UNIVERSITY OF
LIVERPOOL

Scaling of morphogenetic patterns in continuous and discrete models

Thesis submitted in accordance with the requirements of

the University of Liverpool for the degree of Doctor in Philosophy

by

Manan'Iarivo Louis Rasolonjanahary

September 2013

Acknowledgments

Foremost, I would like to express my sincere gratitude to my supervisor Dr Bakhtier Vasiev without whom this thesis would not have been possible. He allowed me to work on this project. I really appreciate his support, guidance, patience and helps during my studies over the past three years.

My special thanks go to my family for their patience, support and encouragement throughout the duration of this project.

I also thank my friends who have supported me during this time.

Contents

General introduction

In biological systems, individuals which belong to the same species can have different sizes. However, the ratios between the different parts of individuals remain the same for individuals of different sizes. For fully developed organism with segmented structure, the number of segment across the size range of the individuals does not change. This morphological scaling plays a major role in the development of the organism and it has been the object of biological studies [18, 22, 74] and mathematical modelling [38, 54] for many decades. Such scaling involves adjusting intrinsic scale of spatial patterns of gene expression that are set up during the development to the size of the system [97]. On the biological side, the evidence of scaling has been demonstrated experimentally on various embryos [88, 36]. For example, a Xenopus embryo was physically cut into dorsal and ventral halves. The dorsal half which contains the "Spermann organizer" developed into a small embryo with normal proportion [88]. Similar experiments carried out for the case of the sea urchin embryo lead to a smaller size of individuals [55]. Also for flies of different species, the number of stripes on their embryos during their development remains the same although they are of different sizes. These stripes, which are visible at an earlier stage of the embryonic development, correspond to the spatial pattern of gene expressions and are the origin of the segmented body of the flies [51, 36, 4]. On the mathematical side, Turing introduced the term morphogens (protein) which is a key factor for pattern formation and he derived a model involving morphogens in which spatial patterns arise under certain conditions. Since then, various mathematical models of pattern formations have been developed. For the diffusion-based models, the spatial pattern do not scale with size. For models using reaction-diffusion equations, (combination of diffusion and biochemical reactions) a characteristic length scale is determined by the diffusion constant and reaction rate. Thus, when the size of the embryo changes, the spacing of the patterning remains fixed. This means that mathematical models based on reaction-diffusion does not show scaling [91].

The motivation of this work is to introduce possible mechanisms of scaling in biological systems and demonstrate those using mathematical models. After a discussion on

how the scaling is considered in a few continuous models, we introduce our definition of scaling. We apply our definition of scaling to analyse properties of concentration profiles arising in various continuous models. Upon analysis of these profiles, we introduce modifications of mathematical models, in particular, two famous continuous models (Turing and Fitzhugh-Nagumo) to achieve scaling of their solutions.

Following a presentation of continuous models, a discrete model of pattern formation based on a chain of logical elements (cellular automata) is also presented. This is more appropriate to represent the discreteness of biological systems with respect to their scaling properties: for a number of problems the issue of scaling doesn't appear in the discrete formulation. This model has been developed to take account of local interactions between cells resulting into stationary pattern formation.

We conclude this thesis by comparing our scaling factor to other scaling factor models and we apply. We also conclude by applying our results to the different stages of the development of the fly segmentation of the fly embryo.

The thesis is structured as follows:

Chapter 1 will discuss about the preliminary background. We will start with patterns in non-biological and biological systems. This is followed by how biological patterns were formed i.e. what mechanisms do we have for these pattern formations. Two of the main properties of biological patterns, which are robustness and scaling, will be briefly discussed in the next section. The mathematical aspects will follow with some examples of mathematical models. The final section will deal with a continuous model.

Chapter 2 will concern the scaling of the continuous models. First, we begin with a simple one-variable model with a diffusion coefficient D and a decay coefficient k. We will investigate whether this model scales with the Dirichlet and Neumann boundary conditions. We consider two mechanisms of scaling of exponential profile. Then, we consider scaling of the morphogen of the annihilation model. We consider the nuclear trapping model and active transport model.

Chapter 3 will concern the two famous models: Turing model and Fitzhugh-Nagumo (FHN) model. For the Turing model, different variants with two variables have been considered. In the variant with three variables, we compute the solution for all variables and then we calculate the scaling factor for one of them. For the FHN model, we start

with the two variables. Then, we move on to the three-variable FHN system. For this latter case, we have computed the scaling factor numerically.

Chapter 4 will concern the presentation of a discrete model based on cellular automaton. We consider the two-state model for which, we determine the transitions giving stationary patterns from an initial periodic solution. Then, we determine the transitions which give periodic stripes from initial random condition. Hereafter, we deal with three- or more states. Biological implementation, of this model, will be discussed in the final section.

Chapter 1

Introduction

1.1 Patterns in living organisms and non-living things

Patterns are defined as orders embedded in randomness or apparent regularities [17]. They can appear in various systems and in different forms.

Living nature is one of the domains very rich in patterns. For instance in animal world, the zebra coat marking consists of a series of black and white stripes. The giraffe's neck has a spotted pattern. Some snakes have also a succession of multi colored ring along their body. Also, patterns can be found on some butterfly wings [69]. These are only a few examples but many more exist in animal world. Patterns can be found also in vegetal world. For instance, on a leaf, the veins exhibit a pattern along the midrib. On the fruit side, pattern is also shown on pineapple skin. Patterns can be seen as well on the flowers of sunflowers or white marguerite [20]. Other examples can be found in vegetal world.
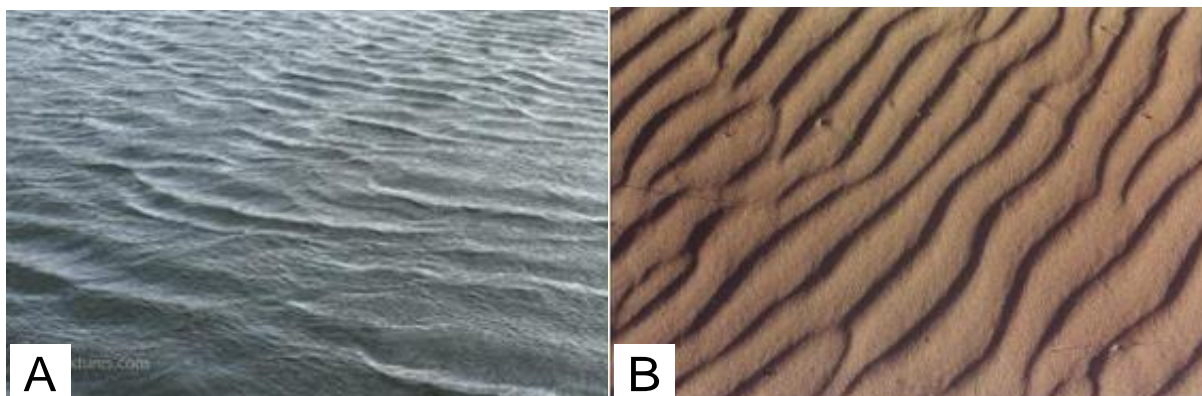
Figure 1.1: **Patterns in Nature. A:** *Waves on the water surface - appear due to an interplay of gravity and pressure when the dissipation of the mechanical energy is slow (low viscosity of water).* **B:** *Sand ripples appear due to an interplay of wind and gravity causing an instability in the shape of surface of the granular material [117].*

Non-living nature is also full of patterns. Patterns can be observed at the surface of bodies of water such as an ocean or a lake (see panel **A** in Figure 1.1). Patterns can be observed at the surface of bodies of water such as an ocean or a lake. These patterns are linked to the transfer of energy from the blowing wind to the water [47]. The size of the resulting wave (so the pattern) depends on the speed and the duration of the wind, and the fetch (length of the interaction area between the wind and the water) [21]. The pattern can have a two dimensional form (succession of rising and failing of water level, for instance) [78, 13]. Steady three-dimensional patterns can exist as well at the surface of the water under certain conditions (constant density, irrational flow, inviscid fluid) [14, 54]. In addition to the wind, a ship cruising at a constant speed on a calm water can induced wave pattern known as the Kelvin wave pattern [73]. Other forms of patterns exist at the surface of water.

For sand, the patterns have the appearance of ripples which can have wavelengths in the range of few centimetres to tens of meters and amplitudes from a few millimetres to a maximum of a few centimetres [77, 48]. They can be observed in desert sand. The sand patterns are believed to be the result of the action of the wind on loose sand [6]. When the wind strength is large enough, the shear stress exerted by the wind on the sand surface lifts individual sand particles [71]. During their flight, the particles have approximately the velocity of the wind. During their impact with the sand surface, other sand particles are ejected [86, 106]. For sufficiently large wind velocities, a cascade process happens, and an entire population of saltating particles hopping on the sand surface emerges [93]. During strong winds, the layer of saltating particles can reach a thickness of more than 1 m [98, 61]. Sand ripple patterns can be found under water as well. For this case, the role of wind is played by the water [117].

Apart from nature, patterns can be encountered in other domains as well. Chemical system is one of them where the famous Belousov-Zhabontisky reaction is an example [49]. Belousov discovered, back in the 1950s, that some chemical reactions containing acid solution and bromate with the presence of a catalyst show a periodic change in concentration of species [75]. This change of concentration is translated to a change of coloration. For example, in the reaction between Cerium-catalysed Bromate and Malonic acid, the ratio of concentration of the cerium(IV) and cerium(III) ions oscillated, causing the color of the solution to oscillate between a yellow solution and a colorless solution [118, 29].

In fluid flow domain, the flow past a cylinder in two-dimensional domain exhibits a

pattern which form depends on the Reynolds number. The Reynolds number is defined as the ratio of the product of the cylinder diameter and the undisturbed free-stream velocity flow and the viscosity of the fluid. When the free stream velocity is increased, a succession of vortices propagates away behind the cylinder [100]. The flow past a cylinder is one of the most studied in aerodynamics and has many engineering applications (see Figure 1.2).
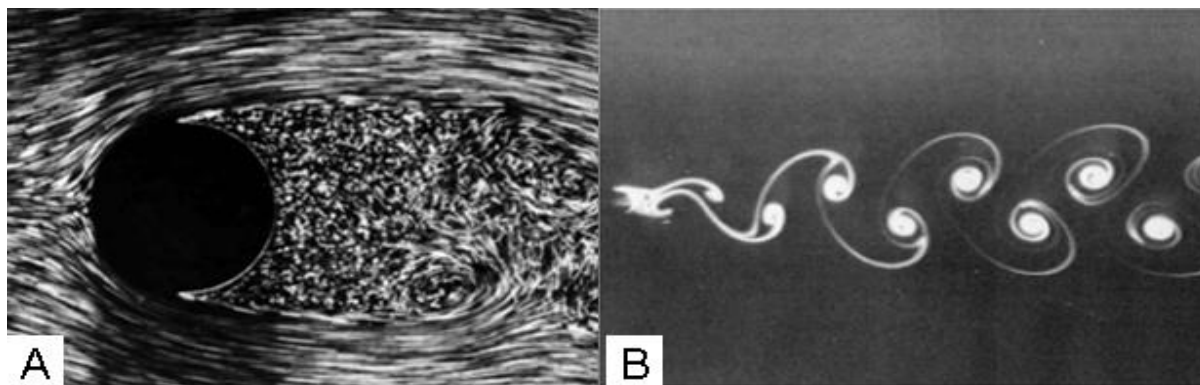
Figure 1.2: **Flows past a circular cylinder. A:** *Birth of vortices behind the cylinder for a Reynolds number of 2000.* **B:** *Two parallel rows of staggered vortices for Reynolds number of 150 [100].*

1.2   Biological patterns

Biology is one of the domains rich in patterns and where the research on patterns has been done extensively. For biological systems, patterns exist in the full spectrum range (from embryo to individual). They have emerged in the origin of life and its evolution [45]. In this part, we deal with more details with some of these domains.

1.2.1   Skin pattern

Skin patterns can have various appearances. Some examples are: stripes for zebras and tigers, spots for leopards [68], patches for giraffes and rings for snakes [67, 2]. Some pictures extracted from various internet sites are shown in Figure 1.3. For zebra, for instance, the hair pattern is considered as black stripes on a white background (the belly and unstriped leg regions are white). The width of these stripes varies, being wide on the neck and narrow on the head. The patterns may differ from a zebra to another or from a zebra specie to another. These different zebra patterns are shown to be generated by a single mechanism forming stripes, operating at different times in embryogenesis [7]. Turing has proposed a possible mechanism explaining how animals get their skin patterns [94]).
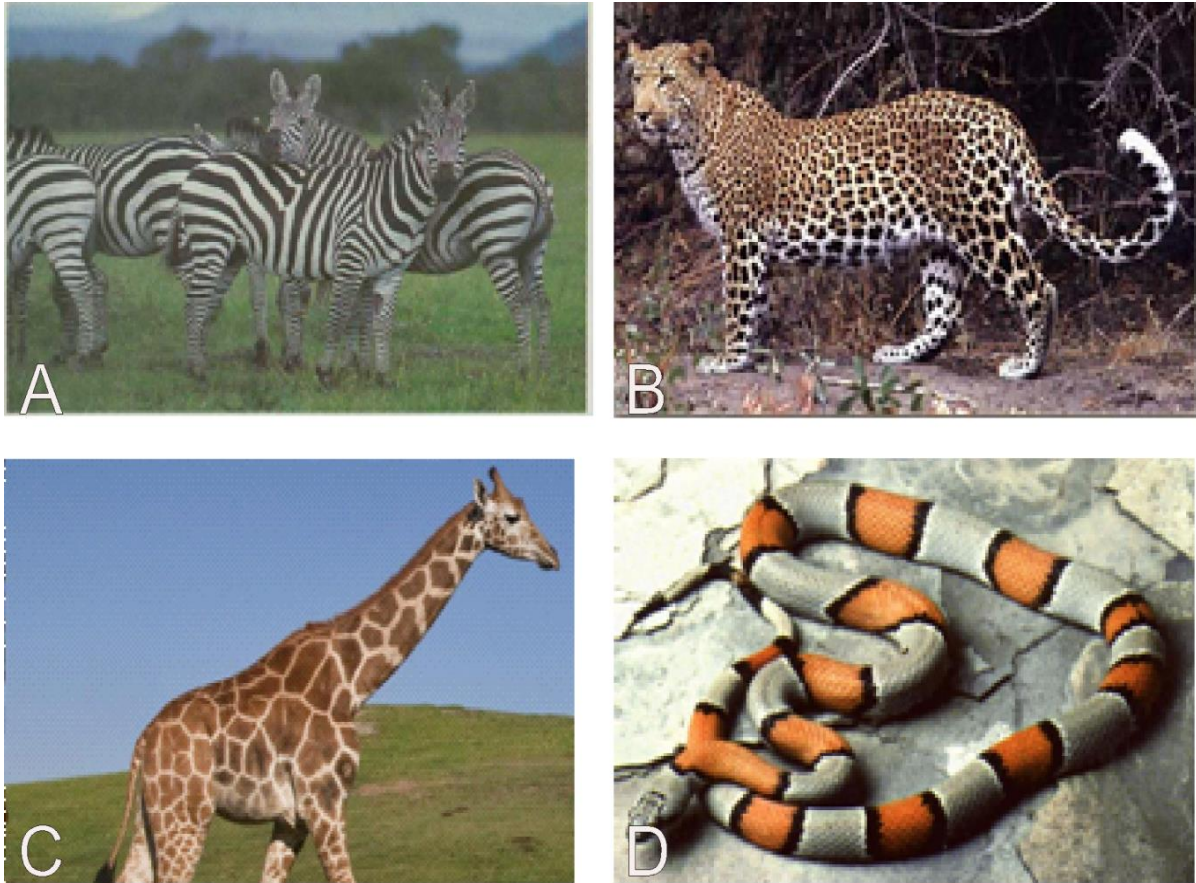
Figure 1.3: **Examples of animal skin patterns.** *A: Black and white stripes for the zebra.* *B: Spots for the leopard.* *C: Patches for the giraffe.* *D: Periodic patterns (orange and grey) for the snake.*

1.2.2 Shells of molluscs

The mollusc shell exhibits one of the more complicated patterns in higher organisms. The patterns on mollusc shell are interesting in two aspects: pigmentation and relief. These two aspects co-exist simultaneously [12]. Moreover, two molluscs of the same species can have different shell patterns and two molluscs from different species can have similar shell patterns. The patterns consist of lines, stripes and patches of different pigmentations or of relief-like structures (ridges, knobs) [104]. The relief-like patterns are believed to have a functional significance (for instance, used to increase friction with sand during burrowing). Therefore, the environment has an effect on relief-like patterns. The shell pattern is formed only on the growing edge of the mollusc shell and therefore, it represents a protocol of what is happened at the growing edge of the particular animal. The patterns are, therefore, space and time plots. More details of mollusc shell patterns are given in [66]. Figure 1.4 shows an example of shells with patterns.

Figure 1.4: **Stripes due to shell pigmentation occurring at regular basis. Upper:** *Stripes are parallel to the axis of the shell.* **Lower:** *Stripes perpendicular to the axis of shell [65].*

1.2.3   Segmentation of the fly embryo (drosophila)

Drosophila embryo is one of the most studied systems for patterning [42]. For the Drosophila embryo, the pattern occurs as a repeated structure called segments arranged along the head to tail axis. These segments have their origin in spatially periodic patterns of gene expressions which are visible at early stages of embryonic development [89]. The patterning in Drosophila embryo is controlled by gradients in the concentration of **maternal genes** (bicoid, caudal, etc.) that arise soon after fertilisation [36]. These genes, located on the poles of the embryo, diffuse spatially from the anterior (bicoid) and posterior (caudal) poles of the embryo and control the spatial pattern of the transcription of the **gap genes** (i.e. hunchback. Krüppel, knirps, etc.) [92]. These genes are amongst the earliest expressed zygotic genes and they encode transcription factors. They act to sub-divide the embryo into broad domains (anterior, middle and posterior). The **gap genes** regulate each other and the next set of genes in the hierarchy which are the **pair-rule genes** (even-skipped, hairy, fushi-tarazu, etc.). **Pair-rule genes** are expressed in 7 stripes of cell and establish the initial expression of **segment-polarity genes** (wingless, hedgehog, engrailed) [50, 87]. **Segment polarity genes**, in turn, are expressed in 14 narrow stripes shortly before gastrulation. These stripes constitute a segmental pre-pattern in that they determine the positions of morphological segment boundaries which form later in development (see Figure 1.5) [76]. The position and identity of body segments which take place during the embryogenesis are specified in the segmentation process [52].
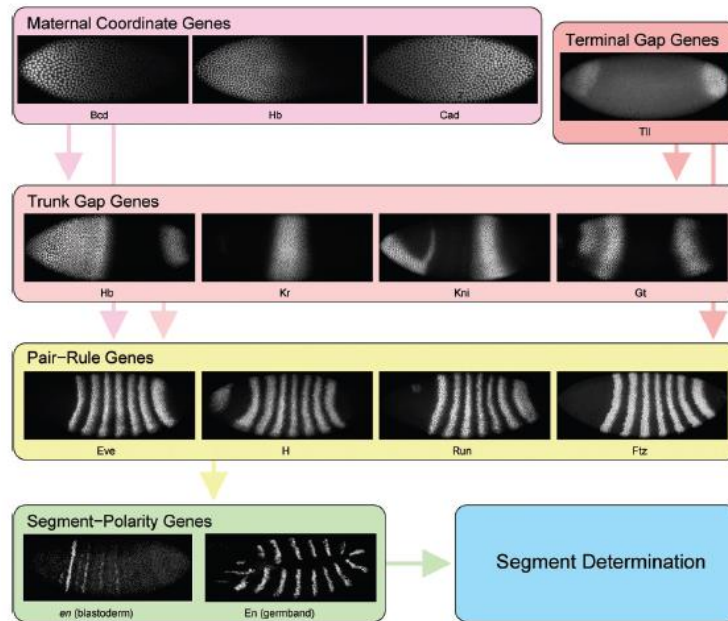
Figure 1.5: **Hierarchy of Gene Control of Segmentation in Drosophila.** *The patterning associated with the segmentation takes place in four levels: Concentration profiles of* **maternity genes** *(bicoid, caudal, etc). These genes control the spatial patterns of transcription of the* **gap genes**. *Spatial patterns of transcription of the* **gap genes** *(Hb, Kr, etc). The* **gap genes** *regulate each other and the next set of genes in the hierarchy, the* **pair-rule genes** *(even-skipped, hairy, etc.).* **Pair-rule genes** *- form seven stripes of transcription around each embryo.* **Pair-rule genes** *determines the initial expression of segment polarity genes.* **Segment polarity genes** *- form fourteen stripes of transcription around each embryo [52].*

For the dorsal-ventral axis, the patterning of the Drosophila dorsal-ventral axis which is controlled by the gradient of Dorsal protein is highest in ventral regions of the embryo [62]. Dorsal protein activates genes in a concentration dependent manner to establish early patterning of the embryo [31, 60]. The patterns are refined by interactions between Dorsal and other activators as well as repressors in both dorsal and ventral regions of the embryo. In the early embryo, the translocation of dorsal protein into ventral nuclei produces a gradient where the ventral cells with the most Dorsal protein become mesoderm. The next higher portion becomes the neurogenic ectoderm. This is followed by the lateral and dorsal ectoderm [33, 79]. The dorsalmost region becomes the amnioserosa (embryonic layer surrounding the embryo)(see Figure 1.6) [34].
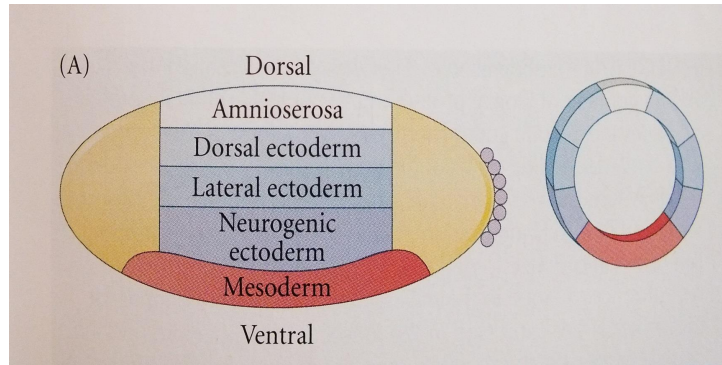
Figure 1.6: **Dorso-ventral regions of early embryo.** *In the early embryo, five distinct regions, which are mesoderm, ventral ectoderm, lateral and dorsal ectoderm and amnioserosa appear.* **Left:** *Lateral view.* **Right:** *Transversal view [34].*

1.3   Mechanisms of pattern formation

Pattern formation is a central process in the development of living organisms. According to Wolpert, it is the process by which spatial organization of cells is established and is related to two other developmental processes which are cell differentiation and change in form [110]. For instance, pattern formation determines where cartilage and muscle will develop on the development of vertebrate limb [111]. The role of pattern formation in the development process in biology can be explained using the concept of positional information. The basic idea behind this concept is that cells acquire positional identities as in coordinate system and then interpret their positions to give rise to spatial patterns. One of the main mechanisms for setting up positional information is based on gradients of morphogens, which are diffusible molecules produced by the cells, whose concentration specifies positions [112]. If the concentration of the morphogen is fixed at the source, then the distribution of its concentration at any point effectively provides the cells with positional information [111].

Mechanisms of pattern formation have been classified into three categories [81, 32]:

1. Autonomous mechanism in which cells enter into specific arrangements (patterns) without interaction.

2. Inductive mechanisms where cells interact with each other by secreting diffusible molecules. This leads to change in pattern by reciprocal or hierarchical alteration of cell phenotypes, and

3. morphogenetic mechanisms where pattern changes by means of cell interactions that do not change cell states.

In theoretical discussion of biological development, it is commonly accepted that pattern formation has two components [108]. First, interaction mechanisms between cells with different states and different spatial relationships using signaling in two and three dimensions. Second, mechanisms that use cell behaviors other than signaling and action previously established pattern to cause the formation of three dimensional tissues and organs.

However, the morphogen gradients are typically dynamic and in many cases their dynamics are conditioned by the movement of cells. Gastrulation in the chick embryo is a good example for which detailed data on the dynamics of gene expression patterns and cell movement is available [5, 90, 16]. An extensive cell motion observed during gastrulation all over the epiblast can be considered as having three distinct parts: (1) cell motion along the embryo midline associated with progression and regression of the primitive streak; (2) lateral movement of cells on both sides of the midline which is vortex-shaped at early gastrulation and form lateral flows toward the midline at later stages and (3) transformation of approaching the midline epithelial cells into mesenchyme which forms a sink in the epiblast along its midline and gives rise to lateral flows formed my mesenchyme cells. As the movement involves different cell groups which express different genes the forming morphogenetic patterns are dynamic and change following the relocation of domains of transcriptions. Furthermore, the movement of cells can, in turn, be affected by morphogen concentrations, which is the case if the movement is chemotactic and morphogens can act as chemotactic agents. These possibilities have recently been explored in studies combining mathematical modelling and experiments [101, 43, 103].

1.4 Symmetry and symmetry breaking in biological pattern formation

Mathematically, symmetry is characterised by a group of transformations that leave certain features of a system unchanged [63]. In physical systems, symmetry can be seen as homogeneity [35] or uniformity [59]. It can be also characterised by the existence of different viewpoints from which the system appears the same [3]. Also, the symmetry properties may be attributed to physical law (equations) or to physical objects or states (solutions) [15]. Symmetry plays fundamental role in physics, for instance, in classical mechanics or quantum mechanics [41].

Symmetry is a very important ingredient in a pattern formation model (spatial hidden symmetries in pattern formation). The application of the concept of symmetry has been extended by Turing in biology. In his famous paper in 1952 [94], Turing showed that, in biology, pattern formation is governed by reaction-diffusion systems involving two chemical substances called morphogens. A spatially homogeneous distribution of these morphogens is unstable if one of them (activator) diffuses more slowly than the other (inhibitor). In this case, small stochastic concentration fluctuations are amplified, leading to a chemical instability (a "Turing instability") and the formation of concentration gradients (or patterns) [99]. These reaction-diffusion systems often possess symmetries. Specifically, the equations which describe them are often left unchanged by certain groups of transformations, such as reflection, translation or rotation.

The process by which the spatially homogeneous distribution is broken to generate a more structured state is called symmetry breaking. For the presence of such structure, a lower symmetry than the absolute one is needed: in the sense that symmetry breaking is essential for the existence of structured things [15]. Symmetry breaking does not imply that no symmetry is present, but rather that the situation is characterized by a lower symmetry than the original one. It refers to the situation in which solutions to the equations have less symmetry than the equations themselves. There are two types of symmetry breaking: spontaneous and explicit [15, 72, 59]. Spontaneous symmetry-breaking occurs when the laws or equations of a system are symmetrical but specific solutions do not respect the same symmetry. Here, spontaneous simply means endogenous to the dynamics of the system and not catalyzed by some exogenous input as in the case of explicit symmetry breaking. Explicit symmetry breaking means a situation where the dynamical equations are not invarivant under the symmetry group [15]. It occurs when the rules governing a system are not manifestly invariant under the symmetry group considered. Also, in this case, the symmetry is broken by external objects.

1.5   Noise-induced pattern formations

Random fluctuations due to environmental effects are always present in natural systems. In addition to deterministic events which lead to pattern formation, these random fluctuations can also generate patterns. These pattern formations are explained as noise induced in the sense that they emerge as a consequence of the randomness of the system's fluctuations. If the noise intensity is set to zero, the noise-induced patterns disappear and the homogeneous stable state is restored. These random drivers have often been related to a symmetry-breaking instability [84]. They destabilise a homogenous (and, thus, symmet-

ric) state of the system and determine a transition to an ordered phase, which exhibits a degree of spatial organisation.

In mathematical modelling of noise induced pattern formation, Gaussian white noise is usually adopted as it provides a reasonable representation of the random fluctuation of the real systems (the spatial and temporal scales of the Gaussian white noise are much shorter than the characteristic scales over which spatio-temporal dynamics of the field variable are evolving). At any point $\boldsymbol{r}(x, y)$ of the system, the spatio-temporal dynamics of the state variable is described by the following equation [84]

$$\frac{\partial \varphi}{\partial t} = f(\varphi) + g(\varphi)\xi(r, t) + DL[\varphi] + \xi_a(r, t).$$

This equation contains three components.

- The deterministic local dynamics $f(\varphi)$ which tends to drive the field variable to a uniform steady state hence do not contribute to pattern formation

- the noise components which consist of the multiplicative part $g(\varphi)\xi(\boldsymbol{r}, \varphi)$ and the additive part $\xi_a(\boldsymbol{r}, \varphi)$ maintain the dynamics away from the uniform steady state, and

- the spatial coupling term represented by $DL[\varphi]$ and which provides spatial coherence. This spatial coupling is characterized by the operator L and its strength D.

Gaussian white noise, with intensity s and zero mean, is usually adopted as it provides a reasonable representation of the random fluctuation of the real systems (the spatial and temporal scales of the Gaussian white noise are much shorter than the characteristic scales over which spatio-temporal dynamics of the field variable are evolving) [84]. For this Gaussian white noise, the correlation is given by

$$\langle \xi(r, t)\xi\left(r', t'\right)\rangle = 2s\delta\left(r - r'\right)\delta\left(t - t'\right).$$

Additive noise

In the case of additive noise, the model is represented by

$$\frac{\partial \varphi}{\partial t} = a\varphi + DL[\varphi] + \xi_a(r, t).$$

The noise effect does not depend on the state of the system. The deterministic part of the dynamics does not generate patterns for any value of a: if $a < 0$, the system is damped to zero without showing any spatial coherence. If $a > 0$, no steady states exist and the dynamics of φ diverge without displaying any ordered spatial structures. Additive noise, ξ_a, is able to keep the dynamics away from the homogenous deterministic steady state even though in the underlying deterministic dynamics $f(\varphi)$ would tend to cause the convergence to the homogenous state. In these conditions patterns emerge and are continuously sustained by noise. These patterns are noise-induced in that they disappear and the homogeneous stable state φ_0 is restored if the noise intensity is set to zero [84].

Multiplicative noise

For this case, the model is represented by

$$\frac{\partial \varphi}{\partial t} = f(\varphi) + g(\varphi)\xi(r,t) + DL[\varphi].$$

In the case of multiplicative noise, the evolution depends on the value of the state variable φ. The cooperation between multiplicative noise and spatial coupling is based on two key actions: (i) the multiplicative random component temporarily destabilizes the homogeneous stable state, φ_0, of the underlying deterministic dynamics, and (ii) the spatial coupling acts during this instability, thereby generating and stabilizing a pattern [84]. The key features of pattern formation induced by multiplicative noise are that for s lower than a critical value s_c, the state variable φ experiences fluctuation about φ_0 but noise does not play any constructive role [83]. For s greater than s_c, the spatial coupling exploits the initial instability of the system to generate ordered structures.

1.6   Robustness and Scaling of biological patterns

In biology, pattern formation results from the response of individual cells to a spatial pattern (gradient) of chemical substances called morphogens [94]. According to Turing, morphogens are responsible for the main phenomena of morphogenesis (generation of form) [94]. One of the key properties of morphogen gradients is "robustness" [56, 95]. The term "robustness" quantifies the aptitude of the morphogen gradients (patterns) to resist to the fluctuations due to internal and external factors [57]. During its development the organ, composed of cells, is exposed to a certain "development noise" i.e. environmental factor, genetic variability and random difference which can lead to variation in gene expression level between individual [46]. Despite these fluctuations, the outcome

of the organ is precise and reproducible, indicating that the mechanisms regulating patterning and growth of organs are robust and able to damp the effects of the variations [85].

Another key property of morphogen gradients is scaling. In Drosophila, development along the anterior-posterior axis is scaled with embryo length i.e. although individuals vary substantially in size, the proportions of different parts of the individuals remain the same, Figure 1.7 [36, 8]. This adaptation of proportion (pattern) with size is termed as scaling. Experiments in scaling have been carried out towards the end of 19th century. In 1883, Whilhem Roux killed one of two cells in a frog embryo and he found that the rest gave rise to only part of the embryo [82]. Hans Driesch, in 1891, he cut two cells of the sea urchin and each gave rise to full embryos (see Figure 1.7)[53]. Four years later, Thomas Morgan repeated Roux's experiment by removing one of two blastomere in a frog embryo and he found out that the amphibian could give rise a complete embryo from half an egg [114, 9, 25].
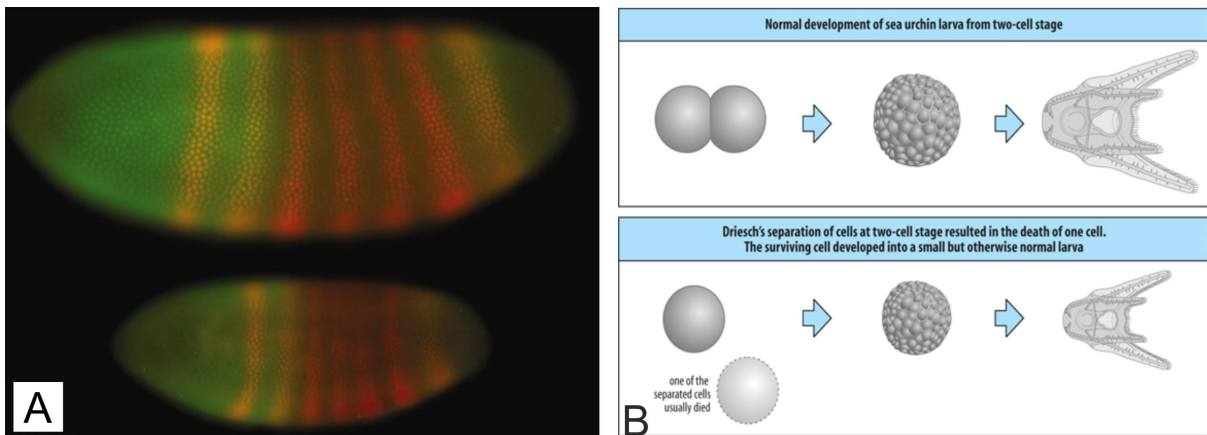
Figure 1.7: **Scalings of fly embryo and sea urchin. A:** Fly embryo of different sizes with the same number of stripes (segments). The upper and lower fly embryo have 485 μm and 344 μm respectively. Scaling was obtained by varying the lifetime of the lifetime of the bicoid protein [36]. **B:** At the two-cell stage, one has the development of the sea urchin. Hans Drieschs separated into two cells resulting that one cell is dead and the other has given rise to a smaller sea urchin [113].

1.7 Mathematical models for pattern formation

Various mathematical models have been developed to help understand pattern formation. The first of these models was introduced by Turing and based on reaction-diffusion equations of morphogens. According to Turing, morphogens react chemically and diffuse through a tissue [94]. These morphogens are, through their gradient, responsible for pattern formation in biological system.

1.7.1 The French Flag Model

The classical illustration of how a morphogen can provide positional information is given by the French Flag model suggested by Lewis Wolpert [110]. This model demonstrates how a simple, linear concentration profile of a morphogen can set domains of cellular determination in an otherwise homogeneous tissue. The linear concentration profiles can form naturally in various settings. The simplest case is when the production and degradation of morphogen take place outside the tissue on its opposing sides and the morphogen passively diffuses along the tissue from the side where it is produced to the side where it is degraded. Mathematically, the concentration of the morphogen in this system should obey so called Laplace's equation with Dirichlet boundary conditions, which for a tissue represented by a one-dimensional domain of length L, is given by the following mathematical formulation [103](Figure 1.8).
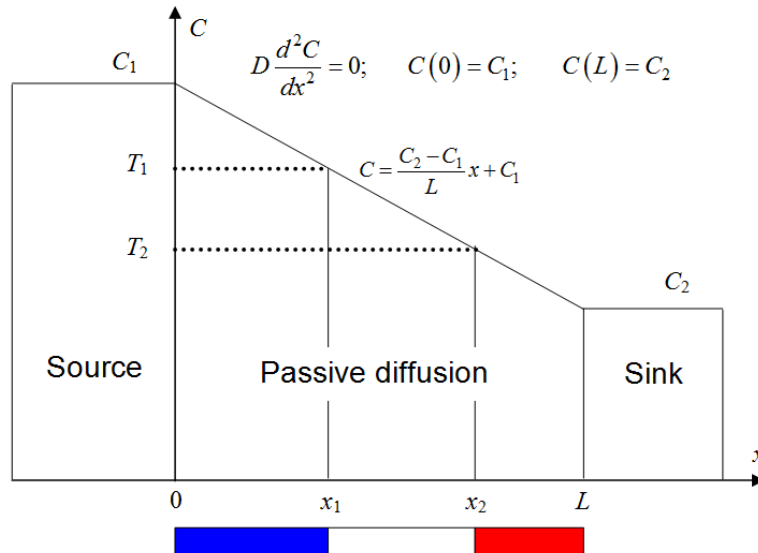
Figure 1.8: **Linear gradient in the French Flag model forms due to passive diffusion of the morphogen.** *x_1 and x_2 have T_1 and T_2 for the threshold concentration values respectively. C is the concentration of morphogen, D is the diffusion coefficient, C_1 and C_2 are the concentrations of the morphogen outside the two sides of the tissue and L is the size of the tissue. We have Dirichlet boundary conditions at both ends.*

In this model, C represents the concentration of the morphogen, D is the diffusion coefficient and C_1 and C_2 are the buffered concentrations of the morphogen outside the two sides of the tissue. In this model, the pattern depends on the level of concentration. This model does scale because if, for example, the size of tissue is doubled then the sizes of all domains of cellular determination which are defined by the threshold concentration values T_1 and T_2 will be also doubled. However, this linear shape is not confirmed by

experimental observations.

1.7.2 Morphogen gradient in system with decay

The linear shape shown in the French Flag model, in the previous section, is not confirmed by experimental observations. Most commonly measurements point to an exponential shape, as, for example, in the case of the transcriptional factor Bicoid in the fly embryo [27, 39]. Formation of the exponential profile can be shown mathematically under the assumption that the morphogen not only diffuses but also degrades inside the domain. The concentration of morphogen can be buffered on the boundaries of the tissue. Alternatively, we can assume that the tissue is isolated (no flows on the boundaries) and the production of the morphogen takes place in a restricted area inside the domain. These assumptions are perfectly reasonable for many studied objects. For example, the maternal Bicoid mRNA in fly embryo is localised in a small region on its apical side and the Bicoid protein produced in this region diffusively spreads and decays along the entire embryo. Stationary concentration of the morphogen in this system will satisfy the following equation [103](Figure 1.9).

In this model, C and D have the same signification as previously, k represents the decay rate, j_0 is a non-zero flux and p is the production of the protein in the apical side region of size a. When the area of the production is small, we can replace it by boundary fluxes (see proof in appendix A). This figure does not scale because of the characteristic length of exponential profile. In other words, the distance required for the concentration to reduce by a certain factor (i.e. $e-$times), depends only on the diffusion coefficient, D, and the degradation rate, k, of the morphogen. For example, if, in the case shown in Figure 1.9, we increase the size of the domain from L to $2L$ then the sizes of blue and white sub-domains will not change while the red sub-domain will increase to cover all added L units of length [103].
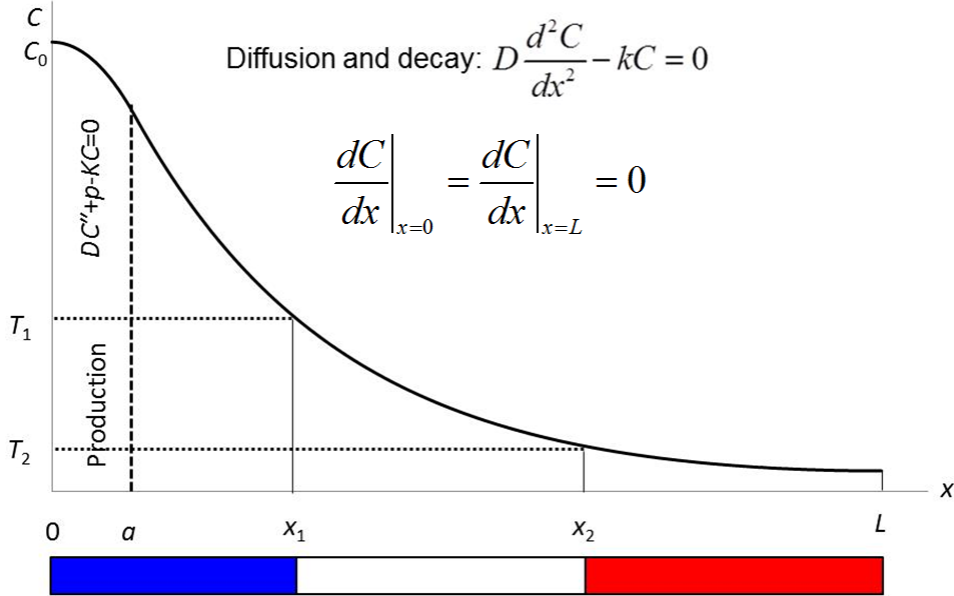
Figure 1.9: ***Exponential profile when the diffusion is combined with the decay.*** *C is the concentration of morphogen, D is the diffusion coefficient, x_1 and x_2 have T_1 and T_2 for the threshold concentration values respectively and C_0 is the concentration at $x = 0$. We have production in the region between 0 and a with parameter p in the equation. And we have Neumann boundary condition at both ends.*

In an attempt to understand pattern formation in more depth, quantitative models of gradient formation have been developed. The addition of a degradation term with rate k to the Fick's second law leads to the equation

$$\frac{\partial C}{\partial t} = D\frac{\partial^2 C}{\partial x^2} - kC. \tag{1.1}$$

The steady state solution to this equation (1.1) with a production from localised source has an exponential form

$$C(x) = C_0 e^{-\frac{x}{\lambda}}, \tag{1.2}$$

where C_0, in equation (1.2) is the concentration at the source boundary ($x = 0$) and λ is the decay length given by $\lambda = \sqrt{D/k}$, i.e. the distance from source at which the concentration is reduced to a fraction $1/e$ of C_0. C_0 depends on the flux of molecules across the source boundary j_0, on the diffusion coefficient D and the degradation rate k as shown in equation (1.3) [107].

$$C_0 = \frac{j_0}{\sqrt{Dk}}. \tag{1.3}$$

1.7.3 Turing model

Turing was the first to propose reaction diffusion theory involving two species (morphogens) as model for pattern formation. He suggested that chemicals can react and diffuse in such a way as to produce steady state heterogeneous spatial patterns of chemical or morphogen concentration [94]. His theory is based on the possibility of a stable state against perturbation, with absence of diffusion phenomenon to become unstable against perturbation in the presence of diffusion.

Turing's pattern formation can be summarised as follows using two morphogen species, u and v. The morphogen u is known as the activator because it is involved in the increase of its own production as well as to the production of the second morphogen v. The second morphogen v is called the inhibitor since it reduces the production rate of the activator and it also enforces its own degradation. For a 2D system (u, v), it is characterised by the set of ordinary differential equations.

$$\frac{du}{dt} = f(u, v), \tag{1.4}$$
$$\frac{dv}{dt} = g(u, v),$$

where $f(u, v)$ and $g(u, v)$ are non-linear functions. The equilibrium point $(u, v) = (u_0, v_0)$ is solution of the LHS=0 of system (1.4). By adding a simple exponential type perturbation $\tilde{u}, \tilde{v} \approx e^{t\lambda}$ to (u_0, v_0), we will find λ from the characteristic equation

$$\begin{vmatrix} f_u - \lambda & f_v \\ g_u & g_v - \lambda, \end{vmatrix} = 0,$$

where f_u, f_v, g_u and g_v are the derivatives with respect to u and v computed at (u_0, v_0). This gives

$$\lambda^2 - \lambda (f_u + g_v) + f_u g_v - f_v g_u = 0.$$

From above, we have

$$\lambda_{1,2} = \frac{f_u + g_v}{2} \pm \sqrt{\frac{(f_u + g_v)^2}{4} - (f_u g_v - f_v g_u)}.$$

In order to have stability, we need to request that Re $\lambda < 0$. From the properties of the roots of quadratic equations, we have the following conditions

$$f_u + g_v < 0, \tag{1.5}$$

and

$$f_u g_v - f_v g_u > 0. \tag{1.6}$$

In the presence of diffusion phenomena, the set of previous ordinary differential equations (1.4) becomes

$$\begin{cases} \frac{\partial u}{\partial t} = D_u \Delta u + f(u, v), \\ \frac{\partial v}{\partial t} = D_v \Delta v + g(u, v), \end{cases} \tag{1.7}$$

where D_u and D_v are the diffusion coefficients of u and v respectively. The equilibrium point $(u, v) = (u_0, v_0)$ is solution of the LHS=0 of system (1.7). To study the effect of small perturbation, let

$$\begin{aligned} \tilde{u} &= u - u_0, \\ \tilde{v} &= v - v_0. \end{aligned}$$

Linearising around (u_0, v_0), we get

$$\begin{aligned} \frac{\partial \tilde{u}}{\partial t} &= D_u \Delta \tilde{u} + \tilde{u} f_u + \tilde{v} f_v, \tag{1.8} \\ \frac{\partial \tilde{v}}{\partial t} &= D_v \Delta \tilde{v} + \tilde{u} g_u + \tilde{v} g_v, \end{aligned}$$

where f_u, f_v, g_u and g_v are the derivatives with respect to u and v computed at (u_0, v_0). We are looking for solutions which can be represented as

$$\begin{aligned} \tilde{u} &= \sum_i \alpha_i e^{\lambda_i t} f_i(x), \\ \tilde{v} &= \sum_i \beta_i e^{\lambda_i t} g_i(x), \end{aligned}$$

where α_i and β_i are constants. Now the functions $f_i(x)$ and $g_i(x)$ can be represented as

$$f_i(x) = g_i(x) = a_i \cos(k_i x) + b_i \sin(k_i x)$$

where a_i and b_i are constants and k_i represents the wavelength. Assume that we have a function which goes from 0 to L and we want to extend it **evenly** i.e. the function is symmetric with respect the vertical axis. Then, in the solutions of $f_i(x)$ and $g_i(x)$, all the *sine* functions will vanish. Therefore, the functions $f_i(x)$ and $g_i(x)$ can be written as

$$f_i(x) = g_i(x) = a_i \cos(k_i x)$$

and the full solutions of $\tilde{u}$ and $\tilde{v}$ can be represented as

$$\tilde{u} = \sum_i \alpha_i e^{\lambda_i t} \cos\left(\frac{\pi i}{L} x\right).$$

$$\tilde{v} = \sum_i \beta_i e^{\lambda_i t} \cos\left(\frac{\pi i}{L} x\right).$$

Any initial concentration profiles for both variables can be represented by above series. These series would represent solution of the system (1.8) if each pair of corresponding terms also satisfies this system. Therefore, we take one particular term from each of the above series

$$\tilde{u} = \alpha_1 \cos(kx) e^{\lambda t},$$

$$\tilde{v} = \beta_1 \cos(kx) e^{\lambda t},$$

and substitute them into equation (1.8), we obtain

$$\alpha_1 \lambda = -k^2 D_u \alpha_1 + f_u \alpha_1 + f_v \beta_1,$$

$$\beta_1 \lambda = -k^2 D_v \alpha_1 + g_u \alpha_1 + g_v \beta_1.$$

The above equations are linear in α_1 and β_1. Non-zero solutions only exist if the determinant of the matrix M is zero i.e.

$$\begin{vmatrix} f_u - \lambda - k^2 D_u & f_v \\ g_u & g_v - \lambda - k^2 D_v \end{vmatrix} = 0.$$

This gives a quadratic equation in λ.

$$\lambda^2 - \lambda\left(f_u + g_v - k^2(D_u + D_v)\right) + \left(k^4 D_u D_v - k^2(f_u D_v + g_v D_u) + f_u g_v - f_v g_u\right) = 0. \quad (1.9)$$

In order to investigate how diffusion phenomenon $(D_u, D_v \neq 0)$ can destabilize the system, let's consider the coefficient of λ and the constant term in (1.9). They are functions of k^2 and denoted respectively as $B(k^2)$ and $C(k^2)$.

$$B\left(k^2\right) = f_u + g_v - k^2\left(D_u + D_v\right), \quad (1.10)$$

and

$$C\left(k^2\right) = k^4 D_u D_v - k^2\left(f_u D_v + g_v D_u\right) + f_u g_v - f_v g_u = 0. \quad (1.11)$$

The function $B(k^2)$ is always negative for any value of k^2 according to (1.5). So, the only way to have instability is that the function $C(k^2)$ is negative. To achieve that, we require that $f_u D_v + g_v D_u > 0$. This is necessary but not sufficient condition. A sufficient condition is to have the minimum of $C(k^2)$ to be negative. The value of k^2 which gives this minimum value, C_{min} is solution of the derivative of $C(k^2)$ with respect to k^2 i.e.

$$2k^2 D_u D_v - (f_u D_v + g_v D_u) = 0.$$

So the sufficient condition to get instability is

$$C_{min} = \frac{(f_u D_v + g_v D_u)^2}{4 D_u D_v} - \frac{(f_u D_v + g_v D_u)^2}{2 D_u D_v} + f_u g_v - f_v g_u < 0.$$

After rearranging, we obtain

$$\frac{(f_u D_v + g_v D_u)^2}{4 D_u D_v} > f_u g_v - f_v g_u. \tag{1.12}$$

In other words, this condition leads to one of the eigenvalues to be positive.

The range of k^2 which corresponds to Turing's instability is given by $k_1^2 < k^2 < k_2^2$ where k_1^2 and k_2^2 are zeros of $C(k^2)$. Their expressions are given by

$$k_{1,2}^2 = \frac{f_u D_v + g_v D_u \pm \sqrt{(f_u D_v + g_v D_u)^2 - 4 D_u D_v (f_u g_v - f_v g_u)}}{2 D_u D_v}.$$

This case corresponding to the instability is represented by the blue curve in Figure 1.10.
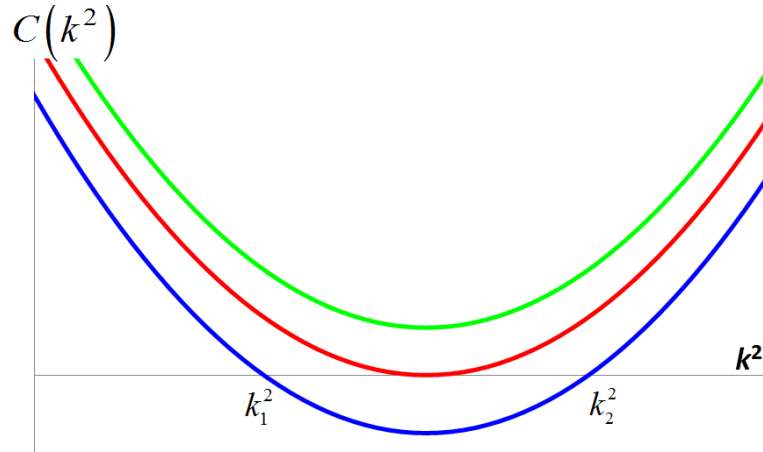
Figure 1.10: **Plot of DET vs k^2.** *The condition (1.12) is satisfied for the blue curve but not satisfied for the green and red ones. The blue curve intersects the k^2 axis at k_1^2 and k_2^2. The instability occurs for k^2 between k_1^2 and k_2^2 i.e. one of the eigenvalues is positive. For the red and green curves, no Turing's patterns occur [69].*

The values k_1 and k_2 are called the boundary wavenumbers. If $k < k_1$ or $k > k_2$ the perturbation due to the diffusion dies out without disturbing the homogeneous stable stationary state. The instability means that any noise with the right wavelength will be amplified by the system and leads to a spatial pattern with the matching wavelength. Turing's instability (pattern) exists not only in biological systems but also in domains such as chemicals, physics, etc.

In summary, the conditions to get the homogeneous stable stationary state to become instable with the presence of diffusion (diffusion driven instability) are as follows:

$$\begin{cases} f_u + g_v < 0, \\ f_u g_v - f_v g_u > 0, \\ f_u D_v + g_v D_u > 2\sqrt{D_u D_v \left(f_u g_v - f_v g_u\right)}. \end{cases} \tag{1.13}$$

The special wavelength of the Turing pattern is defined by the diffusion and kinetics rates of morphogens in equation system (1.9). Neither of these two change when the size of the medium and therefore the patterns forming in the classical Turing model don't scale.

1.7.4 Fitzhugh-Nagumo model

The Fitzhugh-Nagumo model (FHN) belongs to a general class of reaction-diffusion equations [26]. This model has different versions and was originally developed as a generic model for signal propagation along a nerve fibre [30]. Its variant, which introduces the

diffusion of the second variable, also serves as a generic model for morphogenetic pattern formations [102]. It is described by the following system (1.14) which has been obtained after time and space rescaling in order to allow the elimination of one of the diffusion coefficients and one of the kinetic rates

$$\begin{cases} \frac{\partial u}{\partial t} = \Delta u + f(u,v), \\ \frac{\partial v}{\partial t} = D\Delta v + \varepsilon g(u,v). \end{cases} \tag{1.14}$$

In the above system, D is the ratio of the diffusion coefficients and ε is the ratio of the kinetic functions $f(u,v)$ and $g(u,v)$. The kinetic term in the first equation is defined by a cubic function $f(u,v) = -k_u u(u-\alpha)(u-1) - v$ [70] while in the second equation, it is simply represented by a linear function $g(u,v) = k_v u - v$. k_u and k_v represent constants related to the kinetic terms and α is a constant $0 < \alpha \ll 1$ which is called "excitation threshold".

Like in the Turing model, u and v represent the activator and the inhibitor respectively. Unlike the Turing model which patterns result from the difference of diffusion rates, the FHN patterns are based on the excitable dynamics from the reaction terms. By ignoring the diffusion terms, the above system has fixed points which are defined by the intersections of the two nullclines $f(u,v) = 0$ and $g(u,v) = 0$. According to the nature of the intersections, the kinetic system can be classified as excitable, bistable or oscillatory. For $\alpha \geq 0$, one or two steady state solutions can be obtained. The oscillatory solution is obtained for example, by adding an extra term in the function $f(u,v)$ so that the nullcline will move up. These are shown in Figure 1.11.
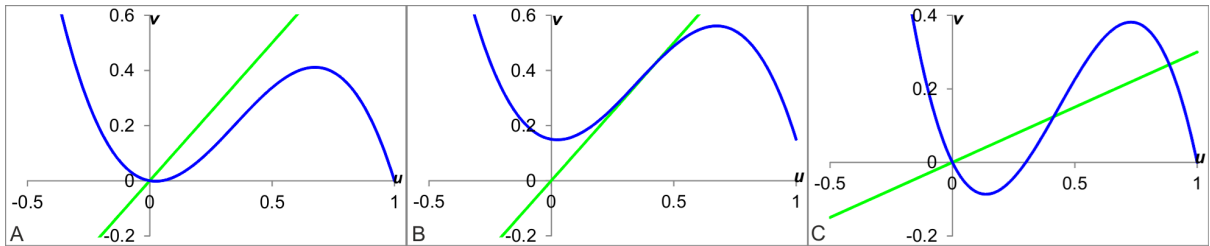
Figure 1.11: **Nullclines for three different dynamical regimes described by the FHN model.** *The blue curve is the cubic nullcline f(u, v)=0 for activator. The green curve corresponds to the linear nullcline g(u, v)=0 for inhibitor. Three different type of system are shown. **A:** The origin is the only equilibrium point. This describes excitable system. **B:** The cubic nullcline has been shifted upward to give an oscillatory system. **C:** There are three equilibrium points. One can have either two unstable and one stable or two stable and one unstable. This system is bistable.*

The model represented by the two equations above allows the understanding of pat-

tern formation phenomena which occur in various chemical, physical and biological systems [102]. Different types of solutions can be obtained by changing the ratio of diffusion D and ratio of kinetic rate ε.

In Figure 1.12, four different scenarios are shown: propagating wave, vanishing spot, pulsating spots and stationary spots. They were obtained with different values of D. Propagating wave was obtained with $D = 1$. $D = 2$ is the case of the vanishing spot. Pulsating spots was simulated with $D = 3.2$. All of these patterns can be classified into four regions which is shown in panel **E** of Figure 1.12.
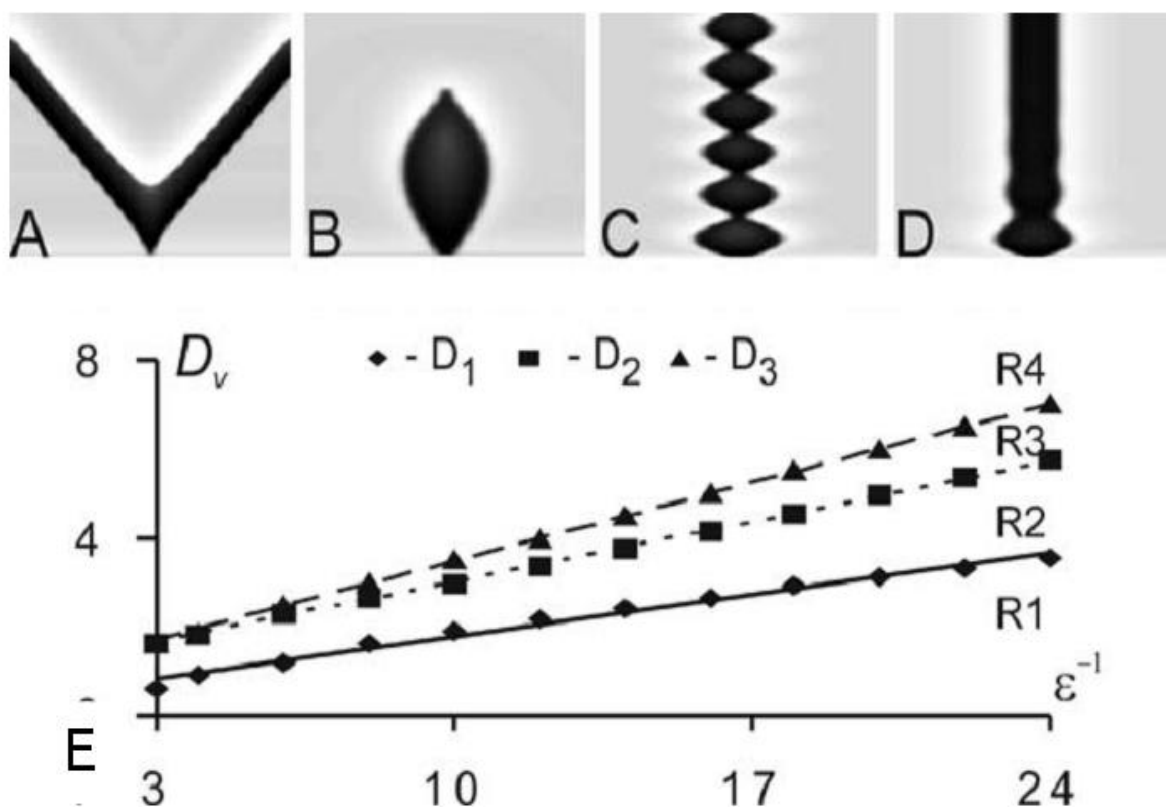
Figure 1.12: **Different 1-dimensional spatio-temporal patterns obtained from the solving of the scaled FHN equations according to the values of the parameters D and ε (Time: vertical axis and space: horizontal axis).** All patterns were stimulated at the middle of the medium. **A:** Unstable patterns and the medium returns to the homogeneous state. **B:** Pulsating spot. **C:** Stationary spots. **D:** Self-replicating waves. **E:** The location of the domains, R_1, R_2, R_3 and R_4 on the (ε^{-1}, D_v) plane. D_v is acting as the ratio of diffusions. D_1, D_2 and D_3 specify the bifurcation parameters. The domain R_1 corresponds to the region with propagating waves, R_2 corresponds to the region where one a domain where the patterns are unstable and the medium as a rule returns to the homogeneous state. R_3 corresponds to the domain where pulsating spots occur and R_4 corresponds to the domain where stationary spots arise [102].

30

1.8 Robustness of morphogen gradient

Mechanisms ensuring the robustness of dorso-ventral patterning in the Drosophila embryo against the changes in production rates (gene dosage) of involved proteins (BMP and Sog) have been studied both experimentally and theoretically in [28]. The analysis was based on detailed consideration of the dynamics of BMP, which is produced on the dorsal side of embryo, Sog, which is produced on the ventral side and inhibits BMP, and BMP/Sog complex which is highly diffusive. The decay of Sog is mediated by Tolloid (Tld) - another protein whose concentration is assumed to be constant. Interactions between these substances can be graphically represented by the following:

$$Sog + Scw \xleftrightarrow{k_b, k_{-b}} Sog - Scw,$$

$$Sog + Tld \xleftrightarrow{\alpha} Tld,$$

$$Sog - Scw + Tld \xleftrightarrow{\gamma} tld + Scw.$$
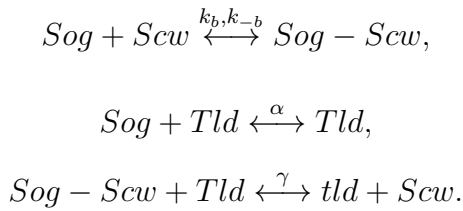
Scw is the morphogen of interest. Sog inhibits the action of Scw by forming the complex $Sog - Scw$. The protease Tld cleaves Sog [28].
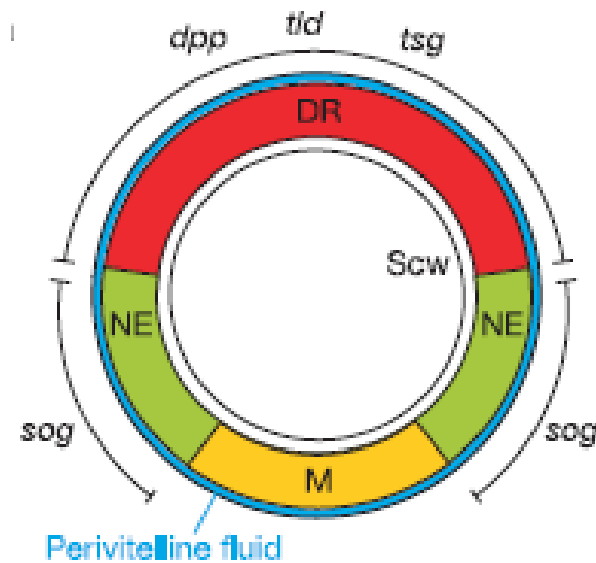
Figure 1.13: **Cross section of the Drosophila embryo.** DR means dorsal region, NE is Neuroectoderm (source of Sog) and M is mesoderm.

These lead to the three reaction-diffusion equations:

$$\frac{\partial[Scw]}{\partial t} = D_{BMP}\nabla^2[Scw] - k_b[Sog][Scw] + \lambda[Tld][Sog-Scw] + k_{-b}[Sog-Scw],$$

$$\frac{\partial[Sog]}{\partial t} = D_S\nabla^2[Sog] - k_b[Sog][Scw] + k_{-b}[Sog-Scw] - \alpha[Tld][Sog],$$

$$\frac{\partial[Sog-Scw]}{\partial t} = D_C[Sog-Scw] + k_b[Sog][Scw] - \lambda[Tld][Sog-Scw] - k_{-b}[Sog-Scw],$$

where D_{BMP}, D_S and D_C are respectively the diffusion rate constants for Sog, Scw and $Sog-Scw$ and k_b, k_{-b}, α and γ are reaction rate constants.

They found out that 0.3% of the systems were stable. In these systems they show changes of less than 10%. We have decided to reproduce their results using different values of boundary fluxes to see if robustness occurs. The left panel shows three profiles with three different values of boundary fluxes. All three profiles have different concentration inside the domain. So there is no robustness. The right panel shows two profiles with two different values of boundary fluxes. As we can see, the two profiles have the same concentration everywhere. So, one can say that we have robustness (see Figure 1.14). Therefore, in this model it was shown that high diffusion of the BMP/Sog complex enhances the dorso-ventral transportation of the BMP (the term used by authors is "shuttling"). Shuttling is obtained when the BMP ligand, binding with the inhibitor, Sog, diffuses. This binding also facilitates the decay of Sog. This mechanism has two advantages. First, it gives rise to a sharp gradient and second it allows robustness to fluctuation in gene dosage [8, 44]. A further modification of this model [11] with two additional equations describing the dynamics of BMP ligand $Admp$, which also forms a highly mobile complex with the BMP inhibitor, was used to demonstrate that a shuttling mechanism can also explain scaling of BMP gradient in Xenopus embryo.
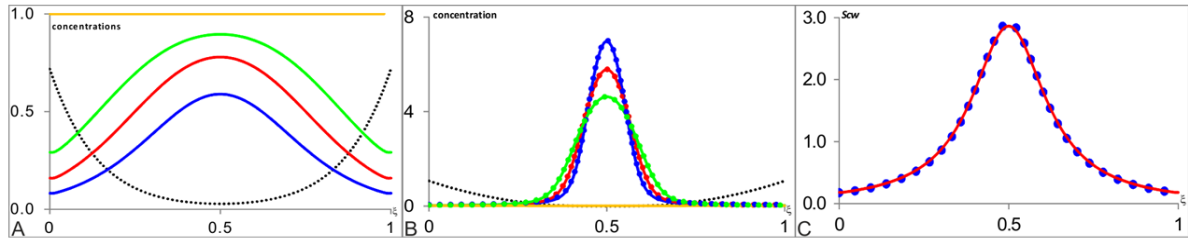
Figure 1.14: **Non-robust and robust profiles of proteins Screw (Scw) using different values of boundary fluxes. A:** *Non-robust profiles. The Sog profile is represented by the black dotted curve. The blue, red and green curves are three profiles of Scw with boundary fluxes values of 10, 5 and 2.5 respectively. And the yellow horizontal profile represents the sum Scw and its complex Scw-Sog. The values of the parameters are as follows: $D_S=1$, $D_{BMP}=D_C=0.01$, $k_b=10$, $k_{-b}=0.5$, $\lambda=2$ and $\alpha=10$.* **B:** *It is robust almost everywhere except when $\xi=0.5$. The values of the parameters are as follows: $D_S=1$, $D_{BMP}=0.01$, $D_C=10$, $k_b=120$, $k_{-b}=1$, $\lambda=200$ and $\alpha=1$. The Sog profiles is represented by the black dotted curve. The blue, red and green curves are three profiles of Scw with boundary fluxes values of 10, 5 and 2.5 respectively. The dotted blue, red and green profiles represents the sum of Scw and its complex. And the yellow horizontal profile represents the sum Scw and its complex.* **C:** *The values of the parameters are as follows: $D_S=1$, $D_{BMP}=10^{-5}$, $D_C=1$, $k_b=10$, $k_{-b}=1$, $\lambda=1000$ and $\alpha=1$. The boundary fluxes of the dotted blue and continuous red profiles are 10 and 5 respectively.*

1.9 Scaling of morphogen gradient

Scaling is a particular case of robustness. Scaling of morphogen gradients is the phenomenon which is persistently observed in experiments and represents one of the central problems in today's mathematical biology. Space-scaling would mean that the characteristic length of morphogen gradient is proportional to the size of the tissue (see Figure 1.15).
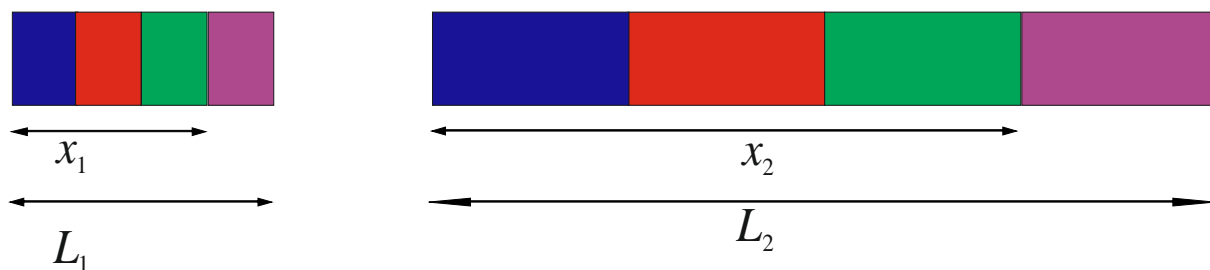
Figure 1.15: **Example of scaling with two patterns of different sizes.** *The ratio x/L of two similar points (x_1 and x_2) of the individual to their respective lengths (L_1 and L_2) remains the same. In this figure x_1 is the distance between the blue and green stripes for the individual of length L_1 and x_2 is the distance between the blue and green stripes for the individual of length L_2.*

There is scaling if for the individuals in the same species, the ratio between the location

of one characteristic point to the length of the individual remains unchanged if we change from an individual to another.

$$\frac{x_1}{L_1} = \frac{x_2}{L_2} = constant.$$

In general, if we call x the location of a characteristic and L the length of the individual, then we have $x/L = constant$ if we change from an individual to another.

$$\frac{x}{L} = constant.$$

We take the natural logarithm on both sides.

$$\ln x - \ln L = \ln\left(constant\right).$$

We take the derivative on both sides.

$$\frac{dx}{x} - \frac{dL}{L} = 0,$$

$$\frac{dx}{x} = \frac{dL}{L},$$
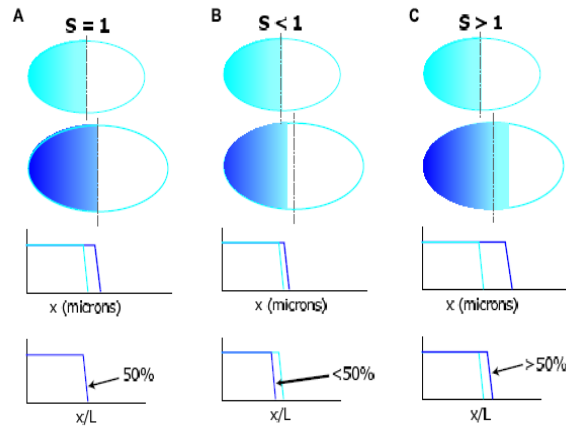
Figure 1.16: **Different scenarios associated with different values of the scaling factor S.** *In the first case S=1. The domain which spans 50% of a small embryo will also span 50% of the bigger embryo. In the case of S < 1, that is hypo-scaling, a domain which spans 50% of the smaller embryo will not expand enough in a bigger embryo. And in the case of hyper-scaling, S > 1, a domain which spans 50% of the smaller embryo will not expand too much in a bigger embryo [24].*

The above formula shows that the fluctuations in embryo length, dL/L, are exactly

compensated by fluctuations in position, dx/x, implying perfectly conserved proportions. In this case [23], considered that $S = 1$ corresponds to perfect scaling. When $S < 1$ and $S > 1$, they refer to the terms hypo- and hyper-scaling, respectively (see Figure 1.16). Hypo-scaling means that there is not enough compensation for a change in embryo size, meaning that in a bigger embryo the absolute position is not shifted enough posteriorward to keep the correct proportions. Hyper-scaling is the tendency to overcompensate for a change in embryo size [24].

$$S = \frac{dx}{dL}\frac{L}{x}.$$ (1.15)

Assuming that the threshold concentration is fixed (implying $dC = (\partial C/\partial x)dx + (\partial C/\partial L)dL = 0$), where C is the morphogen concentration and L is the embryo length), then it follows from equation (1.15) that the scaling coefficient is

$$S(x, L) = - \left(\frac{\partial c}{\partial x}\right)^{-1} \frac{\partial c}{\partial L}\frac{L}{x}.$$ (1.16)

1.9.1 Scaling in Annihilation model

Scaling of morphogen gradients can results from the non-linear interaction of involved morphogens. Assume that the scaling of the Bicoid gradient is possible. This is because the Bicoid and Caudal are expressed in the opposite sides of the embryo, mutually affecting their diffusion and/or degradation rate [52]. This is modelled as

$$\begin{aligned} \frac{\partial u}{\partial t} &= D_u\frac{\partial^2 u}{\partial x^2} - k_u uv, \\ \frac{\partial v}{\partial t} &= D_v\frac{\partial^2 v}{\partial x^2} - k_v uv. \end{aligned}$$ (1.17)

Here D_u and D_v are the diffusion coefficients and k_u and k_v specify the decay rates, D_u, D_v, k_u and k_v are constants. The boundary conditions are:

$$u(x = 0) = u_0, \qquad u(x = L) = u_L,$$

$$v(x = 0) = v_0, \qquad v(x = L) = v_L,$$

u_0 and v_0 are the boundary values at $x = 0$ and u_L and v_L are the boundary values at $x = L$. We shall focus on stationary state of equation (1.18).

$$\begin{aligned} D_u\frac{d^2 u}{dx^2} - k_u uv &= 0, \\ D_v\frac{d^2 v}{dx^2} - k_v uv &= 0. \end{aligned}$$ (1.18)

As it is shown in the appendix C, the relationships between variables u and v is given by the following:

$$k_v D_u u - k_u D_v v = \left(k_v D_u u_L - k_u D_v v_L - k_v D_u u_0 + k_u D_v v_0 \right) \left(\frac{x}{L} \right) + k_v D_u u_0 - k_u D_v v_0.$$

We want to simplify the system (1.11) by considering $D_u = D_v = D$, $k_u = k_v = k$, $u_L = v_0 = 0$ and $v_L = u_0$.

$$D \frac{d^2 u}{dx^2} - kuv = 0, \tag{1.19}$$

$$D \frac{d^2 v}{dx^2} - kuv = 0. \tag{1.20}$$

In this system D is the diffusion coefficient, k is the decay and u_0 is the boundary value. For quantitative analysis, we will consider the sum and the difference of the two morphogens. First, we shall add equations (1.19) and (1.20).

$$D \frac{d^2 (u + v)}{dx^2} - 2kuv = 0.. \tag{1.21}$$

Now, we subtract equation (1.21) from (1.19)

$$D \frac{d^2 (u - v)}{dx^2} = 0. \tag{1.22}$$

Let $s_+ = u + v$ and $s_- = u - v$. Then the equations (1.21) and (1.22), in terms of s_+ and s_-, will become

$$\frac{d^2 s_+}{dx^2} = \frac{2k}{D} uv,$$

$$\frac{d^2 s_-}{dx^2} = 0.$$

The solutions of s_+ and s_- are written as

$$s_- = u_0 \left(1 - 2\xi \right). \tag{1.23}$$

$$s_+ = \frac{8}{\lambda^2 L^2} \left(-1 + \sqrt{1 + \frac{u_0 \lambda^2 L^2}{4}} \right) + \frac{4}{\lambda^2 L^2} \left(-1 + \sqrt{1 + \frac{u_0 \lambda^2 L^2}{4}} \right)^2 (1 - 2\xi)^2 - \frac{\lambda^2 L^2 u_0^2}{96} (1 - 2\xi)^4. \tag{1.24}$$

The solution s_- (see (1.23)) is a function of the relative position x/L, $s_- = s_-(x/L)$ and therefore scales with the size of the medium. However, the solution s_+ (see (1.24)) does not scale since in addition to x/L it depends on the size, L, of the medium, $s_+ = s_+(x/L, L)$.

1.9.2 Scaling by an expansion-repression integral feedback control

Most models of patterning formation by morphogen gradients do not exhibit the scaling property. [10] show that the use of general feedback technology, in which the range of the morphogen gradient increases with the abundance of some molecule, whose production, in turn, is repressed by morphogen signalling. The derivation of their model is reproduced here for sake of clarity. It uses a single morphogen M secreted from a local source and diffuses in a naïve field of cells to establish a concentration gradient that peaks at the source. The distribution of this morphogen is governed by

$$
\begin{aligned}
\frac{\partial [M]}{\partial t} &= D_M \nabla^2 [M] - \frac{\alpha_M}{1 + [E]}[M], \\
\frac{\partial [E]}{\partial t} &= D_E \nabla^2 [E] - \alpha_E [E] + \frac{\beta_E}{1 + ([M]/T_0)^h},
\end{aligned}
$$

where D_M and D_E are the diffusion coefficients of M and E respectively, M and E are the degradation rates of M and E respectively, E is the production rate of E, h is the hill coefficient and T_0 is the threshold concentration.
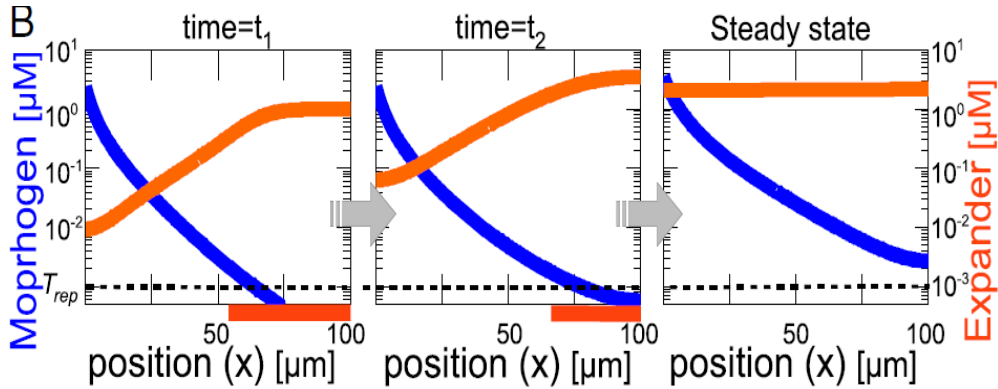
Figure 1.17: **Dynamics of the expansion-repression mechanism.** *Initially, the morphogen and the expander diffuse from opposite ends. The morphogen repressed the expression of the expander when its level is above the threshold reference T_{rep}. The expander which is diffusible and stable expands the morphogen gradient by increasing the diffusion and/or reducing the degradation rate. At a later time, the expander accumulates, the gradient of the morphogen expands and the production domain of the expander shrinks. At steady state, the expander has accumulated and the gradient of the morphogen is wide enough to repress the production of the expender everywhere [10].*

It can be shown that the morphogen profile $M(x)$ can be written as

$$
M(x) = M(x/L, \rho),
$$

37

where L is the size of the medium and ρ the morphogen production rate. This dependency of the morphogen profile $M(x)$ to the ratio x/L shows the scaling property of the expansion-repression model. Perfect scaling occurs if the profile M is insensitive to ρ. However, it has been noticed that this dependency is typically small [10]. This model is not particularly good because the authors did not specify the natures of the morphogen M and E. Hence, the relationship between them is highly speculative. And furthermore, the expander, which is the red profile shown in Figure 1.17, takes too long to reach the steady-state. Our simulations of this model confirm this tendency; it takes about 10^7 time steps to observe levelling of the morphogen in the medium using this model. In the next chapter, we show that we can have scaling with only one assumption.

1.10 Concentration dependent diffusion and scaling of morphogens gradients

In all of the previous reaction-diffusion models of pattern formation, the diffusion and the degradation rates of the morphogens were assumed to be constant. Hence, starting from the reaction-diffusion equation

$$\frac{\partial m}{\partial t} = D_m \frac{\partial^2 m}{\partial x^2} - k_m m,$$

where D_m and k_m are respectively the diffusion and the reaction rates of the morphogen m [97]. have shown that the conditions to achieve scale invariance throughout the domain are that the quantities $q/\sqrt{k_m D_m}$ and $k_m L^2/D_m$ must be independent of the length L. In the first quantity, q represents the input flux of the morphogen m. The second quantity constitutes the ratio between the diffusion time scale L^2/D_m and the reaction time scale $1/k_m$. The second quantity implies that scale invariant distribution of morphogen can be achieved by controlling the time scales of the diffusion and reaction. If each of the parameters D_m, k_m and q vary with L according to a power law, for instance $D_m \sim L^a$ where a is a power, then it can be established all possible ways of parameter variation that lead to global scale invariance.

The above results are valid for a system containing other species in the patterning scheme. A scaling factor for all diffusion coefficients and a scaling factor for all reactions must be identified if the pattern of all species is to be scale invariant.

In order to assess how the change of the diffusion rate with the morphogen concentration affect the scaling property of the morphogens gradient, different models involving

a modulator which is used to adjust the characteristic times scales of diffusion and/or reaction in a size-dependent manner have been introduced [95, 97]. The reaction diffusion equations involving the morphogen m and the modulator M are given by

$$\frac{\partial m}{\partial t} = \nabla \cdot (D_m(M)\nabla(m)) + k(M)R_m(m, M),$$
$$\frac{\partial M}{\partial t} = D_M\nabla^2 M + R_m(m, M).$$

The first equation describes the morphogen transport which includes modulation of diffusion and reaction terms by M. The second provides the balance equation of the modulator M which diffusion rate D_M may or may not be regulated by the morphogen. It has been shown that if the modulator hinders diffusion and/or enhances reaction rates, then scaling can be ensured if M decreases in proportion to the tissue size by an appropriate amount (Table 1.1). For instance, the diffusion and reaction rates are given respectively by $D_m(M) = D_m/(1 + \alpha_1 M)$ and $k(M) = k(1 + \alpha_2 M)$. The general requirements to ensure scaling by modulation of $D_m(M)$ and $k(M)$ are summarised in the table below

Description	α_1	α_2	$D_m(M)$	$k(M)$	M
Enhancer	0	> 0	$constant$	$\sim M$	L^{-2}
Immobiliser	> 0	0	$\sim M^{-1}$	$constant$	L^{-1}
Combination	> 0	> 0	$\sim M^{-1}$	M	L^{-1}

Table 1.1: **Enhancer/Immobiliser.**

Alternatively, if the modulator enhances diffusion and/or hinders reaction rates, then scaling can be ensured if M increases in proportion to the tissue size by an appropriate amount (Table 1.2). For instance, the diffusion and reaction rates are given respectively by $D_m(M) = D_m(1 + \alpha_1 M)$ and $k(M) = k/(1 + \alpha_2 M)$. The general requirements to ensure scaling by modulation of $D_m(M)$ and $k(M)$ are summarised in the table below

Description	α_1	α_2	$D_m(M)$	$k(M)$	M
Inhibitor	0	> 0	$constant$	$\sim M^{-1}$	L^2
Immobiliser	> 0	0	$\sim M$	$\sim M$	L^1
Combination	> 0	> 0	$\sim M$	$\sim M$	L^1

Table 1.2: **Inhibitor/Mobiliser.**

Chapter 2

Scaling in continuous models

In the previous chapter, we have pointed out that biological patterns are commonly scaling with the size of biological objects. We saw a few mathematical models and discussed scaling properties of their solutions. Particularly, we have pointed out that the exponential profiles appearing as solutions of diffusion/decay models do not scale. The aim of this chapter is to incorporate modifications into the model such that its solution scales. A new quantity called "scaling factor" will be introduced to measure scaling properties of morphogen gradients occurring as solutions of mathematical models.

The structure of this chapter is as follows. In section 2.1, we discuss robustness. Then in section 2.2, we deal with a particular case of robustness that is scaling. In this section, we also introduce our definition of the scaling factor. This is follows by a couple of examples. In section 2.3, we analyse the scaling properties of the one-variable model with all the types of boundary conditions. Next, we introduce two mechanisms of scaling of the exponential model in sections 2.4 and 2.5. In section 2.6, we deal with the annihilation model. In section 2.7, we discuss about the nuclear trapping model. And we finish with scaling of the active transport in section 2.8.

2.1 Defining robustness factor

An important aspect of development is robustness. Robustness is the ability of such gradients to resist change in the face of genetic and environmental perturbations. In terms of concentration profiles of morphogens, we can introduce the factor measuring the robustness based on the relocation of the point in the following way. Suppose we change a parameter from p to $p+\Delta p$ then this point shifts from x to $x+\Delta x$. To illustrate this, let's assume that the morphogen profile depends on a certain parameter p and consider two morphogen profiles corresponding to different values of the parameter (see Figure 2.1).
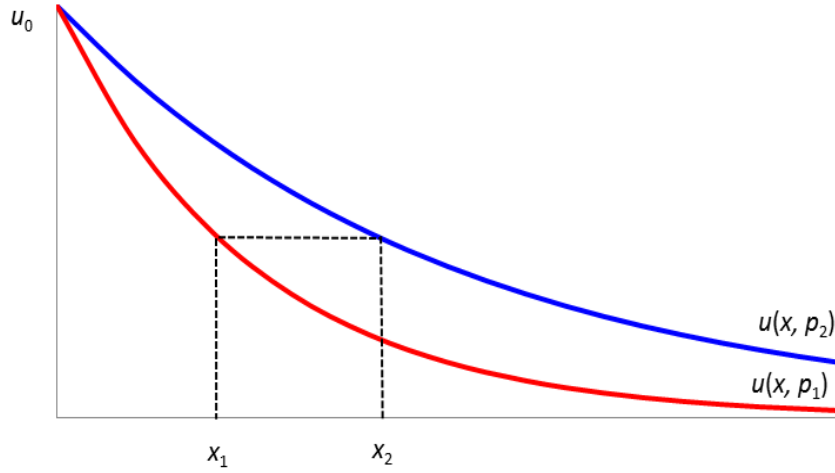
Figure 2.1: **On introduction of robustness factor.** *Hypothetical morphogene profiles for two different values of parameter p are used as an illustration.*

Figure 2.1 shows that the blue profiles is $u(x, 1)$ and the red curve $u(x, 2)$. If $u = u_0$ is a threshold for cell differentiation, then the boundary of differentiated cells domain will shift by Δx. Δx therefore describes robustness of the system (left panel). We have developed a formula for robustness.

Definition. The profile is robust across the two objects if

$$u(x, p_1) = u(x, p_2) \quad for \quad a \quad point \quad x.$$

Generally, this is not true and from $u(x_1, p_1) = u(x_2, p_2)$, it doesn't follow that $x_1 = x_2$. For this case, we can introduce the scaling factor in the following way. Assume that $u(x_1, p_1) = u(x_2, p_2)$. Then, for small variations in p and in x, we can write:

$$u(x_2, p_2) = u(x_1, p_1) + u'_x (x_2 - x_1) + u'_p (p_2 - p_1)$$

$$u'_x (x_2 - x_1) + u'_p (p_2 - p_1) = 0.$$

From the above formula, the relocation of the level point is given as:

$$x_2 - x_1 = -\frac{u'_p}{u'_x} (p_2 - p_1),$$

i.e. the deformation of the profile is proportional to the parameter p of the system with

41

the coefficient of proportionality representing robustness factor:

$$R = -\left(\frac{\partial u}{\partial p}\right)\left(\frac{\partial u}{\partial x}\right)^{-1}.$$

The above formula depends on parameter p and x. The robustness factor R tells us how much shift there is at any point x. If there is no shift at point x, then we say that $R = 0$. This means that we have good robustness. We shall apply the above formula to two examples. The first example, we consider, is for two exponential profiles of u in the form of e^{-px}. In order to determine the robustness factor R, we need to differentiate u with respect to p and x.

$$u'_p = -xe^{px},$$
$$u'_x = -pe^{px}.$$

And, we apply the ratio between u'_p and u'_x.

$$R(x, p) = -\frac{x}{p}. \tag{2.1}$$

The plot of (2.1) is shown in Figure 2.2.
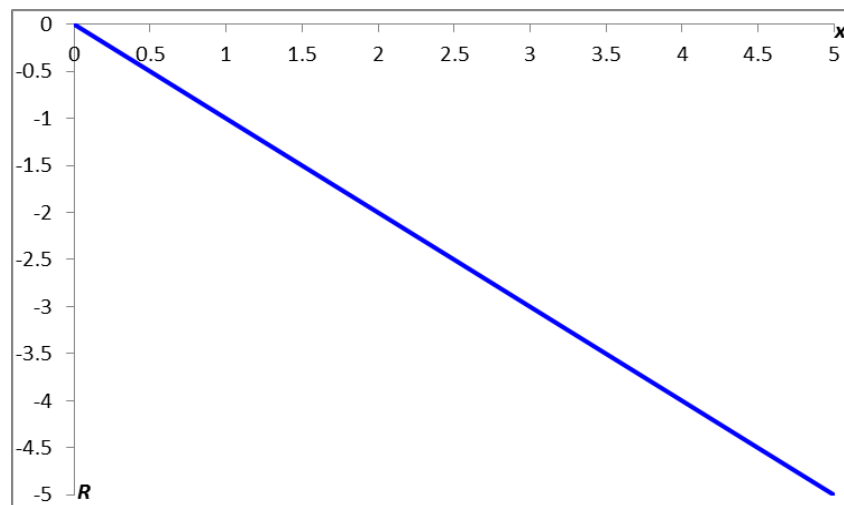
Figure 2.2: **Plot of the robustness factor for the blue exponential profile in Figure 2.1.** *As we can see, the robustness factor gives us a straight profile. This confirms the analytical derivation. We see that at x=0, the robustness factor is 0.*

As second example, we consider the calculation of the robustness factor R for the case of

two quadratic profiles of u. For a quadratic profile, the equation is written as

$$u(x, p) = px(x - 4) + 4 = px^2 - 4px + 4. \tag{2.2}$$

The derivatives of u with respect to x and p are respectively.

$$
\begin{aligned}
u'_p &= x^2 - 4x, \\
u'_x &= 2px - 4p.
\end{aligned}
$$

The robustness factor R is

$$R(x, p) = \frac{x^2 - 4x}{2px - 4p}. \tag{2.3}$$

The above formula shows that at $x = 0$ and $x = 4$, $R = 0$ which means that we have good robustness. The plots of (2.2) and (2.3) are shown in Figure 2.3.
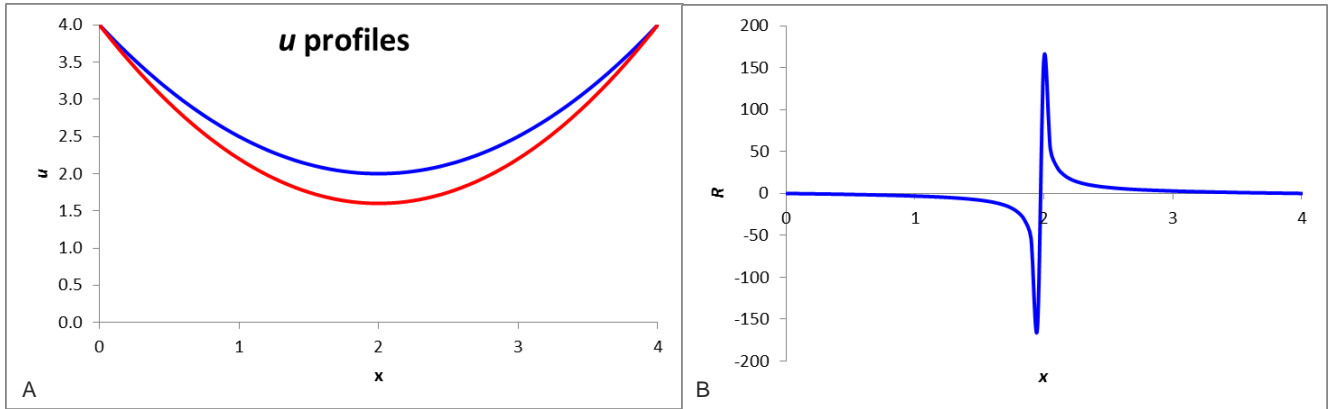
Figure 2.3: **Two quadratic profiles u=px(x-4)+4 for different values of p and plot of the robustness factor for the quadratic profiles of u. A:** p_1=0.5 is the u concentration for the blue profile and p_2=0.6 is the u concentration for the red profile. **B:** The robustness factor is 0 at the end since both profiles have the same concentration. In the middle, the scaling factor is not defined. This is because in panel **A**, the derivative of u-profile at this point is zero.

2.2 Defining Scaling factor

In order to analyse scaling properties of morphogenetic gradients, we need to introduce a formal definition of scaling. For this purpose, let us consider a morphogenetic profile occurring in two objects of different sizes, L_1 and L_2. These profiles can be described by functions $u(\xi, L_1)$ and $u(\xi, L_2)$ where $\xi = x/L$ represents a coordinate in the range $[0, 1]$ for both objects (see Figure 2.4).
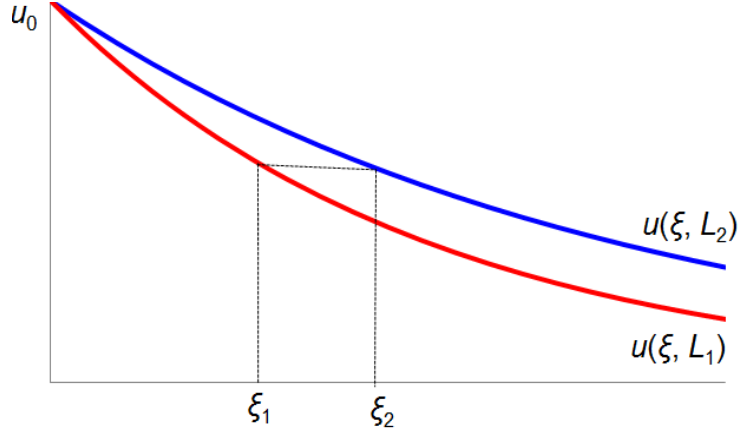
Figure 2.4: **On introduction of scaling factor.** *Sample morphogen profiles for different medium sizes (L_1 and L_2) are presented as functions of relative position ($\xi = x/L$).*

Definition: The profile is scaled across the two objects if

$$u\left(\xi_1, L_1\right) = u\left(\xi_2, L_2\right) \quad for \quad a \quad point \quad \xi.$$

Generally, this is not true and from $u\left(\xi_1, L_1\right) = u\left(\xi_2, L_2\right)$, it doesn't follow that $\xi_1 = \xi_2$. For this case we can introduce the scaling factor in the following way. Assume that $u\left(\xi_1, L_1\right) = u\left(\xi_2, L_2\right)$. Then, for small variations in L and in ξ, we can write:

$$u\left(\xi_2, L_2\right) = u\left(\xi_1, L_1\right) + u'_\xi\left(\xi_2 - \xi_1\right) + u'_L\left(L_2 - L_1\right),$$

$$u'_\xi\left(\xi_2 - \xi_1\right) + u'_L\left(L_2 - L_1\right) = 0.$$

From the above formula, the relocation of the level point is given as:

$$\xi_2 - \xi_1 = -\frac{u'_L}{u'_\xi}\left(L_2 - L_1\right),$$

i.e. the deformation of the profile is proportional to the change in the size of the system with the coefficient of proportionality representing scaling factor:

$$S = -\left(\frac{\partial u}{\partial L}\right)\left(\frac{\partial u}{\partial \xi}\right)^{-1}. \tag{2.4}$$

Thus the scaling factor S is a function of the length of the medium L and the relative position ξ. Our definition of scaling factor is different from the one given by [23](formula 1.16) since it depends on x. Since ξ is between 0 and 1, we are working on dimensionless value. The scaling factor S (see (2.4)) tells us how much shift there is at any point ξ.

If there is no shift at point ξ, then we say that $S = 0$. This means that we have good scaling. This formula is important because if during the development, the proportionality is not maintained then the organism will be deformed. We will use this formula for this and next chapter. Now, we consider a couple of examples of which profiles scale and which do not.

Case 1: Linear profile

Assume that we have a linear profile u which is described by the French Flag model in the form $u = Ax + B$ where A and B are constants to be determined. The Dirichlet boundary conditions are $u(0) = u_0$ and $u(L) = u_L$ with L the size of the tissue. The full solution is given by

$$u = u_0 + (u_L - u_0)\frac{x}{L}, \tag{2.5}$$

with $A = (u_L - u_0)/L$ and $B = u_0$. For the case of a slightly bigger medium size, $L + \Delta L$, the profile will have the same form $u = Ax + B$. The Dirichlet boundary conditions now will take a form: $u(0) = u_0$ and $u(L + \Delta L) = u_L$. The full solution for this case is written as

$$u = u_0 + (u_L - u_0)\frac{x}{L + \Delta L}. \tag{2.6}$$

As we can see, the coefficient B is equal to u_0 for both cases but for the medium of larger size the coefficient A is smaller than for the medium of smaller size. For the case of solution (2.5), we can replace x/L by ξ. But for the case of solution (2.6), we should replace $x/(L + \Delta L)$ by ξ. Therefore, the solutions (2.5) and (2.6) in terms of ξ are written as

$$u = u_0 + (u_L - u_0)\xi.$$

The above solution is independent of L. The scaling factor for this solution calculated according to the formula (2.4) shows that the scaling factor is 0 for all locations and all medium sizes. This shows that we have perfect scaling.

Case 2: Exponential profile

Let's consider and exponential profile which has an equation of the form $u = e^{-kx} = e^{-k\xi L}$. We apply the formula for the scaling factor. First, we differentiate u with respect to L.

$$u'_L = -k\xi e^{-k\xi L}.$$

And then, we differentiate u with respect to ξ.

$$u'_\xi = -kLe^{-k\xi L}.$$

The calculation of the scaling factor gives

$$S = -\frac{\xi}{L}. \tag{2.7}$$

The above formula shows that at $\xi = 0$, we have good scaling. We can also have good scaling as L gets bigger. The plot of (2.7) for the case of $L = 1$ is shown in Figure 2.7.
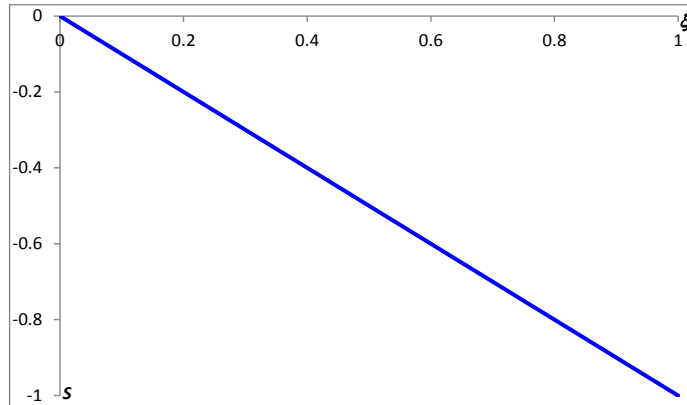
Figure 2.5: **Scaling factor for the exponential profile** $u = e^{-\xi}$. *The scaling factor is 0 at $\xi=0$ meaning that we have good scaling. As ξ increases, the scaling factor decreases.*

2.3   Scaling in one-variable model

The body plan of the fly embryo along the anterior-posterior axis is determined by a cascade of regulatory events. Maternal mRNA (messenger Ribonucleic acid) such as bicoid is required for early patterning. It is located at the anterior pole ($x = 0$). Once synthesized, the Bicoid protein diffuses posteriorly forming a protein gradient exponentially. This phenomenon can be illustrated by the single gradient model (see (1.1)) [64, 80]. We want to investigate the scaling properties of this model. Let u be the concentration of the morphogen which obeys the stationary equation of (1.1)(see (2.8)).

$$D_u \frac{d^2u}{dx^2} - k_u u = 0. \tag{2.8}$$

Here D_u is the diffusion coefficient and k_u is the degradation rate. Both D_u and k_u are constants. The features of the solution including its scaling strongly depend on the boundary conditions. Regarding this, let us consider a few different cases:

Case A: We have the Dirichlet boundary conditions at both ends

$$u(x = 0) = u_0, \qquad u(x = L) = u_L,$$

where u_0 and u_L are the boundary values at $x = 0$ and $x = L$ respectively. The stationary solution of u of equation (2.8) is

$$u = \frac{\left(u_L - u_0 e^{-L\lambda}\right) e^{x\lambda} + \left(u_0 e^{L\lambda} - u_L\right) e^{-x\lambda}}{e^{L\lambda} + e^{-L\lambda}},$$

with $\lambda = \sqrt{k_u/D_u}$. We shall rewrite the solution of u as a function of ξ in order to determine the scaling factor.

$$u = \frac{u_L e^{\xi L\lambda} - u_0 e^{L\lambda(\xi-1)} + u_0 e^{L\lambda(1-\xi)} - u_L e^{-\xi L\lambda}}{e^{L\lambda} + e^{-L\lambda}}. \tag{2.9}$$

The formula of the scaling factor is too long for the general case. We have decided to take some representative values of u_0 and u_L for example $u_0 = 1$ and $u_L = 0$. The expression of the scaling factor with these values is defined as

$$S = -\frac{(\xi - 2)\left(e^{\xi L} - e^{-\xi L}\right) + \xi\left(e^{-L(\xi-2)} - e^{L(\xi-2)}\right)}{L\left(e^L - e^{-L}\right)\left(e^{L(\xi-1)} + e^{-L(\xi-1)}\right)}. \tag{2.10}$$

This formula shows that S is a function of both L and ξ. The plots of (2.9) and (2.10) are shown in Figure 2.6.
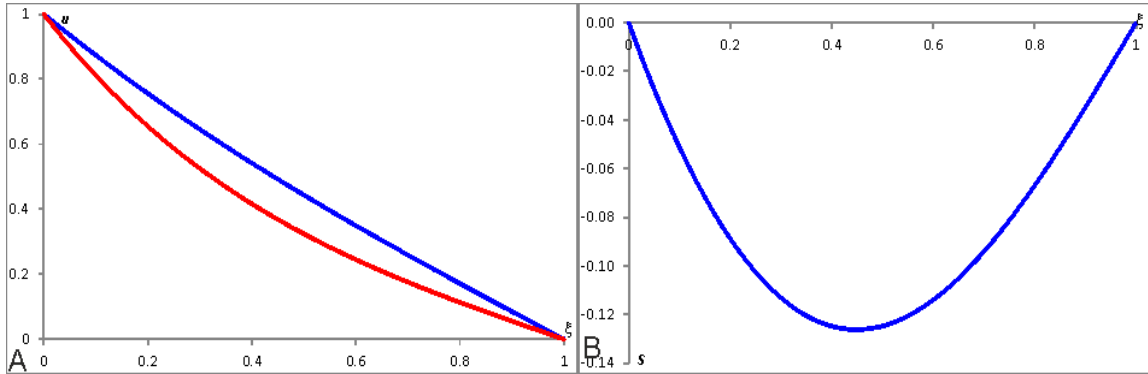
Figure 2.6: **Plots of profiles for L=1 and L=2, and the scaling factor for L=1. A:** *The blue and red profiles represent for L=1 and L=2 respectively. We use k_u=D_u=1 to give λ=1.* **B:** *We see that the scaling factor at ξ=0 and ξ=1 is zero. This is because the two profile in panel* **A** *have the same concentration at these two points. Elsewhere, the scaling factor is negative since the blue red profile is below the blue profile.*

Case B: So far, we had Dirichlet boundary conditions at both ends ($x = 0$ and $x = L$). Now, one can have Dirichlet boundary condition at $x = 0$ and Neumann boundary condition at $x = L$ or vice versa. This is known as mixed boundary conditions. We consider equation (2.8) with the following boundary conditions: Neumann boundary condition at $x = 0$, $u'(x = 0) = -j_0$ and Dirichlet boundary condition at $x = L$, $u(x = L) = u_L$ is

$$u = \frac{\left(\lambda u_L + j_0 e^{-L\lambda}\right) e^{x\lambda} + \left(\lambda u_L + j_0 e^{L\lambda}\right) e^{-x\lambda}}{\lambda \left(e^{L\lambda} + e^{-L\lambda}\right)},$$

where j_0 is the boundary flux at $x = 0$, u_L is the boundary value at $x = L$ and $\lambda = \sqrt{k_u/D_u}$. We shall rewrite the solution of u as a function of ξ in order to compute the scaling factor.

$$u = \frac{\left(\lambda u_L + j_0 e^{-L\lambda}\right) e^{L\xi\lambda} + \left(\lambda u_L + j_0 e^{L\lambda}\right) e^{-L\xi\lambda}}{\lambda \left(e^{L\lambda} + e^{-L\lambda}\right)}. \tag{2.11}$$

The formula of the scaling factor will be too long for the general case. Therefore, we have decided two subcases:

Case B$_1$: For the first case, we choose $j_0 = 0$ and $u_L = 1$. Therefore, the scaling factor with these values is written as

$$S = -\frac{(\xi - 1)\left(e^{L(1+\xi)} - e^{-L(1+\xi)}\right) + (\xi + 1)\left(e^{L(\xi-1)} - e^{L(1-\xi)}\right)}{L\left(e^L + e^{-L}\right)\left(e^{L\xi} + e^{-L\xi}\right)} \tag{2.12}$$

This formula shows that S is a function of both L and ξ. The plots of (2.11) and (2.12) are shown in Figure 2.7.
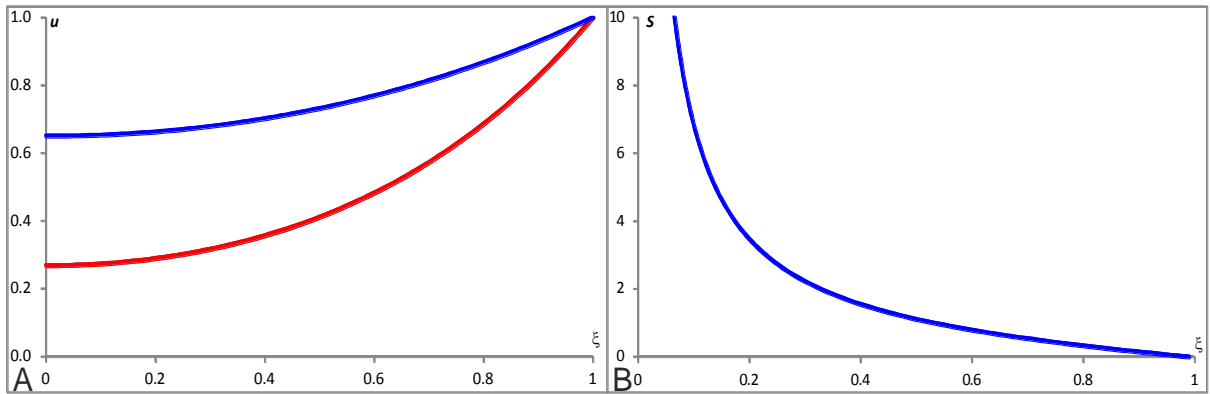
*Figure 2.7: **Plots of profiles for L=1 and L=2 and the scaling factor for L=1. A:** The blue and red profiles represent for L=1 and L=2 respectively. We use k_u=D_u=1 to give λ=1. **B:** At ξ=0, the scaling factor is at infinity. As ξ increases, the scaling factor decreases fast. This is because the two profiles are getting closer to each other. The scaling factor at ξ=1 is zero since the two profiles, in panel **A**, end up with the same initial concentration.*

Case B$_2$: For the second case, we take $j_0 = 1$ and $u_L = 0$. The scaling factor formula with these values of j_0 and u_L is given as

$$S = -\frac{(\xi - 2)\left(e^{\xi L} - e^{-\xi L}\right) + \xi\left(e^{L(\xi-2)} + e^{-L(\xi-2)}\right)}{L\left(e^L - e^{-L}\right)\left(e^{L(\xi-1)} + e^{-L(\xi-1)}\right)}. \tag{2.13}$$

The plots of (2.11) and (2.13) are shown in Figure 2.8.
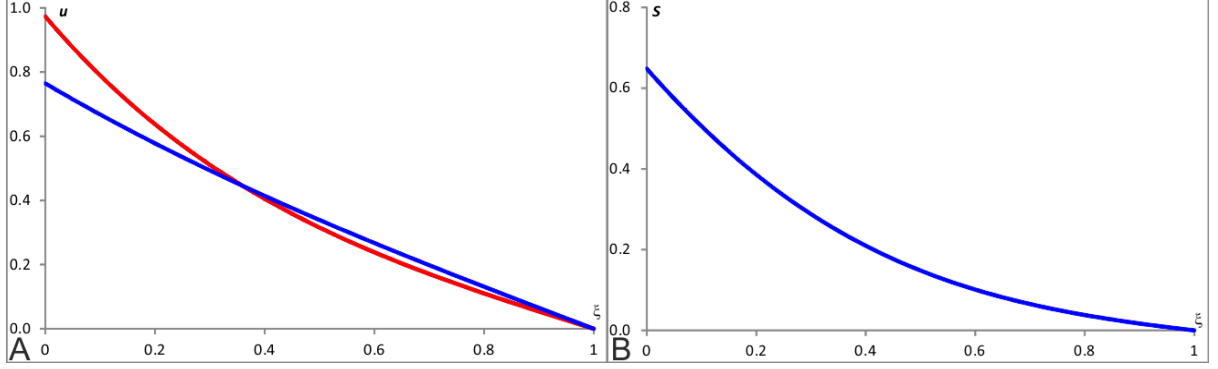
Figure 2.8: **Plots of profiles for L=1 and L=2, and the scaling factor for L=1. A:** *The blue and red profiles represent for L=1 and L=2 respectively. We use $k_u=D_u=1$ to give $\lambda=1$.* **B:** *As ξ increases, the scaling factor gets smaller.*

Case C: From **Case A**, we had Dirichlet boundary condition at both ends and from **Case B**, we had mixed boundary conditions. From the latter case, we didn't consider the second type of mixed boundary condition (Dirichlet boundary condition at $x = 0$ and Neumann boundary condition at $x = L$) because the profiles with this type of boundary condition will be symmetric compared in Figure 2.7 and Figure 2.8. One can consider the Neumann boundary condition at both $x = 0$, $(u'(x = 0) = j_0)$ and $x = L$, $(u'(x = L) = j_L)$. The solution of u with the Neumann boundary condition is written as

$$u = \frac{\left(j_L - j_0 e^{-L\lambda}\right)e^{x\lambda} + \left(j_L - j_0 e^{L\lambda}\right)e^{-x\lambda}}{\lambda\left(e^{L\lambda} - e^{-L\lambda}\right)},$$

where j_0 and j_L are the boundary fluxes at $x = 0$ and $x = L$ respectively and $\lambda = \sqrt{k_u/D_u}$. We shall rewrite the solution of u as a function of ξ in order to compute the scaling factor.

$$u = \frac{\left(j_L - j_0 e^{-L\lambda}\right)e^{L\xi\lambda} + \left(j_L - j_0 e^{L\lambda}\right)e^{-L\xi\lambda}}{\lambda\left(e^{L\lambda} - e^{-L\lambda}\right)}. \tag{2.14}$$

The formula of the scaling factor will be too long for the general case. We choose $j_0 = -1$

and $j_L = 0$. Therefore the scaling factor with these values is written as

$$S = -\frac{(\xi - 2)\left(e^{\xi L} + e^{-\xi L}\right) - \xi\left(e^{L(\xi-2)} + e^{-L(\xi-2)}\right)}{L\left(e^L - e^{-L}\right)\left(e^{L(\xi-1)} - e^{-L(\xi-1)}\right)}. \tag{2.15}$$

This formula shows that S is a function of both L and ξ.The plots of (2.14) and (2.15) are shown in Figure 2.9.
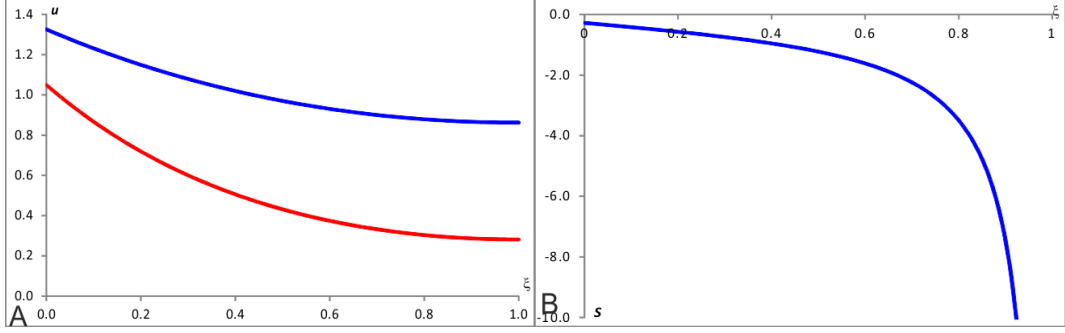
Figure 2.9: **Plots of profiles for L=1 and L=2, and the scaling factor for L=1. A:** *The blue and red profiles represent for L=1 and L=2 respectively. We use $k_u=D_u=1$ to give $\lambda=1$.* **B:** *The scaling factor at $\xi=0$ is zero since the two profiles, in panel* **A**, *start with the same initial concentration. Elsewhere the scaling factor is negative since the red profile is below the blue profile. As ξ increases, the scaling factor decreases fast. This is because the two profiles are getting away from each other. Furthermore, the scaling factor tends to $-\infty$ at $\xi=1$ since the denominator of S is 0.*

2.3.1 Effect of λ for the Dirichlet boundary condition

Previously, we have investigated scaling for all boundary conditions. We see that in Figure 2.6 to Figure 2.9, the exponential profiles and their scaling factor depends on the values of L and λ. Now, we will investigate the effect of λ for scaling properties of exponential profiles under the Dirichlet boundary condition. Let's use the same values of u_0 and u_L. The scaling factor S is given as follows.

$$S = -\frac{(\xi - 2)\left(e^{L\lambda\xi} - e^{-L\lambda\xi}\right) + \xi\left(e^{-L\lambda(\xi-2)} - e^{L\lambda(\xi-2)}\right)}{L\left(e^{L\lambda} - e^{-L\lambda}\right)\left(e^{L\lambda(\xi-1)} + e^{-L\lambda(\xi-1)}\right)}, \tag{2.16}$$

where $\xi = x/L$. Assume that $\lambda \ll 1$ meaning that $k_u \ll D_u$. Then, the first order of the Taylor expansions of the exponentials gives

$$e^{\xi L\lambda} \approx 1 + \xi L\lambda,$$

$$e^{-\xi L\lambda} \approx 1 - \xi L\lambda,$$

$$e^{L\lambda(-2+\xi)} \approx 1 + L\lambda(-2+\xi) = 1 + L\lambda\xi - 2L\lambda,$$

$$e^{-L\lambda(-2+\xi)} \approx 1 - L\lambda(-2+\xi) = 1 - L\lambda\xi + 2L\lambda,$$

$$e^{L\lambda} \approx 1 + L\lambda,$$

$$e^{-L\lambda} \approx 1 - L\lambda,$$

$$e^{L\lambda(-1+\xi)} \approx 1 + L\lambda(-1+\xi) = 1 + L\lambda\xi - L\lambda,$$

$$e^{-L\lambda(-1+\xi)} \approx 1 - L\lambda(-1+\xi) = 1 - L\lambda\xi + L\lambda,$$

By substituting these approximations into the scaling solution S (2.16), we obtain

$$S \approx -\frac{(\xi-2)\left(1+L\xi\lambda-1+L\xi\lambda\right)+\xi\left(1-L\xi\lambda+2L\lambda-1-L\lambda\xi+2L\lambda\right)}{L\left(1+L\lambda-1-(1-L\lambda)\right)\left(1+L\lambda\xi-L\lambda+1-L\lambda\xi+L\lambda\right)},$$

$$\approx -\frac{2L\xi\lambda\left(\xi-2\right)+\xi\left(-2L\xi\lambda+4L\lambda\right)}{L\left(1+L\lambda-1-(1-L\lambda)\right)\left(1+L\lambda\xi-L\lambda+1-L\lambda\xi+L\lambda\right)},$$

$$\approx -\frac{2L\xi^2\lambda-4L\lambda\xi-2L\xi^2\lambda+4L\lambda\xi}{L\left(1+L\lambda-1-(1-L\lambda)\right)\left(1+L\lambda\xi-L\lambda+1-L\lambda\xi+L\lambda\right)},$$

Therefore

$$S \approx 0.$$

We end up with $S \approx 0$ which implies that we have perfect scaling. The plot with three different values of λ is shown in Figure 2.10.
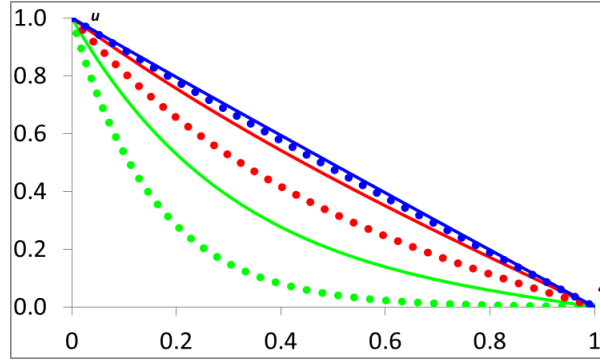
Figure 2.10: **Plots of $u-$ profiles for two different medium sizes and three values of** λ. *The continuous and dotted profiles stand for L=1 and L=2 respectively. The green, red and blue curves are plotted for λ=10, 1 and 0.1. As λ gets smaller, the two profiles get closer to each other. Therefore, the scaling factor tends to zero. This is getting closer to the French Flag model since in this model, there is no degradation term (see Figure 1.8).*

2.3.2 Effect of λ for the Neumann boundary condition

Previously, we saw that we had perfect scaling if the degradation rate k_u is much smaller than the diffusion rate D_u for the case of Dirichlet boundary condition. Now, we shall

analyze the scaling properties of exponential profile under the Neumann boundary condition. Let's use the same values of j_0 and j_L. The formula of the scaling factor including λ is written as

$$S = -\frac{(\xi - 2)\left(e^{\xi L\lambda} + e^{-\xi L\lambda}\right) - \xi\left(e^{L\lambda(\xi-2)} + e^{-L\lambda(\xi-2)}\right)}{L\left(e^{L\lambda} - e^{-L\lambda}\right)\left(e^{L\lambda(\xi-1)} - e^{-L\lambda(\xi-1)}\right)}, \tag{2.17}$$

where $\xi = x/L$. First, we assume that $\lambda \ll 1$. Then, the first order of the Taylor expansions of the exponentials gives

$$e^{\xi L\lambda} \approx 1 + \xi L\lambda,$$

$$e^{-\xi L\lambda} \approx 1 - \xi L\lambda,$$

$$e^{L\lambda(-2+\xi)} \approx 1 + L\lambda(-2 + \xi) = 1 + L\lambda\xi - 2L\lambda,$$

$$e^{-L\lambda(-2+\xi)} \approx 1 - L\lambda(-2 + \xi) = 1 - L\lambda\xi + 2L\lambda,$$

$$e^{L\lambda} \approx 1 + L\lambda,$$

$$e^{-L\lambda} \approx 1 - L\lambda,$$

$$e^{L\lambda(-1+\xi)} \approx 1 + L\lambda(-1 + \xi) = 1 + L\lambda\xi - L\lambda,$$

$$e^{-L\lambda(-1+\xi)} \approx 1 - L\lambda(-1 + \xi) = 1 - L\lambda\xi + L\lambda.$$

The numerator of (2.17) can be approximated as

$$(\xi - 2)\left(e^{\xi L\lambda} + e^{-\xi L\lambda}\right) - \xi\left(e^{L\lambda(\xi-2)} + e^{-L\lambda(\xi-2)}\right) \approx (\xi - 2)\left(1 + L\xi\lambda + 1 - L\xi\lambda\right) - \xi\left(1 + L\xi\lambda - 2L\lambda + 1 - L\xi\lambda + 2L\lambda\right)$$

$$= -4.$$

The denominator of (2.17) can be approximated as

$$L\left(e^{L\lambda} - e^{-L\lambda}\right)\left(e^{L\lambda(\xi-1)} - e^{-L\lambda(\xi-1)}\right) \approx L\left(1 + L\lambda - (1 - L\lambda)\right)\left(1 + L\lambda(\xi - 1) - (1 - L\lambda(\xi - 1))\right)$$

$$= 4L^3\lambda^2(\xi - 1).$$

The scaling factor S can be approximated as

$$S \approx \frac{1}{L^3\lambda^2(\xi - 1)}. \tag{2.18}$$

The above formula, for the case when $\lambda \ll 1$, shows that at $\xi = 0$, the scaling factor is negative. As $\xi = 1$, the scaling factor is at $-\infty$. Hence, scaling doesn't occur at all. And

second, we assume that $\lambda \gg 1$. The numerator of (2.17) can be approximated as

$$(\xi - 2)\left(e^{\xi L\lambda} + e^{-\xi L\lambda}\right) - \xi\left(e^{L\lambda(\xi-2)} + e^{-L\lambda(\xi-2)}\right) \approx e^{L\xi\lambda}(\xi - 2) - \xi e^{-L\lambda(\xi-2)}.$$

And the the denominator of (2.17) can be approximated as

$$L\left(e^{L\lambda} - e^{-L\lambda}\right)\left(e^{L\lambda(\xi-1)} - e^{-L\lambda(\xi-1)}\right) \approx -Le^{L\lambda\xi}e^{-L\lambda(\xi-1)} = -Le^{L\lambda(2-\xi)}.$$

The scaling factor S can be approximated as

$$S \approx \frac{e^{L\lambda\xi}(\xi - 2) - \xi e^{-L\lambda(\xi-2)}}{Le^{L\lambda(2-\xi)}} = \frac{(\xi - 2)\,e^{2L\lambda}}{Le^{L\lambda(2-\xi)}} - \frac{\xi}{L}$$

$$= \frac{(\xi - 2)e^{2L\lambda(\xi-1)}}{L} - \frac{\xi}{L},$$

or after further simplifications

$$S \approx -\frac{\xi}{L}. \tag{2.19}$$

The above formula, for the case when $\lambda \gg 1$, shows that at $\xi = 0$, we have good scaling. We can also have good scaling as L gets bigger. The plots of (2.18) and (2.19) are shown in Figure 2.11.
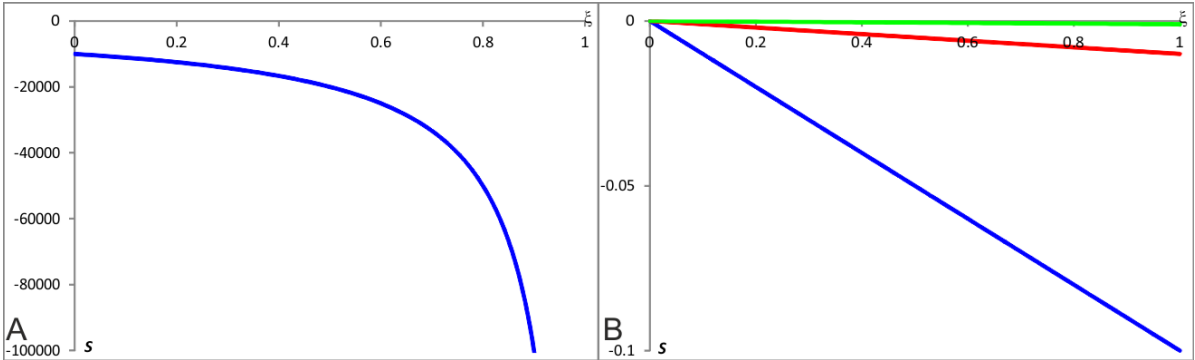
Figure 2.11: **Plots of scaling factor for the Neumann boundary condition. A:** *Scaling factor for the case when λ is very small. As ξ increases, the scaling factor tends to $-\infty$ since at $\xi=1$, the denominator of (2.17) is zero. We used $L=1$ and $\lambda=0.01$.* **B:** *Scaling factor for the case when λ is very big. The blue, red and green profiles correspond for $L=10$, 100 and 1000 respectively. We have good scaling at $\xi=0$ for all profiles. As L gets bigger, (see (2.18)) the scaling factor tends to zero.*

As we can notice, if λ is very small then the scaling factor will be high which will not be very good. If λ is large, then the scaling factor will tends to zero under certain conditions.

Now, let's come back to the solution of u

$$u = \frac{e^{L\lambda(\xi-1)} + e^{-L\lambda(1-\xi)}}{\lambda\left(e^{L\lambda} - e^{-L\lambda}\right)}.$$

Assume that $\lambda \ll 1$. Then, the exponential terms in the above solution u can be approximated by

$$u \approx \frac{1 + L\lambda\left(\xi-1\right) + 1 - L\lambda\left(1-\xi\right)}{\lambda\left(1 + L\lambda - (1 - L\lambda)\right)} = \frac{1 + L\lambda\xi - L\lambda + 1 + L\lambda - L\lambda\xi}{2L\lambda^2} = \frac{1}{L\lambda^2}$$

$$= \frac{D_u}{k_u L}. \tag{2.20}$$

As we can see, the solution (2.19) is represented by a constant value (leveled up profile) which is inverse proportional to the size of the medium. The solution (2.19) is not scaling at all (scaling factor $S = -\infty$). However it can be used for coupling with other variable in a way that that variable is scaled. This technique will be demonstrated in the next section.

2.4 Scaling of exponential profile (mechanism 1)

In the previous section, we found out that scaling occurs when λ is very small for the case of the Dirichlet boundary condition. For the case of the Neumann boundary condition, there is no scaling at all when λ is very small. And when λ is large, scaling occurs if L is large. We apply the solution (2.20) in this section. Assume that there is another morphogen whose decay is affected by the first morphogen so that its concentration v is given by the equation 2.21 [103].

$$D_v \frac{d^2 v}{dx^2} - k_v v u^2 = 0; \qquad v(x=0) = v_0; \qquad \left.\frac{dv}{dx}\right|_{x=L} = j_v. \tag{2.21}$$

where v_0 is the boundary at $x = 0$ and j_v is the boundary flux at $x = L$. The solution of equation (2.21) of v is written as a superposition of two exponents. But if the size of the medium is large enough, then $v(x)$ can be approximated by only one exponent (see appendix B for full derivation).

$$v \approx v_0 e^{-x\sqrt{\frac{k_v u^2}{D_v}}} = v_0 e^{-xu\sqrt{\frac{k_v}{D_v}}} = v_0 e^{-x\frac{D_u}{k_u L}\sqrt{\frac{k_v}{D_v}}} = v_0 e^{-\xi\frac{D_u}{k_u}\sqrt{\frac{k_v}{D_v}}}. \tag{2.22}$$

The solution of equation (2.22) is a function of the relative position $\xi = x/L$ rather than the position x and therefore scales with the size of the medium. The plot of (2.22) is

shown in Figure 2.12.
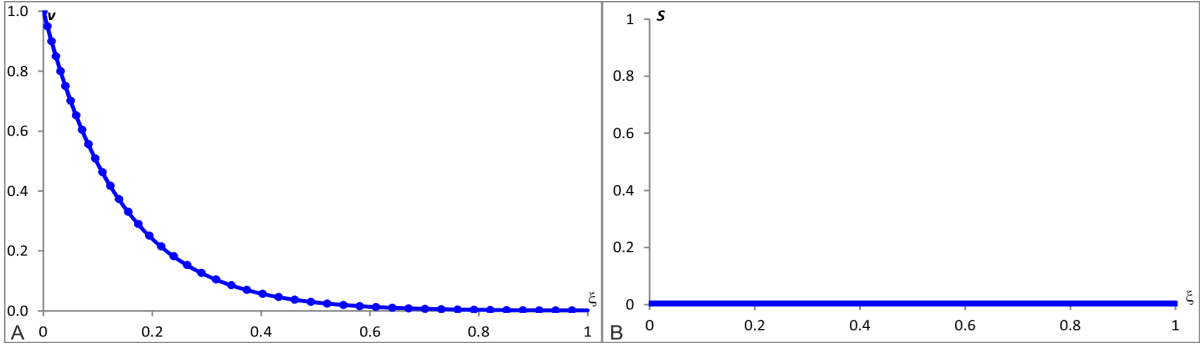
Figure 2.12: **Profile of v for two different medium size and scaling factor.** *In our simulations, we chose the values for these parameters: $D_u=10$, $D_v=1$, $k_u=0.005$, $k_v=1$, $v_0=1$ and $j_v=0$ for two different medium sizes L=1 and L=2.* **A:** *The continuous curve is for L=1 and the dotted curve is for L=2.* **B:** *The scaling factor is zero everywhere since the two profiles have the same concentration everywhere.*

One of the mechanisms of scaling, (which is also behind the expansion-repression model [10]), can be illustrated in a simple setting. Assume that the production rate of a certain morphogen is constant and it degrades uniformly in the medium. Also assume that the morphogen diffuses quickly so that its level is roughly the same over the entire medium. If u denotes the concentration of the morphogen and it degrades with rate $k_u u$ at each "point", then the total degradation rate over the medium of size L is $k_u u L$. If the total production rate over the entire medium is p (and constant), then balance is achieved if $p = k_u u L$, indicating that the concentration, u, is inversely proportional to the size of the medium $u = p/k_u L$. Furthermore, assume that there is another morphogen whose decay is affected by the first morphogen so that its concentration v is given by the equation [103].

2.5 Scaling of exponential profile (mechanism 2)

Assume that we have a domain of size L, where the morphogen with concentration u is produced and diffuses. Furthermore, assume that there is a region of size a in the middle of this domain where the morphogen decays. This setting can be illustrated by Figure 2.13 and modelled by the following equation:

$$\frac{\partial u}{\partial t} = D_u \frac{\partial^2 u}{\partial x^2} - k(x)u + p,$$

where

$$k(x) = \begin{cases} k_u, & \text{for } \frac{L-a}{2} < x < \frac{L+a}{2} \\ 0, & \text{otherwise.} \end{cases}$$

with the following boundary conditions.

$$\left.\frac{\partial u}{\partial x}\right|_{x=0} = \left.\frac{\partial u}{\partial x}\right|_{x=L} = 0.$$

Here D_u represents the diffusion coefficient, p the production rate and k_u the decay rate.
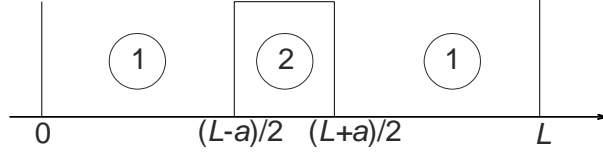
Figure 2.13: **Domain with production and decay in the middle. Region 1:** *Domain where the morphogen with concentration u is produced with rate p and diffusing.* **Region 2:** *Domain where the morphogen is decaying with rate k_u.*

The analytical solution of $u(x)$ is represented in three parts:

$$u(x) = \begin{cases} p\left(-\frac{x^2}{2D_u} + \frac{(L-a)\left(2+e^{-a\lambda}+e^{a\lambda}\right)}{2\lambda D_u\left(e^{-a\lambda}-e^{a\lambda}\right)} + \frac{1}{k_u} + \frac{(L-a)^2}{8D_u}\right), & \text{for } x < \frac{L-a}{2} \\[3ex] p\left(-\frac{(L-a)\left(e^{\frac{\lambda(L+a)}{2}}+e^{\frac{\lambda(L-a)}{2}}\right)\left(e^{x\lambda}+e^{\lambda(L-x)}\right)}{2\lambda D_u\left(e^{(L-a)\lambda}-e^{(L+a)\lambda}\right)} + \frac{1}{k_u}\right), & \text{for } \frac{L-a}{2} < x < \frac{L+a}{2} \\[3ex] p\left(-\frac{x^2}{2D_u} + \frac{Lx}{D_u} + \frac{(L-a)\left(2+e^{-a\lambda}+e^{a\lambda}\right)}{2\lambda D_u\left(e^{-a\lambda}-e^{a\lambda}\right)} + \frac{1}{k_u} + \frac{(L-a)^2}{8D_u} - \frac{L(L+a)}{2D_u}\right), & \text{for } x > \frac{L+a}{2} \end{cases} \tag{2.23}$$

where $\lambda = \sqrt{k_u/D_u}$. For full derivation see appendix D.

For large diffusion coefficient D_u, the solution can be approximated (see appendix D) as

$$u \approx \frac{pL}{ak_u},$$

which indicates that fast diffusion results to levelling up of the morphogen over the entire domain so that its level is proportional to the size of the domain.

Now let us consider another morphogen whose dynamics is given by the following equation:

$$\frac{\partial v}{\partial t} = D_v\frac{\partial^2 v}{\partial x^2} - k_v\frac{v}{u^2}; \qquad v(x=0) = v_0; \qquad \left.\frac{\partial v}{\partial x}\right|_{x=L} = j_v. \tag{2.24}$$

where v_0 is the boundary value at $x = 0$ and j_v is the boundary flux at $x = L$. In

order to have scaling, the decay is represented by the ration of v and u^2. Although the plots of $u-$profiles can be done using analytical solution for u (see (2.23)) in order to see $v-$profiles, we had to numerically integrate equations (2.24). The plots of u and v from simulations are shown in Figure 2.14.
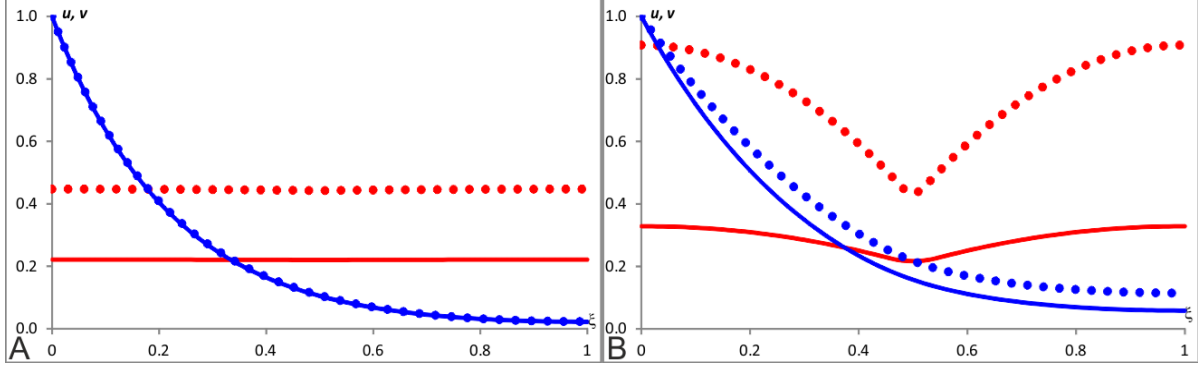
Figure 2.14: ***u- and v- profiles from numerical integration of equations (2.22) and (2.23).*** *Profiles (the blue and red curve stand for u and v profiles respectively) are presented for two different medium sizes (L=1, solid line and L=2 dashed line) and two different values of D_u (D_u=1 on panel **A** and D_u=0.01 in panel **B**). Values for other model parameters are D_v=1, k_v=1, p=0.01, k_u=0.5, v_0=1 and j_v=0, for two different medium sizes L=1 and L=2. In panel **A**, we see that the u-profile is constant but in panel **B**, the $u-$profile is not constant.*

For both plots in Figure 2.14, we have calculated the scaling factor numerically using our formula (2.4). The $u-$profile scales perfectly well for the case when $D_u = 1$: the scaling factor calculated for this case does not exceed 0.1. But for the case when $D_u = 0.01$, its scaling is increases rapidly to 10. Hence, this is much worse compared to the scaling factor for $D_u = 1$.

2.6 Scaling of morphogen in annihilation model

In section 1.7.1, we have dealt with scaling involving two morphogens which are expressed in opposite sides of the embryo. In this model, u and v can be seen as representing Bicoid and Nanos profiles in fly embryo respectively. We already know that only s_- can scale.

We can deduce the expression of u and v using the facts that s_+ (see (1.19)) is the sum of u and v and s_- (see (1.19)) is the difference between u and v. The formulae of s_+ and s_- in terms of u and v are given as $s_+ = u + v$ and $s_- = u - v$. We can compute

the expressions of u and v by adding and subtracting the two equations respectively.

$$\left.\begin{array}{l} s_+ = u + v \\ s_- = u - v \end{array}\right\} \Rightarrow 2u = s_+ + s_- \Rightarrow u = \frac{1}{2}\left(s_+ + s_-\right),$$

$$\left.\begin{array}{l} s_+ = u + v \\ s_- = u - v \end{array}\right\} \Rightarrow 2v = s_+ - s_- \Rightarrow v = \frac{1}{2}\left(s_+ - s_-\right).$$

Therefore the full expressions of u and v are

$$u = \frac{1}{2}\left(\frac{8}{\lambda^2 L^2}\left(-1 + \sqrt{1 + \frac{u_0\lambda^2 L^2}{4}}\right) + \frac{4}{\lambda^2 L^2}\left(-1 + \sqrt{1 + \frac{u_0\lambda^2 L^2}{4}}\right)^2(1-2\xi)^2 - \frac{\lambda^2 L^2 u_0^2}{96}(1-2\xi)^4 + u_0(1-2\xi)\right),$$
$$(2.25)$$

$$v = \frac{1}{2}\left(\frac{8}{\lambda^2 L^2}\left(-1 + \sqrt{1 + \frac{u_0\lambda^2 L^2}{4}}\right) + \frac{4}{\lambda^2 L^2}\left(-1 + \sqrt{1 + \frac{u_0\lambda^2 L^2}{4}}\right)^2(1-2\xi)^2 - \frac{\lambda^2 L^2 u_0^2}{96}(1-2\xi)^4 - u_0(1-2\xi)\right),$$
$$(2.26)$$

where $\xi = x/L$. Assume that $\lambda^2 \ll 1$, then the first term and the coefficient of $(1 - 2\xi)^2$ of the solution u inside the bracket, in equation (2.24) can be approximated using the binomial distribution.

$$\frac{8}{\lambda^2 L^2}\left(-1 + \sqrt{1 + \frac{u_0\lambda^2 L^2}{4}}\right) \approx \frac{8}{\lambda^2 L^2}\left(-1 + 1 + \frac{u_0\lambda^2 L^2}{8}\right) = u_0$$

$$\frac{4}{\lambda^2 L^2}\left(-1 + \sqrt{1 + \frac{u_0\lambda^2 L^2}{4}}\right)^2 \approx \frac{4}{\lambda^2 L^2}\left(-1 + 1 + \frac{u_0\lambda^2 L^2}{8}\right)^2 = \frac{u_0^2\lambda^2 L^2}{16}.$$

So far u is approximated by

$$u \approx \frac{1}{2}\left(u_0 + \frac{u_0^2\lambda^2 L^2}{16}(1-2\xi)^2 - \frac{\lambda^2 L^2 u_0^2}{96}(1-2\xi)^4 + u_0(1-2\xi)\right).$$

As λ is small, we can neglect the second and the third terms and therefore, u is approximated by

$$u \approx \frac{1}{2}\left(u_0 + u_0(1-2\xi)\right) = \frac{1}{2}\left(2u_0 - 2u_0\xi\right) = u_0\left(1 - \xi\right). \tag{2.27}$$

The solution of v in equation (2.25) can be approximated similarly to the solution of u. Therefore v can be approximated by

$$v \approx \frac{1}{2}\left(u_0 - u_0(1-2\xi)\right) = \frac{1}{2}\left(2u_0\xi\right) = u_0\xi. \tag{2.28}$$

u_0 in (2.27) and (2.28) is a constant. We see that u and v are independent of L. Hence, the scaling factor will be zero for both approximations. The plot of equation (2.27) is shown in Figure 2.15.
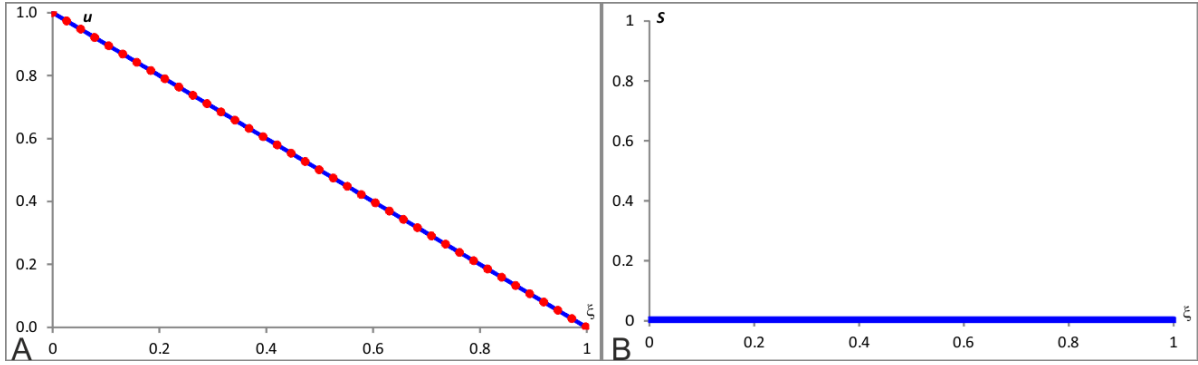
Figure 2.15: **Two plots for the annihilation model and scaling factor.** *In our simulations, we use k=10⁻⁵ and D=u₀=1.* ***A:*** *The continuous blue profile is for the case when L=1 and the red dotted profile is for the case when L=2.* ***B:*** *The scaling factor is 0 everywhere since in panel* ***A****, we have two linear profiles.*

2.7 Scaling of nuclear trapping model

Scaling of Bicoid gradient in Drosophila embryo is well established experimental fact [37]. Formations of Bicoid gradient have been addressed in a number of modelling studies [40]. Its exponential profile can be easy modelled and the real challenge is to construct a model which shows scaling. It is known that one part of Bicoid molecules is located in the syncytium and freely diffuses, while another part is bounded by the nuclei. The only hypothesis concerning the scaling of Bicoid gradient is related to the predominant degradation of Bicoid in nuclei compared to the degradation in syncytium [36]. This hypothesis can be checked using the modification of so-called nuclear trapping model [19, 23] which described the dynamics of free and bound Bicoid in the embryo (see Figure 2.16).
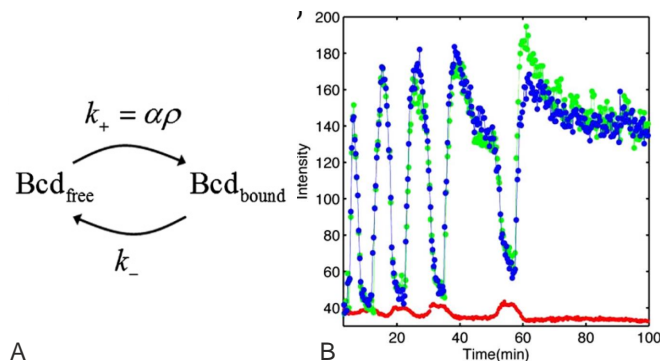
Figure 2.16: **Nuclear trapping model.** ***A:*** *Bicoid exists in two states: freely diffusing and immobile/nuclear bound. The forward nuclear trapping rate constant (k_+) is proportional to the nuclear density [19].* ***B:*** *Experimentally measured concentrations of free (red) and bound (blue and green) Bicoid from [36].*

The fly embryo has a shape of ellipsoid [115, 58]. All the nuclei in the embryo are located near the surface of the embryo in a layer called syncytium. Bicoid molecules are produced at the anterior pole of the embryo and diffuse along the syncytium [1]. These molecules are also captured by nuclei so that there are two fractions of Bicoid: free (u), where it is moving with diffusivity D, and bound (v), where it is confined to the nucleus and can be considered immobile. The transitions between the free and bound states are modelled by first order processes with the rate constants k_+ and k_-, the original equation of the model can be found in [19]. We have extended the model by adding terms counting for the degradation of Bicoid and by focusing on the stationary solution of the system.

$$
\begin{aligned}
\frac{\partial u}{\partial t} &= D\frac{\partial^2 u}{\partial x^2} - k_u u - \rho\left(uk_1 - vk_2\right), \\
\frac{\partial v}{\partial t} &= uk_1 - vk_2 - vk_v,
\end{aligned}
$$

where D defines the rate of free Bicoid diffusion, k_u and k_v are the degradation rates of free and bound Bicoid, k_1 and k_2 define the rate of nuclear trapping and release of Bicoid respectively and ρ is the nuclei density (number of nuclei per unit length). The scaling in this model is possible because the total amount of nuclei, N, in embryos of different sizes is the same at the same developmental stage. Furthermore, the nuclei are located in the thin (two-dimensional) syncytium covering the embryo and therefore their density is inversely proportional to the square length of the embryo, $\rho = N/L^2$. These equations can be considered under different boundary conditions. For the mixed boundary conditions $u(x = 0) = 1$ and $u'(x = L) = 0$, where $u(x = 0) = 1$ counts for the production of Bicoid in the apical side of the embryo, the stationary solution of $u(x)$ is given by

$$
u(x) = \frac{e^{-L\sqrt{\beta}}}{e^{-L\sqrt{\beta}} - e^{L\sqrt{\beta}}},
$$

which can be approximated as (see appendix E for full derivation)

$$
u \approx e^{-\xi\sqrt{\frac{k_u}{D}L^2 + \frac{Nk_1 k_v}{D(k_2 + k_v)}}}. \tag{2.29}
$$

The above approximation depends on both ξ and L. If the first term, of solution (2.29), under the square root is smaller than the second term then the solution would scale.

For the Neumann boundary conditions $u'(x = 0) = -\gamma$ and $u'(x = L) = 0$, the sta-

tionary solution of $u(x)$ is given by

$$u(x) = \frac{\gamma \left(e^{(x-L)\sqrt{\beta}} + e^{(L-x)\sqrt{\beta}} \right)}{\sqrt{\beta} \left(e^{L\sqrt{\beta}} - e^{-L\sqrt{\beta}} \right)}.$$

The above solution can be approximated as (see appendix F for full derivation)

$$u(\xi, L) \approx L \frac{\gamma}{\sqrt{\frac{k_u}{D}L^2 + \frac{Nk_1k_v}{D(k_2+k_v)}}} e^{-\xi\sqrt{\frac{k_u}{D}L^2 + \frac{Nk_1k_v}{D(k_2+k_v)}}}. \tag{2.30}$$

The above approximation depends on both ξ and L. We have two possible scenarios both not permitting the scaling of the $u-$profile. Indeed, if the first term, of the solution (2.30), under the square root is smaller than the second term, then the exponential would scale but not the coefficient since it depends on L. If the second term under the square root is smaller compared to the first, then the coefficient of the exponential term would scale but not the exponential itself. Therefore the solution cannot scale in opposition to [96] since this author claimed that this solution would scale. In equation (2.29) and (2.30), $\beta = \left(k_u \left(k_2 + k_v \right) + k_1 k_v \right) / \left(D \left(k_2 + k_v \right) \right)$ and $\xi = x/L$. In order to check for scaling, k_u should be a very small number. We perform simulations for two different mediums sizes for the mixed boundary condition. The results are shown in Figure 2.17.
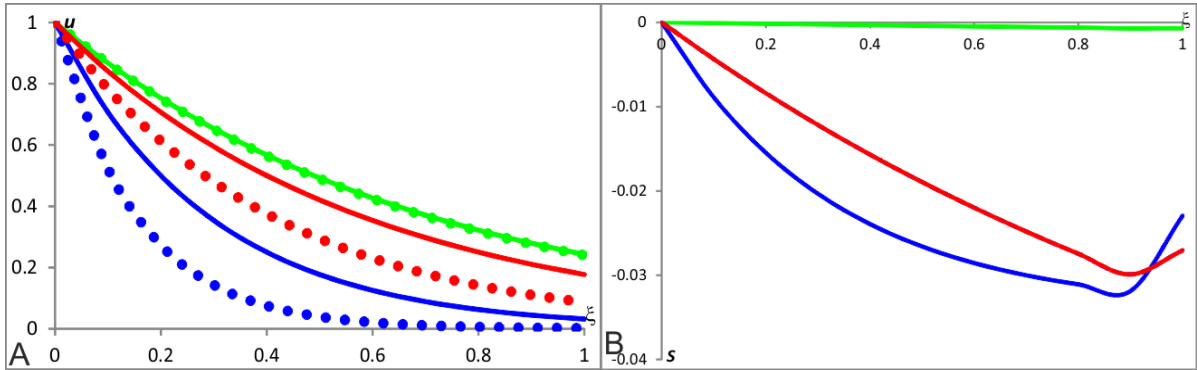
Figure 2.17: **Profiles for mixed boundary conditions for two different medium sizes and their scaling factor.** *The following parameters values are used: D=10, k_2=2, k_v=0.5 and N=k_1=ρ=1. **A:** Continuous and dotted profiles are for L=1 and L=2 respectively for the mixed boundary condition. The blue, red and green profiles are for k_u=0.1, 0.01 and 0.001 respectively. **B:** Scaling factor for the mixed boundary condition. The blue, red and green profiles are for k_u=0.1, 0.01 and 0.001 respectively. The blue curve corresponds to the worst scaling out of all three. The green profile has the best scaling factor out of all three since its scaling factor tends to zero.*

2.8 Scaling in a system with active transport

To explore other mechanisms of scaling we can assume that all nuclei are connected by microtubules which can enforce active Bicoid transportation which can be predominantly oriented in the anterior-to-posterior direction. This is highly hypothetical statement but we can show that it leads to the scaling of gradient even if don't consider nuclear trapping. The active transportation is mathematically represented by an advection term, so that the Bicoid concentration, c, can be described by the modification of the equation in Figure 1.9:

$$D\frac{d^2c}{dx^2} + s\rho\frac{dc}{dx} - kc = 0; \qquad c(x = 0) = 1; \qquad \frac{dc}{dx}(x = L) = 0. \qquad (2.31)$$

Here parameter s defines the strength of Bicoid flow due to the active transportation. Since we are interested in a flow along the anterio-posterior axis, the nuclei density is considered only in this direction and therefore it is inversely proportional to the size of the embryo: $\rho = N/L$. The solution of the equation (2.3) is approximated by the exponent:

$$c \approx e^{-\xi\left(\alpha+\sqrt{\alpha^2+\beta}\right)}, \qquad (2.32)$$

where $\alpha = sN/2D$ and $\beta = kL^2/D$. The above solution (2.32) scales with the size of embryo if the rate of Bicoid transportation is high compared to its degradation rate. If α is positive, then the active transport is directed to the left. If α is negative, then the active transport is directed to the right. We can only have scaling for the case with α positive, that is, when the advection flow is directed against the diffusive flow and points towards the source emitting the morphogen. The plot of solution (2.32) is shown in Figure 2.18.
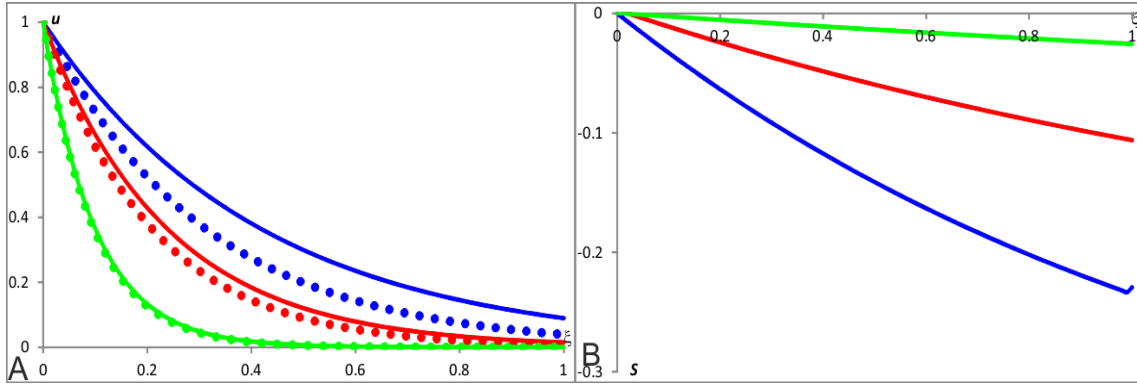
Figure 2.18: **Profiles for mixed boundary conditions for two different medium sizes and their scaling factor in active transport model.** *We chose D=k=1.* **A:** *Continuous and dotted profiles are for L=1 and L=2 respectively for the mixed boundary condition. The blue, red and green profiles are for α=1, 2 and 5 respectively.* **B:** *Scaling factor for the mixed boundary condition. The blue, red and green profiles are for for α=1, 2 and 5 respectively. The blue curve corresponds to the worst scaling out of all three. The scaling factor of the green profile has the best scaling factor out of all three since its scaling factor tends to zero.*

2.9   Summary

The aim of this chapter was to design a model such that its solution can be represented by an exponential function which scales with the medium size. We have also developed a tool which allows to measure robustness and scaling. Scaling is a particular case of robustness. We have introduced our definition of scaling factor and tested it throughout this chapter. We have tested our scaling factor for two simple cases. The first case was a linear profile and the second case was an exponential profile. We have noticed the linear profile will always scale no matter what the size of the medium is. However, the exponential profile generally doesn't scale. We have considered the one-variable model with all boundary conditions. We saw that the solution can scale under the Dirichlet boundary condition. This is getting closer to the French Flag model. For the case of Neumann boundary condition, the solution doesn't scale at all. But we can use the latter result for our two mechanisms of scaling of exponential profile. In these two models, the morphogen u could represent a hypothetical morphogen while v could reflect the bicoid concentration profile in fly oocyte. These two mechanisms can illustrate the scenario where the bicoid protein diffuse posteriorly forming a protein gradient. Bicoid is not only the only maternal genes for early patterning. Nanos is another maternal gene which is located at the posterior pole $(x = L)$. It diffuses anteriorly. The annihilation model in section 2.6 allowed us to illustrate this phenomenon. We have also shown that solutions for nuclear trapping model and active transport model can exhibit good scaling properties for the mixed

boundary conditions. The fact that we have Dirichlet boundary condition on one side, in all our models, allows us to have scaling. In this chapter, we had good scaling with only one assumption compared to [10]. Our assumption was if the degradation rate of one morphogen is much smaller than the diffusion coefficient, then this morphogen will diffuse faster and this enables a second morphogen to have its concentration scaled across the profile.

Chapter 3

Scaling of Turing patterns

In the first chapter, we have seen that the solutions of Turing and FHN models do not scale similarly to exponential solutions of diffusion/decay model. In the second chapter, we have introduced a few modifications of diffusion/decay models such that their solutions are represented by exponential profiles having good scaling properties. The objective of this chapter is to modify Turing and FHN models to allow scaling properties for solutions of new models. This could be seen as mathematical representation of the fact that the patterning (number of stripe) remains the same for two individual of the same species. The spatial positions of these stripes depend on the concentration of morphogens. The Turing's model is a prototype model commonly used for illustration of stationary patterns appearing in inhibitor/activator systems. The second one is the Fitzhugh-Nagumo model which is used for illustration of formation of excitation waves in inhibitor/activator systems. We will analyse the link between these two models and show that Turing's model can be transformed into modification of FitzHugh Nagumo model and also, we want see if scaling occurs using our formula (2.4). In the first chapter, we have seen that the solutions of Turing and FHN models do not scale similarly to exponential solutions of diffusion/decay model. In the second chapter we have introduced a few modifications of diffusion/decay models such that their solutions are represented by exponential profiles having good scaling properties. The objective of this chapter is to modify Turing and FHN models to allow scaling properties. This could be seen as mathematical representation of the fact that the patterning (number of stripe) remains the same for two individuals of the same species. The spatial positions of these stripes depend on the concentration of morphogens. The Turing's model is a prototype model commonly used for illustration of stationary patterns appearing in inhibitor/activator systems. The second one is the Fitzhugh-Nagumo model which is used for illustration of formation of excitation waves in inhibitor/activator systems. We will analyse the link between these two models and show that Turing's model can be transformed into FitzHugh-Nagumo

model and also, we will investigate if scaling occurs using our formula (2.4).

We start with section 3.1 by discussing the original Turing model. We shall, in section 3.2, discuss about our extended Turing's model. In sections 3.3 and 3.4, we shall investigate the effects of the medium size and the diffusion of the inhibitor on the number of stripes. The stripes are used to characterise patterns. The three-variable Turing's model will be dealt in section 3.5. In this section, we also test the scaling problem. In section 3.6, we move on to the standard Fitzhugh-Nagumo model. Section 3.7 will be about the conversion of the Turing model to the Fitzhugh-Nagumo model. The three-variable FHN model will be dealt in section 3.8. We also test the scaling formula for this model.

3.1   Original Turing Model

Let's find out the conditions for existence of Turing instability for the following system (see (3.1)).

$$
\begin{pmatrix} \dot{u} \\ \dot{v} \end{pmatrix} = A \begin{pmatrix} u \\ v \end{pmatrix},
\tag{3.1}
$$

where $A = \begin{pmatrix} a & b \\ c & d \end{pmatrix}$ and a, b, c and d are real constants. The nullclines are determined by equating the LHS to zero of (3.1). Hence, we have two straight nullclines

$$
\begin{aligned}
v &= -\frac{a}{b} &&\text{for} &&\dot{u} = 0 \\
v &= -\frac{c}{d} &&\text{for} &&\dot{v} = 0.
\end{aligned}
\tag{3.2}
$$

The first nullcline in (3.2) is for the case when $du/dt = 0$ and the second one is for the case when $dv/dt = 0$. The equilibrium point is at the origin and for its stability, we require that the $trace = a + d < 0$ and the $determinant = ad - bc > 0$. In total, we have six cases for stability. These cases can be defined as the following. Assume that $a > 0$. Then, $d < 0$, such that $|a| < |d|$, to satisfy $trace < 0$. Hence, it follows that if $b < 0$, then $c > 0$ or other way around to satisfy $determinant > 0$. Thus, the first two cases are:

1. $a > 0$, $d < 0$, $b < 0$ and $c > 0$ or

2. $a > 0$, $d < 0$, $b > 0$ and $c < 0$.

Now assume that $a < 0$. To satisfy $trace < 0$, $d < 0$. Hence, it follows that if, $b < 0$ then $c > 0$ or other way around to satisfy $determinant > 0$. Thus, the next two cases are:

3. $a < 0$, $d < 0$, $b > 0$ and $c < 0$ or

4. $a < 0$, $d < 0$, $b < 0$ and $c > 0$.

The *trace* < 0 by assuming that $a < 0$ and $d > 0$ provided that $|a| > |d|$. Hence, it follows that if $b < 0$ then $c > 0$ or other way around to satisfy *determinant* > 0. Thus, the last two cases are:

5. $a < 0$, $d > 0$, $b > 0$ and $c < 0$ or

6. $a < 0$, $d > 0$, $b > 0$ and $c < 0$.

Let's consider the first case, $a > 0$, $d < 0$ $b < 0$ and $c > 0$. The trace is already satisfied since the parameters a and d are opposite signs. We check for the case of the determinant.

$$ad - bc \; > \; 0$$
$$ad \; > \; bc.$$

We shall divide by b on both sides. Since b is negative, the sign of the inequality will change.
$$\frac{ad}{b} < c.$$

Next, we shall divide by d on both sides. Again, since d is negative, the sign of the inequality will change again.
$$\frac{a}{d} > \frac{c}{d}.$$

We shall multiply by -1 on both sides.

$$-\frac{a}{d} < -\frac{c}{d}.$$

As we can see, in order to have stability, the slope of $du/dt = 0$, $-a/b$ should be less than the slope of $dv/dt = 0$, $-c/d$. Now, we shall consider the reaction-diffusion system.

$$\frac{\partial u}{\partial t} \; = \; D_u \frac{\partial^2 u}{\partial x^2} + \gamma_1 \left(au + bv\right),$$
$$\frac{\partial v}{\partial t} \; = \; D_v \frac{\partial^2 v}{\partial x^2} + \gamma_2 \left(cu + dv\right),$$

where D_u, D_v are the diffusion coefficients of u and v respectively. Any solutions $u(x,t)$ are $v(x,t)$ can be represented as a superposition of functions

$$
\begin{aligned}
u_k(x,t) = f_k(t)g_k(x) &\approx \hat{u}(t)\cos(kx), \\
v_k(x,t) = f_k(t)g_k(x) &\approx \hat{v}(t)\cos(kx).
\end{aligned}
$$

By substituting these two solutions into the above system, we will have

$$
\begin{aligned}
\frac{\partial \hat{u}}{\partial t} &= -k^2 D_u \hat{u} + \gamma_1(a\hat{u} + b\hat{v}), \\
\frac{\partial \hat{v}}{\partial t} &= -k^2 D_v \hat{v} + \gamma_2(c\hat{u} + d\hat{v}).
\end{aligned}
$$

We can determine the two nullclines by equating $\partial \hat{u}/\partial t$ and $\partial \hat{v}/\partial t$ to 0.

$$
\begin{aligned}
-k^2 D_u \hat{u} + \gamma_1(a\hat{u} + b\hat{v}) &= 0, \\
-k^2 D_v \hat{v} + \gamma_2(c\hat{u} + d\hat{v}) &= 0.
\end{aligned}
$$

From the above equations, we can write $\hat{v}$ as a function of $\hat{u}$.

$$
\hat{v} = \frac{k^2 D_u - a\gamma}{b\gamma}\hat{u}, \tag{3.3}
$$

$$
\hat{v} = \frac{c\gamma}{k^2 D_v - d\gamma}\hat{u}. \tag{3.4}
$$

The first nullcline, 3.3), is for the case when $du/dt = 0$ and the second one, 3.4), is for the case when $dv/dt = 0$. The parameters a, b, c, d, D_u, D_v and γ_1 and γ_2 have arbitrary values. Since we have diffusion terms, we will have instability. The range of the parameter k^2 which leads to instability is the solution of the inequality below.

$$
\frac{k^2 D_u - a\gamma_1}{b\gamma_1} > \frac{c\gamma_2}{k^2 D_v - d\gamma_2}.
$$

From the above inequality, we can get a quartic equation in terms of k.

$$
k^4 D_u D_v - k^2 (a\gamma_1 D_v + d\gamma_2 D_u) + \gamma_1\gamma_2(ad - bc).
$$

The critical points of k^2 are when the above equation is equal to 0. These solutions are given by

$$k_{1,2}^2 = \frac{a\gamma_1 D_v + d\gamma_2 D_u \pm \sqrt{(a\gamma_1 D_v - d\gamma_2 D_u)^2 + 4D_u D_v \gamma_1 \gamma_2 (ad - bc)}}{2D_u D_v}.$$

Now, we shall consider these different cases.

Case 1. $a > 0$, $d < 0$, $b < 0$ and $c > 0$.

The graph on the left below shows the phase portrait without diffusion. This represents the stability. The relative position of the two slopes $(-a/b < -c/d)$. On the right, the slops intersect at two points called instability critical points. The unstable region occurs between these two points (see Figure 3.1).
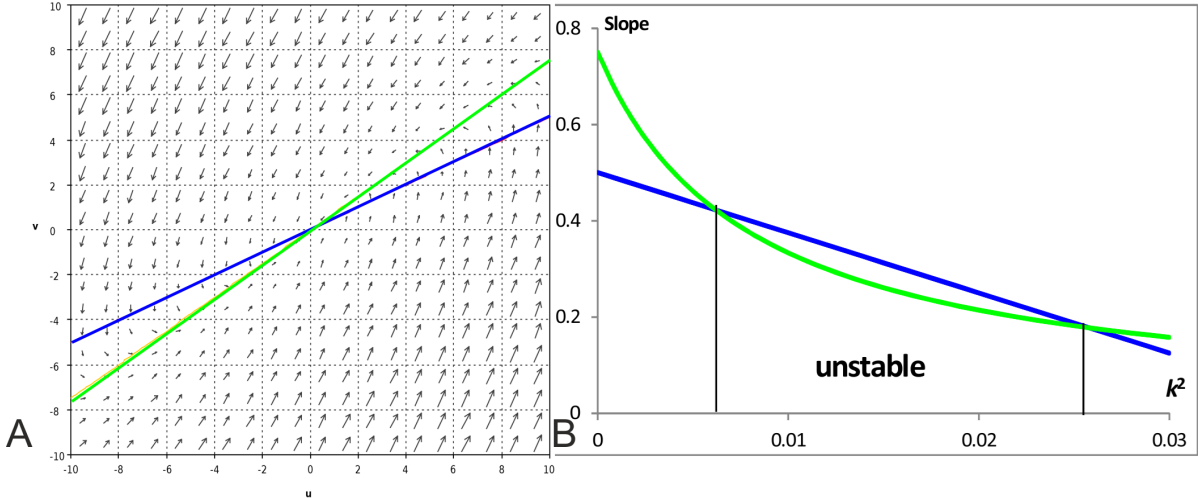
Figure 3.1: **Phase portrait for case 1.** *A: The u and v nullclines are represented by the blue and green line respectively for the system with no diffusion. The arrows represent the phase trajectory.* **B:** *Slopes of $\dot{u}$ and $\dot{v}$ versus k^2 for harmonic solutions of the equations (3.3) and (3.4) containing cos(kx).*

Case 2. $a > 0, d < 0, b > 0$ and $c < 0$.

The graph on the left below shows the phase portrait without diffusion. This represents the stability. The relative position of the two slopes $(-a/b > -c/d)$. On the right, the slops intersect at two points called instability critical points. The unstable region occurs between these two points (see Figure 3.2).
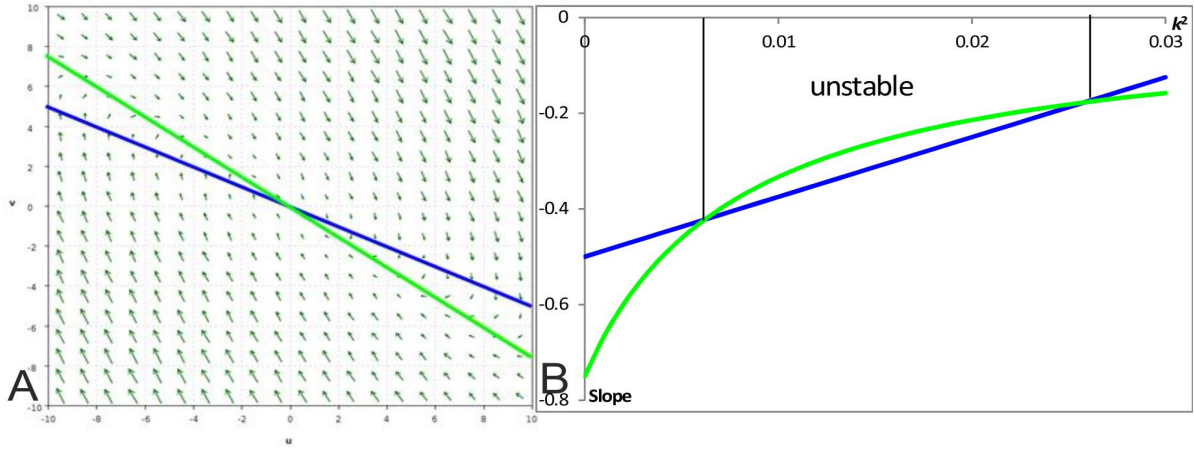
Figure 3.2: **Phase portrait for case 2.** *A: The u and v nullclines are represented by the blue and green line respectively for the system with no diffusion. The arrows represent the phase trajectory.* **B:** *Slopes of $\dot{u}$ and $\dot{v}$ versus k^2 for harmonic solutions of the equations (3.3) and (3.4) containing cos(kx).*

Case 3. $a < 0, d < 0, b < 0$ and $c > 0$.

The graph on the left below shows the phase portrait without diffusion. This represents the stability. The relative position of the two slopes $(-a/b < -c/d)$. The graph on the right shows that the two slopes don't intersect. Therefore, it will always be stable (see Figure 3.3).
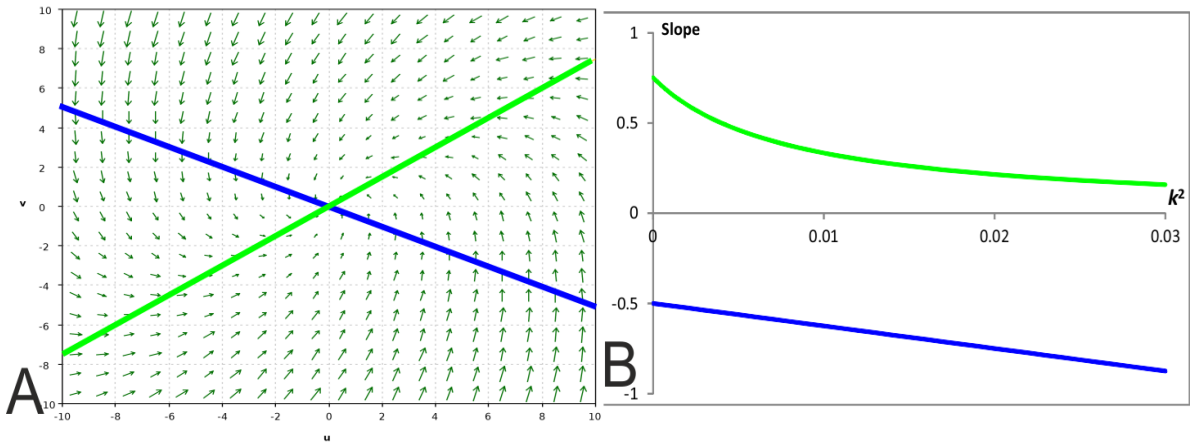
Figure 3.3: **Phase portrait for case 3.** *A: The u and v nullclines are represented by the blue and green line respectively for the system with no diffusion. The arrows represent the phase trajectory.* **B:** *Slopes of $\dot{u}$ and $\dot{v}$ versus k^2 for harmonic solutions of the equations (3.3) and (3.4) containing cos(kx).*

Case 4. $a < 0, d < 0, b > 0$ and $c < 0$.

70

The graph on the left below shows the phase portrait without diffusion. This repre-
sents the stability $(-a/b > -c/d)$. The graph on the right shows that the two slopes
don't intersect. Therefore, it will always be stable (see Figure 3.4).
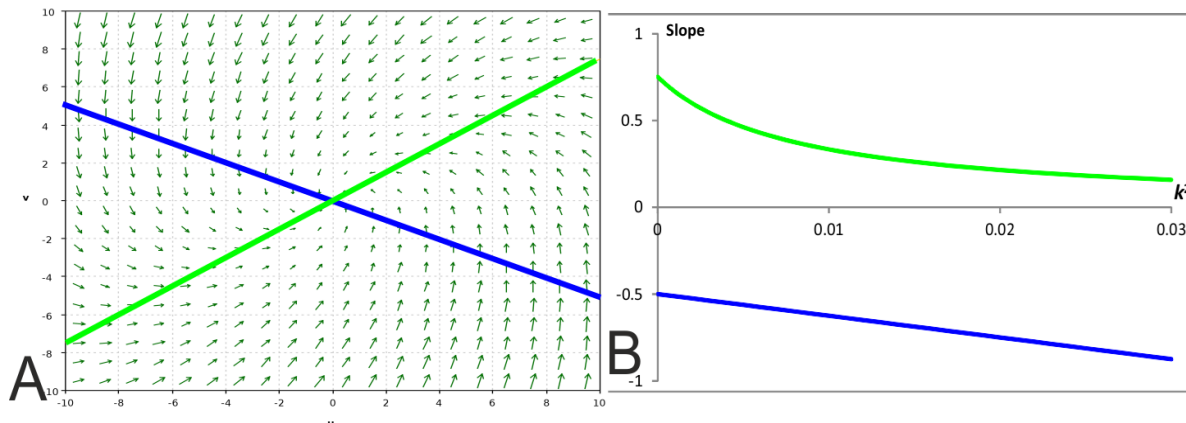
Figure 3.4: **Phase portrait for case 4. A:** The u and v nullclines are represented by the blue
and green line respectively for the system with no diffusion. The arrows represent the phase
trajectory. **B:** Slopes of $\dot{u}$ and $\dot{v}$ versus k^2 for harmonic solutions of the equations (3.3) and
(3.4) containing cos(kx).

Case 5. $a < 0, d > 0, b > 0$ and $c < 0$.

The graph on the left below shows the phase portrait without diffusion. This repre-
sents the stability. The relative position of the two slopes $(-a/b < -c/d)$. The graph on
the right shows that the two slopes don't intersect. Therefore, it will always be stable
(see Figure 3.5).
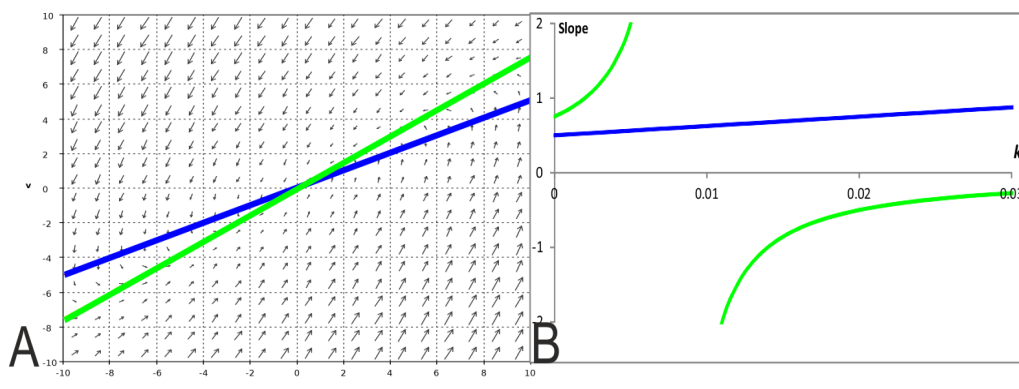
Figure 3.5: **Phase portrait for case 5. A:** The u and v nullclines are represented by the blue
and green line respectively for the system with no diffusion. The arrows represent the phase
trajectory. **B:** Slopes of $\dot{u}$ and $\dot{v}$ versus k^2 for harmonic solutions of the equations (3.3) and
(3.4) containing cos(kx).

Case 6. $a < 0, d > 0, b < 0$ and $c > 0$.

The graph on the left below shows the phase portrait without diffusion. This represents the stability. The relative position of the two slopes $(-a/b > -c/d)$. The graph on the right shows that the two slopes don't intersect. Therefore, it will always be stable (see Figure 3.6).
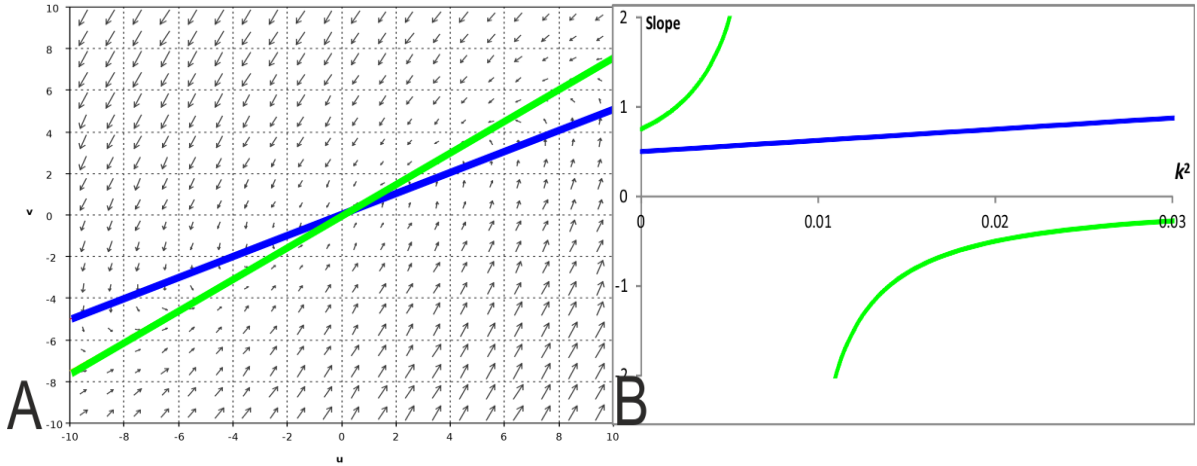
Figure 3.6: **Phase portrait for case 6. A:** *The u and v nullclines are represented by the blue and green line respectively for the system with no diffusion. The arrows represent the phase trajectory.* **B:** *Slopes of $\dot{u}$ and $\dot{v}$ versus k^2 for harmonic solutions of the equations (3.3) and (3.4) containing $\cos(kx)$.*

In order to analyse the linear model, we will need to consider six cases when the model is stable. Cases 1 and 2 give Turing instability. The other four cases will always be stable. For case 1, u is called the activator because it is responsible for production of v and v is called inhibitor because it is involved in the decay of u. Case 2 describes the kinetics which are not directly associate with known interactions of biochemical substances [69].

3.2 Turing instability in the model extended with cubic terms

In the linear model, the concentrations u and v tend to the infinity with time. To avoid this, we extend the linear model (3.1) by adding cubic terms for both equations with

coefficients α_u and α_v.

$$\frac{\partial u}{\partial t} = D_1 \frac{\partial^2 u}{\partial x^2} + \gamma\left(au + bv\right) - \alpha_u u^3; \quad \left.\frac{\partial u}{\partial x}\right|_{x=0} = \left.\frac{\partial u}{\partial x}\right|_{x=L} = 0, \quad (3.5)$$

$$\frac{\partial v}{\partial t} = D_2 \frac{\partial^2 v}{\partial x^2} + \gamma\left(cu + dv\right) - \alpha_u v^3; \quad \left.\frac{\partial v}{\partial x}\right|_{x=0} = \left.\frac{\partial v}{\partial x}\right|_{x=L} = 0, \quad (3.6)$$

where D_u, D_v are the diffusion coefficients of u and v respectively, a, b, c, d are constant parameters and γ_1 and γ_2 are parameters which we can change to see how many stripes can have unstable modes in a medium of a given size.
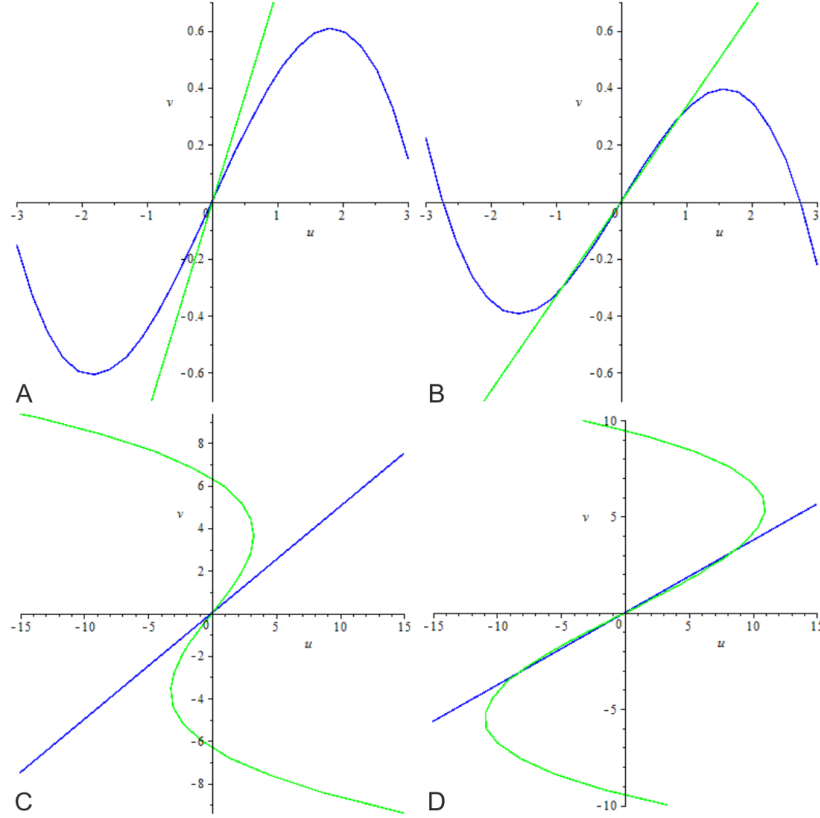
*Figure 3.7: **Cubic and linear nullclines of the system (3.5) and (3.6).** The two top panel are for the cases when $\alpha_u=0.1$ and $\alpha_v=0$. **A:** Both nullclines when k=0. **B:** Both nullclines for k=0.5. The two above panel are for the cases when $\alpha_u=0$ and $\alpha_v=-0.1$. **C:** Both nullclines when k=0. **D:** Both nullclines for k=0.5. Values of model parameters are as follows: a=1, b=-2, c=3, d=-4, $D_u=1$ and $D_v=20$.*

Figure 3.7 shows the nullclines of the system (3.5) and (3.6). Panels **A** and **B** show the cases when $\alpha_v = 0$. Panel **A** has one equilibrium point. This is stable. Panel **B** is similar to panel **A** except that it has three equilibrium points. The origin is unstable and the other two are stable. Panels **C** and **D** show the cases when $\alpha_u = 0$. The parameter α_v in

these two panels is negative otherwise we will never get the two extra equilibrium points. Panel **C** has one equilibrium point. This is stable. Panel **D** is similar to panel **C** except that it has three equilibrium points. The origin is unstable and the other two are stable. In panels **B** and **D**, as the origin is unstable the direction fields around the origin will be repelled. But since we have two stable equilibrium points, the the phase trajectories which are repelled from the origin will be attracted to these two stable equilibrium points. They will prevent the direction field to go to infinity. That's why, we choose cubic terms. Consider the case when one has square terms. For this case, we only have two equilibrium points. One of them is stable and the other is unstable. The direction field at the unstable point will be repelled and they will be attracted to the stable equilibrium point. But since we only have one stable equilibrium point, some direction field will go to ∞. That is the reason why, we don't consider square terms. The same argument applies for the general case u^{2n}, where n is positive. We shall consider the cases when $\alpha_u = 0$ and $\alpha_v = 0$.

3.3 Effect of the size of the medium on the number of stripes

There can be many unstable special modes in the same system [69]. In section 1.5.3, the condition to allow Turing's instability has been shown by condition (1.12). By applying the results obtained in section 1.5.3 to our model defined by (3.5) and (3.6), the two bounds k_1^2 and k_2^2 are given by

$$k_{1,2}^2 = \frac{aD_v\gamma_1 + dD_u\gamma_2 \pm \sqrt{(aD_v\gamma_1 + dD_u\gamma_2)^2 - 4D_uD_v\gamma_1\gamma_2 det}}{2D_uD_v},$$

where $det = ad - bc$. The range of square wavenumber k^2 corresponding to Turing's instability is

$$k_1^2 < k^2 < k_2^2.$$

Using the expression of k_1^2 and k_2^2, we obtain

$$\frac{aD_v\gamma_1 + dD_u\gamma_2 - \sqrt{(aD_v\gamma_1 + dD_u\gamma_2)^2 - 4D_uD_v\gamma_1\gamma_2 det}}{2D_uD_v} < k^2 < \frac{aD_v\gamma_1 + dD_u\gamma_2 + \sqrt{(aD_v\gamma_1 + dD_u\gamma_2)^2 - 4D_uD_v\gamma_1\gamma_2 det}}{2D_uD_v}.$$

Since k is a wavenumber, it can be written as $k = n\pi/L$, when n is the number of stripes. By substituting $k = n\pi/L$ into the above inequality and after rearranging, we get

$$\frac{L}{\pi}\sqrt{\frac{aD_v\gamma_1 + dD_u\gamma_2 - \sqrt{(aD_v\gamma_1 + dD_u\gamma_2)^2 - 4D_uD_v\gamma_1\gamma_2 det}}{2D_uD_v}} < n < \frac{L}{\pi}\sqrt{\frac{aD_v\gamma_1 + dD_u\gamma_2 + \sqrt{(aD_v\gamma_1 + dD_u\gamma_2)^2 - 4D_uD_v\gamma_1\gamma_2 det}}{2D_uD_v}}.$$

$$(3.7)$$

Our first investigation consists of assessing the effect of the medium size on the number of stripes. To do so, we fix a, b, c, d, D_u and D_v. For each set of value of γ_1 and γ_2, the range of number of stripes n is given by (3.8)

$$\frac{L}{\pi}\sqrt{\frac{20\gamma_1-4\gamma_2-\sqrt{(20\gamma_1+4\gamma_2)^2-480\gamma_1\gamma_2}}{40}} < n < \frac{L}{\pi}\sqrt{\frac{20\gamma_1-4\gamma_2+\sqrt{(20\gamma_1+4\gamma_2)^2-480\gamma_1\gamma_2}}{40}}$$
(3.8)

From (3.8), the two bounds of the number of stripes are linear functions with respect to L. The plots of bounds defined by the left and right hand side of inequality (3.8) for different set of values of γ_1 and γ_2 are shown in Figure 3.8.
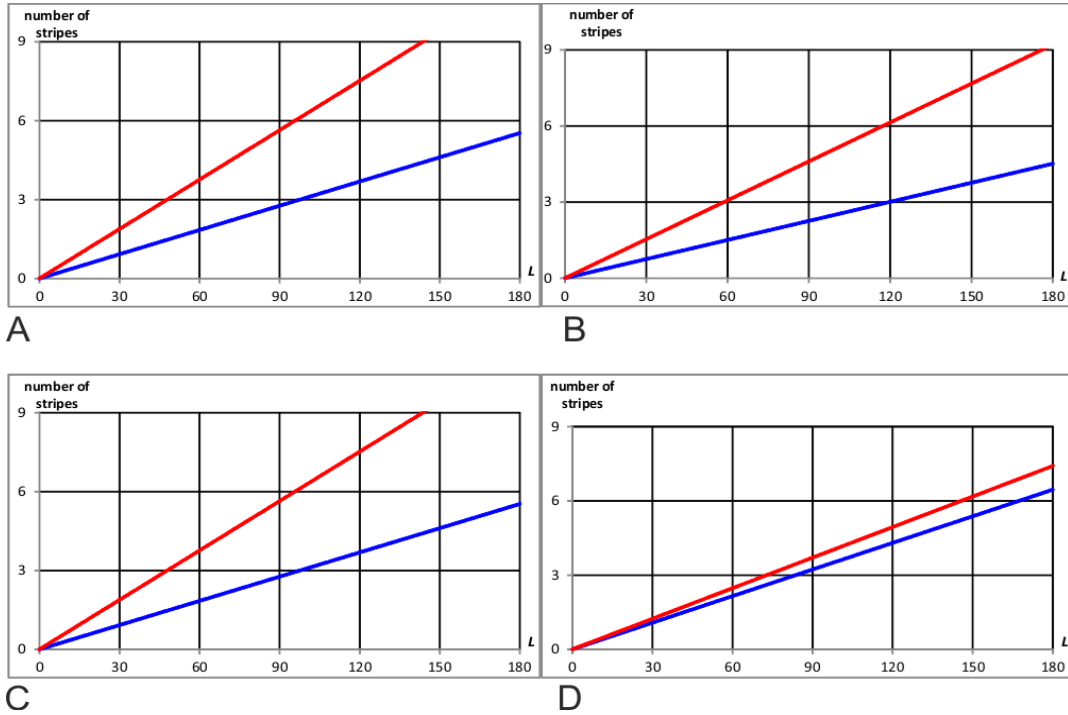
Figure 3.8: **Graph showing the effect of the medium size L on the number of stripes for four different sets of values of γ_1 and γ_2.** *Each horizontal line between red and blue lines corresponds to a pattern of different special periodicity. The blue and the red lines correspond respectively to the left and right hand side of (3.8). Shown simulations are performed using the following parameter values: a=1, b=-2, c=3, d=-4, D_u=1, D_v=20, α_u=0.1 and α_v=-0.1.* **A:** $\gamma_1=\gamma_2=0.06$. **B:** $\gamma_1=\gamma_2=0.04$. **C:** $\gamma_1=0.053$ and $\gamma_2=0.04$. **D:** $\gamma_1=0.04$ and $\gamma_2=0.053$.

Consider the case with both γ_1 and γ_2 equal to 0.06. If we take for example $L = 140$, several possibilities of number of stripes can occur (2.5 to 4 stripes)(see Figure 3.8 in panel **A**). If we decrease the value of both γ_1 are γ_2 to 0.04, the two curves get closer and the number of stripes, for $L = 140$, is reduced (see Figure 3.8 in panel **B**). For this case it can be between 2 and 3.5 stripes. Next, the value of γ_1 is increased to 0.053 and

γ_2 remains fixed to 0.04. The two curves are getting away for each other. For this case the number of possible stripes increases (see Figure 3.8 in Panel **C**). In the last panel, if we swap the values of γ_1 and γ_2, the two curves get much closer. We can only get one possible number of stripes. For $L = 160$, we can only have 2.5 stripes (see Figure 3.8 panel **D**). We are particular interested in panel **D** because for some medium size, it can only have one possibility. This is shown by the graph below (see Figure 3.9). No matter how many locations we stimulate, we will always get the same number of stripes. This panel is particularly useful for scaling. For example if in a small medium we have two stripes and in a bigger medium, we either have two or three stripes. Then scaling might not be obvious. On the other hand, if we only have two stripes in a small and big medium then scaling will occur.
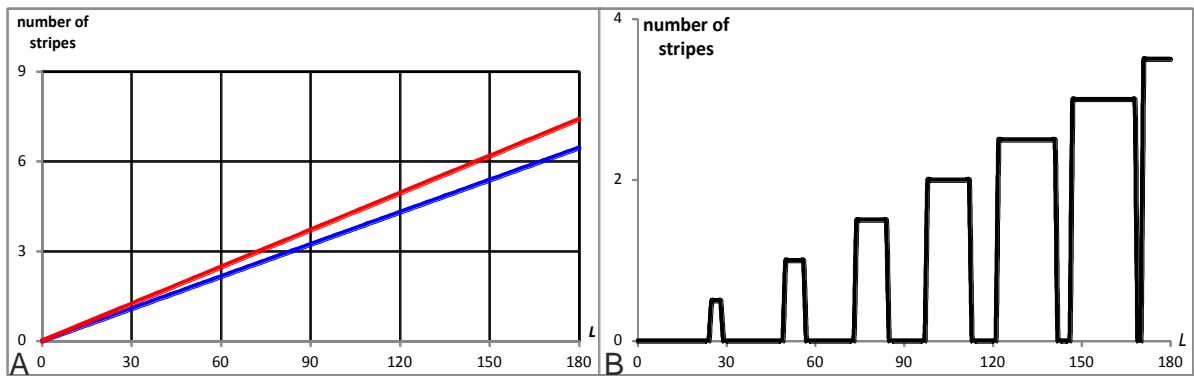
Figure 3.9: **Case of a unique unstable mode.** *By variation of model parameters, it is possible to reduce the number of unstable modes (bringing the red and red lines closer bounding the region of instability).* **A:** γ_1=0.04 *and* γ_2=0.053. **B:** *The effect of the size of the medium on the number of stripes. Any perturbation of homogenous state will always get the same plots.*

3.4   Effect of the diffusion of the inhibitor on the number of stripes

We have previously investigated the effect of L on the number of stripes. By changing the values of γ_1 and γ_2, the blue and red lines in Figure 3.9 get closer to each other. This has reduced the number of unstable modes.

Now, we examine the effect of the diffusion D_v of the inhibitor v on the number of stripes. To do so, We fix $a, b, c, d, D_u, \alpha_u, \alpha_v, \gamma_1, \gamma_2$ and L. Their values are given below

in Figure 3.10. The range of n given previously by (3.7) is written in terms of D_v as

$$\frac{140}{\pi}\sqrt{\frac{0.04D_v-0.16-\sqrt{(0.04D_v+0.16)^2-0.0384D_v}}{2D_v}} < n < \frac{140}{\pi}\sqrt{\frac{0.04D_v-0.16+\sqrt{(0.04D_v+0.16)^2-0.0384D_v}}{2D_v}}.$$
(3.9)

The two limits of the range of n in (3.9) are non-linear functions of D_v. Their plots are shown in Figure 3.10 (blue lower limit and red higher limit).
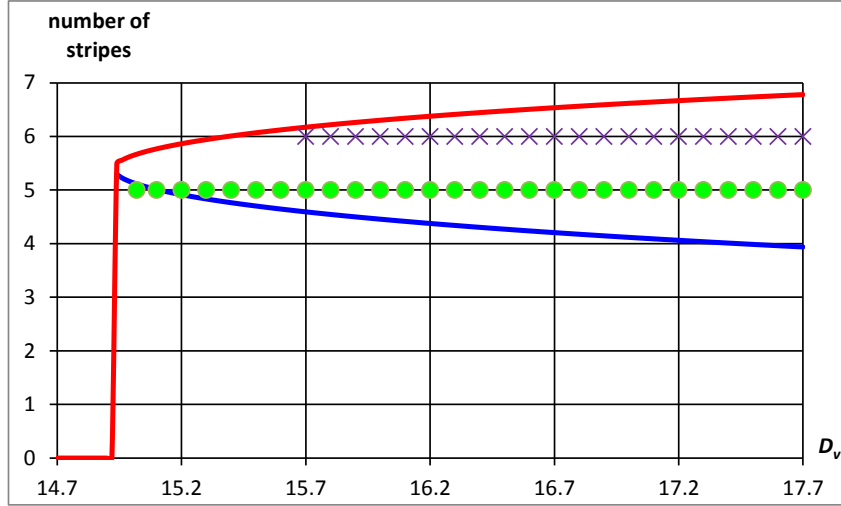
Figure 3.10: **Graph showing the effect of the diffusion of the inhibitor D_v on the number of stripes for $L=140$.** *The blue and the red curves are the lower and higher limits respectively. Simulations results are shown by green circles and purple crossings. The green circles indicate patterns with 2.5 stripes and the purple crossings - with 3 stripes. The following parameter values were used: a=1, b=-2, c=3, d=-4, D_u=1, D_v=20, α_u=0.1, α_v=-0.1 and γ_1=γ_2=0.04. For D_v=15.2, we will always have 2.5 stripes no matter how many places we stimulate. For D_v=15.7, one can either have 2.5 stripes or 3 stripes.*

3.5 Scaling of Turing patterns in the three-variable model

All of our simulations confirm that adding cubic terms prevent the concentration from going to infinity. Furthermore, our simulations confirmed the results from Figure 3.9 and Figure 3.10. Changing the values of α_u and α_v affect the amplitudes of the stripes. The smaller the values of both α_u and α_v are, the bigger the amplitudes of the stripes will be. We will use our model (3.5) and (3.6) to perform scaling like in sections 2.4 and 2.5. To introduce scaling into the Turing model, we extend it with a third variable z satisfying the two following conditions:

1. z is maintained at a constant level which depends on the size of the medium and

2. z affects the kinetics rate of two original variables so that the space scaling of the pattern is proportional to the medium size.

The extended three-variable model is given by the system (3.10)

$$
\begin{aligned}
\frac{\partial u}{\partial t} &= D_u \frac{\partial^2 u}{\partial x^2} + \left(\gamma\left(au+bv\right) - \alpha_u u^3\right) z^2; \quad \left.\frac{\partial u}{\partial x}\right|_{x=0} = \left.\frac{\partial u}{\partial x}\right|_{x=L} = 0, \\
\frac{\partial v}{\partial t} &= D_v \frac{\partial^2 v}{\partial x^2} + \left(\gamma\left(cu+dv\right) - \alpha_v v^3\right) z^2; \quad \left.\frac{\partial v}{\partial x}\right|_{x=0} = \left.\frac{\partial v}{\partial x}\right|_{x=L} = 0, \qquad (3.10) \\
\frac{\partial z}{\partial t} &= D_z \frac{\partial^2 z}{\partial x^2} - k_z z; \quad \left.\frac{\partial z}{\partial x}\right|_{x=0} = -j_0, \left.\frac{\partial z}{\partial x}\right|_{x=L} = j_z,
\end{aligned}
$$

where D_u, D_v and D_z are the diffusion coefficients of u, v and z respectively, k_z defines the degradation rate of z and j_0 and j_z specify the boundary fluxes of z at $x = 0$ and $x = L$ respectively. The plots of all three variables are shown in Figure 3.11.

For both medium sizes, they have the same number of stripes (4.5 stripes) with the same magnitudes. Now, we want to determine the scaling factor, for u for instance. Since there is no analytical formula for its scaling factor, we compute it numerically. The plot of the scaling factor of u is shown in Figure 3.12.
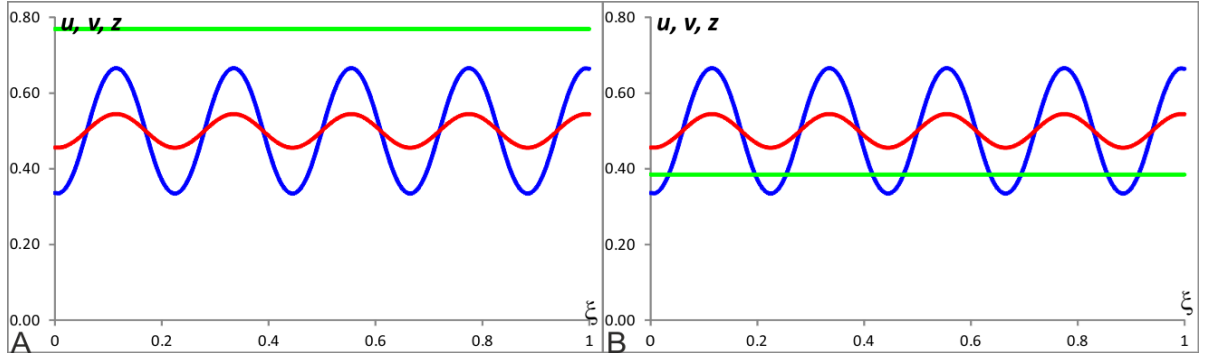
Figure 3.11: **Scaling of the three-variable Turing model for system (3.10)**. *The blue curve represents the concentration u, the red curve is for v and the green curve is for z. For the simulations, we used the following values for the following parameters: D_u=1, D_v=20, D_z=50, γ=0.2, k_z=0.00001, j_0=j_z=0.0001, a=1, b=-2, c=3, d=-4, α_u=0.1 and α_v=0.1. **A:** Plot for L=1. **B:** Plot for L=2. The above graphs show patterns forming in the extended Turing model for the case of two different medium lengths (L_2=2L_1). The concentration z is constant. Profiles of u and v are identical for these two medium sizes-indicating the perfect scaling.*
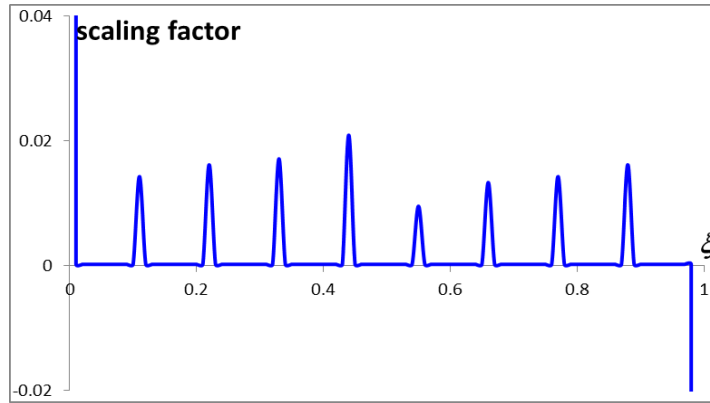
Figure 3.12: ***Scaling factor for u-profile from Figure 3.11 across the relative position*** $\xi = x/L$.

Figure 3.12 leads us to 2 remarks. First, the scaling factor is zero almost everywhere across the relative position ($\xi = x/L$) except at the boundaries ($\xi = 0$ and $\xi = 1$). At both ends, the zero-flux boundary condition has been applied. At $\xi = 0$, the concentration does not change suddenly ($\partial u/\partial \xi = 0$). This makes the denominator of the scaling factor to be zero. At the other end, $\xi = 1$, similar argument can be applied. And second, there are crests at some points. This is because the derivatives at theses point is 0.

3.6 Fitzhugh-Nagumo model

All the analysis was done for the Turing model. The Fitzhugh-Nagumo model (FHN) without the diffusion term transfers into the following system of ODEs:

$$\begin{aligned}
\frac{du}{dt} &= f(u,v) = -k_u u(u-\alpha)(u-1) - v, & (3.11) \\
\frac{dv}{dt} &= g(u,v) = \varepsilon(lu - v),
\end{aligned}$$

where k_u is the membrane conductance, α represents the threshold potential, ε specifies the recovery rate constant and l is the positive slope of the $v-$nullcline.
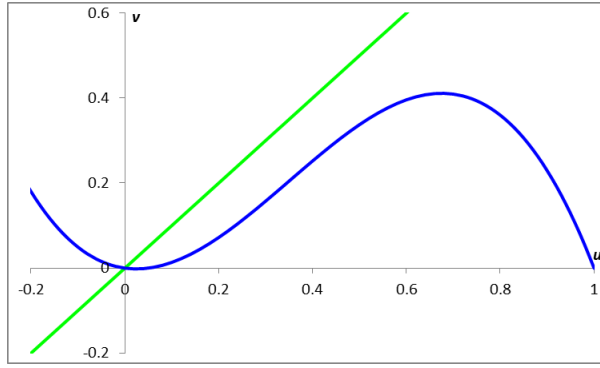
Figure 3.13: **The two nullclines of the FHN model describing excitable system on the (u, v) axis of system (3.15).** *The blue curve is the cubic nullcline, that is when du/dt=0. The green curve is the linear nullcline, that is when dv/dt=0. For this case, α=0.05, ε=0.05, k_u=3 and l=1.*

The only equilibrium point, in Figure 3.13, is the origin. We want to show that this is stable. We investigate the stability of this equilibrium point. To do so, we need to calculate the Jacobian matrix at this point. This is written as

$$J = \begin{pmatrix} f_u & f_v \\ g_u & g_v \end{pmatrix},$$

where the entries $f_u = -k_u\alpha$, $f_v = -1$, $g_u = l\varepsilon$ and $g_v = -\varepsilon$. The trace and the determinant, computed at the origin, are defined as

$$trace = f_u + g_v = -k_u\alpha - \varepsilon < 0,$$

$$det = f_u g_v - f_v g_u = k_u\alpha + l > 0.$$

This shows that the origin is stable. Now, we modify the FHN model such that the equilibrium point (point of intersection between cubic and linear nullclines) is not at the origin. To do this, we add a term called *up* in the first kinetic term $f(u,v)$. Furthermore, we assume that there is only one equilibrium point, which can be ensured by either having a high value of l or sufficiently low value of k_u.

$$\frac{du}{dt} = f(u,v) = -k_u u(u-\alpha)(u-1) - v + up, \qquad (3.12)$$
$$\frac{dv}{dt} = g(u,v) = \varepsilon(lu - v).$$

The linear nullcline will be the same as in (3.11) but the cubic nullcline will be shifted up. The plots of the two nullclines of (3.12) are shown in Figure 3.14.
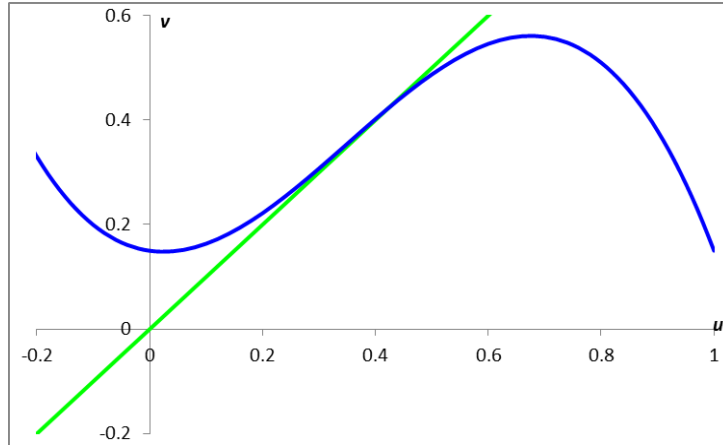
Figure 3.14: **The two nullclines of the FHN model describing an oscillatory system on the (u, v) plane of system (3.16).** *The blue curve is the cubic nullcline, that is when du/dt=0. The green curve is the linear nullcline, that is when dv/dt=0. The equilibrium point is between the minimum and the maximum of the cubic nullcline. For this case, we chose: $\alpha=0.05$, $\varepsilon=0.05$, $k_u=3$, $l=1$ and up=0.15.*

At this equilibrium point, the Jacobian matrix has the same entries as the previous case except for f_u. This is because the value of f_u will be different at this equilibrium point. This matrix is written as follows

$$J = \begin{pmatrix} f_u & -1 \\ l\varepsilon & -\varepsilon \end{pmatrix},$$

The trace and the determinant are defined by

$$
\begin{aligned}
trace &= f_u - \varepsilon, \\
det &= \varepsilon\left(l - f_u\right).
\end{aligned}
$$

In order to have stability, it is required

$$
\begin{aligned}
f_u &< \varepsilon, \\
l &> f_u.
\end{aligned}
$$

In FHN model, it is assumed that ε is very small: $\varepsilon \ll l$. Hence, we can conclude that the conditions for Turing instability is given by

$$0 < f_u < \varepsilon.$$

Now, we transform the FHN (3.12) model using the following change of variables

$$u = \tilde{u} - u_0,$$

$$v = \tilde{v} - v_0,$$

where (u_0, v_0) is the equilibrium point of system (3.12) and $\tilde{u}$ and $\tilde{v}$ are the new variables axes. We substitute them into the equations (3.12).

$$\frac{d\tilde{u}}{dt} = -k_u (\tilde{u} - u_0)(\tilde{u} - u_0 - \alpha)(\tilde{u} - u_0 - 1) - (\tilde{v} - v_0) + up,$$
$$\frac{d\tilde{v}}{dt} = \varepsilon (l(\tilde{u} - u_0) - (\tilde{v} - v_0)).$$

We can multiply out in the second equation.

$$\frac{d\tilde{v}}{dt} = \varepsilon l(\tilde{u} - u_0) - \varepsilon (\tilde{v} - v_0).$$

From the above, we can deduce that $lu_0 - v_0 = 0$. This is because there are no constant terms in the second equation of (3.12). Therefore, $v_0 = lu_0$. From the first equation, we multiply out and collect terms containing power of $\tilde{u}$.

$$\left[\tilde{u}^3\right] \qquad k_u = \alpha_u,$$

$$\left[\tilde{u}^2\right] \qquad k_u(1 + \alpha + 3u_0) = 0,$$

$$\left[\tilde{u}^1\right] \qquad k_u(-u_0(u_0 + \alpha) - (2u_0 + \alpha)(u_0 + 1)) = a,$$

$$\left[\tilde{u}^0\right] \qquad k_u u_0(u_0 + \alpha)(u_0 + 1) = 0.$$

From the second equation, we can determine the expression of α.

$$\alpha = -(1 + 3u_0).$$

The third equation says that the LHS is equal to a i.e. the kinetic term in (3.5). And the last equation says that the LHS is equal to 0. The considered modification of FHN model after adding diffusion terms is equivalent to the Turing model (3.5) and (3.6) by taking the values of the following parameters as follows: $a = f_u$, $b = -1$, $c = l\varepsilon$, $d = -\varepsilon$, $\gamma_1 = \gamma_2 = 1$ and $\alpha_u = k_u$.

$$\frac{\partial u}{\partial t} = au - v + \beta u^2 - \alpha_u u^3, \qquad (3.13)$$
$$\frac{\partial v}{\partial t} = cu + dv. \qquad (3.14)$$

The above modification of the FHN models shows that we have a cubic and a linear null-cline in the (u, v) plane. The two nullclines of (3.13) and (3.14) are plotted in Figure 3.15.
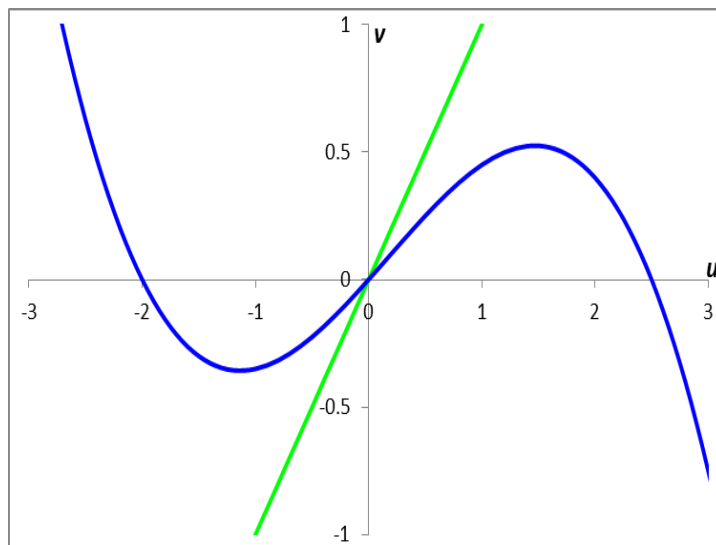
Figure 3.15: **The two nullclines of the converted Turing model to FHN model.** *The blue curve is the cubic nullcline (du/dt=0). The green curve is the linear nullcline (dv/dt=0). The plot was obtained with α_u=0.1, a=0.5, b=-1, c=ε and d=-ε with ε=0.05 and β=0.05.*

For the system without diffusion in (3.13) and (3.14) the matrix A computed at the origin is given by

$$A = \begin{pmatrix} a & -1 \\ \varepsilon & -\varepsilon \end{pmatrix}.$$

The trace and the de determinant are defined by

$$trace = a - \varepsilon$$
$$det = \varepsilon(1 - a).$$

In order to have stability

$$a < \varepsilon,$$
$$a < 1.$$

These can be assemble as $a < \varepsilon \ll 1$ knowing that $\varepsilon \ll 1$.

3.7 Transition from oscillations to stripes

As a result of Turing instability stationary inhomogeneous, solutions merge from stable homogeneous solutions. In the case of FHN model, as we have shown in the previous section, there can be observed oscillating solution. In order to have oscillating solution, we require that the trace and determinant are both positive i.e. $f_u > \varepsilon$ and $l > f_u$. Assuming that $\varepsilon \ll l$, we can assemble these two conditions to $\varepsilon < f_u < l$. To see if we have Turing's patterns, we add diffusion to the system (3.12). The full reaction-diffusion for FHN model is shown below (see (3.15)).

$$
\begin{aligned}
\frac{\partial u}{\partial t} &= D_u \frac{\partial^2 u}{\partial x^2} - k_u u(u - \alpha)(u - 1) - v + up, \qquad (3.15)\\
\frac{\partial v}{\partial t} &= D_v \frac{\partial^2 v}{\partial x^2} + \varepsilon(lu - v).
\end{aligned}
$$

Both trace and determinant depend on the sign of f_u. For the case of the determinant, it will remain positive no matter the sign of f_u is. For the case of the trace, the sign of f_u can have different scenarios. They are shown in Figure 3.16. First if $f_u < 0$, then we will have nothing (blue region). If f_u is between 0 and ε shown by the orange region, we start with stable solution and in the presence of diffusion, we have the classical Turing instability. The green region shows that f_u is greater than ε. In the absence of diffusion, we have oscillating solutions. In the presence of diffusion, we may have stripes.
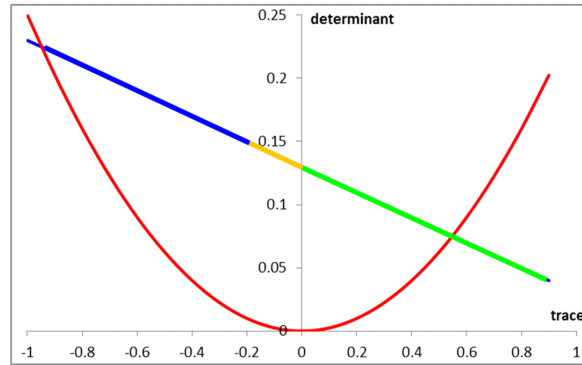
Figure 3.16: **Graph (blue curve) showing relationship between trace and determinant when f_u is changed.** *The curve is represented by a linear function which is* **det=ε(l-trace-ε).** *The red curves is represented by a parabola* **det=trace^2/4** *separating regions with and without oscillations. For this plot, l=1 and ε=0.1.*

Instead of dealing with the standard FHN model (see (3.15)), we have decided to work with the modification of the FHN model (see (3.13) and (3.14)). In (3.13), we choose

$\beta = 0$. The full reaction-diffusion of this model is given as

$$\frac{\partial u}{\partial t} = D_u \frac{\partial^2 u}{\partial x^2} + au + bv - \alpha_u u^3,$$ (3.16)

$$\frac{\partial v}{\partial t} = D_v \frac{\partial^2 v}{\partial x^2} + cu + dv,$$

where D_u and D_v are the diffusion coefficients of u and v respectively and a, b, c, d and α_u are constants. In Figure 3.16, we start from the second quadrant. By adding diffusions, we will end up in the third quadrant. This is for the case of Turing model. For the case of FHN model, we start from the first quadrant. The addition of diffusions means that we may end up in the third quadrant. For the latter model, we did the following. For three values of D_v say 10, 20 and 30, we chose a few values of k starting from $k = 0$. For each value of k, we compute the values of $B(k^2)$ (see (1.10) and $C(k^2)$ (see (1.11). Figure 3.17 shows that for $k = 0$, we are in the first quadrant. For the case $D_v = 10$, Turing's instability doesn't occur. This is because, there is no range of values of k which satisfies $B(k^2) < 0$ and $C(k^2) < 0$. For the case $D_v = 20$, there is a small range of k which Turing's instability occurs. And for the case $D_v = 30$, there is a bigger range value of k which Turing patterns appear (Figure 3.17).
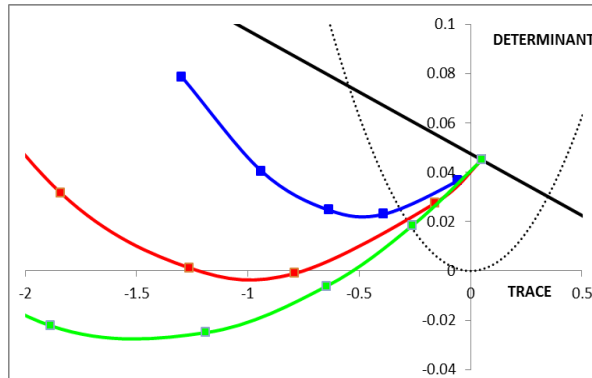
Figure 3.17: **Graph showing relationship between trace and determinant.** *We use a=0.1, b=-1, c=ε, d=-ε with ε=0.05 and D_u=1. The blue, red, green, purple and orange curves are simulations for the cases when D_v=10, 20, 30, 40 and 50 respectively. The black curve is represented by a linear function which is **det=ε(1-trace-ε)**. The black dotted curve represents **det=trace²/4**. For the case when k=0, we are situated in the first quadrant.*

As a reminder, the Jacobian matrix A computed at the origin using (3.13) and (3.14) is given by

$$A = \begin{pmatrix} a & -1 \\ \varepsilon & -\varepsilon \end{pmatrix}.$$

Now, we investigate the possibility to have oscillating solution in the absence of diffusion.

We recall that without diffusion, the trace and the determinant of the Jacobian matrix are respectively

$$
\begin{aligned}
trace &= a - \varepsilon, \\
det &= \varepsilon(1-a).
\end{aligned}
$$

The case giving oscillatory solution require that the trace and the determinant are both positive.

$$
\begin{aligned}
trace &= a - \varepsilon > 0, \\
det &= \varepsilon(1-a) > 0.
\end{aligned}
$$

These lead to the following conditions: $\varepsilon < a$ and $a < 1$. Assuming that $\varepsilon \ll 1$, these can be combined as $\varepsilon < a < 1$. In the presence of diffusions, the Jacobian matrix B is written as

$$
B = \begin{pmatrix} a - k^2 D_u & -1 \\ \varepsilon & -\varepsilon - k^2 D_v \end{pmatrix}.
$$

The trace and the determinant of matrix B are given as follows.

$$
\begin{aligned}
traceB &= -k^2(D_u + D_v) + trace, \\
detB &= k^4 D_u D_v - k^2(aD_v - \varepsilon) + det.
\end{aligned}
$$

In section 1.7.3, we saw that the only way to get instability is that equation (1.11) has to be negative. Turing instability can be obtained if the trace and the determinant of Jacobian matrix B are both negative.

$$
\begin{aligned}
traceB &= -k^2(D_u + D_v) + a - \varepsilon < 0, \\
detB &= k^4 D_u D_v - k^2(aD_v - \varepsilon) - \varepsilon(1-a) < 0.
\end{aligned}
$$

From above, assuming that $D_u = 1$, the conditions for k^2 to get Turing instability are

$$
k^2 > \frac{a - \varepsilon}{1 + D_v},
$$

$$
\frac{aD_v - \varepsilon - \sqrt{(aD_v + \varepsilon)^2 - 4D_v\varepsilon}}{2D_v} < k^2 < \frac{aD_v - \varepsilon + \sqrt{(aD_v + \varepsilon)^2 - 4D_v\varepsilon}}{2D_v}.
$$

To find the limiting value of k^2, we proceed as follow

$$\sqrt{(aD_v + \varepsilon)^2 - 4D_v\varepsilon} = \sqrt{(aD_v)^2\left(1 + \frac{\varepsilon}{aD_v}\right)^2 - 4D_v\varepsilon} = aD_v\sqrt{\left(1 + \frac{\varepsilon}{aD_v}\right)^2 - \varepsilon\frac{4}{a^2D_v}}.$$

Since ε is very small, we have

$$aD_v\sqrt{\left(1 + \frac{\varepsilon}{aD_v}\right)^2 - \varepsilon\frac{4}{a^2D_v}} \approx aD_v\sqrt{1 + \frac{2\varepsilon}{aD_v} - \frac{4\varepsilon}{a^2D_v}} \approx aD_v\left(1 + \frac{\varepsilon}{aD_v} - \frac{2\varepsilon}{a^2D_v}\right).$$

So, the lower bound k_1^2 can be approximated by

$$k_1^2 = \frac{aD_v - \varepsilon - \sqrt{(aD_v + \varepsilon)^2 - 4D_v\varepsilon}}{2D_v} \approx \frac{aD_v - \varepsilon - aD_v\left(1 + \frac{\varepsilon}{aD_v} - \frac{2\varepsilon}{a^2D_v}\right)}{2D_v}.$$

Therefore,

$$k_1^2 \approx \left(\frac{1 - a}{aD_v}\right)\varepsilon.$$

And the higher bound k_2^2 can be approximated by

$$k_2^2 = \frac{aD_v - \varepsilon + \sqrt{(aD_v + \varepsilon)^2 - 4D_v\varepsilon}}{2D_v} \approx \frac{aD_v - \varepsilon + aD_v\left(1 + \frac{\varepsilon}{aD_v} - \frac{2\varepsilon}{a^2D_v}\right)}{2D_v}.$$

Therefore,

$$k_2^2 \approx a - \frac{\varepsilon}{aD_v}.$$

k^2 can be bounded between

$$\left(\frac{1 - a}{aD_v}\right)\varepsilon < k^2 < a - \frac{\varepsilon}{aD_v}. \tag{3.17}$$

Let's consider the LHS of (3.17), that is we estimate the minimal value of k, k_{min}.

$$\left(\frac{1 - a}{aD_v}\right)\varepsilon < k_{min}^2. \tag{3.18}$$

We already know that $k_{min} = \pi n_{min}/L$. By substituting into (3.18), we obtain.

$$\left(\frac{1 - a}{aD_v}\right)\varepsilon < \left(\frac{\pi n_{min}}{L}\right)^2. \tag{3.19}$$

From (3.19), L, a and D_v are fixed. Hence, we can deduce that n^2 is proportional to ε.

This is shown in equation (3.20)

$$(n_{min})^2 > \left(\frac{\varepsilon}{D_v}\right)\left(\frac{L}{\pi}\right)^2 \frac{1-a}{a},$$

or

$$n_{min}^2 \sim \varepsilon. \tag{3.20}$$

Thus, the number of stripes increases when the kinetic rate increases. This is confirmed by numerical simulations as shown in Figure 3.18. The graph below shows that as ε increases, the number of stripes increases quickly.
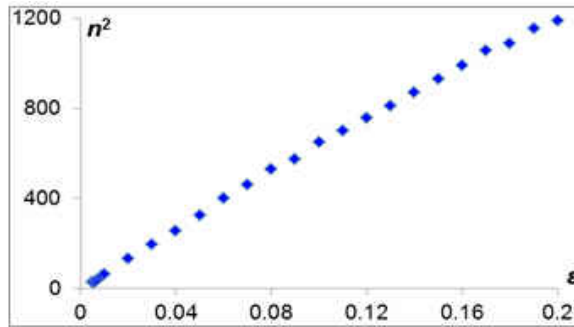
Figure 3.18: **Effect of ε on the minimal number of stripes which can be stimulated in the medium described by the equation (3.21).** *Model parameters are: $D_u=1$, $D_v=50$, $k_u=4$, $\alpha=0.05$, $up=0.1$, $l=1$ and $L=2000$.*

3.8 Three-variable FHN model

Previously, we started with oscillating solution and by adding diffusions, we have stripes. This was done with our considered modification of the FHN model (see (3.16)). We will use the proper FHN model (see (3.13)) to perform scaling. Like in Turing model, to introduce scaling into the Fitzhugh-Nagumo model we have extended it with the third variable with a diffusion coefficient D_z and a decay rate k_z. We assume that the kinetic of the inhibitor in FitzHugh-Nagumo system is affected by the concentration of the third variable (which has an exponential profile) and therefore in the second equation, we multiplied the second term on the RHS by k^2. So the extended FHN model is given by

(3.21).

$$
\begin{aligned}
\frac{\partial u}{\partial t} &= D_u \frac{\partial^2 u}{\partial x^2} - k_u u \left(u - \alpha \right) \left(u - 1 \right) - v + up; & \left. \frac{\partial u}{\partial x} \right|_{x=0} &= \left. \frac{\partial u}{\partial x} \right|_{x=L} = 0, \\
\frac{\partial v}{\partial t} &= D_v \frac{\partial^2 z}{\partial x^2} - \varepsilon \left(lu - v \right) z^2; & \left. \frac{\partial v}{\partial x} \right|_{x=0} &= \left. \frac{\partial v}{\partial x} \right|_{x=L} = 0, & (3.21) \\
\frac{\partial z}{\partial t} &= D_z \frac{\partial^2 z}{\partial x^2} - k_z z; & \left. \frac{\partial z}{\partial x} \right|_{x=0} &= -j_0, \left. \frac{\partial z}{\partial x} \right|_{x=L} = j_z,
\end{aligned}
$$

where D_u, D_v and D_z are the diffusion coefficients of u, v and z respectively, k_u represents the membrane conductance, α is the threshold potential, ε is the recovery rate constant, k_z defines the degradation rate of z and j_0 and j_z specify the boundary fluxes of z at $x = 0$ and $x = L$ respectively. The solution of z, provided that the ratio $(k_z/D_z)^{1/2}$ is very small, is given by: $z = D_z \left(j_0 + j_z \right) / k_z L$. The concentrations u, v and z are plotted in Figure 3.19.
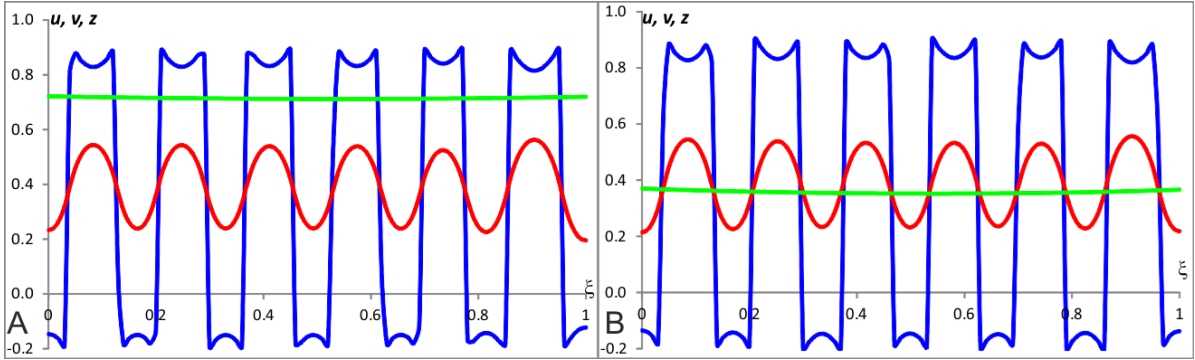
Figure 3.19: **Scaling of the three-variable FHN model.** *The values of the parameters used to plots these profiles are: $D_u=1$, $D_v=50$, $D_z=50$, $k_u=4$, $\alpha=0.05$, $\varepsilon=0.05$, $up=0.1$, $l=1$, $k_z=0.00001$ and $j_0=j_z=0.0001$. The blue, red and green curves represent u, v and z profiles respectively.* **A:** *Simulation for the case $L=700$.* **B:** *Simulation for the case $L=1400$.*

As we can see, the above graphs show that z is a constant solution. For u and v, they are periodic solutions. For both medium sizes, they have the same number of stripes with the same magnitudes. Now, we want to determine the scaling factor for v for example. As no analytical formula exists for it we compute it numerically. Its graph is shown in the Figure 3.20. As we can see, it is practically zero which corresponds to perfect scaling.
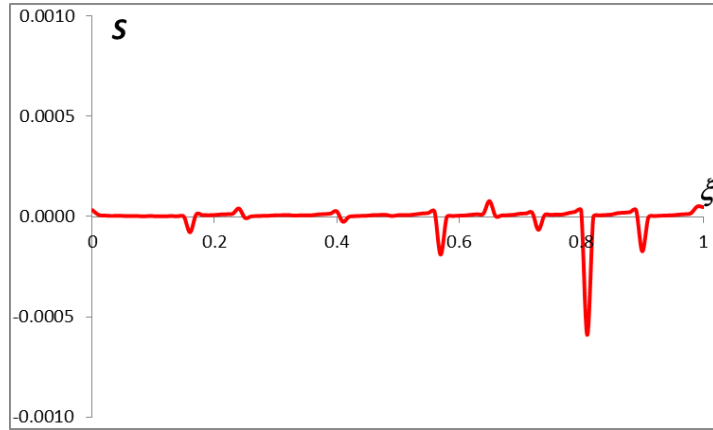
Figure 3.20: **Scaling factor for v.**

3.9 Summary

In this chapter, we had considered two more continuous model namely Turing and Fitzhugh-Nagumo models. Starting with the linear version of Turing model (two-variable), we found that there were two cases which can give Turing's instability. The first case corresponds to the activator/inhibitor systems while the second for activator/substrate ones. In our study, we have extended the activator/inhibitor system represented by a Turing model with cubic nonlinearity and by FHN model to derive two counterpart models whose solutions exhibit good scaling property.

Generally the patterns forming due to Turing instability are not unique. There can be many unstable special modes in the same system [69]. Extending the Turing model with cubic terms on the RHS prevents the concentrations going to infinity arising for unstable modes of solution and observes patterns of different periodicity arising in the same system. Coexistence of different patterns creates difficulties in maintenance of scaling. By variation of model parameters it is possible to reduce the number of unstable modes. To introduce scaling in Turing's model, we added a third variable. The level of this third variable remains constant across the field.

For the Fitzhugh-Nagumo model, it is converted to the Turing model using most of its parameters. The transition from oscillating to stripes has been investigated. Then we introduced scaling in the FHN model like in the Turing's model.

90

Chapter 4

Discrete model

Besides the continuous model based on reaction-diffusion equation systems, discrete model also exist for pattern formation studies. Unlike the continuous models based on the calculation of the gradient of morphogens (proteins), discrete models work on the cell-to-cell contact. We can have scaling if the number of nuclei, in embryos of different sizes, is the same. First, the model is based on cellular automata (CA). Cellular automaton is a collection of cells on a grid which evolve on a number of discrete time-step according to a set of rules based on the state of the cells. CA has been invented by John Von Neumann in the 1940s [105]. A detailed description of cellular automaton can be found in [116]. And second, a derived version of the CA which is called the hybrid cellular automata model. In this chapter, we will focus on the application of the cellular automata model to describe pattern formation. The patterning is due to cell-to-cell contact. The outcome of this contact depends on the genes contained in each cell. The objective of this chapter is to see whether we can have stationary patterns using CA model. In section 4.1, we shall describe the technique of the cellular automata in pattern formation. This is followed by the two-state model analysis presented in section 4.2. Section 4.3 deals with Wolfram's model followed by some of our simulation works. Section 4.4 deals with the three-state model. This is followed by four- or more- state models in section 4.5. Biological implementation will be discussed in section 4.6.

4.1   Technique of cellular automata

A cellular automaton technique requires a regular lattice of cell. This can have one, two or three dimensions. The procedure of the application of cellular automata to pattern formation is shown in Figure 4.1. In this flowchart, N represents the number of cells, t_{end} is the current time and tend is the end of simulation time. Before applying cellular automata to pattern formation modelling, the following definitions are required.

1. State: possible value a cell can have.

2. Neighbour: the set of cells which can interact with one cell.

3. Updating or transition rules: rules which define the future state of a cell according to its current state and that of its neighbours. In the cellular automaton technique, the reaction diffusion equation is transformed into updating rules.

This technique can provide nontrivial patterns including stationary, oscillating and propagating waves.
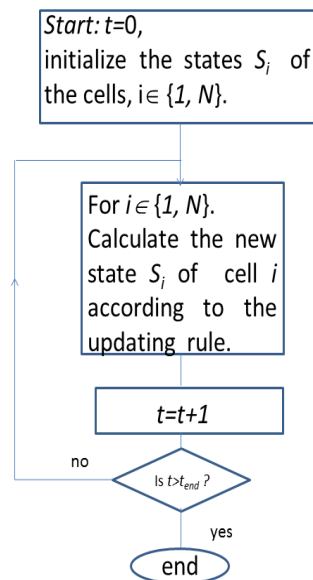
Figure 4.1: Flow chart of cellular automata technique applied to pattern formation.

4.2 Chain of logical elements

A one-dimensional regular lattice of cells is used in the modelling of pattern formation. Each cell can have two or more states. A one-dimensional regular lattice with two-state cells is called a chain of logical elements. The state S_i of each cell i can be denoted by 0 (black) or 1 as (white), i.e. the cell is represented by a logical element. In application in biology, the state can reflect the expression of certain genes. The case of two-state represents whether a simple gene is expressed or not.

4.3 Wolfram's model

Wolfram derived a one-dimensional variant of von Neumann's cellular automata. This consists of a regular lattice of cells which can have two states ($S_i = 0$ or $S_i = 1$). Each cell is surrounded by only two other cells (its two closest neighbours). The state S_1^{t+1} of a cell i in the next generation is determined by the current state of cells $i-1$, i, and $i+1$ according to a transition rule f defined by $S_i^{t+1} = f\left(S_{i-1}^t, S_i^t, S_{i+1}^t\right)$ [109]. This Wolfram model is called a two-state cellular automaton. A noise is introduced in order to assess the robustness of the obtained pattern. This means that a probability equal to the noise level is used to alter the result from the transition rule. An example of transition rule is

$$\text{If } (\text{cell}(i-1) = 1 \text{ and } \text{cell}(i+1) = 0) \text{ then } \text{cell}(i) = 0.$$

A cell interacting with its two closest neighbours leads to the following findings.

- There are $2^3 = 8$ possible configurations, which are 111, 110, 101, 100, 011, 010, 001, and 000.

- For the above configurations, the resulting states are as follows (function f is for compactness is replaced by the arrow):

$$\begin{aligned}
&\text{Configuration 0:} \quad && (000) \to (0\boldsymbol{S_0}0) \\
&\text{Configuration 1:} \quad && (001) \to (0\boldsymbol{S_1}1) \\
&\text{Configuration 2:} \quad && (010) \to (0\boldsymbol{S_2}0) \\
&\text{Configuration 3:} \quad && (011) \to (0\boldsymbol{S_3}1) \\
&\text{Configuration 4:} \quad && (100) \to (1\boldsymbol{S_4}0) \\
&\text{Configuration 5:} \quad && (101) \to (1\boldsymbol{S_5}1) \\
&\text{Configuration 6:} \quad && (110) \to (1\boldsymbol{S_6}0) \\
&\text{Configuration 7:} \quad && (111) \to (0\boldsymbol{S_7}1)
\end{aligned}$$

- This set of transition rule can be characterised by a binary number $\boldsymbol{S_7 S_6 S_5 S_4 S_3 S_2 S_1 S_0}$ which varies from 0 to 255. In other words, the configurations above allow $2^8 = 256$ possible cellular automata.

- The binary number $\boldsymbol{S_7 S_6 S_5 S_4 S_3 S_2 S_1 S_0}$ translated in decimal bases is taken to be the transition rule number.

We want to find a set of rules which cause formation of stationary periodic patterns.

4.4 Effects of initial condition and noise in the patterning for two-state model

In order to assess transition rules for their ability to produce stationary periodic patterns, we have performed a number of simulations. In the first set of simulations, we aimed finding out transition rules which do not destroy already existing periodic pattern. Therefore, these simulations have been started with two-periodic initial conditions (1 white + 1 black) shown in Figure 4.2.

Figure 4.2: Pattern with periodicity of 2 in two-state model.

The results are as follows. Starting with initial periodic solution, 64 transition rules out 256 (25 %) wouldn't destroy it. Their values are in decimal format are as follows

4, 5, 6, 7, 12, 13, 14, 15, 20, 21, 22, 23, 28, 29, 30, 31, 68, 69, 70, 71, 76, 77, 78, 79, 84, 85, 86, 87 , 92, 93, 94, 95, 132, 133, 134, 135, 140, 141, 142, 143, 148, 149, 150, 151, 156, 157, 158, 159, 196, 197, 198, 199, 204, 205, 206, 207, 212, 213, 214, 215, 220, 221, 222 and 223.

Their binary expression is written in the form: $\boldsymbol{XX0XX1XX}$, where $\mathbf{X}$ can be 0 or 1.

$$\text{Configuration 2:} \qquad (010) \to (0\boldsymbol{S_2}0)$$

$$\text{Configuration 5:} \qquad (101) \to (1\boldsymbol{S_5}1).$$

From one generation to the next, this pattern consisting of a repetition of black and white remains the same.

The second set of simulations were aimed to find out transition rules such that when we start with periodic initial conditions (see Figure 4.2) and apply a noise this rules will let the pattern to recover from noise. The noise level of 0.1% has been applied meaning that the state of one out of 1000 cells was altered each time step. Simulations show that 25 out of the above 64 transitions (which would keep the pattern when no noise is set) would "resist" to the perturbation caused by the noise. These transition rules are given by the following numbers:

6, 13, 14, 15, 28, 30, 69, 70, 77, 78, 79, 85, 86, 92, 93, 134, 135, 141, 149, 197, 198, 199, 213, 214, and 215.

For the analysis of this set of rules, we shall point out that if the probability of changing the state of one cell is small, then the probability of changing the state of two cells will be smaller and therefore, we can neglect it. Other rules restore periodic patterns from the noise in more than one time step, often taking the irregularity in a wave fashion to the left or right border. Let's consider rule 77. Assume we have the sequence

$$0101 0101 \ldots$$

Assume that the digit **1** will change to **0**, due to noise, to give

$$0100 0101 \ldots$$

Assume that, the digit **0** will change back to **1**.

$$01010101 \ldots$$

Let's analyse the scenario when the **0** change back to **1**. Let's start with the first the three digits 010. The one in the middle of 010 will stay as it is. This is because the configuration says that $(010) \rightarrow (010)$. The next three digits are 100. The zero in the middle of 100 will stay as it is. This is because the configuration says that $(100) \rightarrow (100)$. The next three digits are 000. The zero in the middle of 000 will change into 1. This is because the configuration says that $(000) \rightarrow (010)$. The next three digits are 001. The zero in the middle of 001 will remain as it is. This is because, the configuration says that $(001) \rightarrow (011)$. So far, the four configurations are configurations are

$$(010) \rightarrow (010)$$

$$(000) \rightarrow (010)$$

$$(100) \rightarrow (100)$$

$$(001) \rightarrow (011).$$

Now, let's get back to the sequence

$$01\mathbf{0}0101\ldots$$

Assume that the digit **0** will change to **1**, due to noise, to give

$$01\mathbf{1}0101.\ldots$$

Assume that, the digit **1** will change back to **0**.

$$01\mathbf{0}10101 \ldots.$$

Let's analyse the scenario when the **1** change back to **0**. Let's start with the first the three digits, 011. The one in the middle of 011 will stay as it is. This because, the configuration says that $(011) \rightarrow (011)$. The next three digits are 1**1**1. The one in the middle of 1**1**1 will change into a **0**. This is because the configuration says that $(111) \rightarrow (101)$. The next three digits are 110. The one in the middle of 110 will remain as it is. This is because, the configuration says that $(110) \rightarrow (110)$. The next three digits are 101. The zero in the middle of 101 will remain as it is. This is because the configuration says that $(101) \rightarrow (101)$ So far, the four configurations are

$$(011) \rightarrow (011)$$

$$(111) \rightarrow (101)$$

$$(101) \rightarrow (101)$$

$$(110) \rightarrow (110).$$

In total, the configuration rules are

$$(000) \rightarrow (010)$$

$$(001) \rightarrow (011).$$

$$(010) \rightarrow (010)$$

$$(011) \rightarrow (011)$$

$$(100) \rightarrow (100)$$

$$(101) \rightarrow (101)$$

$$(110) \rightarrow (110).$$

$$(111) \rightarrow (101)$$

This binary number (**01001101**) is 77.

The third set of simulations aimed finding transition rules such that starting with random initial condition the same periodic stationary patterns were obtained. These simulations have shown that such transition rules exist and given by the following numbers:

$$15, 30, 85, 86, 135 \text{ and } 149.$$

Two transition rules, 15 and 85, converge faster towards the periodic stationary pattern (two time-steps to produce a new stripe).

Now let's analyse in details how the transition rule 15 results into formation of stationary periodic structure from any initial conditions. Shown below is some example of simulation forming periodic stationary patterns for transition rule 15.

t=0	1 0 1 1 1 1 1 1	t=0	0 1 0 1 1 0 1 1	t=0	0 1 0 0 0 1 0 0
t=1	1 0 1 0 0 0 0 1	t=1	0 1 0 1 0 0 1 1	t=1	0 1 0 1 1 1 0 0
t=2	1 0 1 0 1 1 1 1	t=2	0 1 0 1 0 1 1 1	t=2	0 1 0 1 0 0 0 0
t=3	1 0 1 0 1 0 0 1	t=3	0 1 0 1 0 1 0 1	t=3	0 1 0 1 0 1 1 0
t=4	1 0 1 0 1 0 1 1	t=4	0 1 0 1 0 1 0 1	t=4	0 1 0 1 0 1 0 0
t=5	1 0 1 0 1 0 1 1	t=5	0 1 0 1 0 1 0 1	t=5	0 1 0 1 0 1 0 0

Figure 4.3: Three different types of simulation with three different ends at $t = 5$.

The table on the left shows that at $t = 0$, we start with 10111111. As the time increases, the sequence 101 builds gradually. At $t = 4$, we have the sequence $101\ldots$ except on the right hand side where we have a broken sequence 011. The table on the middle shows that at $t = 0$, we start with 01011011. As the time increases, the sequence 010 builds gradually. At $t = 4$, we have the full sequence $101\ldots$. The table on the right shows that at $t = 0$, we start with 01000100. At the time increases, the sequence 010 builds gradually. At $t = 4$, we have the sequence $010\ldots$ except on the right hand side where we have a broken sequence 100.

We shall write 15 into the configuration rule.

$$15= \textbf{00001111}$$

$$(000) \rightarrow (0\mathbf{1}0)$$

$$(001) \rightarrow (0\mathbf{11})$$

$$(010) \rightarrow (0\mathbf{1}0)$$

$$(011) \rightarrow (0\mathbf{11})$$

$$(100) \rightarrow (1\mathbf{0}0)$$

$$(101) \rightarrow (1\mathbf{0}1)$$

$$(110) \rightarrow (1\mathbf{0}0)$$

$$(111) \rightarrow (1\mathbf{0}1).$$

PROPOSITION 1. *For **rule 15**, starting from any initial conditions in the chain of k elements, we will end up with two-periodic structures (010101... or 10101...) coming from the left which appears during k iterations. The final stationary sequence may have either 00 or 11 on the right hand side.* ∎

Proof. We have noted that under the transition rule 15, periodic patterns form first on the left and then expand over the chain from the left to the right. Therefore, we will consider various initial combinations occurring on the left side of the chain and analyse how they allow the growth of the periodic structure to the right. First, we consider four cases starting with the first digit 1 on the left of the structure.

Case A: $100x$.

$$100x \rightarrow \mathbf{101}x. \qquad \text{(1TS)}$$

For **Case A**, one has initially $100x$ (white, black, black, x is either black or white). Let's start with the first three digits. The first digit, 1, is fixed. The next digit, 0, remains the same. This is because the configuration says that $(100) \rightarrow (1\mathbf{0}0)$. The next three digits are $00x$. Two configurations which contain $00x$ are $(000) \rightarrow (0\mathbf{1}0)$ and $(001) \rightarrow (0\mathbf{11})$. Whatever the value of x is, the zero in the middle of $00x$ will turn into 1. At the end, we obtain the sequence $\mathbf{101}$.

Case B: $101x$.

$$\mathbf{101}x. \qquad \text{(0TS)}$$

For **Case B**, the sequence **101** is already established.

Case C: $110x$.

$$110x \to 100x \to \mathbf{101}x. \qquad \text{(2TS)}$$

For **Case C**, one has initially $110x$. Let's start with the first three digits. The first digit is fixed. The next digit, 1, turns into 0. This is because the configuration says that $(110) \to (1\mathbf{0}0)$. The next three digits are $10x$. Two configurations containing $10x$ are $(100) \to (1\mathbf{0}0)$ and $(101) \to (1\mathbf{0}1)$. No matter what the value of x will be, the 0 in the middle of $10x$ will stays the same. Thus, we obtain $100x$. We need one more procedure in order to reach $\mathbf{101}x$. The first digit is fixed. The next digit of $100x$, 0, remains as it is. This is because the configuration says that $(100) \to (1\mathbf{0}0)$. The next three digits are $00x$. Two configurations containing $00x$ are $(000) \to (0\mathbf{1}0)$ and $(001) \to (0\mathbf{1}1)$. No matter what the value of x will be, the 0 in the middle of $00x$ will turn into a 1. Thus, we obtain the sequence **101**.

Case D: $111x$.

$$111x \to 100x \to \mathbf{101}x. \qquad \text{(2TS)}$$

For **Case D**, one has initially $111x$. Let's start with the first three digits. The first digit is fixed. The next digit, 1, turns into 0. This is because the configuration says that $(111) \to (1\mathbf{0}1)$. The next three digits are $11x$. Two configurations containing $11x$ are $(110) \to (1\mathbf{0}0)$ and $(111) \to (1\mathbf{0}1)$. No matter what the value of x will be, the 1 in the middle of $11x$ will change into a 0. Thus, we obtain $100x$. We need one more procedure in order to reach $\mathbf{101}x$. The first digit is fixed. The next digit of $100x$, 0, remains as it is. This is because the configuration says that $(100) \to (1\mathbf{0}0)$. The next three digits are $00x$. Two configurations containing $00x$ are $(000) \to (0\mathbf{1}0)$ and $(001) \to (0\mathbf{1}1)$. No matter what the value of x will be, the 0 in the middle of $00x$ will turn into a 1. Thus, we obtain the sequence **101**.

Cases E-H: For other cases when one has $0xx$, if one starts with $000x$, we will reach $\mathbf{010}x$ with two time-steps. This is similar to case **Case D**, except that one replaces **1** by **0**. For the case when one starts with $001x$, we will reach $\mathbf{010}x$ with two time-steps. This

is similar to **Case C**,except that one replaces the **1** by **0** and the **0** by **1**. If one starts with **010**x, then we already have the sequence **010**x. For the case starting with $011x$, we will reach **010**x one time-step. This is similar to **Case A**, except that one replaces the **1** by **0** and the **0** by **1**.

Concerning the right hand side, one might have either 00 or 11. For the case when one has two 00, the element before the two 00 can be either 0 or 1. If the element before 00 is 0, then one will have a full pattern. This is because the configuration in transition rule 15 says that $(000) \rightarrow (0\mathbf{1}0)$. If the element before 00 is 1, then one will have a broken pattern. This is because, the configuration says that $(100) \rightarrow (100)$. Consider the case when one might have 11 at the end. The element before the two 11 can be either 0 or 1. If the element before 11 is 1, then one will have a full pattern. This is because, the configuration in transition rule 15 says that $(111) \rightarrow (1\mathbf{0}1)$. If the element before 11 is 0, then one will have a broken pattern. This is because, the configuration says that $(011) \rightarrow (0\mathbf{1}\mathbf{1})$.

Thus, the slowest way of formation of periodic structure implies the formation of one stripe during 2 time-steps. Therefore, in the medium containing k elements periodic structure (containing $k/2$ stripes) forms during k iterations. $\square$

We will consider the counterpart of 15 which is 85. We shall write 85 into the configuration rule.

$$85 = \mathbf{01010101}$$

$$(000) \rightarrow (0\mathbf{1}0)$$

$$(001) \rightarrow (0\mathbf{0}\mathbf{1})$$

$$(010) \rightarrow (0\mathbf{1}0)$$

$$(011) \rightarrow (0\mathbf{0}\mathbf{1})$$

$$(100) \rightarrow (1\mathbf{1}0)$$

$$(101) \rightarrow (1\mathbf{0}\mathbf{1})$$

$$(110) \rightarrow (1\mathbf{1}0)$$

$$(111) \to (1\mathbf{0}1)$$

PROPOSITION 2. *For **rule 85**, starting from any initial conditions in the chain of k elements, we will end up with two-periodic structures (...101010 or ...010101) coming from the right which appears during k iterations. The final stationary sequence may have either 00 or 11 on the left hand side.* ∎

Proof. We have noted that under the transition rule 85, periodic pattern forms first on the right and then expand over the chain from the right to the left. Therefore, we will consider various initial combinations occurring on the right side of the chain and analyse how they allow the growth of the periodic structure to the left. Let's consider four cases starting with the first digit 0 on the right of the structure.

Case A: $x000$.

$$x000 \to x110 \to x\mathbf{101}. \qquad \text{(2TS)}$$

For **Case A**, one has initially $x000$ (x is either black or white, black, black, black). Let's start with the last three digits. The last digit, 0, is fixed. The next digit from right to left, 0, turns into 1. This is because the configuration says that $(000) \to (0\mathbf{1}0)$. The next three digits from right to left are $x00$. Two configurations containing $x00$ are $(100) \to (1\mathbf{1}0)$ and $(000) \to (0\mathbf{1}0)$. Whatever the value of x is, the zero in the middle of $x00$ will turn into 1. Thus, we have $x110$. We need to repeat the procedure in order to reach **010**. The last digit, 0, is fixed. The next digit from right to left, $x110$, 1, remains as it is. This is because the configuration says that $(110) \to (1\mathbf{1}0)$. The next three digits from right to left are $x11$. Two configurations containing $x11$ are $(011) \to (0\mathbf{0}1)$ and $(111) \to (101)$. Whatever the value of x is, the one in the middle of $x11$ will turn into 0. Thus, we have the sequence **010**.

Case B: $x010$.

$$x\mathbf{010}. \qquad \text{(0TS)}$$

For **Case B**, the sequence **010** is already established.

Case C: $x100$.

101

$$x100 \rightarrow x110 \rightarrow x\mathbf{010}. \qquad \text{(2TS)}$$

For **Case C**, one has initially $x100$. Let's start with the last three digits. The last digit, 0, is fixed. The next digit from right to left, 0, changes to 1. This is because the configuration says that $(100) \rightarrow (1\mathbf{1}0)$. The next three digits from right to left are $x10$. Two configurations containing $x10$ are $(010) \rightarrow (0\mathbf{1}0)$ and $(110) \rightarrow (1\mathbf{1}0)$. Whatever the value of x is, the one in the middle of $x10$ will remain 1. Thus, we obtain $x110$. We need to repeat the procedure in order to get **010**. The last digit, 0, is fixed. The next digit from right to left of $x110$, 1, remains as it is. This is because the configuration says that $(110) \rightarrow (1\mathbf{1}0)$. The next three digits from right to left are $x11$. Two configurations containing $x11$ are and $(011) \rightarrow (0\mathbf{0}1)$ and $(111) \rightarrow (1\mathbf{0}1)$. Whatever the value of x is, the one in the middle of $x11$ will turn into 0. Thus, we have the sequence **010**.

Case D: $x110$.

$$x110 \rightarrow x\mathbf{010}. \text{ (1TS)}$$

For **Case D**, one has initially $x110$. Let's start with the last three digits. The last digit, 0, is fixed. The next digit from right to left, 1, remains the same. This is because, the configuration says that $(110) \rightarrow (1\mathbf{1}0)$. The next three digits from right to left are $x11$. Two configurations containing $x11$ are $(011) \rightarrow (0\mathbf{0}1)$ and $(111) \rightarrow (1\mathbf{0}1)$. Whatever the value of x is, the one in the middle of $x11$ will change to 0. At the end, we obtain the sequence **010**.

Cases E-H: For other cases when $xx1$, if one starts with $x001$, we will reach $x101$ with one time-step. This is similar to **Case D**, except that one replaces the **1** by **0** and the **0** by **1**. For the case when one has $x011$, we will reach $x\mathbf{101}$ with two time-steps. This is similar to **Case C**, except that one replaces the **1** by **0** and the **0** by **1**. If one starts with $x101$, then we already have the sequence $x\mathbf{101}$. For the case starting with $x111$, we will reach $x\mathbf{101}$ with two time-steps. This is similar to **Case A**, except that one replaces the **0** by **1**.

Concerning on the left hand side, one might have either 00 or 11. The proof will be similar to transition rule 15 except that, one starts from the right hand side. $\qquad \square$

Let's consider transition rule 30. We shall write 30 into the configuration rule.

$$30 = \mathbf{0001110}$$

$$(000) \rightarrow (0\mathbf{0}0)$$

$$(001) \rightarrow (0\mathbf{11})$$

$$(010) \rightarrow (0\mathbf{1}0)$$

$$(011) \rightarrow (0\mathbf{11})$$

$$(100) \rightarrow (\mathbf{11}0)$$

$$(101) \rightarrow (1\mathbf{0}1)$$

$$(110) \rightarrow (1\mathbf{0}0)$$

$$(111) \rightarrow (1\mathbf{0}1)$$

PROPOSITION 3. *For **rule 30**, starting from any initial conditions in the chain of k elements, we will end up with two-periodic structures (101010... or 010101...) which appears from left to right during 4.5k iterations. The final sequence may have irregularity or even oscillations of the second rightmost element in the sequence.* ∎

Proof. For the trivial case $0000\ldots0\ldots0$ - nothing happens, that is rule 30 does not give periodic structure from this initial condition. Any configuration $0000\ldots01xxx$, where the first occurrence of **1** is on n^{th} location ($n > 1$), transfers into $\mathbf{010}xxxx$, (where first and third elements in the chain are **0** and the second is **1**), after $(n-1)$ time steps.

For the case when $n = 2$, **010** is already established and 011 transfers into **010** in one time-step.

For the case when $n = 3$, the number of time-steps to reach $\mathbf{010}x$ is 2.

$$001xxx \rightarrow 01xxx \rightarrow \mathbf{010}x. \qquad \mathbf{2TS}$$

103

Let us use mathematical induction. Assume that the statement is true for $n = i$. Then, let us prove the statement for the case $n = i + 1$.

$$000 \ldots 0\mathbf{1}xxx,$$

where the digit $\mathbf{1}$ is in position $i + 1$. Then

$$000 \ldots 0\mathbf{1}xxx \rightarrow 000 \ldots \mathbf{1}1xxx.$$

At one time-step, the digit 1 will be at position n. But according to the previous case ($n = i$), we require $(n - 1)$ time-step to reach $\mathbf{010}$. In total, we need $(n - 1 + 1 = n)$ time-steps.

For any initial condition starting with $1xx$, see appendix G.

Concerning the right hand side, one might have oscillation. This is because, the configuration in transition rule 30 says that $(100) \rightarrow (110)$ and $(110) \rightarrow (100)$. Also, one might have an irregularity (e.g. 11 at the end). This is because, if the element before the 11 is 0 the configuration says that $(011) \rightarrow (011)$. If the element before the 11 is 1, one will have a full pattern since the configuration says that $(111) \rightarrow (101)$. $\qquad\square$

Consideration for the transition rule 86 shows that it is very similar to the rule of 30 except, for transition rule 86, the pattern forms from the other direction. Therefore, we can make the following proposition.

PROPOSITION 4. *For **rule 86**, starting from any initial conditions in the chain of k elements, we will end up with two-periodic structures ($\ldots 101010$ or $\ldots 010101$) which appears from right to left during $4.5k$ iterations. The final sequence may have irregularity or even oscillations of the second leftmost element in the sequence.* $\qquad\blacksquare$

Proof. For the trivial case $0000 \ldots 0 \ldots 0$ - nothing happens, that is rule 86 does not give periodic structure from this initial condition. Any configuration $xxx\mathbf{1}0 \ldots 000$, where the first occurrence of $\mathbf{1}$ is on n^{th} location ($n > 1$), transfers into $xxxx\mathbf{010}$, (where on the right side, first and third elements in the chain are $\mathbf{0}$ and the second is $\mathbf{1}$), after $(n - 1)$ time-steps. For any initial condition starting with $xx1$, the proof will be similar to rule 30 except that we start from the right hand side.

Concerning the left hand side, the proof will be analogous to 30 except that for 86, we are dealing with the left hand side. $\square$

For the two remaining transition rules (135 and 149) which cause the formation of stationary periodic structures, we can make the following propositions.

PROPOSITION 5. *For **rule 135**, starting from any initial conditions in the chain of k elements, we will end up with two-periodic structures (101010... or 010101...) which appears from left to right during $4.5k$ iterations. The final sequence may have irregularity or even oscillations of the second rightmost element in the sequence.* $\blacksquare$

Proof. For the trivial case $1111\ldots 1\ldots 1$ - nothing happens, that is rule 135 does not give periodic structure from this initial condition. Any configuration $1111\ldots 10xxx$, where the first occurrence of **0** is on n^{th} location ($n > 1$), transfers into $\mathbf{101}xxxx$, (where first and third elements in the chain are **1** and the second is **0**), after ($n-1$) time steps. The proof is similar to transition rule 30 except that, we replace **1** by **0**. This is also valid for any initial condition starting with $0xx$. Concerning the right hand side, the proof will be similar to 30 except that in rule 135, one replaces the **1** by **0**.

Concerning the right hand side, the proof will be similar to 30 except that in rule 135, one replaces the **1** by **0**. $\square$

PROPOSITION 6. *For **rule 149**, starting from any initial conditions in the chain of k elements, we will end up with two-periodic structure (...101010 or ...010101) which appears from right to left during $4.5k$ iterations. The final sequence may have irregularity or even oscillations of the second leftmost element in the sequence.* $\blacksquare$

Proof. For the trivial case $1111\ldots 1\ldots 1$ - nothing happens, that is rule 149 does not give periodic structure from this initial condition. Any configuration $xxx01\ldots 111$, where the first occurrence of **0** is on n^{th} location ($n > 1$), transfers into $xxxx\mathbf{101}$, (where on the right side, first and third elements in the chain are **1** and the second is **0**), after ($n-1$) time-steps. For any initial condition starting with $xx0$ the proof will be similar to rule 86 except we replace **1** by **0**. Concerning the left hand side, the proof will be similar to 86 except that in rule 149, one replaces the **1** by **0**. $\square$

We have proved that all four transitions can form two-periodic structure of the form $(101010\ldots$ or $010101\ldots)$. The differences between 30, 86, 135 and 149 are: 86 forms the patterns from the other direction compared to 30. For the case of 135, if one has initially all **1** then nothing happens. But if there is at least one **0** on the nth position, then it transfers into **101**$xxxx$, (where first and third elements in the chain are **1** and the second is **0**), after $(n-1)$ time-steps. For the cases of 30 and 86, it's the opposite way. For the case of 149, if one has initially all **1**, then nothing happens. But if there is at least one **0** on the nth position, then it transfers into $xxxx$**101**, (where the first and the third elements on the right side of the chain are **1** and the second is **0**), after $(n-1)$ time-steps. This is opposite to 135.

4.4.1 Formation of three-periodic stationary structures in the general cellular automata (two-state model)

The previous results have been obtained with periodicity of 2 of the two-state model. With a periodicity of 3, the following results have been obtained.

With initial periodic conditions shown on Figure 4.4, 32 transition rules conserve 2 blacks and 1 white (see Figure 4.4). These transition rules are given by the following numbers:

4, 5, 12, 13, 36, 37, 44, 45, 68, 69, 76, 77, 100, 101, 108, 109, 132, 133, 140, 141, 164, 165, 172, 173, 196, 197, 204, 205, 228, 229, 236 and 237.

Figure 4.4: **Three-periodic pattern in two states (two blacks and one white)**

All of these numbers have a binary expression in the form of

$$xxx\mathbf{0}x\mathbf{10}x$$

Configuration 1: $(001) \to (00\mathbf{1})$

Configuration 2: $(010) \to (0\mathbf{1}0)$

Configuration 4: $(100) \to (\mathbf{1}00)$

32 transition rules conserve 2 whites and 1 black (see Figure 4.5). These transition rules are given by the following numbers:

72, 73, 74, 75, 76, 77, 78, 79, 88, 89, 90, 91, 92, 93, 94, 95, 200, 201, 202, 203, 204, 205, 206, 207, 216, 217, 218, 219, 220, 221, 222 and 223.
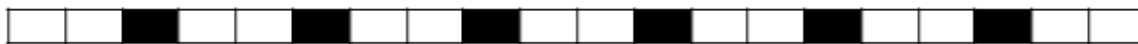
Figure 4.5: **Three-periodic pattern in two states (two whites and one black).**

They have in common the binary expression in the form of

$$x\mathbf{10}x\mathbf{1}xxx$$

Configuration 3: $(011) \rightarrow (0\mathbf{11})$

Configuration 5: $(101) \rightarrow (\mathbf{1}0\mathbf{1})$

Configuration 6: $(110) \rightarrow (\mathbf{11}0)$

Starting from random initial periodic solutions, there are four transition rules which can produce 3−periodic patterns. These simulations have shown that such transition rules exist and given by the following numbers:

45, 75, 89 and 101.

The transition rules 45 and 75 produce 3-periodic stationary pattern from left to right. And transition rules 89 and 101 produce 3-periodic stationary pattern from right to left. Transition rules 45 and 101 produce 2 blacks and 1 white patterns. And transition rules 75 and 89 produce 2 whites and 1 black patterns.

4.4.2 General comment on periodic patterns in two-state model

Above we have considered in details two- and three- periodic structures forming in two-state model. Simulations indicated that no structures of higher periodicity can form in this model. Our analysis of this phenomenon brought to the following proposition.

PROPOSITION 7. *The maximum periodicity for stationary patterns forming in two-state model is 3.* ∎

Proof. First, we will prove that 4-periodic structures can't be stationary in this model. Let's consider the following 4-periodic patterns:

$$a_1 a_2 a_3 a_4 a_1 a_2 a_3 a_4 \ldots,$$

where the above elements can be either 0 or 1. We have 16 possible cases for 4-periodicity in two states. These are as follows:

0000, 0001, 0010, 0011, 0100, 0101, 0110, 0111, 1000, 1001, 1010, 1011, 1100, 1101, 1110 and 1111.

For the first and last cases (0000 and 1111), these are trivial and essentially not periodic. They are not interesting. For the cases 0101 and 1010, these are the two-periodicity elements. For the cases 0001, 0010, 0100, 0111, 1000, 1110, 1101 and 1011, these are acceptable. Now, for the last four cases which are 0011, 0110, 1100 and 1001, theses can be represented as

$$(0011)^n \text{ or } (0001)^n,$$

where n gives the number of recurrence of the sequence in the brackets. Let's consider the first case and look into the part of the sequence containing two periods 00110011. The first three digits from left to right are 001. Between 0 and 1, one has 0. The next three digits from left to right are 011. Between 0 and 1, one has 1. This is a contradiction to the fact that between 0 and 1, one has 0 in the middle. Let's consider the second case ($00010001xxx$). The first three digits from left to right are 000. Between 0 and 0, one has 0. The next three digits from left to right are 001. Between 0 and 1, one has 0. So, this is fine. The next three digits from left to right are 010. Between 0 and 0, one has

1. This contradicts the fact that between 0 and 0, one has 0 in the middle. The same argument applies for 5- or more-periodicity. □

In summary, for the two-state model, the following have been noticed: the initial condition and the level of noise affect the number of transition rules leading to the periodic stationary patterns. Without noises, two transition rules (15 and 85) converge faster to the periodic stationary patterns than the others. The increase of the periodicity of the solution reduces the number of transition rules.

4.5 Three-state model

The two-state model is expanded to allow three or more states per cell. The transitions in a chain of logically elements having three states are given by a set of 27 configurations, as each cell in the triple (considered cell and its two neighbours) has three possible states (black, grey and white that is 0, 1 and 2 respectively). The three-state system can have a periodicity of 3. One example is shown in Figure 4.6.

Figure 4.6: **Pattern with periodicity of 3 in three-state model.**

The three-state model gives the 27 following configurations:

Configuration 0: $(000) \rightarrow (0\boldsymbol{S_0}0)$

Configuration 1: $(001) \rightarrow (0\boldsymbol{S_1}1)$

Configuration 2: $(002) \rightarrow (0\boldsymbol{S_2}2)$

Configuration 3: $(010) \rightarrow (0\boldsymbol{S_3}0)$

Configuration 4: $(011) \rightarrow (0\boldsymbol{S_4}1)$

Configuration 5: $(012) \rightarrow (0\boldsymbol{S_5}2)$

Configuration 6: $(020) \rightarrow (0\boldsymbol{S_6}0)$

Configuration 7: $(021) \rightarrow (0\boldsymbol{S_7}1)$

$$\text{Configuration 8:} \quad (022) \rightarrow (0\boldsymbol{S_8}2)$$

$$\text{Configuration 9:} \quad (100) \rightarrow (1\boldsymbol{S_9}0)$$

$$\text{Configuration 10:} \quad (101) \rightarrow (1\boldsymbol{S_{10}}1)$$

$$\text{Configuration 11:} \quad (102) \rightarrow (1\boldsymbol{S_{11}}2)$$

$$\text{Configuration 12:} \quad (110) \rightarrow (1\boldsymbol{S_{12}}0)$$

$$\text{Configuration 13:} \quad (111) \rightarrow (1\boldsymbol{S_{13}}1)$$

$$\text{Configuration 14:} \quad (112) \rightarrow (1\boldsymbol{S_{14}}2)$$

$$\text{Configuration 15:} \quad (120) \rightarrow (1\boldsymbol{S_{15}}0)$$

$$\text{Configuration 16:} \quad (121) \rightarrow (1\boldsymbol{S_{16}}1)$$

$$\text{Configuration 17:} \quad (122) \rightarrow (1\boldsymbol{S_{17}}2)$$

$$\text{Configuration 18:} \quad (200) \rightarrow (2\boldsymbol{S_{18}}0)$$

$$\text{Configuration 19:} \quad (201) \rightarrow (2\boldsymbol{S_{19}}1)$$

$$\text{Configuration 20:} \quad (202) \rightarrow (2\boldsymbol{S_{20}}2)$$

$$\text{Configuration 21:} \quad (210) \rightarrow (2\boldsymbol{S_{21}}0)$$

$$\text{Configuration 22:} \quad (211) \rightarrow (2\boldsymbol{S_{22}}1)$$

$$\text{Configuration 23:} \quad (212) \rightarrow (2\boldsymbol{S_{23}}2)$$

$$\text{Configuration 24:} \quad (220) \rightarrow (2\boldsymbol{S_{24}}0)$$

$$\text{Configuration 25:} \quad (221) \rightarrow (2\boldsymbol{S_{25}}1)$$

$$\text{Configuration 26:} \quad (222) \rightarrow (2\boldsymbol{S_{26}}2).$$

Each transition rule can be characterised by a number to the base of 3
$$\boldsymbol{S_{26}S_{25}S_{24}S_{23}S_{22}S_{21}S_{20}S_{19}S_{18}S_{17}S_{16}S_{15}S_{14}S_{13}S_{12}S_{11}S_{10}S_9S_8S_7S_6S_5S_4S_3S_2S_1S_0}$$
which varies from 0 to $3^{27} - 1$ (3^{27}).

Similarly, we want to find which transition rules do not destroy existing patterns which is shown in Figure 4.6. The results are as follows. Starting with initial periodic solution, $2\,(3^{24})$ transition rules out $3^{27}(4.7\%)$ wouldn't destroy it. Their expression in base 3 is written in the form of

$$XXXXXXX0XXX2XXXXXXXXXX1XXXXX$$

or

$$XXXXX1XXXXXXXXXX0XXX2XXXXXXX$$

where X can be 0, 1 or 2.

$$\text{Configuration 5:} \quad (012) \to (0\mathbf{1}2)$$

$$\text{Configuration 15:} \quad (120) \to (1\mathbf{2}0)$$

$$\text{Configuration 19:} \quad (201) \to (2\mathbf{0}1)$$

Examples of transition rules for the three-state are: 28698057, 28875204, 10460357577 and 10460889018. Similarly as in the two-state model, this pattern consisting of a repetition of black, grey and white remains the same from one generation to the next.

We found that they are four transition rules, which take three time-steps to produce stripes. These simulations have shown that such transition rules exist and given by the following numbers:

$$387410647, \ 2053045476727, \ 3226214320571 \text{ and } 3812605051931.$$

Transition rules 387410647 and 3812605051931 give periodic stationary patterns from left to right like transition rule 15. And the other two 2053045476727 and 3226214320571 give periodic stationary patterns from right to left like transition rule 85. Let's deal with 387410647.

$$387410647 = \mathbf{000000000222222222111111111}$$

$$(000) \to (0\mathbf{1}0)$$

$$(001) \to (0\mathbf{1}1)$$

$$(002) \to (0\mathbf{1}2)$$

$$(010) \to (0\mathbf{1}0)$$

111

$$(011) \rightarrow (0\mathbf{11})$$

$$(012) \rightarrow (0\mathbf{12})$$

$$(020) \rightarrow (0\mathbf{10})$$

$$(021) \rightarrow (0\mathbf{11})$$

$$(022) \rightarrow (0\mathbf{12})$$

$$(100) \rightarrow (1\mathbf{20})$$

$$(101) \rightarrow (1\mathbf{21})$$

$$(102) \rightarrow (1\mathbf{22})$$

$$(110) \rightarrow (1\mathbf{20})$$

$$(111) \rightarrow (1\mathbf{21})$$

$$(112) \rightarrow (1\mathbf{22})$$

$$(120) \rightarrow (1\mathbf{20})$$

$$(121) \rightarrow (1\mathbf{21})$$

$$(122) \rightarrow (1\mathbf{22})$$

$$(200) \rightarrow (2\mathbf{00})$$

$$(201) \rightarrow (2\mathbf{01})$$

$$(202) \rightarrow (2\mathbf{02})$$

$$(210) \rightarrow (2\mathbf{00})$$

$$(211) \rightarrow (2\mathbf{01})$$

$$(212) \rightarrow (2\mathbf{02})$$

$$(220) \rightarrow (2\mathbf{00})$$

$$(221) \rightarrow (2\mathbf{01})$$

$$(222) \rightarrow (2\mathbf{02}).$$

PROPOSITION 8. *For **rule 387410647**, starting from any initial conditions in the chain of k elements, we will end up with three-periodic structures (012012...or 120120...or 201201...) coming from the left which appears during k iterations.* ∎

Proof. See appendix H □

PROPOSITION 9. *For **rule 3812605051931**, Starting from any initial conditions in the chain of k elements, we will end up with three-periodic structures (021021...or 102102...or 210210...) coming from the left which appears during k iterations.* ∎

Proof. The proof is similar to the case of transition rule 387410647. By considering twenty seven cases starting with the first digit 1 on the left of the structure, some of them will end with three time-steps. The same proofs can be applied for the cases if one starts with the first digit 0 or 2 on the left of the structure. □

PROPOSITION 10. *For **rule 2053045476727**, starting from any initial conditions in the chain of k elements, we will end up with three-periodic structures (...210210 or ...021021 or ...102102) coming from the right which appears during k iterations.* ∎

Proof. By considering 27 cases starting with the first digit 1 on the right of the structure, some of them will end with three time-steps. The same proofs can be applied for the cases if one starts with the first digit 0 or 2 on the right of the structure. □

PROPOSITION 11. *For **rule 3226214320571**, starting from any initial conditions in the chain of k elements, we will end up with three-periodic structures (...120120 or ...201201 or ...012012) coming from the right which appears during k iterations.* ∎

Proof. The proof is similar to the case of transition rule 3226214320571. By considering 27 cases starting with the first digit 1 on the right of the structure, some of them will end

with three time-steps. The same proofs can be applied for the cases if one starts with the first digit 0 or 2 on the right of the structure. ☐

4.6 Four- and more- state models

The transitions in a chain of logically elements having four states are given by a set of 64 configurations. The four-state system can have a maximum periodicity of 6 as shown in Figure 4.7.
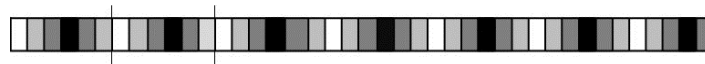
Figure 4.7: **Pattern with periodicity of 6 in 4-state model.**

As the number of state increases, the number of transition rule becomes astronomical. For instance, with the four-state systems, the total number is 4^{64} and with five-state system the total number is 5^{125}. The transition in a chain of logically elements having n states thus would include n^3 configurations and will have in total n^{n^3} . We shall make some preliminary analyses to find interesting transitions. As a guidance, the same methodology as in analysis of two-state system can be used. This permits to make reasonable assumptions on "interesting" sets of rules for n-state systems and therefore to avoid blind simulation of all possible transition sets.

As major findings on cellular automata with higher states, the number of transition rules increases astronomically with the number of states.

4.7 Biological implementations

The results in patterning due to local interactions of logical elements can be used to explain biological pattern formations. Such interactions can represent contact (membrane-to-membrane) interactions between cells in biological tissues resulting into differentiation of cells. For example two-state model can represent chain of locally interacting cells, where cells in state "1" express some particular gene while in state "0" don't (see Figure 4.8). Therefore the modelled interactions can be seen as regulating the differentiation of cells.

The periodic stationary pattern forming in a two-state model represents a chain of cells where each second cell expresses the gene. These patterns can form under various interactions (transitions) from wide range of initial conditions.
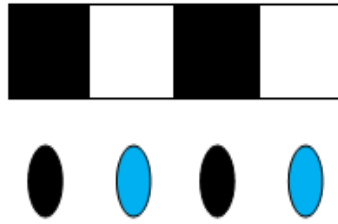
Figure 4.8: **Generation of two-periodic pattern.** *The black stripe has a cell which is not expressed and the white stripe has a cell which is expressed.*
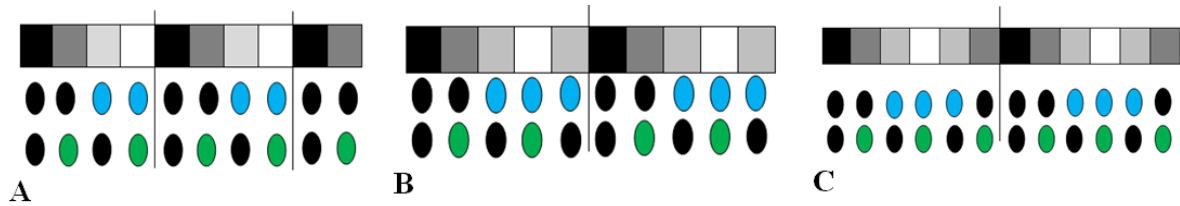
Figure 4.9: **Generation of four-, five- and six-periodic patterns. A:** *The black stripe element has two cells which are not expressed. The dark and light grey stripes have one cell which is expressed and the other one is not. The white stripe has two cells which are expressed.* **B:** *The black stripe element has two cells which are not expressed. The dark and light grey stripes have one cell which is expressed and the other one is not. The white stripe has two cells which are expressed.* **C:** *The black stripe element has two cells which are not expressed. The dark and light grey stripes have one cell which is expressed and the other one is not. The white stripe has two cells which are expressed.*

The three-state model doesn't have direct biological implementation, while the four-state model can be viewed as modelling cells whose differentiation is associated with expression of pair of genes. The four-periodic pattern (i.e. 0, 1, 2, 3, 0, 1, 2, 3, ...) or alternating **black, dark grey, light grey** and **white**) can correspond to the following alternation of gene expression (Figure 4.9 panel **A**). The four-state model can have a five-periodic pattern that is 0, 1, 2, 3, 2, 0, 1, 2, 3, 2, ... or alternating **black, dark grey, light grey, white** and **light grey** (see Figure 4.9 panel **B**). The four-state model can also have a six-periodic pattern that is 0, 1, 2, 3, 2, 1, 0, 1, 2, 3, 2, 1, ... or alternating **black, dark grey, light grey, white, light grey** and **dark grey** (see Figure 4.9 panel **C**).

Formation of periodic stationary patterns in four-state model are extremely sensitive to the initial conditions, i.e. these patterns forms only when very special initial conditions are met. This may explain the multi- (four-) level of segmentation in the fly embryo (Figure 1.5). The model can account for interactions between segment polarity genes with specific initial conditions set by above three levels of patterning.

4.8 Summary

The pattern formation which is governed by cell-to-cell interactions has been modelled using a 1-dimensional chain of logical element. A cell is represented by a logical element of the chain. The expression of gene inside the cell defines the state of the logical element. In this model, the cells interact with two closest neighbours according to a set of rules. This model can be applied to simulate pattern formation in some biological systems including segmentation. It allows the modelling of stationary patterns forming in one dimensional chain of cells. The findings are as follows.

With a two-state model, the transition is characterised by a binary number which varies from 0 to 255 which means, there are 256 transitions. 64 out of these 256 transitions gave periodic stationary patterns using fixed initial conditions (preset stationary patterns are not destroyed). Out of these 64 transitions, 25 are resistive to noise which represents the external effect to the cells. Out of these 64 transitions, there were 6 which gave periodic stationary patterns using random initial conditions. According to the initial condition, the patterning can start from either side. Also, the initial condition affects the timescale of the pattern formation.

For three-state model, a few transitions can produce three-periodic patterns. However, they don't have any direct biological implementation. Four-state model can be viewed as modelling cells whose differentiation is associated with expression of pair of genes. The allowance of multi-gene in a cell can be specified by four or more states. For instance, four-state model expresses the presence of a pair of genes. All of these multi-state models might exhibit stationary patterns.

Chapter 5

Conclusion and discussion

This thesis is devoted to study of scaling properties of morphogenetic patterns. For pattern formations in biological systems, the robustness with respect to the developmental conditions is an important property. One of the particularities of robustness is the scaling with the size of developing object. This has been demonstrated experimentally in fly and sea urchin embryos [55, 36]. Also, recent observations [74] confirm that scaling of biological patterns takes place at the echelon of morphogen gradients. Biological pattern formations have been the subject of extensive research for many decades (since Turing's work in 1952). Many research groups are working towards revealing the mechanisms underlying robustness and scaling of biological patterns. In this thesis, a few hypothetical mechanisms of scaling which can take place during morphogenetic patterning and differentiation of cells in tissues have been explored. It was proposed that scaling in continuous systems can take place due to interplay of morphogens such that the level of one morphogen depends on the size of the medium and it modifies the kinetics of another morphogen in a way that the second scales. Correspondingly, modifications of diffusion/decay and Turing-type models have been designed (in chapters 2 and 3) such that their solutions scale with the medium size. Also, we have designed a discrete-type model (chapter 4) which relates the properties of patterns to number of interacting entities (i.e. number of nuclei in fly oocyte) so that the forming patterns scale with the number of interacting entities rather than with the physical size of the object and therefore insensitive to the size (i.e. scale).

5.1   Summary

The motivation of chapter 2 was to modify the diffusion/decay model such that its exponential solution scales. This chapter is started with the analysis of scaling properties of exponential profiles forming in simple diffusion/decay systems. We have shown that

with the Dirichlet boundary condition, scaling occurs under certain conditions. For the case of Neumann, the solution does not exhibit any scaling property. From the Neumann boundary condition result, a new model called Scaling of exponential profile has been derived. The analysis of the morphogens in annihilation model, where both variables have the same diffusion and decay coefficients, has shown some scaling property. For the nuclear trapping model, we found out that the solution for the case of mixed boundary condition scales under some conditions. But for the case of Neumann boundary condition, the solution doesn't scale. This contradicts to the result of [96] since he claims that the solution can scale.

The main mechanism of scaling studied in the 2nd chapter can be summarised as the following. There is a morphogen which is produced in a region of fixed size with a constant rate and this rate doesn't depend on the size of the tissue. This morphogen is degraded everywhere in the tissue with a functional rate which also doesn't depend on the size of the medium (however, the overall degradation rate as an integral over the medium will increase with the size of the medium). In addition, this morphogen diffuses quickly enough to maintain roughly constant level all over the tissue and this level is inversely proportional to the medium size. This morphogen affects the kinetics rates of another morphogen (also forming diffusion/decay system) responsible for patterning in the tissue and therefore, the kinetics of the morphogen depends on the size of the tissue. By tuning the interactions between morphogens, we can get the kinetics rate which is inversely proportional to the size of the medium and then the forming morphogenetic pattern scale perfectly well

The motivation of chapter 3 was to modify the Turing and FHN models in order that scaling occurs i.e. the number of stripes is the same for two medium sizes. In this chapter, the investigations were carried out with the original Turing model and FHN model. The extension of the Turing model with addition of cubic terms prevents the concentrations going to infinity. Turing patterns have been obtained from stable solution by "turning" on diffusions. The objective is to assess the effects of the size of the medium L and the diffusion of the inhibitor on the number of stripes. A third variable has been included to measure scaling in the Turing model. For the FHN model, oscillating solution can be obtained by shifting up the cubic nullcline. The FHN model is equivalent to the Turing model by removing the second cubic terms in the latter model. In this equivalent model (modified Turing model) without diffusion, Turing patterns have been obtained from oscillating solutions. A third variable is included in the FHN model to allow for scaling.

In chapter 4, the investigations focused on discrete model where the pattern formation is governed by cell-to-cell interactions. The patterning can be affected by the noises and the initial conditions. Also, the initial condition affects the timescale of the pattern formation. The discrete model of pattern formation does consider scaling issue. However, the scale of patterning (special periodicity) is related to the number of cells in the chain rather than to cell sizes or size of the embryo.

5.2 Comparison of our definition for scaling factor with others

In term of scaling, many indications show that it is based on the discrete nature (with discrete entities represented by cells or nuclei) of biological objects. Some of the mathematical models presented exhibit the scaling property (French Flag for instance) but others do not satisfy this property (models allowing exponential profile forming in systems with decay or Turing patterns). Following the investigation on how scaling is considered in a few continuous models, we introduced a new formula of scaling factor (see (5.1)) and tested it in continuous models where analytical formula is not available. For our scaling factor S, the perfect scaling is characterised by $S = 0$. This formula is different from the one proposed by de Lachapelle and Bergmann [23] where the perfect scaling is characterised by $S = 1$. In order to compare our scaling factor with theirs [23], we need to convert theirs in terms of ξ. Their scaling factor in terms of ξ (relative position) is shown in (see (5.2)).

$$S_o = -\left(\frac{\partial u}{\partial L}\right)\left(\frac{\partial u}{\partial \xi}\right)^{-1} \tag{5.1}$$

$$S_L = -\left(\frac{\partial u}{\partial L}\right)\left(\frac{\partial u}{\partial \xi}\right)^{-1}\frac{L}{\xi}. \tag{5.2}$$

Our formula (5.1) does not show a singularity at $\xi = 0$ (S tends towards infinity) which is not the case for (5.2). Furthermore, for two symmetric profiles from two different lengths, the scaling factor should be symmetric (see Figure 5.1). Consequently, our definition of scaling factor (implying that perfect scaling correspond to $S = 0$) seems to be more suitable for analysis of the concentration profiles.
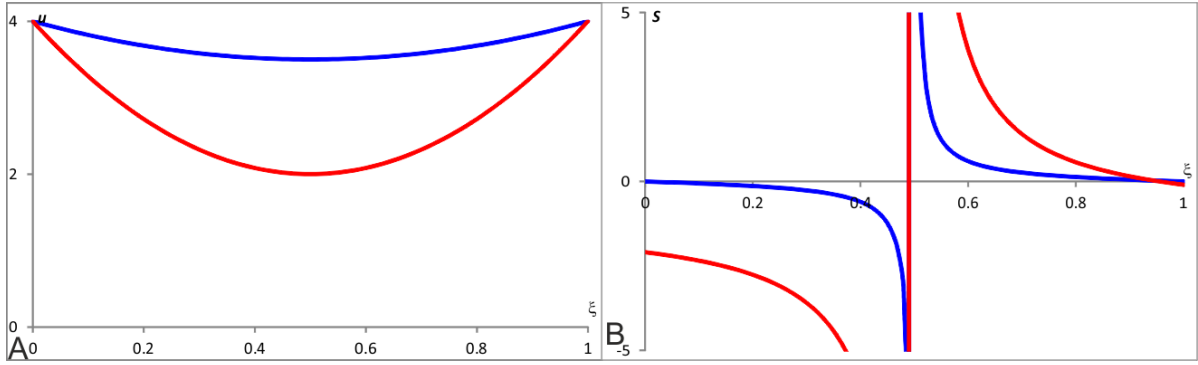
Figure 5.1: **Two quadratic profiles u=0.5ξL²(ξ-1)+4 for different values of L and plots of the scaling factors for the quadratic profiles of u. A:** *The blue and red profiles are for L=2 and L=4 respectively.* **B:** *The blue curve indicates our scaling factor and the red curve indicates [23] scaling factor. In panel **A**, we have symmetric profiles. Our scaling factor, calculated according to formula (5.1) and shown by blue line on panel **B** is also symmetric, while scaling factor calculated according to (5.2) is not symmetric. The scaling factor at ξ=0.5 is at infinity because the derivative at this point is 0. Furthermore, the scaling factor at both ξ=0 and ξ=1 is zero since the two profiles have the same concentration. Their scaling factor is not symmetric at all. Furthermore, at both ends, their scaling factor has different values. That's why our definition is better than the one which has been done by [23].*

5.3 Application of our result to the segmentation of fly embryo

As discussion, the various mathematical models of pattern formations reported are of two types: continuous one and discrete one. The application of these models to a biological system where the scaling has been demonstrated is very useful to understand the scaling property. The Drosophila embryo is one of the best understood of these biological systems. The development of Drosophila embryo occurs in four levels of patterns (see Figure 1.5). In the first level which consists of the maternity genes, the gradient of Bicoid after fertilisation should be addressed by a continuous reaction-diffusion model (exponential model) (see Figure 5.2). Models analysing possible interactions (mutual influence to decay kinetics) between maternal genes could give some ideas on the mechanisms of 1st level scaling. The scaling of the 2nd and 3rd(and even 4th) levels are, most likely, preconditioned by the scaling in the 1st level. The second level involves the gap genes which spatial patterns are controlled by the maternity genes. A good modelling tool is

provided by the Turing model (see (5.3)).

$$\frac{\partial u}{\partial t} = D_u \frac{\partial^2 u}{\partial x^2} + \left(\gamma\left(au + bv\right) - \alpha_u u^3\right) z^2; \quad \left.\frac{\partial u}{\partial x}\right|_{x=0} = \left.\frac{\partial u}{\partial x}\right|_{x=L} = 0,$$

$$\frac{\partial v}{\partial t} = D_v \frac{\partial^2 v}{\partial x^2} + \left(\gamma\left(cu + dv\right) - \alpha_v v^3\right) z^2; \quad \left.\frac{\partial v}{\partial x}\right|_{x=0} = \left.\frac{\partial v}{\partial x}\right|_{x=L} = 0, \qquad (5.3)$$

$$\frac{\partial z}{\partial t} = D_z \frac{\partial^2 z}{\partial x^2} - k_z z; \quad z(x=0) = z_0, \quad z(x=L) = z_L,$$

where D_u, D_v, and D_z are the diffusion coefficients of u, v and z respectively, k_z defines the degradation rate of z, a, b, c, d, α_u, α_v, γ are parameters and z_0 and z_L specify the boundary values of z at $x = 0$ and $x = L$ respectively. The plot of system (5.3) is shown in Figure 5.2. The third and fourth levels are well described by discrete models. The third level which comprises the pair-rule genes is formed by stripes which are regulated by the gap genes. The two-state discrete model permits the modelling of pair-rule genes patterning (see Figure 4.2). The last genes on the hierarchy are the segment-polarity genes. They consist of fourteen stripes of transcription around each embryo. The four-state discrete model is well suited to describe segment-polarity genes (see Figure 4.7). The logical interactions between cells, which we have explored here, are rather assumed (on the basis of biological observations) to stabilise the fourth level patterning. Therefore, those of explored here transitions which result into stationary patterns should be compared with biological observations on interactions between 4th level genes to support and/or complete those observations.
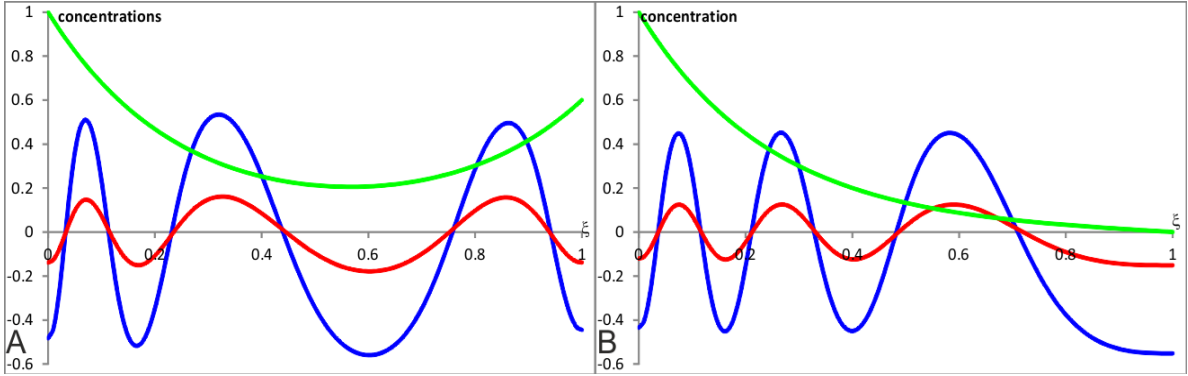
Figure 5.2: **Graph modelling the first and second level of the fly embryo development.** *The first level consisting of the maternity genes can be shown by the green curve. The second level involving the gap genes is represented by the blue and red curves. The concentrations u, v and z are represented by the blue, red and green curves respectively. Zero−flux boundary conditions are used for u and v, and Dirichlet boundary condition for z. **A:** The model parameters are as follows: $D_u=1$, $D_v=20$, $D_z=50$, $\gamma=0.15$, $k_z=0.02$, $a=1$, $b=-2$, $c=3$, $d=-4$, $z_0=1$, $z_L=0.6$, $\alpha_u=0.1$ and $\alpha_v=0.1$. **B:** The model parameters are as follows: $D_u=1$, $D_v=20$, $D_z=50$, $\gamma=0.2$, $k_z=0.02$, $a=1$, $b=-2$, $c=3$, $d=-4$, $z_0=1$, $z_L=0.6$, $\alpha_u=0.1$ and $\alpha_v=0.1$.*

5.4 Future works

Concerning stationary patterns forming in FHN model, we have noted that different number of spikes can be initiated in the same medium. For these patterns, the spatial profiles of spikes can be of different width while their amplitude is pretty much the same. This gave us an idea of scaling mechanism which can take place when the stripe should fit a limited space: that is, it is possible that under some conditions the width of the strip is proportional to the space given and therefore scales. To check whether it is true, it is proposed to stimulate a single stripe in the medium of small size and investigate its scaling properties. The size of the medium will be varied.

For the discrete system, we have seen in the previous chapter that 25 out of 64 transitions were resistive to noise. There are two types of noises. The first type is that in some transition, the disturbance to the stationary pattern is extinct locally. We have already considered one example. And the second type is that the noise is expelled by propagation towards their edge of the medium. We will investigate the latter one for future work.

For the 3-periodic in two-state model, we saw that there were 32 out of 256 transitions which would conserve 3-periodic stationary pattern stating from initial 3-periodic solutions. But there were only 4 out of these 32 transitions which would exhibit patterns stating from random initial condition. Some initial conditions give patterns and some do not. This requires extensive research.

For the case of 4-state model, we have 4^{4^3} transition rules. This number makes the analysis of 4-state models to be a challenging task. One way in approaching this problem would be by reducing the problem to that in two-state system. That is, the state of an element in 4-state system can be represented by a state of two elements each taken from one of two two-state systems. That is, the sequence formed by 4-state elements $(e_1, e_2, \ldots, e_n)$ can be represented by two interlinked sequences of 2-state elements $(e_1 = (x_1, y_1), e_2 = (x_2, y_2), \ldots, e_n = (x_n, y_n))$ as shown in Figure 5.3. The simplest case to analyse is represented by rules such that they are represented by a pair of rules for 2-state systems, i.e.x_n is affected only by $x_n - 1$ and $x_n + 1$ and y_n is only affected by $y_n - 1$ and $y_n + 1$. The total amount of such transition rules is 2^9 (which is a tiny fraction for 4^{64} of all possible transition rules).

x_1	x_2	x_3	x_4	x_5	$\cdots$	x_n
y_1	y_2	y_3	y_4	y_5	$\cdots$	y_n

Figure 5.3: **Representation of 4-state (e) elements by two 2-state (x, y) elements.** *The pair (x, y) can have four states: 00, 01, 10 and 11.*

This approach for example can allow us to find out all rules (out of those which can be considered in a given way) resulting into periodic solutions. As pattern in each of the sequences can be 2 or 3 periodic, the combined pattern can only be 2, 3 or 6 periodic. By allowing interactions between elements from different sequences, we can consider other transition rules. This is a large task to be considered in a future work.

Appendix A

One variable systems with decay

The maternal Bicoid mRNA in fly embryo is localised in a small region on its apical side and the Bicoid protein produced in this region diffusively spreads and decays along the entire embryo (Figure 1.9 is an illustration of this system). Here, we show that when the area of the production is small, we can replace it by a boundary flux at $x = 0$ in which this will be derived in this appendix.

For $\boldsymbol{0 < x < a}$, we have

$$D\frac{d^2C}{dx^2} + p - kC = 0. \tag{A.1}$$

For $\boldsymbol{a \leq x < L}$, we have

$$D\frac{d^2C}{dx^2} - kC = 0. \tag{A.2}$$

The solutions of the equations (A.1) and (A.2) are given respectively by $C_1(x)$ and $C_2(x)$.

$$C(x) = \begin{cases} C_1(x) = Ae^{x\lambda} + Be^{-x\lambda} + \frac{p}{k}, & 0 < x < a \\ C_2(x) = Ee^{x\lambda} + Fe^{-x\lambda}, & a \leq x < L, \end{cases} \tag{A.3}$$

where $\lambda = (k/D)^{1/2}$. Since we have four unknowns, we need four conditions. Two conditions are the boundary fluxes at $x = 0$ and $x = L$: $(C_1(x = 0))' = 0$ and $(C_2(x = L))' = 0$. The other two conditions are the continuity, i.e. $C_1(x) = C_2(x)$ and the derivatives i.e. $(C_1(x))' = (C_2(x))'$ at $x = a$. First, we shall differentiate both solutions.

$$\frac{dC_1(x)}{dx} = A\lambda e^{x\lambda} - B\lambda e^{-x\lambda}, \tag{A.4}$$

$$\frac{dC_2(x)}{dx} = E\lambda e^{x\lambda} - F\lambda e^{-x\lambda}. \tag{A.5}$$

We compute equation (A.4) at $x = 0$.

$$\frac{dC_1(x = 0)}{dx} = A - B = 0 \Rightarrow A = B.$$

We compute equation (A.5) at $x = L$.

$$\frac{dC_2(x = L)}{dx} = Ee^{x\lambda} - Fe^{-x\lambda} = 0 \Rightarrow Ee^{x\lambda} = Fe^{-x\lambda} \Rightarrow F = Ee^{2x\lambda}.$$

We use the other two conditions: $C_1(x) = C_2(x)$ and the derivative, $(C_1(x))' = (C_2(x))'$ of the function at $x = a$. We will use the first condition which is $C_1(a) = C_2(a)$ in equation (A.3).

$$Ae^{a\lambda} + Ae^{-a\lambda} + \frac{p}{k} = Ee^{a\lambda} + Ee^{\lambda(2L-a)} \Rightarrow$$

$$A\left(e^{a\lambda} + e^{-a\lambda}\right) + \frac{p}{k} = E\left(e^{a\lambda} + e^{\lambda(2L-a)}\right). \tag{A.6}$$

We shall use the second condition which is $(C_1(a))' = (C_2(a))'$ in equations (A.4) and (A.5).

$$Ae^{a\lambda} - Ae^{-a\lambda} = Ee^{a\lambda} - Ee^{\lambda(2L-a)} \Rightarrow$$

$$A\left(e^{a\lambda} - e^{-a\lambda}\right) = E\left(e^{a\lambda} - e^{\lambda(2L-a)}\right). \tag{A.7}$$

In equation (A.7), E can be written as

$$E = \frac{\left(e^{a\lambda} - e^{-a\lambda}\right)}{e^{a\lambda} - e^{\lambda(2L-a)}}. \tag{A.8}$$

Putting the expression of E into equation (A.6), we have

$$A\left(e^{a\lambda} + e^{-a\lambda}\right) + \frac{p}{k} = \frac{A\left(e^{a\lambda} - e^{-a\lambda}\right)\left(e^{a\lambda} + e^{\lambda(2L-a)}\right)}{e^{a\lambda} - e^{\lambda(2L-a)}} \Rightarrow$$

$$A\left(e^{a\lambda} + e^{-a\lambda}\right) - \frac{A\left(e^{a\lambda} - e^{-a\lambda}\right)\left(e^{a\lambda} + e^{\lambda(2L-a)}\right)}{e^{a\lambda} - e^{\lambda(2L-a)}} = -\frac{p}{k} \Rightarrow$$

$$A\left(\left(e^{a\lambda} + e^{-a\lambda}\right) - \frac{\left(e^{a\lambda} - e^{-a\lambda}\right)\left(e^{a\lambda} + e^{\lambda(2L-a)}\right)}{e^{a\lambda} - e^{\lambda(2L-a)}}\right) = -\frac{p}{k} \Rightarrow$$

$$A\left(\frac{\left(e^{a\lambda} + e^{-a\lambda}\right)\left(e^{a\lambda} - e^{\lambda(2L-a)}\right) - \left(e^{a\lambda} - e^{-a\lambda}\right)\left(e^{a\lambda} - e^{\lambda(2L-a)}\right)}{e^{a\lambda} - e^{\lambda(2L-a)}}\right) = -\frac{p}{k} \Rightarrow$$

$$A = \left(\frac{2 - 2e^{a\lambda + \lambda(2L-a)}}{e^{a\lambda} - e^{\lambda(2L-a)}}\right) = -\frac{p}{k} \Rightarrow$$

$$A = \left(\frac{2 - 2e^{2L\lambda}}{e^{a\lambda} - e^{\lambda(2L-a)}} \right) = -\frac{p}{k} \Rightarrow$$

$$A = B = -\frac{p\left(e^{a\lambda} - e^{\lambda(2L-a)}\right)}{k\left(2 - 2e^{2L\lambda}\right)}.$$

We need to compute the expression of E.

$$E = -\frac{p\left(e^{a\lambda} - e^{-a\lambda}\right)}{2k\left(1 - e^{2L\lambda}\right)}.$$

We already know that

$$F = Ee^{2L\lambda} = -\frac{p\left(e^{a\lambda} - e^{-a\lambda}\right)}{2k\left(1 - e^{2L\lambda}\right)}e^{2L\lambda}.$$

In summary, the expressions of A, B, E and F are as follows

$$A = B = -\frac{p\left(e^{a\lambda} - e^{\lambda(2L-a)}\right)}{2k\left(1 - e^{2L\lambda}\right)},$$

$$E = -\frac{p\left(e^{a\lambda} - e^{-a\lambda}\right)}{2k\left(1 - e^{2L\lambda}\right)},$$

$$F = -\frac{p\left(e^{a\lambda} - e^{-a\lambda}\right)}{2k\left(1 - e^{2L\lambda}\right)}e^{2L\lambda}.$$

By putting the expressions of A, B, E and F, the solutions of $C_1(x)$ and $C_2(x)$ are written as

$$C_1(x) = -\frac{p\left(e^{a\lambda} - e^{\lambda(2L-a)}\right)}{k\left(2 - 2e^{2L\lambda}\right)}e^{x\lambda} - \frac{p\left(e^{a\lambda} - e^{\lambda(2L-a)}\right)}{k\left(2 - 2e^{2L\lambda}\right)}e^{-x\lambda} + \frac{p}{k},$$

$$C_2(x) = -\frac{p\left(e^{a\lambda} - e^{-a\lambda}\right)}{2k\left(1 - e^{2L\lambda}\right)}e^{x\lambda} - \frac{p\left(e^{a\lambda} - e^{-a\lambda}\right)}{2k\left(1 - e^{2L\lambda}\right)}e^{2L\lambda}e^{-x\lambda}.$$

By simplifying the above solutions, we get

$$C_1(x) = \frac{p}{k}\left(1 - \frac{\left(e^{a\lambda} - e^{\lambda(2L-a)}\right)\left(e^{x\lambda} - e^{-x\lambda}\right)}{2k\left(1 - e^{2L\lambda}\right)}\right),$$

$$C_2(x) = -\frac{p\left(e^{a\lambda} - e^{-a\lambda}\right)\left(e^{x\lambda} - e^{(2L-x)\lambda}\right)}{2k\left(1 - e^{2L\lambda}\right)}.$$

We replace p by p/a in $C_2(x)$.

$$C_2(x) = -\frac{p\left(e^{a\lambda} - e^{-a\lambda}\right)\left(e^{x\lambda} - e^{(2L-x)\lambda}\right)}{2ka\left(1 - e^{2L\lambda}\right)}.$$

As a gets smaller, we use the linear approximations of the exponentials.

$$e^{a\lambda} \approx 1 + a\lambda,$$
$$e^{-a\lambda} \approx 1 - a\lambda.$$

Substituting these linear approximations in $C_2(x)$.

$$C_2(x) \approx -p\lambda \left(\frac{e^{x\lambda} - e^{(2L-x)\lambda}}{k \left(1 - e^{2L\lambda}\right)} \right).$$

Differentiating and symplifying $C_2(x)$.

$$(C_2(x))' = -\frac{p \left(e^{x\lambda} - e^{(2L-x)\lambda}\right)}{D \left(1 - e^{2L\lambda}\right)}.$$

Evaluating $(C_2(x))'$ at $x = 0$ and at $x = L$.

$$(C_2(x))'\big|_{x=0} = -\frac{p \left(1 - e^{2L\lambda}\right)}{D \left(1 - e^{2L\lambda}\right)} = -\frac{p}{D},$$

$$(C_2(x))'\big|_{x=L} = -\frac{p \left(e^{L\lambda} - e^{(2L-L)\lambda}\right)}{D \left(1 - e^{2L\lambda}\right)} = \frac{p \left(e^{L\lambda} - e^{L\lambda}\right)}{D \left(1 - e^{2L\lambda}\right)} = 0.$$

Thus, we have shown that when the area of production, on the left side, is small compared to the medium size, we can replace the internal production by a boundary flux.

Appendix B

Scaling of exponential profile (mechanism 1)

In Section 2.3, we have shown that the solution of u for the case of Neumann boundary condition doesn't scale at all. However, under certain conditions (when the diffusion is too fast or decay is slow) this solution levels up to the value inversely proportional to the medium size. We can use this result for coupling with another variable such that the latter one can be scaled. In chapter 2, the solution of $v(x)$ (see (2.22)) can be approximated by only one exponent. It does scale indeed. In this appendix, we derive the solution (2.22). We introduce a second reaction-diffusion equation for v and we multiply the decay term by u^2 as shown below.

$$D_v \frac{d^2 v}{dx^2} - k_v v u^2 = 0; \quad v(x = 0) = v_0 \quad \frac{dv}{dx}(x = L) = j_v, \tag{B.1}$$

where v_0 is the boundary value at $x = 0$ and j_v is the boundary flux at $x = L$. We already know the approximation of u from section 2.3.2. We can put it into the equation (B.1).

$$D_u \frac{d^2 v}{dx^2} - k_v v \left(\frac{D_u}{k_u L} \right)^2 = 0. \tag{B.2}$$

The solution of (B.2) is written as

$$v = C_1 e^{x\alpha} + C_2 e^{-x\alpha},$$

where C_1 and C_2 are coefficients to be determined and

$$\alpha = \sqrt{\frac{k_v}{D_v} \left(\frac{D_u}{k_u L} \right)^2}.$$

We need to compute the derivative of v in order to use the Neumann boundary condition at $x = L$.

$$v' = C_1 \alpha e^{x\alpha} + C_2 \alpha e^{-x\alpha}.$$

We use the Dirichlet boundary condition at $x = 0$ which is $v(x = 0) = v_0$.

$$v(x = 0) = C_1 + C_2 = v_0. \tag{B.3}$$

We use the Neumann boundary condition which is $v'(x = L) = j_v$.

$$v'(x = L) = j_v \Rightarrow C_1 e^{L\alpha} - C_2 e^{-L\alpha} = \frac{j_v}{\alpha}. \tag{B.4}$$

We can get C_1 from equation (B.3).

$$C_1 = v_0 - C_2. \tag{B.5}$$

We can substitute the expression of C_1 into the equation (B.4).

$$(v_0 - C_2) e^{L\alpha} - C_2 e^{-L\alpha} = \frac{j_L}{\alpha} \Rightarrow$$

$$-C_2 e^{L\alpha} - C_2 e^{-L\alpha} = \frac{j_L}{\alpha} - v_0 e^{L\alpha} \Rightarrow$$

$$-C_2 \left(e^{L\alpha} + e^{-L\alpha} \right) = \frac{j_L - v_0 \alpha e^{L\alpha}}{\alpha} \Rightarrow$$

$$C_2 = -\frac{j_L - v_0 \alpha e^{L\alpha}}{\alpha \left(e^{L\alpha} + e^{-L\alpha} \right)}.$$

We can determine the expression of C_1 in equation (B.5) since we know C_2.

$$C_1 = v_0 + \frac{j_L - v_0 \alpha e^{L\alpha}}{\alpha \left(e^{L\alpha} + e^{-L\alpha} \right)} = \frac{v_0 \left(e^{L\alpha} + e^{-L\alpha} \right) + j_L - v_0 \alpha e^{L\alpha}}{\alpha \left(e^{L\alpha} + e^{-L\alpha} \right)} = \frac{j_L + v_0 \alpha e^{-L\alpha}}{\alpha \left(e^{L\alpha} + e^{-L\alpha} \right)}.$$

In summary, the coefficients C_1 and C_2 are

$$C_1 = \frac{j_L + v_0 \alpha e^{-L\alpha}}{\alpha \left(e^{L\alpha} + e^{-L\alpha} \right)},$$

$$C_2 = -\frac{j_L - v_0 \alpha e^{L\alpha}}{\alpha \left(e^{L\alpha} + e^{-L\alpha} \right)}.$$

The full solution of v is

$$v = \frac{j_L + v_0 \alpha e^{-L\alpha}}{\alpha \left(e^{L\alpha} + e^{-L\alpha} \right)} e^{x\alpha} - \frac{j_L - v_0 \alpha e^{L\alpha}}{\alpha \left(e^{L\alpha} + e^{-L\alpha} \right)} e^{-x\alpha}.$$

This can be simplified to

$$v = \frac{\left(\left(j_L + u_0\alpha e^{-L\alpha}\right)e^{x\alpha} - \left(j_L - u_0\alpha e^{L\alpha}\right)e^{-x\alpha}\right)}{\alpha\left(e^{L\alpha} + e^{-L\alpha}\right)}.$$

We assume that L goes to infinity, Then, v can be approximated by

$$v = \frac{\left(j_L + v_0\alpha e^{-L\alpha}\right)e^{x\alpha} - \left(j_L - v_0\alpha e^{L\alpha}\right)e^{-x\alpha}}{\alpha e^{L\alpha}} \Rightarrow$$

$$v = \frac{\left(j_L + v_0\alpha e^{-L\alpha}\right)e^{x\alpha}}{\alpha e^{L\alpha}} - \frac{\left(j_L - v_0\alpha e^{L\alpha}\right)e^{-x\alpha}}{\alpha e^{L\alpha}} \Rightarrow$$

$$v \approx -\frac{\left(j_L - v_0\alpha e^{L\alpha}\right)e^{-x\alpha}}{\alpha e^{L\alpha}}.$$

Therefore,

$$v \approx v_0 e^{-x\alpha}.$$

By putting back the expression of α, v can be approximated by

$$v \approx v_0 e^{-\xi\frac{D_u}{k_u}\sqrt{\frac{k_v}{D_v}}},$$

where $\xi = x/L$. Under the mixed boundary condition when L is large, the approximation of v is written as a single exponent.

Appendix C

Annihilation model

In this appendix, we show the derivation of the solutions (1.23) and (1.24) discussed in section 1.9.1.

$$\frac{\partial u}{\partial t} = D_u \frac{\partial^2 u}{\partial x^2} - k_u uv, \tag{C.1}$$

$$\frac{\partial v}{\partial t} = D_v \frac{\partial^2 v}{\partial x^2} - k_v uv, \tag{C.2}$$

where D_u and D_v are the diffusion coefficients and k_u and k_v specify the decay rates. D_u, D_v, k_u, and k_v are constants. The boundary conditions are:

$$u(x = 0) = u_0, \qquad u(x = L) = u_L,$$

$$v(x = 0) = v_0, \qquad v(x = L) = v_L.$$

u_0 and v_0 are the boundary values at $x = 0$ and u_L and v_L are the boundary values at $x = L$. We shall focus on stationary state of equations (C.1) and (C.2).

$$D_u \frac{d^2 u}{dx^2} - k_u uv = 0, \tag{C.3}$$

$$D_v \frac{d^2 v}{dx^2} - k_v uv = 0. \tag{C.4}$$

We multiply equation (C.3) and (C.4) respectively by k_v and k_u. This will give

$$k_v D_u \frac{d^2 u}{dx^2} - k_u k_v uv = 0, \tag{C.5}$$

$$k_u D_v \frac{d^2 v}{dx^2} - k_u k_v uv = 0. \tag{C.6}$$

After subtracting equation (C.6) from (C.5), this yields

$$k_v D_u \frac{d^2 u}{dx^2} - k_u D_v \frac{d^2 v}{dx^2} = 0 \Rightarrow$$

$$\frac{d^2 \left(k_v D_u u \right)}{dx^2} - \frac{d^2 \left(k_u D_v v \right)}{dx^2} = 0 \Rightarrow$$

$$\frac{d^2 \left(k_v D_u u - k_u D_v v \right)}{dx^2} = 0.$$

Integrating the above equation twice gives

$$k_v D_u u - k_u D_v v = Ax + B. \tag{C.7}$$

Applying the boundary condition at $x = 0$ in equation (C.7), gives

$$B = k_v D_u u_0 - k_u D_v v_0.$$

Applying the boundary condition at $x = L$ in equation (C.7), gives

$$k_v D_u u_L - k_u D_v v_L = AL + k_v D_u u_0 - k_u D_v v_0.$$

We can get A from the above equation

$$A = \frac{k_v D_u u_L - k_u D_v v_L - k_v D_u u_0 + k_u D_v v_0}{L}.$$

The full solution of equation (C.7) is

$$k_v D_u u - k_u D_v v = \left(k_v D_u u_L - k_u D_v v_L - k_v D_u u_0 + k_u D_v v_0 \right) \left(\frac{x}{L} \right) + k_v D_u u_0 - k_u D_v v_0.$$

We want to simplify the problem by considering $D_u = D_v = D$, $k_u = k_v = k$, $u_L = v_0 = 0$ and $v_L = u_0$ in equations (C.3) and (C.4).

$$D \frac{d^2 u}{dx^2} - kuv = 0, \tag{C.8}$$

$$D \frac{d^2 v}{dx^2} - kuv = 0. \tag{C.9}$$

with the Dirichlet boundary conditions

$$u(x = 0) = u_0, \qquad u(x = L) = 0,$$

$$v(x = 0) = 0, \qquad v(x = L) = u_0.$$

For quantitative analysis, we will consider the sum and the difference of the two morphogens. The addition and subtraction of equations (C.8) and (C.9) lead respectively to

$$D\frac{d^2\left(u+v\right)}{dx^2} - 2kuv = 0, \tag{C.10}$$

$$\frac{d^2\left(u-v\right)}{dx^2} = 0. \tag{C.11}$$

Let $s_+ = u + v$ and $s_- = u - v$. Then, the equations (C.10) and (C.11), in terms of s_+ and s_-, will become

$$\frac{d^2 s_+}{dx^2} = \frac{2k}{D}uv, \tag{C.12}$$

$$\frac{d^2 s_-}{dx^2} = 0. \tag{C.13}$$

The differential equation involving s_+ (see (C.12)) still has a term containing u and v namely uv. So, we shall write uv in terms of s_+ and s_-.

$$uv = \frac{\left(u+v\right)^2 - \left(u-v\right)^2}{4} = \frac{s_+^2 - s_-^2}{4}.$$

As we can see, uv is written as the quarter of the difference of the squares of s_+ and s_-. By putting the expression of uv in terms of s_+ and s_-, the equations containing s_+ and s_- will be

$$\frac{d^2 s_+}{dx^2} = \frac{k\left(s_+^2 - s_-^2\right)}{2D}, \tag{C.14}$$

$$\frac{d^2 s_-}{dx^2} = 0. \tag{C.15}$$

The boundary conditions associated with s_+ and s_- are derived from the boundary conditions associated with u and v. For s_+, the boundary condition at $x = 0$ and $x = L$ is the sum of the boundary condition of u and v at these ends. For s_-, it is the difference of the boundary conditions of u and v at both $x = 0$ and $x = L$.

$$s_+(x = 0) = u(x = 0) + v(x = 0) = u_0, \tag{C.16}$$

$$s_+(x = L) = u(x = L) + v(x = L) = u_0, \tag{C.17}$$

$$s_-(x = 0) = u(x = 0) - v(x = 0) = u_0, \tag{C.18}$$

$$s_-(x = L) = u(x = L) - v(x = L) = -u_0. \tag{C.19}$$

We can integrate equation (C.15) twice.

$$\frac{d^2 s_-}{dx^2} = 0 \Rightarrow s_- = C_1 x + C_2.$$

$$s_- = C_1 x + C_2. \tag{C.20}$$

The solution of s_- (C.20) is a linear profile. We use the boundary conditions involving s_- to determine the constants C_1 and C_2.

$$s_-(x = 0) = u_0 \Rightarrow C_2 = u_0.$$

$$C_2 = u_0$$

$$s_-(x = L) = -u_L \Rightarrow -u_0 = LC_1 + u_0 \Rightarrow -2u_0 = LC_1 \Rightarrow$$

$$C_1 = -\frac{2u_0}{L}.$$

Using the expression of the constants C_1 and C_2, the full solution of s_- is

$$s_- = u_0 \left(1 - 2\frac{x}{L}\right). \tag{C.21}$$

Coming back to (C.13).

$$\frac{d^2 s_+}{dx^2} = \frac{k\left(s_+^2 - s_-^2\right)}{2D}.$$

It is rewritten by putting all the terms containing s_+ on the left hand side. Knowing the expression of s_- (C.21), and after its substitution into (C.14), one has

$$\frac{d^2 s_+}{dx^2} - \frac{k}{2D}s_+^2 = -\frac{k}{2D}u_0^2 \left(1 - 2\frac{x}{L}\right)^2. \tag{C.22}$$

Multiplying both sides by $2D/k$ in equation (C.21) gives

$$\frac{2D}{k}\frac{d^2 s_+}{dx^2} - s_+^2 = -u_0^2 \left(1 - 2\frac{x}{L}\right)^2.$$

Let $\beta = 2\lambda^2$ where $\lambda^2 = k/D$. The above equation can be rewritten as

$$\beta\frac{d^2 s_+}{dx^2} - s_+^2 = -u_0^2 \left(1 - 2\frac{x}{L}\right)^2. \tag{C.23}$$

As s_+ is the sum of two continuous functions u and v (concentrations) in the interval $[0, L]$, it is a continuous function. Since we can't solve (C.23) analytically, we use power series method. s_+ can be approximated by a polynomial function. So, it can be written

as

$$s_+ = \sum_{n=0}^{\infty} s_n \left(1 - 2\frac{x}{L}\right)^n. \tag{C.24}$$

We shall differentiate the above series twice (see C.24).

$$s'_+ = -\left(\frac{2}{L}\right) \sum_{n=1}^{\infty} n s_n \left(1 - 2\frac{x}{L}\right)^{n-1}, \tag{C.25}$$

$$s''_+ = \left(\frac{2}{L}\right)^2 \sum_{n=2}^{\infty} n(n-1) s_n \left(1 - 2\frac{x}{L}\right)^{n-2}. \tag{C.26}$$

We square the power series of s_+ (see C.24).

$$s_+^2 = \left(\sum_{n=0}^{\infty} s_n \left(1 - 2\frac{x}{L}\right)^n\right)^2. \tag{C.27}$$

We write a few terms from expression (C.26).

$$s''_+ = \frac{8s_2}{L^2} + \frac{24s_3}{L^2}\left(1 - 2\frac{x}{L}\right) + \frac{48s_4}{L^2}\left(1 - 2\frac{x}{L}\right)^2 + \frac{80s_5}{L^2}\left(1 - 2\frac{x}{L}\right)^3$$
$$+ \frac{120s_6}{L^2}\left(1 - 2\frac{x}{L}\right)^4 + \frac{168s_7}{L^2}\left(1 - 2\frac{x}{L}\right)^5 + \frac{224s_8}{L^2}\left(1 - 2\frac{x}{L}\right)^6 +$$
$$+ \frac{228s_9}{L^2}\left(1 - 2\frac{x}{L}\right)^7 + \cdots.$$

Similarly, we write a few terms from (C.27).

$$s_+^2 = s_0^2 + 2s_0 s_1 \left(1 - 2\frac{x}{L}\right) + \left(s_1^2 + 2s_0 s_2\right)\left(1 - 2\frac{x}{L}\right)^2 + \left(2s_0 s_3 + 2s_1 s_2\right)\left(1 - 2\frac{x}{L}\right)^3$$
$$+ \left(s_2^2 + 2s_1 s_3 + 2s_0 s_4\right)\left(1 - 2\frac{x}{L}\right)^4 + \left(2s_0 s_5 + 2s_1 s_4 + 2s_2 s_3\right)\left(1 - 2\frac{x}{L}\right)^5$$
$$+ \left(s_3^2 + 2s_0 s_6 + 2s_1 s_5 + 2s_2 s_4\right)\left(1 - 2\frac{x}{L}\right)^6 +$$
$$\left(2s_0 s_7 + 2s_1 s_6 + 2s_2 s_5 + 2s_3 s_4\right)\left(1 - 2\frac{x}{L}\right)^7 + \cdots.$$

Substituting all of the terms in (C.23)

$$\beta \left(\frac{8s_2}{L^2} + \frac{24s_3}{L^2}\left(1 - 2\frac{x}{L}\right) + \frac{48s_4}{L^2}\left(1 - 2\frac{x}{L}\right)^2 + \frac{80s_5}{L^2}\left(1 - 2\frac{x}{L}\right)^3 + \frac{120s_6}{L^2}\left(1 - 2\frac{x}{L}\right)^4 + \cdots\right)$$

$$- \left(s_0^2 + 2s_0 s_1 \left(1 - 2\frac{x}{L}\right) + \left(s_1^2 + 2s_0 s_2\right)\left(1 - 2\frac{x}{L}\right)^2 + \left(2s_0 s_3 + 2s_1 s_2\right)\left(1 - 2\frac{x}{L}\right)^3 + \cdots\right)$$

$$= -u_0^2 \left(1 - 2\frac{x}{L}\right)^2.$$

Identifying the coefficients of different powers of $\left(1 - 2\frac{x}{L}\right)$ at both sides of the equality.

$$\left[1 - 2\frac{x}{L}\right]^0 \quad : \quad \frac{8s_2}{L^2} - s_0^2 = 0, \tag{C.28}$$

$$\left[1 - 2\frac{x}{L}\right]^1 \quad : \quad \frac{24\beta s_3}{L^2} - 2s_0 s_1 = 0, \tag{C.29}$$

$$\left[1 - 2\frac{x}{L}\right]^2 \quad : \quad \frac{48\beta s_4}{L^2} - \left(s_1^2 + 2s_0 s_2\right) = -u_0^2, \tag{C.30}$$

$$\left[1 - 2\frac{x}{L}\right]^3 \quad : \quad \frac{80\beta s_5}{L^2} - \left(2s_0 s_3 + 2s_1 s_2\right) = 0, \tag{C.31}$$

$$\left[1 - 2\frac{x}{L}\right]^4 \quad : \quad \frac{120\beta s_6}{L^2} - \left(s_2^2 + 2s_0 s_4 + 2s_1 s_3\right) = 0. \tag{C.32}$$

$$\cdots$$

Assuming that $u_0 = v_L$, s_+ has a minimum at $x = L/2$. We write a few terms of equation (C.24).

$$s'_+ = -\frac{2}{L}s_1 - \frac{4}{L}s_2\left(1 - 2\frac{x}{L}\right) - \frac{6}{L}s_3\left(1 - 2\frac{x}{L}\right)^2 - \frac{8}{L}s_4\left(1 - 2\frac{x}{L}\right)^3 - \cdots .$$

We substitute $x = L/2$ into this series

$$s'_+\left(x = \frac{L}{2}\right) = 0 \Rightarrow s_1 = 0.$$

Putting $s_1 = 0$ in equation (C.29) will imply that $s_3 = 0$. Substituting $s_1 = 0$ and $s_3 = 0$ in equation (C.31) will lead to $s_5 = 0$ and so on. In general, the coefficients s_{2n+1}, where $n \in \mathbb{N}$, are equal to 0. The solution of s_+ will be written in the form

$$s_+ = s_0 + s_2\left(1 - 2\frac{x}{L}\right)^2 + s_4\left(1 - 2\frac{x}{L}\right)^4 + s_6\left(1 - 2\frac{x}{L}\right)^6 + \cdots . \tag{C.33}$$

We can write s_2 in terms of s_0 from equation (C.28).

$$\frac{8s_2}{L^2} - s_0^2 = 0 \Rightarrow s_2 = \frac{L^2 s_0^2}{8\beta} = \frac{L^2 s_0^2}{8\left(\frac{2}{\lambda^2}\right)} = \frac{\lambda^2 L^2 s_0^2}{16} \Rightarrow s_2 = \frac{\lambda^2 L^2 s_0^2}{16}.$$

The coefficient s_4 can be determined from equation (C.30).

$$\frac{48\beta s_4}{L^2} - \left(s_1^2 + 2s_0 s_2\right) = -u_0^2 \Rightarrow s_4 = \frac{L^2\left(2s_0 s_2 - u_0^2\right)}{48\beta} \Rightarrow \frac{L^2\left(2s_0\frac{\lambda^2 L^2 s_0^2}{16} - u_0^2\right)}{48\left(\frac{2}{\lambda^2}\right)}$$

$$\Rightarrow s_4 = \frac{\lambda^2 L^2\left(2\lambda^2 L^2 s_0^3 - 16u_0^2\right)}{1536}.$$

Therefore,

$$s_4 = \frac{s_0^3 L^4 \lambda^4 - 8L^2 u_0^2 \lambda^2}{768}.$$

The coefficient s_6 can be obtained from equation (C.32).

$$\frac{120\beta s_6}{L^2} - \left(s_2^2 + 2s_0 s_4\right) = 0$$

$$\Rightarrow s_6 = \frac{L^2 \left(s_2^2 + 2s_0 s_4\right)}{120\beta}$$

$$\Rightarrow s_6 = \frac{L^2 \left(\left(\frac{\lambda^2 L^2 s_0^2}{16}\right)^2 + 2s_0 \left(\frac{s_0^3 L^4 \lambda^4 - 8\lambda^2 L^2 u_0^2}{768}\right)\right)}{120 \left(\frac{2}{\lambda^2}\right)}$$

$$\Rightarrow s_6 = \frac{\lambda^2 L^2 \left(\frac{L^4 s_0^4 \lambda^4}{256} + \frac{2L^4 s_0^4 \lambda^4 - 16 s_0 \lambda^2 L^2 u_0^2}{768}\right)}{240}$$

$$= \frac{\lambda^2 L^2 \left(\frac{3L^4 s_0^4 \lambda^4}{768} + \frac{2L^4 s_0^4 \lambda^4 - 16 s_0 L^2 u_0^2 \lambda^2}{768}\right)}{240}$$

$$s_6 = \frac{\lambda^2 L^2 \left(\frac{5\lambda^4 L^4 s_0^4 - 16 s_0 \lambda^2 L^2 u_0^2}{768}\right)}{240} = \frac{\left(\frac{5\lambda^6 L^6 s_0^4 - 16 s_0 u_0^2 \lambda^4 L^4}{768}\right)}{240}.$$

Therefore,

$$s_6 = \frac{5s_0^4 L^6 \lambda^6 - 16 s_0 u_0^2 L^4 \lambda^4}{184320}.$$

Now assume that $\lambda^2 = k/D \ll 1$. The coefficients s_6, s_8, s_{10}, etc will have terms containing λ of higher degree. Therefore, equation (C.33) can be approximated as

$$s_+ \approx s_0 + \frac{\lambda^2 L^2 s_0^2}{16} \left(1 - 2\frac{x}{L}\right)^2 - \frac{\lambda^2 L^2 u_0^2}{96} \left(1 - 2\frac{x}{L}\right)^4. \tag{C.34}$$

In order to determine the expression of s_0, we shall use the boundary conditions at $x = 0$ and $x = L$ (see (C.16) or (C.17)).

$$u_0 = s_0 + \frac{\lambda^2 L^2 s_0^2}{16} - \frac{\lambda^2 L^2 u_0^2}{96}. \tag{C.35}$$

We rearrange the equation (C.35) in order to have a quadratic equation in s_0.

$$\frac{\lambda^2 L^2}{16} s_0^2 + s_0 - \left(u_0 + \frac{\lambda^2 L^2 u_0^2}{96}\right) = 0. \tag{C.36}$$

We have two possible solutions of s_0 from equation (C.36).

$$s_0 = \frac{-1 \pm \sqrt{1 + 4\left(\frac{\lambda^2 L^2}{16}\right)\left(u_0 + \frac{\lambda^2 L^2 u_0^2}{96}\right)}}{2\frac{\lambda^2 L^2}{16}}. \tag{C.37}$$

The positive solution of equation (C.37) can be approximated by

$$s_0 \approx \frac{8}{\lambda^2 L^2}\left(-1 + \sqrt{1 + \frac{u_0 \lambda^2 L^2}{4}}\right). \tag{C.38}$$

Using (C.38), the expression of s_+ from (C.34) becomes

$$s_+ = \frac{8}{\lambda^2 L^2}\left(-1 + \sqrt{1 + \frac{u_0 \lambda^2 L^2}{4}}\right) + \frac{4}{\lambda^2 L^2}\left(-1 + \sqrt{1 + \frac{u_0 \lambda^2 L^2}{4}}\right)^2\left(1 - 2\frac{x}{L}\right)^2 - \frac{\lambda^2 L^2 u_0^2}{96}\left(1 - 2\frac{x}{L}\right)^4. \tag{C.39}$$

After further simplifications, (C.39) can be written as

$$s_+ = \frac{8}{\lambda^2 L^2}\left(-1 + \sqrt{1 + \frac{u_0 \lambda^2 L^2}{4}}\right) + \frac{4}{\lambda^2 L^2}\left(-1 + \sqrt{1 + \frac{u_0 \lambda^2 L^2}{4}}\right)^2\left(1 - 2\frac{x}{L}\right)^2 - \frac{\lambda^2 L^2 u_0^2}{96}\left(1 - 2\frac{x}{L}\right)^4.$$

In summary, the solution of s_- is given by

$$s_- = u_0\left(1 - 2\xi\right),$$

and s_+ is approximated by

$$s_+ \approx \frac{8}{\lambda^2 L^2}\left(-1 + \sqrt{1 + \frac{u_0 \lambda^2 L^2}{4}}\right) + \frac{4}{\lambda^2 L^2}\left(-1 + \sqrt{1 + \frac{u_0 \lambda^2 L^2}{4}}\right)^2\left(1 - 2\xi\right)^2 - \frac{\lambda^2 L^2 u_0^2}{96}\left(1 - 2\xi\right)^4,$$

where $\xi = x/L$, $\lambda^2 = k/D$ and u_0 is the boundary value from the boundary conditions (C.16) to (C.19). These formulae are used in the section 2.6.

Appendix D

Scaling of exponential profile (mechanism 2)

In chapter 2, the morphogen with concentration u is produced and diffuses. We assume that the morphogen decays in a region of size a in the middle. In this appendix, we shall derive three solutions of u: One solution coming from region (2) and the other two coming from region (1). From these solutions, we can show that all of them are proportional to the size of the domain.
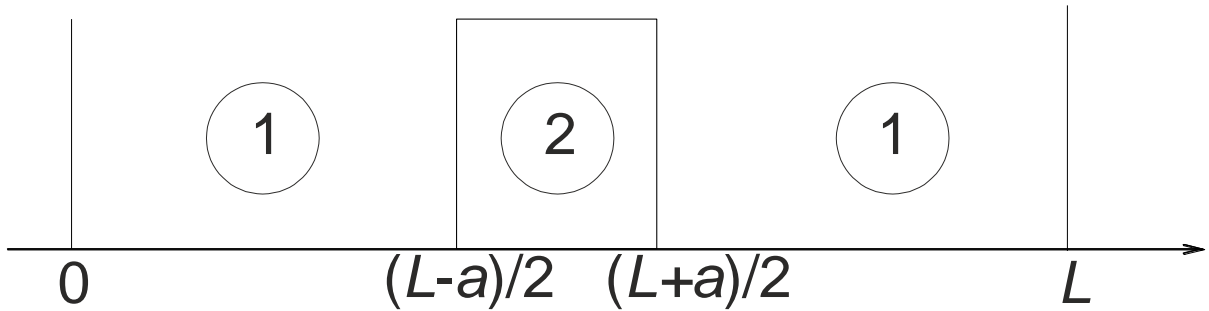
In region (1), we have

$$D_u \frac{d^2u}{dx^2} + p = 0.$$

In region (2), we have

$$D_u \frac{d^2u}{dx^2} - k_u u + p = 0.$$

The solution in region (1) for x between 0 and $(L-a)/2$ is written as

$$u_1 = -\frac{p}{2D_u}x^2 + Cx + D. \tag{D.1}$$

The solution in region (2) is written as

$$u_2 = Ae^{x\lambda} + Be^{-x\lambda} + \frac{p}{k_u}. \tag{D.2}$$

The solution in region (1) for x between $(L + a)/2$ and L is written as

$$u_3 = -\frac{p}{2D_u}x^2 + Ex + F. \tag{D.3}$$

In solution (D.2), $\lambda = (k_u/D_u)^{1/2}$. Since we have six unknowns (A, B, C, D, E and F), we need six conditions. The first two conditions are the boundary fluxes at $x = 0$ and $x = L$: $u_1'(0) = u_3'(L) = 0$. Two are the continuity at $x = (L - a)/2$ and $x = (L + a)/2$. And the other two are the derivative at $x = (L - a)/2$ and $x = (L + a)/2$. Let's use the first two conditions. We need to derive solution (D.1).

$$u_1' = -\frac{p}{D_u}x + C.$$

By using $u_1'(0) = 0$, we see that $C = 0$. Hence, the solution (D.1) is

$$u_1 = -\frac{p}{2D_u}x^2 + D.$$

We need to derive the expression (D.4)

$$u_3' = -\frac{p}{D_u}x + E. \tag{D.4}$$

We use $u_3'(L) = 0$.

$$0 = -\frac{p}{D_u}L + E \Rightarrow E = \frac{pL}{D_u}$$

So far, the solution of u_3 is written as

$$u_3 = -\frac{p}{2D_u}x^2 + \frac{pL}{D_u}x + F.$$

We use the continuity at $x = (L - a)/2$ and $x = (L + a)/2$. First $u_1((L - a)/2) = u_2((L + a)/2)$

$$-\frac{p}{2D_u}\left(\frac{L - a}{2}\right)^2 + D = Ae^{\left(\frac{L-a}{2}\right)\lambda} + Be^{-\left(\frac{L-a}{2}\right)\lambda} + \frac{p}{k_u}. \tag{D.5}$$

140

Second, $u_2((L+a)/2) = u_3((L+a)/2)$

$$-\frac{p}{2D_u}\left(\frac{L+a}{2}\right)^2 + -\frac{pL}{D_u}\left(\frac{L+a}{2}\right) + F = Ae^{\left(\frac{L-a}{2}\right)\lambda} + Be^{-\left(\frac{L-a}{2}\right)\lambda} + \frac{p}{k_u}. \qquad (D.6)$$

Third, by equating the derivatives of u_1 and u_2 at $x = (L-a)/2$, we obtain

$$-\frac{p}{\lambda D_u}\left(\frac{L-a}{2}\right) = Ae^{\left(\frac{L-a}{2}\right)\lambda} + Be^{-\left(\frac{L-a}{2}\right)\lambda}. \qquad (D.7)$$

Similarly, by equating the derivatives of u_2 and u_3 at $x = (L+a)/2$, we obtain

$$-\frac{p}{\lambda D_u}\left(\frac{L+a}{2}\right) + \frac{pL}{\lambda D_u} = Ae^{\left(\frac{L+a}{2}\right)\lambda} + Be^{-\left(\frac{L+a}{2}\right)\lambda} \qquad (D.8)$$

Multiply (D.7) by $e^{\left(\frac{L-a}{2}\right)\lambda}$.

$$-\frac{-p\,(L-a)\,e^{\left(\frac{L-a}{2}\right)\lambda}}{2\lambda D_u} = Ae^{(L-a)\lambda} - B. \qquad (D.9)$$

Multiply (D.8) by $e^{\left(\frac{L+a}{2}\right)\lambda}$.

$$-\frac{-p\,(L-a)\,e^{\left(\frac{L+a}{2}\right)\lambda}}{2\lambda D_u} = Ae^{(L+a)\lambda} - B \qquad (D.10)$$

Subtract (D.10) from (D.9).

$$A\left(e^{(L-a)\lambda} - e^{(L+a)\lambda}\right) = -\frac{p\,(L-a)}{2\lambda D_u}\left(e^{\left(\frac{L+a}{2}\right)\lambda} + e^{\left(\frac{L-a}{2}\right)\lambda}\right).$$

We can deduce A from above.

$$A = -\frac{p\,(L-a)\left(e^{\left(\frac{L+a}{2}\right)\lambda} + e^{\left(\frac{L-a}{2}\right)\lambda}\right)}{2\lambda D_u\left(e^{(L-a)\lambda} - e^{(L+a)\lambda}\right)}.$$

Putting the expression of A into $(D.7)$

$$-\frac{p}{\lambda D_u}\left(\frac{L-a}{2}\right) = \left(-\frac{p\,(L-a)\left(e^{\left(\frac{L+a}{2}\right)\lambda} + e^{\left(\frac{L-a}{2}\right)\lambda}\right)}{2\lambda D_u\left(e^{(L-a)\lambda} - e^{(L+a)\lambda}\right)}\right)e^{\left(\frac{L-a}{2}\right)\lambda} + Be^{-\left(\frac{L-a}{2}\right)\lambda}.$$

From above, B can be written as

$$Be^{-\left(\frac{L-a}{2}\right)\lambda} = \frac{p}{\lambda D_u}\left(\frac{L-a}{2}\right) = \left(-\frac{p\left(L-a\right)\left(e^{\left(\frac{L+a}{2}\right)\lambda} + e^{\left(\frac{L-a}{2}\right)\lambda}\right)}{2\lambda D_u\left(e^{(L-a)\lambda} - e^{(L+a)\lambda}\right)}\right)e^{\left(\frac{L-a}{2}\right)\lambda}.$$

$$B = \left(-\frac{p\left(L-a\right)\left(e^{\left(\frac{L+a}{2}\right)\lambda} + e^{\left(\frac{L-a}{2}\right)\lambda}\right)}{2\lambda D_u\left(e^{(L-a)\lambda} - e^{(L+a)\lambda}\right)}\right)e^{(L-a)\lambda} + \frac{p\left(L-a\right)}{2\lambda D_u}e^{\left(\frac{L-a}{2}\right)\lambda}.$$

We can simplify the above expression

$$B = -\frac{p\left(L-a\right)}{2\lambda D_u}\left(\frac{e^{\frac{\lambda}{2}(3L+a)} + e^{\frac{\lambda}{2}(3L-a)}}{e^{(L-a)\lambda} - e^{(L+a)\lambda}}\right).$$

Since we know A and B, we can determine the coefficient D from equation (D.5).

$$-\frac{p}{2D_u}\left(\frac{L-a}{2}\right)^2 + D = -\frac{p(L-a)\left(e^{\left(\frac{L+a}{2}\right)\lambda} + e^{\left(\frac{L-a}{2}\right)\lambda}\right)}{2\lambda D_u\left(e^{(L-a)\lambda} - e^{(L+a)\lambda}\right)}e^{\left(\frac{L-a}{2}\right)\lambda} - \frac{p(L-a)}{2\lambda D_u}\left(\frac{e^{\frac{\lambda}{2}(3L+a)} + e^{\frac{\lambda}{2}(3L-a)}}{e^{(L-a)\lambda} - e^{(L+a)\lambda}}\right)e^{-\left(\frac{L-a}{2}\right)\lambda} + \frac{p}{k_u}.$$

From above, D can be written as

$$D = -\frac{p(L-a)\left(e^{\left(\frac{L+a}{2}\right)\lambda} + e^{\left(\frac{L-a}{2}\right)\lambda}\right)}{2\lambda D_u\left(e^{(L-a)\lambda} - e^{(L+a)\lambda}\right)}e^{\left(\frac{L-a}{2}\right)\lambda} - \frac{p(L-a)}{2\lambda D_u}\left(\frac{e^{\frac{\lambda}{2}(3L+a)} + e^{\frac{\lambda}{2}(3L-a)}}{e^{(L-a)\lambda} - e^{(L+a)\lambda}}\right)e^{-\left(\frac{L-a}{2}\right)\lambda} + \frac{p}{k_u} + \frac{p}{2D_u}\left(\frac{L-a}{2}\right)^2.$$

This gives after further simplification

$$D = -\frac{p(L-a)\left(e^{L\lambda} + e^{(L-a)\lambda}\right)}{2\lambda D_u\left(e^{(L-a)\lambda} - e^{(L+a)\lambda}\right)} - \frac{p\left(L-a\right)\left(e^{\lambda(L+a)} + e^{L\lambda}\right)}{2\lambda D_u\left(e^{(L-a)\lambda} - e^{(L+a)\lambda}\right)} + \frac{p}{k_u} + \frac{p\left(L-a\right)}{8D_u}.$$

The full solution of u_1 is then

$$u_1 = -\frac{p}{2D_u}x^2 - \frac{p(L-a)\left(e^{L\lambda} + e^{(L-a)\lambda}\right)}{2\lambda D_u\left(e^{(L-a)\lambda} - e^{(L+a)\lambda}\right)} - \frac{p\left(L-a\right)\left(e^{\lambda(L+a)} + e^{L\lambda}\right)}{2\lambda D_u\left(e^{(L-a)\lambda} - e^{(L+a)\lambda}\right)} + \frac{p}{k_u} + \frac{p\left(L-a\right)}{8D_u}$$

and the full solution of u_2 is

$$u_2 = -\frac{p\left(L-a\right)\left(e^{\left(\frac{L+a}{2}\right)\lambda} + e^{\left(\frac{L-a}{2}\right)\lambda}\right)}{2\lambda D_u\left(e^{(L-a)\lambda} - e^{(L+a)\lambda}\right)}e^{x\lambda} - \frac{p\left(L-a\right)}{2\lambda D_u}\left(\frac{e^{\frac{\lambda}{2}(3L+a)} + e^{\frac{\lambda}{2}(3L-a)}}{e^{(L-a)\lambda} - e^{(L+a)\lambda}}\right)e^{-x\lambda} + \frac{p}{k_u}.$$

We can determine the expression of F in equation (D.6).

$$-\frac{p}{2D_u}\left(\frac{L+a}{2}\right)^2 + \frac{pL}{D_u}\left(\frac{L+a}{2}\right) + F = -\frac{p(L-a)\left(e^{\left(\frac{L+a}{2}\right)\lambda}+e^{\left(\frac{L-a}{2}\right)\lambda}\right)}{2\lambda D_u\left(e^{(L-a)\lambda}-e^{(L+a)\lambda}\right)}e^{\left(\frac{L-a}{2}\right)\lambda} - \frac{p(L-a)}{2\lambda D_u}\left(\frac{e^{\frac{\lambda}{2}(3L+a)}+e^{\frac{\lambda}{2}(3L-a)}}{e^{(L-a)\lambda}-e^{(L+a)\lambda}}\right)e^{-\left(\frac{L-a}{2}\right)\lambda} + \frac{p}{k_u}$$

$$F = -\frac{p(L-a)\left(e^{\left(\frac{L+a}{2}\right)\lambda}+e^{\left(\frac{L-a}{2}\right)\lambda}\right)}{2\lambda D_u\left(e^{(L-a)\lambda}-e^{(L+a)\lambda}\right)}e^{\left(\frac{L-a}{2}\right)\lambda} - \frac{p(L-a)}{2\lambda D_u}\left(\frac{e^{\frac{\lambda}{2}(3L+a)}+e^{\frac{\lambda}{2}(3L-a)}}{e^{(L-a)\lambda}-e^{(L+a)\lambda}}\right)e^{-\left(\frac{L-a}{2}\right)\lambda} + \frac{p}{k_u} + \frac{p}{2D_u}\left(\frac{L+a}{2}\right)^2 - \frac{pL}{D_u}\left(\frac{L+a}{2}\right).$$

We can simplify the above expression

$$F = -\frac{p\,(L-a)\left(e^{(L+a)\lambda}+e^{L\lambda}\right)}{2\lambda D_u\left(e^{(L-a)\lambda}-e^{(L+a)\lambda}\right)} - \frac{p\,(L-a)\left(e^{L\lambda}+e^{(L-a)\lambda}\right)}{2\lambda D_u\left(e^{(L-a)\lambda}-e^{(L+a)\lambda}\right)} + \frac{p}{k_u} + \frac{p\,(L+a)^2}{8D_u} - \frac{pL\,(L+a)}{2D_u}.$$

Therefore, the full solution of u_3 is written as

$$u_3 = -\frac{p}{2D_u}x^2 + \frac{pL}{D_u}x - \frac{p(L-a)\left(e^{(L+a)\lambda}+e^{L\lambda}\right)}{2\lambda D_u\left(e^{(L-a)\lambda}-e^{(L+a)\lambda}\right)} - \frac{p(L-a)\left(e^{L\lambda}+e^{(L-a)\lambda}\right)}{2\lambda D_u\left(e^{(L-a)\lambda}-e^{(L+a)\lambda}\right)} + \frac{p}{k_u} + \frac{p(L+a)^2}{8D_u} - \frac{pL(L+a)}{2D_u}.$$

Our three simplified functions are represented as

$$u_1(x) = p\left(-\frac{x^2}{2D_u} - \frac{(L-a)\left(2+e^{-a\lambda}+e^{a\lambda}\right)}{2\lambda D_u\left(e^{-a\lambda}-e^{a\lambda}\right)} + \frac{1}{k_u} + \frac{(L-a)^2}{8D_u}\right)$$

$$u_2(x) = p\left(-\frac{(L-a)\left(e^{\frac{\lambda(L+a)}{2}}+e^{\frac{\lambda(L-a)}{2}}\right)\left(e^{x\lambda}+e^{\lambda(L-x)}\right)}{2\lambda D_u\left(e^{(L-a)\lambda}-e^{(L+a)\lambda}\right)} + \frac{1}{k_u}\right)$$

$$u_3(x) = p\left(-\frac{x^2}{2D_u} + \frac{Lx}{D_u} - \frac{(L-a)\left(2+e^{-a\lambda}+e^{a\lambda}\right)}{2\lambda D_u(e^{-a\lambda}-e^{a\lambda})} + \frac{1}{k_u} + \frac{(L+a)^2}{8D_u} - \frac{L\,(L+a)}{2D_u}\right).$$

Assume that D_u is large. Then, u_1 can be approximated by

$$u_1 \approx p\left(-\frac{(L-a)\left(2+e^{-a\lambda}+e^{a\lambda}\right)}{2\lambda D_u\left(e^{-a\lambda}-e^{a\lambda}\right)} + \frac{1}{k_u}\right) \tag{D.11}$$

Assume that λ is very small, then

$$e^{-a\lambda} \approx 1 - a\lambda$$

$$e^{a\lambda} \approx 1 + a\lambda$$

$$u_1 \approx p\left(-\frac{(L-a)\left(2+1-a\lambda+1+a\lambda\right)}{2\lambda D_u\left(1-a\lambda-1-a\lambda\right)} + \frac{1}{k_u}\right)$$

$$u_1 \approx p\left(-\frac{4\,(L-a)}{4\lambda D_u a\lambda} + \frac{1}{k_u}\right)$$

143

$$u_1 \approx p\left(-\frac{L-a}{ak_u} + \frac{1}{k_u}\right)$$

$$u_1 \approx p\left(-\frac{L}{ak_u} - \frac{1}{k_u} + \frac{1}{k_u}\right)$$

$$u_1 \approx \frac{pL}{ak_u}. \tag{D.12}$$

Assume that D_u is large. Then, u_3 can be approximated by

$$u_3 \approx p\left(-\frac{(L-a)\left(2 + e^{-a\lambda} + e^{a\lambda}\right)}{2\lambda D_u \left(e^{-a\lambda} - e^{a\lambda}\right)} + \frac{1}{k_u}\right).$$

This is identical to the approximation of u_1 (see (D.11)). Therefore u_3 can be approximated by

$$u_3 \approx \frac{pL}{ak_u}. \tag{D.13}$$

Let's come back to the solution u_2.

$$u_2(x) = p\left(-\frac{(L-a)\left(e^{\frac{\lambda(L+a)}{2}} + e^{\frac{\lambda(L-a)}{2}}\right)\left(e^{x\lambda} + e^{\lambda(L-x)}\right)}{2\lambda D_u \left(e^{(L-a)\lambda} - e^{(L+a)\lambda}\right)} + \frac{1}{k_u}\right).$$

Assume that D_u is large. Then, u_2 can be approximated by taking the following approximations of terms occurring in the above equation:

$$e^{\frac{\lambda(L+a)}{2}} + e^{\frac{\lambda(L-a)}{2}} \approx \left(1 + \frac{\lambda(L+a)}{2} + 1 + \frac{\lambda(L-a)}{2}\right) = 2 + L\lambda$$

$$e^{x\lambda} + e^{\lambda(L-x)} \approx 1 + x\lambda + 1 + \lambda(L-x) = 2 + L\lambda,$$

and therefore:

$$u_2(x) \approx p\left(-\frac{(L-a)(2+L\lambda)^2}{2\lambda D_u (-2a\lambda)} + \frac{1}{k_u}\right),$$

which can be further approximated as:

$$u_2(x) \approx p\left(-\frac{(L-a)\left(2\left(1+\frac{L\lambda}{2}\right)\right)^2}{2\lambda D_u (-2a\lambda)} + \frac{1}{k_u}\right) \approx p\left(\frac{(L-a)(1+L\lambda)}{ak_u} + \frac{1}{k_u}\right) \approx$$

$$\approx p\left(\frac{(L-a)}{ak_u} + \frac{1}{k_u}\right) \approx p\left(\frac{L}{ak_u} - \frac{a}{ak_u} + \frac{1}{k_u}\right) \approx p\left(\frac{L}{ak_u} - \frac{1}{k_u} + \frac{1}{k_u}\right) \approx \frac{pL}{ak_u}. \tag{D.14}$$

In this appendix, there are three solutions of u (u_1, u_2 and u_3). When the diffusion is large or the decay is small, all solutions level up and are proportional to the size of the

medium. This allows for the solution of the second variable v (see (2.24)) to be scaled. We see that the approximations (D.12), (D.13) and (D.14) are proportional to the size of the medium.

Appendix E

Nuclear trapping model (Mixed boundary condition)

In chapter 2, one part of Bicoid molecules is located in the syncytium and freely diffuses, while another part is bounded by the nuclei. Let u be the molecules which are moving with diffusivity D in syncytium and v be the bounded molecule, where it is confined to the nucleus and can be considered immobile. In this appendix, we want to show that u scales with the mixed boundary condition.

$$\frac{\partial u}{\partial t} = D\frac{\partial^2 u}{\partial x^2} - uk_u - \rho\left(uk_1 - vk_2\right), \tag{E.1}$$

$$\frac{\partial v}{\partial t} = uk_1 - vk_2 - vk_u. \tag{E.2}$$

Equating (E.2) to zero, we will have

$$uk_1 - vk_2 - vk_u = 0 \Rightarrow uk_1 - v\left(k_2 + k_v\right) = 0 \Rightarrow$$

$$v = \frac{uk_1}{k_2 + k_v}. \tag{E.3}$$

Equating (E.1) to zero and putting the expression of v from equation (E.3), we obtain

$$D\frac{d^2 u}{dx^2} - uk_u - \rho\left(uk_u - \frac{uk_1 k_2}{k_2 + k_v}\right) = 0 \Rightarrow$$

$$D\frac{d^2 u}{dx^2} - uk_u - u\rho\left(k_1 - \frac{k_1 k_2}{k_2 + k_v}\right) = 0 \Rightarrow$$

$$D\frac{d^2 u}{dx^2} - uk_u - u\rho\left(\frac{k_1\left(k_2 + k_v\right) - k_1 k_2}{k_2 + k_v}\right) = D\frac{d^2 u}{dx^2} - uk_u - u\rho\left(\frac{k_1 k_v}{k_2 + k_v}\right) = 0 \Rightarrow$$

$$D\frac{d^2u}{dx^2} - u\left(k_u + \frac{\rho k_1 k_v}{k_2 + k_v}\right) = D\frac{d^2u}{dx^2} - u\left(\frac{k_u(k_2 + k_v) + \rho k_1 k_v}{k_2 + k_v}\right) = 0 \Rightarrow$$

$$\frac{d^2u}{dx^2} - u\left(\frac{k_u(k_2 + k_v) + \rho k_1 k_v}{D(k_2 + k_v)}\right) = 0. \tag{E.4}$$

The solution of $u(x)$ from equation (E.4) is

$$u(x) = Ae^{x\sqrt{\beta}} + Be^{-x\sqrt{\beta}}, \tag{E.5}$$

where

$$\beta = \frac{k_u(k_2 + k_v) + \rho k_1 k_v}{D(k_2 + k_v)}.$$

We apply the mixed boundary conditions which are $u(x = 0) = 1$ and $u'(x = L) = 0$. Using the first boundary condition $u(x = 0) = 1$, we have

$$u(0) = A + B = 1. \tag{E.6}$$

Using the second boundary condition $u'(x = L) = 0$, we obtain

$$u(L) = Ae^{L\sqrt{\beta}} - Be^{-L\sqrt{\beta}} = 0. \tag{E.7}$$

We can, for example, get B from equation (E.6).

$$B = 1 - A. \tag{E.8}$$

Substitute B, from equation (E.8), into equation (E.7).

$$Ae^{L\sqrt{\beta}} - (1 - A)e^{-L\sqrt{\beta}} = Ae^{L\sqrt{\beta}} - e^{-L\sqrt{\beta}} + Ae^{-L\sqrt{\beta}} = A\left(e^{L\sqrt{\beta}} + e^{-L\sqrt{\beta}}\right) - e^{-L\sqrt{\beta}} = 0.$$

$$\Rightarrow A\left(e^{L\sqrt{\beta}} + e^{-L\sqrt{\beta}}\right) = -e^{-L\sqrt{\beta}} \Rightarrow A = \frac{e^{-L\sqrt{\beta}}}{e^{-L\sqrt{\beta}} + e^{L\sqrt{\beta}}}.$$

We can now compute the coefficient B in equation (E.8).

$$B = 1 - \frac{e^{-L\sqrt{\beta}}}{e^{-L\sqrt{\beta}} + e^{L\sqrt{\beta}}} = \frac{\left(e^{-L\sqrt{\beta}} + e^{L\sqrt{\beta}}\right) - e^{-L\sqrt{\beta}}}{e^{-L\sqrt{\beta}} + e^{L\sqrt{\beta}}} = \frac{e^{L\sqrt{\beta}}}{e^{-L\sqrt{\beta}} + e^{L\sqrt{\beta}}}.$$

In summary, the coefficients of A and B are

$$A = \frac{e^{-L\sqrt{\beta}}}{e^{-L\sqrt{\beta}} + e^{L\sqrt{\beta}}},$$

$$B = \frac{e^{L\sqrt{\beta}}}{e^{-L\sqrt{\beta}} + e^{L\sqrt{\beta}}}.$$

The full solution of $u(x)$ from equation (E.5) is written as

$$u(x) = \frac{e^{-L\sqrt{\beta}}}{e^{-L\sqrt{\beta}} + e^{L\sqrt{\beta}}} e^{x\sqrt{\beta}} + \frac{e^{L\sqrt{\beta}}}{e^{-L\sqrt{\beta}} - e^{L\sqrt{\beta}}} e^{-x\sqrt{\beta}}. \qquad (E.9)$$

As L tends to infinity, $u(x)$ from equation (E.9) can be approximated as

$$u(x) \approx \frac{e^{(x-L)\sqrt{\beta}} - e^{(L-x)\sqrt{\beta}}}{e^{L\sqrt{\beta}}} = -\frac{e^{x\sqrt{\beta}}}{e^{2L\sqrt{\beta}}} + e^{-x\sqrt{\beta}} \approx e^{-x\sqrt{\beta}}. \qquad (E.10)$$

By putting the expression of β, in equation (E.10), $u(x)$ is represented as

$$u(x) \approx e^{-x\sqrt{\frac{k_u(k_2+k_v)+\rho k_1 k_v}{D(k_2+k_v)}}}.$$

Here, if k_u tends to 0 and $\rho = N/L^2$, then $u(x)$ can be approximated as

$$u(x) \approx e^{-\frac{x}{L}\sqrt{\frac{Nk_1 k_v}{D(k_2+k_v)}}}. \qquad (E.11)$$

i.e. $u(x)$ does scale. The formal quantity to measure scaling of morphogen gradient is given by

$$S = -\left(\frac{\partial u}{\partial L}\right)\left(\frac{\partial u}{\partial \xi}\right)^{-1}.$$

Since $\xi = x/L$, the solution of $u(x)$ from equation (E.11) can be written as

$$u \approx e^{-\xi\sqrt{\frac{Nk_1 k_v}{D(k_2+k_v)}}}.$$

The calculation of the derivatives of u with respect to ξ and L gives

$$\frac{\partial u}{\partial L} = 0,$$

$$\frac{\partial u}{\partial \xi} = -\sqrt{\frac{Nk_1 k_v}{D(k_2 + k_v)}} e^{-\xi\sqrt{\frac{Nk_1 k_v}{D(k_2+k_v)}}},$$

$$S = 0,$$

which shows a perfect scaling. Thus, under the mixed boundary condition when L tends to infinity, scaling tends to be perfect ($S \to 0$).

Appendix F

Nuclear trapping model (Neumann boundary conditions)

This is similar to the previous appendix except that we use Neumann boundary condition. From here, we show that the solution u doesn't scale.

$$\frac{\partial u}{\partial t} = D\frac{\partial^2 u}{\partial x^2} - uk_u - \rho\left(uk_1 - vk_2\right), \qquad (F.1)$$

$$\frac{\partial v}{\partial t} = uk_1 - vk_2 - vk_v. \qquad (F.2)$$

Equating (F.2) to zero, we will have

$$uk_1 - vk_2 - vk_u = 0 \Rightarrow uk_1 - v\left(k_2 + k_v\right) = 0 \Rightarrow$$

$$v = \frac{uk_1}{k_2 + k_v}. \qquad (F.3)$$

Equating (F.1) to zero and putting the expression of v from equation (F.3), we obtain

$$D\frac{d^2 u}{dx^2} - uk_u - \rho\left(uk_u - \frac{uk_1 k_2}{k_2 + k_v}\right) = 0 \Rightarrow$$

$$D\frac{d^2 u}{dx^2} - uk_u - u\rho\left(k_1 - \frac{k_1 k_2}{k_2 + k_v}\right) = 0 \Rightarrow$$

$$D\frac{d^2 u}{dx^2} - uk_u - u\rho\left(\frac{k_1\left(k_2 + k_v\right) - k_1 k_2}{k_2 + k_v}\right) = D\frac{d^2 u}{dx^2} - uk_u - u\rho\left(\frac{k_1 k_v}{k_2 + k_v}\right) = 0 \Rightarrow$$

$$D\frac{d^2 u}{dx^2} - u\left(k_u + \frac{\rho k_1 k_v}{k_2 + k_v}\right) = D\frac{d^2 u}{dx^2} - u\left(\frac{k_u\left(k_2 + k_v\right) + \rho k_1 k_v}{k_2 + k_v}\right) = 0 \Rightarrow$$

$$\frac{\partial^2 u}{\partial x^2} - u\left(\frac{k_u\left(k_2 + k_v\right) + \rho k_1 k_v}{D\left(k_2 + k_v\right)}\right) = 0. \tag{F.4}$$

The solution of $u(x)$ from equation (E.4) is

$$u(x) = Ae^{x\sqrt{\beta}} + Be^{-x\sqrt{\beta}}, \tag{F.5}$$

where

$$\beta = \frac{k_u\left(k_2 + k_v\right) + \rho k_1 k_v}{D\left(k_2 + k_v\right)}.$$

We shall use the Neumann boundary conditions which are $u'(x = 0) = -\gamma$ and $u'(x = L) = 0$. We need to compute the derivative of $u(x)$.

$$u'(x) = A\sqrt{\beta}e^{x\sqrt{\beta}} - B\sqrt{\beta}e^{-x\sqrt{\beta}}. \tag{F.6}$$

Using the first boundary condition $u'(x = 0) = -\gamma$, equation (F.6) is written as

$$A - B = -\frac{\gamma}{\sqrt{\beta}}. \tag{F.7}$$

Using the second boundary condition, $u'(x = L) = 0$, equation (F.6) is written as

$$Ae^{L\sqrt{\beta}} - Be^{-L\sqrt{\beta}} = 0.. \tag{F.8}$$

We can, for example, get A, from equation (F.7)

$$A = B - \frac{\gamma}{\sqrt{\beta}}. \tag{F.9}$$

Substitute A, from equation (F.9), into equation (F.8)

$$\left(B - \frac{\gamma}{\sqrt{\beta}}\right)e^{L\sqrt{\beta}} - Be^{-L\sqrt{\beta}} = Be^{L\sqrt{\beta}} - \frac{\gamma}{\sqrt{\beta}}e^{L\sqrt{\beta}} - Be^{-L\sqrt{\beta}} = 0$$

$$\Rightarrow B\left(e^{L\sqrt{\beta}} - e^{-L\sqrt{\beta}}\right) = \frac{\gamma}{\sqrt{\beta}}e^{L\sqrt{\beta}} \Rightarrow B = \frac{\gamma}{\sqrt{\beta}}\left(\frac{e^{L\sqrt{\beta}}}{e^{L\sqrt{\beta}} - e^{-L\sqrt{\beta}}}\right).$$

We can now compute the coefficient A in equation (F.9).

$$A = \frac{\gamma}{\sqrt{\beta}}\left(\frac{e^{L\sqrt{\beta}}}{e^{L\sqrt{\beta}} - e^{-L\sqrt{\beta}}}\right) - \frac{\gamma}{\sqrt{\beta}} = \frac{\gamma}{\sqrt{\beta}}\left(\frac{e^{L\sqrt{\beta}}}{e^{L\sqrt{\beta}} - e^{-L\sqrt{\beta}}} - 1\right) = \frac{\gamma}{\sqrt{\beta}}\left(\frac{e^{L\sqrt{\beta}} - \left(e^{L\sqrt{\beta}} - e^{-L\sqrt{\beta}}\right)}{e^{L\sqrt{\beta}} - e^{-L\sqrt{\beta}}}\right)$$

$$\Rightarrow A = \frac{\gamma}{\sqrt{\beta}}\left(\frac{e^{-L\sqrt{\beta}}}{e^{L\sqrt{\beta}} - e^{-L\sqrt{\beta}}}\right).$$

In summary, the coefficients of A and B are

$$A = \frac{\gamma}{\sqrt{\beta}}\left(\frac{e^{-L\sqrt{\beta}}}{e^{L\sqrt{\beta}} - e^{-L\sqrt{\beta}}}\right),$$

$$B = \frac{\gamma}{\sqrt{\beta}}\left(\frac{e^{L\sqrt{\beta}}}{e^{L\sqrt{\beta}} - e^{-L\sqrt{\beta}}}\right).$$

The full solution of $u(x)$ from equation (F.5) is written as

$$u(x) = \frac{\gamma\left(e^{(x-L)\sqrt{\beta}} + e^{(L-x)\sqrt{\beta}}\right)}{\sqrt{\beta}\left(e^{L\sqrt{\beta}} - e^{-L\sqrt{\beta}}\right)}. \tag{F.10}$$

As L tends to infinity, $u(x)$ from equation (F.10), can be approximated as

$$u(x) \approx \frac{\gamma\left(e^{(x-L)\sqrt{\beta}} + e^{(L-x)\sqrt{\beta}}\right)}{\sqrt{\beta}e^{L\sqrt{\beta}}} = \frac{\gamma}{\sqrt{\beta}}\left(\frac{e^{x\sqrt{\beta}}}{e^{2L\sqrt{\beta}}} + e^{-x\sqrt{\beta}}\right) \approx \frac{\gamma}{\sqrt{\beta}}e^{-x\sqrt{\beta}}. \tag{F.11}$$

By putting the expression of β, $u(x)$ can be represented as

$$u(x) = \frac{\gamma}{\sqrt{\frac{k_u(k_2+k_v)+\rho k_1 k_v}{D(k_2+k_v)}}}e^{-x\sqrt{\frac{k_u(k_2+k_v)+\rho k_1 k_v}{D(k_2+k_v)}}}. \tag{F.12}$$

Here, if k_u tends to 0 and $\rho = N/L^2$ then, $u(x)$ from equation (F.12), can be approximated as

$$u(x) \approx L\frac{\gamma}{\sqrt{\frac{Nk_1 k_v}{D(k_2+k_v)}}}e^{-\frac{x}{L}\sqrt{\frac{Nk_1 k_v}{D(k_2+k_v)}}}.$$

We can replace x/L by ξ. The solution of $u(x)$ can be written as

$$u \approx L\frac{\gamma}{\sqrt{\frac{Nk_1 k_v}{D(k_2+k_v)}}}e^{-\xi\sqrt{\frac{Nk_1 k_v}{D(k_2+k_v)}}}. \tag{F.13}$$

The formal quantity to measure scaling of morphogen gradient is given by

$$S = -\left(\frac{\partial u}{\partial L}\right)\left(\frac{\partial u}{\partial \xi}\right)^{-1}.$$

Let's compute the scaling factor of equation (F.13). We differentiate u with respect to L and ξ.

$$\frac{\partial u}{\partial L} = \frac{\gamma}{\sqrt{\frac{Nk_1 k_v}{D(k_2+k_v)}}}e^{-\xi\sqrt{\frac{Nk_1 k_v}{D(k_2+k_v)}}},$$

$$\frac{\partial u}{\partial \xi} = -L\gamma e^{-\xi\sqrt{\frac{Nk_1 k_v}{D(k_2+k_v)}}} \Rightarrow \left(\frac{\partial u}{\partial \xi}\right)^{-1} = -\frac{e^{\xi\sqrt{\frac{Nk_1 k_v}{D(k_2+k_v)}}}}{L\gamma},$$

$$S = -\left(\frac{\gamma e^{-\xi\sqrt{\frac{Nk_1 k_v}{D(k_2+k_v)}}}}{\sqrt{\frac{Nk_1 k_v}{D(k_2+k_v)}}}\right)\left(-\frac{e^{\xi\sqrt{\frac{Nk_1 k_v}{D(k_2+k_v)}}}}{L\gamma}\right) = \frac{1}{L\sqrt{\frac{Nk_1 k_v}{D(k_2+k_v)}}} \neq 0.$$

The above scaling factor formula depends on parameters in contrast with the formula which was derived in the previous appendix. Scaling occurs if L, N, k_1 or k_v is large. Alternatively, we can achieve scaling if D or $k_2 + k_v$ is very small.

Appendix G

Rule 30

In chapter 4, we have proved that, for the cases of transition rules 15 and 85, they will take two-time steps to produce a new stripe $\mathbf{101}$. In this appendix, we want to show that if we start with $1xxxxx$ for the case of transition rule 30, it will take nine-time steps to produce a stripe $\mathbf{101}$.

$$30 = \mathbf{0001110}$$

$$(000) \rightarrow (0\mathbf{0}0)$$

$$(001) \rightarrow (0\mathbf{11})$$

$$(010) \rightarrow (0\mathbf{1}0)$$

$$(011) \rightarrow (0\mathbf{11})$$

$$(100) \rightarrow (1\mathbf{1}0)$$

$$(101) \rightarrow (1\mathbf{01})$$

$$(110) \rightarrow (1\mathbf{0}0)$$

$$(111) \rightarrow (1\mathbf{01})$$

Case A: $10000x$.

$$10000x \rightarrow 1100x \rightarrow \mathbf{101}x. \qquad (2 \text{ TS})$$

Case B: $10001x$.

$10001x \rightarrow 11011x \rightarrow 10010x \rightarrow 1111x \rightarrow 1000x \rightarrow 110x \rightarrow 10x$. **We need to consider more elements**.

Case B$_1$: $10001\textcolor{blue}{0}x$.

$10001\textcolor{blue}{0}x \rightarrow 11011x \rightarrow 10010x \rightarrow 1111x \rightarrow 1000x \rightarrow 110x \rightarrow 10x$. **We need to consider more elements**.

Case B$_{11}$: $10001\textcolor{blue}{0}\textcolor{red}{0}x$.

$10001\textcolor{blue}{0}\textcolor{red}{0}x \rightarrow 110111x \rightarrow 100100x \rightarrow 11111x \rightarrow 10000x \rightarrow 1100x \rightarrow \mathbf{101}x$. **(6TS)**

Case B$_{12}$: $10001\textcolor{blue}{0}\textcolor{red}{1}x$.

$10001\textcolor{blue}{0}\textcolor{red}{1}x \rightarrow 1101101x \rightarrow 1001001x \rightarrow 1111111x \rightarrow 1000000x \rightarrow 110000x \rightarrow \mathbf{101}00x$. **(6TS)**

Case B$_2$: $10001\textcolor{blue}{1}x$.

$10001\textcolor{blue}{1}x \rightarrow 110110x \rightarrow 10010x \rightarrow 1111x \rightarrow 1000x \rightarrow 110x \rightarrow 10x$. **We need to consider more elements**.

Case B$_{21}$: $10001\textcolor{blue}{1}\textcolor{red}{0}x$.

$10001\textcolor{blue}{1}\textcolor{red}{0}x \rightarrow 110110x \rightarrow 10010x \rightarrow 1111x \rightarrow 1000x \rightarrow 110x \rightarrow 10x$. **We need to consider more elements**.

Case B$_{211}$: $10001\textcolor{blue}{1}\textcolor{red}{0}\textcolor{green}{0}x$.

$10001\textcolor{blue}{1}\textcolor{red}{0}\textcolor{green}{0}x \rightarrow 110100x \rightarrow 100111x \rightarrow 111110x \rightarrow 10000x \rightarrow 1100x \rightarrow \mathbf{101}00x$. **(6TS)**

Case B$_{212}$: $10001\textcolor{blue}{1}\textcolor{red}{0}\textcolor{green}{1}x$.

$10001\textcolor{blue}{1}\textcolor{red}{0}\textcolor{green}{1}x \rightarrow 11011001x \rightarrow 1001011x \rightarrow 11110100x \rightarrow 1000010x \rightarrow 110011x \rightarrow \mathbf{101}110x$. **(6TS)**

Case B$_{22}$: $10001\textcolor{blue}{1}\textcolor{red}{1}x$.

$$100011\textcolor{red}{1}x \to 1101100x \to 100101x \to 111101x \to 100001x \to 110011x \to \mathbf{101}110x.$$
$$\textbf{(6TS)}$$

Case C: $10010x$.

$10010x \to 1111x \to 1000x \to 110x \to 10x$. **We need to consider more elements**.

Case C$_1$: $10010\textcolor{blue}{0}x$.

$$100100\textcolor{blue}{0}x \to 11111x \to 10000x \to 1100x \to \mathbf{101}x. \textbf{ (4TS)}$$

Case C$_2$: $10010\textcolor{blue}{1}x$.

$$10010\textcolor{blue}{1}x \to 111101x \to 100001x \to 110011x \to \mathbf{101}110x. \textbf{ (4TS)}$$

Case D: $10011x$.

$10011x \to 11110x \to 1000x \to 110x \to 10x$. **We need to consider more elements**.

Case D$_1$: $10011\textcolor{blue}{0}x$.

$10011\textcolor{blue}{0}x \to 11110x \to 1000x \to 110x \to 10x$. **We need to consider more elements**.

Case D$_{11}$: $10011\textcolor{red}{00}x$.

$$10011\textcolor{red}{00}x \to 111101x \to 100001x \to 110011x \to \mathbf{101}110x. \textbf{ (4TS)}$$

Case D$_{12}$: $10011\textcolor{red}{01}x$.

$$10011\textcolor{red}{01}x \to 1111001x \to 1000111x \to 1101100x \to 100100x \to 11111x \to 10000x \to$$
$$1100x \to \mathbf{101}x. \textbf{ (8TS)}$$

Case D$_2$: $10011\textcolor{blue}{1}x$.

$$10011\textcolor{blue}{1}x \to 111100x \to 10001x \to 11011x \to 10010x \to 1111x \to 1000x \to 110x \to 10x.$$
$$\textbf{We need to consider more elements}.$$

Case D$_{21}$: $= 100111\textcolor{red}{0}x$.

$10011\textcolor{blue}{1}\textcolor{red}{0}x \to 1111000x \to 10001x \to 110011x \to 10010x \to 1111x \to 1000x \to 110x \to$
$10x$. **We need to consider more elements**.

Case D$_{211}$: $10011\textcolor{red}{1}\textcolor{green}{0}0x$.

$10011\textcolor{red}{1}\textcolor{green}{0}0x \to 1111001x \to 100011x \to 1100110x \to 100101x \to 111101x \to 100001x \to$
$110011x \to \mathbf{101}110x.$ **(8TS)**

Case D$_{212}$: $10011\textcolor{green}{1}\textcolor{red}{0}1x$.

$10011\textcolor{red}{1}\textcolor{green}{0}1x \to 11110001x \to 10001011x \to 11011010x \to 1001001x \to 1111111x \to$
$1000000x \to 110000x \to \mathbf{101}00x.$ **(8TS)**

Case D$_{22}$: $100111\textcolor{blue}{1}x$.

$10011\textcolor{red}{1}\textcolor{blue}{1}x \to 1111000x \to 100010x \to 11011x \to 10010x \to 1111x \to 1000x \to 110x \to$
$10x$. **We need to consider more elements**.

Case D$_{221}$: $10011\textcolor{red}{1}\textcolor{green}{1}0x$.

$10011\textcolor{red}{1}\textcolor{green}{1}0x \to 111100x \to 100010x \to 11011x \to 10010x \to 1111x \to 1000x \to 110x \to$
$10x$. **We need to consider more elements**.

Case D$_{2211}$: $100111\textcolor{red}{1}\textcolor{green}{0}0x$.

$100111\textcolor{red}{1}\textcolor{green}{0}0x \to 1111001x \to 10001011x \to 11011010x \to 1001001x \to 1111111x \to$
$1000000x \to 110000x \to \mathbf{101}00x.$ **(8TS)**

Case D$_{2212}$: $100111\textcolor{red}{1}\textcolor{green}{0}1x$.

$100111\textcolor{red}{1}\textcolor{green}{0}1x \to 111100001x \to 100010011x \to 110111110x \to 10010000x \to 1111100x \to$
$100001x \to 110011x \to \mathbf{101}110x.$ **(8TS)**

Case D$_{222}$: $10011\textcolor{red}{1}\textcolor{green}{1}\textcolor{blue}{1}x$.

$$10011\textcolor{red}{11}\textcolor{blue}{1}x \to 11110000x \to 1000100x \to 110111x \to 100100x \to 11111x \to 10000x \to$$
$$1100x \to \mathbf{101}x. \ (\mathbf{8TS})$$

Case E-H. For the cases of $10100x$, $10101x$, $10110x$ and $10111x$, the time step to reach **101** is 0.

Case I: $11000x$.

$$11000x \to \mathbf{101}0x. \ (\mathbf{1TS})$$

Case J: $11001x$.

$$11001x \to \mathbf{101}11x. \ (\mathbf{1TS})$$

Case K: $11010x$.

$$11010x \to 1001x \to 1111x \to 100x \to 110x \to 10x. \ \textbf{We need to consider more}$$
$$\textbf{elements}.$$

Case K_1: $11010\textcolor{blue}{0}x$.

$$11010\textcolor{blue}{0}x \to 10011x \to 11110x \to 1000x \to 110x \to 10x. \ \textbf{We need to consider more}$$
$$\textbf{elements}.$$

Case K_{11}: $11010\textcolor{blue}{0}\textcolor{red}{0}x$.

$$11010\textcolor{blue}{0}\textcolor{red}{0}x \to 100110x \to 11110x \to 1000x \to 110x \to 10x. \ \textbf{We need to consider}$$
$$\textbf{more elements}.$$

Case K_{111}: $11010\textcolor{blue}{0}\textcolor{red}{0}\textcolor{green}{0}x$.

$$11010\textcolor{blue}{0}\textcolor{red}{0}\textcolor{green}{0}x \to 1001100x \to 111101x \to 100001x \to 110011x \to \mathbf{101}110x. \ (\mathbf{5TS})$$

Case K_{112}: $11010\textcolor{blue}{0}\textcolor{red}{0}\textcolor{green}{1}x$.

$$11010\textcolor{blue}{0}\textcolor{red}{0}\textcolor{green}{1}x \to 10011011x \to 11110010x \to 1000111x \to 1101100x \to 100100x \to$$
$$11111x \to 10000x \to 1100x \to \mathbf{101}x. \ (\mathbf{9TS})^{*}$$

158

Case K$_{12}$: $110100\textcolor{red}{1}x$.

$$110100\textcolor{red}{1}x \rightarrow 1001111x \rightarrow \mathbf{101}1000x. \ \mathbf{(2TS)}$$

Case K$_2$: $11010\textcolor{blue}{1}x$.

$$11010\textcolor{blue}{1}x \rightarrow 100101x \rightarrow 111101x \rightarrow 100001x \rightarrow 110011x \rightarrow \mathbf{101}110x. \ \mathbf{(5TS)}$$

Case L: $11011x$.

$$11011x \rightarrow 10010x \rightarrow 1111x \rightarrow 100x \rightarrow 110x \rightarrow 10x. \ \textbf{We need to consider more elements}.$$

Case L$_1$: $11011\textcolor{blue}{0}x$.

$$11011\textcolor{blue}{0}x \rightarrow 10010x \rightarrow 1111x \rightarrow 1000x \rightarrow 110x \rightarrow 10x. \ \textbf{We need to consider more elements}.$$

Case L$_{11}$: $11011\textcolor{red}{00}x$.

$$11011\textcolor{red}{00}x \rightarrow 100100x \rightarrow 11111x \rightarrow 10000x \rightarrow 1100x \rightarrow \mathbf{101}x. \ \mathbf{(5TS)}$$

Case L$_{12}$: $11011\textcolor{red}{01}x$.

$$11011\textcolor{red}{01}x \rightarrow 1001001x \rightarrow 1111111x \rightarrow 1000000x \rightarrow 110000x \rightarrow \mathbf{101}00x. \ \mathbf{(5TS)}$$

Case L$_2$: $11011\textcolor{blue}{0}x$.

$$11011\textcolor{blue}{0}x \rightarrow 100100x \rightarrow 11111x \rightarrow 10000x \rightarrow 1100x \rightarrow \mathbf{101}x. \ \mathbf{(5TS)}$$

Case M: $11100x$.

$$11100x \rightarrow 1001x \rightarrow 1111x \rightarrow 100x \rightarrow 110x \rightarrow 10x. \ \textbf{We need to consider more elements}.$$

Case M$_1$: $11100\textcolor{blue}{0}x$.

$$1110\textcolor{blue}{0}x \to 10010x \to 1111x \to 100x \to 110x \to 10x. \textbf{ We need to consider more}$$
$$\textbf{elements}.$$

Case M$_{11}$: $1110\textcolor{red}{0}\textcolor{blue}{0}x$.

$$1110\textcolor{red}{0}\textcolor{blue}{0}x \to 100100x \to 11111x \to 10000x \to 1100x \to \textbf{101}x. \textbf{ (5TS)}$$

Case M$_{12}$: $1110\textcolor{red}{0}\textcolor{blue}{1}x$.

$$1110\textcolor{red}{0}\textcolor{blue}{1}x \to 1001011x \to 1111010x \to 100001x \to 110001x \to \textbf{101}x. \textbf{ (5TS)}$$

Case M$_{2}$: $11100\textcolor{blue}{1}x$.

$$11100\textcolor{blue}{1}x \to 100111x \to 111100x \to 10001x \to 11011x \to 10010x \to 1111x \to 1000x \to$$
$$110x \to 10x. \textbf{ We need to consider more elements}.$$

Case M$_{21}$: $11100\textcolor{red}{1}\textcolor{blue}{0}x$.

$$11100\textcolor{red}{1}\textcolor{blue}{0}x \to 100111x \to 111100x \to 10001x \to 11011x \to 10010x \to 1111x \to 1000x \to$$
$$110x \to 10x. \textbf{ We need to consider more elements}.$$

Case M$_{211}$: $11100\textcolor{red}{1}\textcolor{green}{0}0x$.

$$11100\textcolor{red}{1}\textcolor{green}{0}0x \to 1001111x \to 1111000x \to 100010x \to 11011x \to 10010x \to 1111x \to$$
$$1000x \to 110x \to 10x. \textbf{ We need to consider more elements}.$$

Case M$_{2111}$: $11100\textcolor{blue}{1}\textcolor{green}{0}\textcolor{purple}{0}0x$.

$$11100\textcolor{blue}{1}\textcolor{green}{0}\textcolor{purple}{0}0x \to 10011110x \to 1111000x \to 100010x \to 11011x \to 10010x \to 1111x \to$$
$$1000x \to 110x \to 10x. \textbf{ We need to consider more elements}.$$

Case M$_{21111}$: $11100\textcolor{red}{1}\textcolor{blue}{0}\textcolor{green}{0}\textcolor{orange}{0}x$.

$$11100\textcolor{red}{1}\textcolor{blue}{0}\textcolor{green}{0}\textcolor{orange}{0}x \to 100111100x \to 11110001x \to 10001011x \to 11011010x \to 1001001x \to$$
$$1111111x \to 1000000x \to 11000x \to \textbf{101}00x. \textbf{ (9TS)}^{*}$$

Case M$_{21112}$: $11100\textcolor{red}{1}\textcolor{blue}{0}\textcolor{green}{0}\textcolor{orange}{1}x$.

$1110010001x \rightarrow 1001111011x \rightarrow 1111000010x \rightarrow 100010011x \rightarrow 110111110x \rightarrow$
$10010000x \rightarrow 1111100x \rightarrow 100001x \rightarrow 110011x \rightarrow \mathbf{101}110x$. $(\mathbf{9TS})^*$

Case M$_{2112}$: $1110010 01x$.

$11100 1001x \rightarrow 100111111x \rightarrow 111100000x \rightarrow 10001000x \rightarrow 110111x \rightarrow 100100x \rightarrow$
$11111x \rightarrow 10000x \rightarrow 1100x \rightarrow \mathbf{101}x$. $(\mathbf{9TS})^*$

Case M$_{212}$: $11100101x$.

$11100 101x \rightarrow 10011101x \rightarrow 11110001x \rightarrow 10001011x \rightarrow 11011010x \rightarrow 1001001x \rightarrow$
$1111111x \rightarrow 1000000x \rightarrow 110000x \rightarrow \mathbf{101}00x$. $(\mathbf{9TS})^*$

Case M$_{22}$: $1110011x$.

$1110011x \rightarrow 1001110x \rightarrow 111100x \rightarrow 10001x \rightarrow 11001x \rightarrow \mathbf{101}11x$. $(\mathbf{5TS})$

Case N: $11101x$.

$11101x \rightarrow 10001x \rightarrow 11011x \rightarrow 10010x \rightarrow 1111x \rightarrow 1000x \rightarrow 110x \rightarrow 10x$. **We need to consider more elements**.

Case N$_1$: $111010x$.

$111010x \rightarrow 10001x \rightarrow 11011x \rightarrow 10010x \rightarrow 1111x \rightarrow 1000x \rightarrow 110x \rightarrow 10x$. **We need to consider more elements**.

Case N$_{11}$: $1110100x$.

$1110100x \rightarrow 100011x \rightarrow 110110x \rightarrow 10010x \rightarrow 1111x \rightarrow 1000x \rightarrow 110x \rightarrow 10x$. **We need to consider more elements**.

Case N$_{111}$: $11101000x$.

$11101000x \rightarrow 1000110x \rightarrow 110110x \rightarrow 10010x \rightarrow 1111x \rightarrow 1000x \rightarrow 110x \rightarrow 10x$. **We need to consider more elements**.

Case N$_{1111}$: $11101\textcolor{blue}{0}\textcolor{red}{0}\textcolor{green}{0}\textcolor{magenta}{0}x$.

$$11101\textcolor{blue}{0}\textcolor{red}{0}\textcolor{green}{0}\textcolor{magenta}{0}x \rightarrow 10001100x \rightarrow t1101101x \rightarrow 1001001x \rightarrow 1111111x \rightarrow 1000000x \rightarrow$$
$$110000x \rightarrow \mathbf{101}00x. \ (\mathbf{7TS})$$

Case N$_{1112}$: $11101\textcolor{blue}{0}\textcolor{red}{0}\textcolor{green}{0}\textcolor{magenta}{1}x$.

$$11101\textcolor{blue}{0}\textcolor{red}{0}\textcolor{green}{0}\textcolor{magenta}{1}x \rightarrow 100011011x \rightarrow 110110010x \rightarrow 10010111x \rightarrow 11110100x \rightarrow 1000010x \rightarrow$$
$$110011x \rightarrow \mathbf{101}110x. \ (\mathbf{7TS})$$

Case N$_{112}$: $11101\textcolor{blue}{0}\textcolor{red}{0}\textcolor{green}{1}x$.

$$11101\textcolor{blue}{0}\textcolor{red}{0}\textcolor{green}{1}x \rightarrow 10001111x \rightarrow 11011000x \rightarrow 1001010x \rightarrow 111101x \rightarrow 100001x \rightarrow$$
$$110011x \rightarrow \mathbf{101}110x. \ (\mathbf{7TS})$$

Case N$_{12}$: $11101\textcolor{blue}{0}\textcolor{red}{1}x$.

$$t11101\textcolor{blue}{0}\textcolor{red}{1}x \rightarrow 1000101x \rightarrow 1101101x \rightarrow 1001001x \rightarrow 1111111x \rightarrow 1000000x \rightarrow$$
$$110000x \rightarrow \mathbf{101}00x. \ (\mathbf{7TS})$$

Case N$_{2}$: $11101\textcolor{blue}{1}x$.

$$11101\textcolor{blue}{1}x \rightarrow 100010x \rightarrow 11011x \rightarrow 10010x \rightarrow 1111x \rightarrow 1000x \rightarrow 110x \rightarrow 10x. \ \mathbf{We \ need}$$
$$\mathbf{more \ elements}.$$

Case N$_{21}$: $11101\textcolor{blue}{1}\textcolor{red}{0}x$.

$$11101\textcolor{blue}{1}\textcolor{red}{0}x \rightarrow 100010x \rightarrow 11011x \rightarrow 10010x \rightarrow 1111x \rightarrow 1000x \rightarrow 110x \rightarrow 10x. \ \mathbf{We}$$
$$\mathbf{need \ to \ consider \ more \ elements}.$$

Case N$_{211}$: $11101\textcolor{blue}{1}\textcolor{red}{0}\textcolor{green}{0}x$.

$$11101\textcolor{blue}{1}\textcolor{red}{0}\textcolor{green}{0}x \rightarrow 1000101x \rightarrow 1101101x \rightarrow 1001001x \rightarrow 1111111x \rightarrow 1000000x \rightarrow$$
$$110000x \rightarrow \mathbf{101}00x. \ (\mathbf{7TS})$$

Case N$_{212}$: $11101\textcolor{blue}{1}\textcolor{red}{0}\textcolor{green}{1}x$.

$11101\textbf{101}x \rightarrow 10001001x \rightarrow 11011111x \rightarrow 10010000x \rightarrow 1111100x \rightarrow 100000x \rightarrow 11000x \rightarrow \textbf{101}0x.$ **(7TS)**

Case N$_{22}$: $11101\textbf{11}x$.

$110101\textbf{11}x \rightarrow 1000100x \rightarrow 110111x \rightarrow 100100x \rightarrow 11111x \rightarrow 10000x \rightarrow 1100x \rightarrow \textbf{101}x.$
(7TS)

Case O: $11110x$.

$11110x \rightarrow 1000x \rightarrow 110x \rightarrow 10x.$ **We need to consider more elements**.

Case O$_1$: $11110\textbf{0}x$.

$11110\textbf{0}x \rightarrow 10001x \rightarrow 11011x \rightarrow 10010x \rightarrow 1111x \rightarrow 1000x \rightarrow 110x \rightarrow 10x.$ **We need to consider more elements**.

Case O$_{11}$: $11110\textbf{00}x$.

$11110\textbf{00}x \rightarrow 100010x \rightarrow 11011x \rightarrow 10010x \rightarrow 1111x \rightarrow 1000x \rightarrow 110x \rightarrow 10x.$ **We need to consider more elements**.

Case O$_{111}$: $11110\textbf{000}x$.

$11110\textbf{000}x \rightarrow 1000100x \rightarrow 110111x \rightarrow 100100x \rightarrow 11111x \rightarrow 10000x \rightarrow 1100x \rightarrow \textbf{101}x.$
(7TS)

Case O$_{112}$: $11110\textbf{001}x$.

$11110\textbf{001}x \rightarrow 10001011x \rightarrow 11011010x \rightarrow 1001001x \rightarrow 1111111x \rightarrow 1000000x \rightarrow 110000x \rightarrow \textbf{101}00x.$ **(7TS)**

Case O$_{12}$: $11110\textbf{01}x$.

$11110\textbf{01}x \rightarrow 1000111x \rightarrow 1101100x \rightarrow 100101x \rightarrow 1111101x \rightarrow t100001x \rightarrow 110011x \rightarrow \textbf{101}110x.$ **(7TS)**

Case O$_2$: $111101x$.

$$111101x \rightarrow 100001x \rightarrow 110011x \rightarrow \mathbf{101}110x. \ \mathbf{(3TS)}$$

Case P: $11111x$.

$$11111x \rightarrow 10000x \rightarrow 1100x \rightarrow \mathbf{101}x. \ \mathbf{(3TS)}$$

We can see that the maximum number of time−steps to get $\mathbf{101}xxx$ is 9. 10 is the minimum number of cells to reach 9 time-steps.

Appendix H

Rule 387410647

In chapter 4, we found that there are only four transition rules which give three-periodic stationary pattern in three states using random initial conditions. In this appendix, we want to see the maximum number of time-steps this transition takes to produce periodic stationary patterns.

We have noted that under the transition rule 387410647, periodic pattern forms first on the left and then expand over the chain from the left to the right. Therefore, we will consider various initial combinations occurring on the left side of the chain and analyse how they allow the growth of the periodic structure to the right. Let's consider twenty seven cases starting with the first digit 1 on the left of the structure.

Case A: $1000x$.

$$1000x \rightarrow 1211x \rightarrow 1202x \rightarrow \mathbf{1201}x. \qquad \text{(3TS)}$$

For **Case A**, one has initially $1000x$. Let's start with the first three digits. The first digit is fixed. The next digit, 0, turns into 2. This is because the configuration says that $(100) \rightarrow (1\mathbf{2}0)$. The next three digits are 000. The 0 in the middle of 000 turns to 1. This is because the configuration says that $(000) \rightarrow (0\mathbf{1}0)$. The next three digits are $00x$. Three configurations containing $00x$ are $(000) \rightarrow (0\mathbf{1}0)$, $(001) \rightarrow (0\mathbf{1}1)$ and $(002) \rightarrow (0\mathbf{1}2)$. No matter what the value of x will be, the 0 in the middle of $00x$ change to 1. Thus, we obtain $1211x$. We start again. The first digit is fixed. The next digit, 2, remains as it is. This is because the configuration says that $(121) \rightarrow (1\mathbf{2}1)$. The next three digits are 211. The 1 in the middle of 211 turns to 0 because the configuration says that $(211) \rightarrow (2\mathbf{0}1)$. The next three digits are $11x$. Three configurations containing $11x$ are $(110) \rightarrow (1\mathbf{2}0)$, $(111) \rightarrow (1\mathbf{2}1)$ and $(112) \rightarrow (1\mathbf{2}2)$. No matter what the value

165

of x will be, the 1 in the middle of $11x$ will change to 2. Thus, we obtain $1202x$. We need one more procedure in order to reach $\mathbf{1201}x$. The first digit is fixed. The next digit, 2, remains the same because the configuration says that $(120) \to (1\mathbf{2}0)$. The next three digits are 202. The 0 in the middle of 202 remains the same since the configuration says that $(202) \to (2\mathbf{0}2)$. The next three digits are $02x$. Three configurations containing $02x$ are $(020) \to (0\mathbf{1}0)$, $(021) \to (0\mathbf{1}1)$ and $(022) \to (0\mathbf{1}2)$. No matter what the value of x will be, the 2 in the middle of $02x$ will change to 1. Thus, we obtain the sequence $\mathbf{1201}$.

Case B: $1001x$.

$$1001x \to 1211x \to 1202x \to \mathbf{1201}x. \qquad \text{(3TS)}$$

For **Case B**, one has initially $1001x$. Let's start with the first three digits. The first digit is fixed. The next digit, 0, turns into 2. This is because the configuration says that $(100) \to (1\mathbf{2}0)$. The next three digits are 001. The 0 in the middle of 001 turns to 1. This is because the configuration says that $(001) \to (0\mathbf{1}1)$. The next three digits are $01x$. Three configurations containing $01x$ are $(010) \to (0\mathbf{1}0)$, $(011) \to (0\mathbf{1}1)$ and $(012) \to (0\mathbf{1}2)$. No matter what the value of x will be, the 0 in the middle of $00x$ will remain as it is. Thus, we obtain $1211x$. We start again. The first digit is fixed. The next digit, 2, remains as it is. This is because the configuration says that $(121) \to (1\mathbf{2}1)$. The next three digits are 211. The 1 in the middle of 211 turns to 0 because the configuration says that $(211) \to (2\mathbf{0}1)$. The next three digits are $11x$. Three configurations containing $11x$ are $(110) \to (1\mathbf{2}0)$, $(111) \to (1\mathbf{2}1)$ and $(112) \to (1\mathbf{2}2)$. No matter what the value of x will be, the 1 in the middle of $11x$ will change to 2. Thus, we obtain $1202x$. We need one more procedure in order to reach $\mathbf{1201}x$. The first digit is fixed. The next digit, 2, remains the same because the configuration says that $(120) \to (1\mathbf{2}0)$. The next three digits are 202. The 0 in the middle of 202 remains the same since the configuration says that $(202) \to (2\mathbf{0}2)$. The next three digits are $02x$. Three configurations containing $02x$ are $(020) \to (0\mathbf{1}0)$, $(021) \to (0\mathbf{1}1)$ and $(022) \to (0\mathbf{1}2)$. No matter what the value of x will be, the 2 in the middle of $02x$ will change to 1. Thus, we obtain the sequence $\mathbf{1201}$.

Case C: $1002x$.

$$1002x \to 1211x \to 1202x \to \mathbf{1201}x. \qquad \text{(3TS)}$$

For **Case C**, one has initially $1002x$. Let's start with the first three digits. The first digit is fixed. The next digit, 0, turns into 2. This is because the configuration says

166

that $(100) \rightarrow (1\mathbf{2}0)$. The next three digits are 002. The 0 in the middle of 002 turns to 1. This is because the configuration says that $(002) \rightarrow (0\mathbf{1}2)$. The next three digits are $02x$. Three configurations containing $02x$ are $(020) \rightarrow (0\mathbf{1}0)$, $(021) \rightarrow (0\mathbf{1}1)$ and $(022) \rightarrow (0\mathbf{1}2)$. No matter what the value of x will be, the 0 in the middle of $00x$ change to 1. Thus, we obtain $1211x$. We start again. The first digit is fixed. The next digit, 2, remains as it is. This is because the configuration says that $(121) \rightarrow (1\mathbf{2}1)$. The next three digits are 211. The 1 in the middle of 211 turns to 0 according to the configuration $(211) \rightarrow (2\mathbf{0}1)$. The next three digits are $11x$. Three configurations containing $11x$ are $(110) \rightarrow (1\mathbf{2}0)$, $(111) \rightarrow (1\mathbf{2}1)$ and $(112) \rightarrow (1\mathbf{2}2)$. No matter what the value of x will be, the 1 in the middle of $11x$ will change to 2. Thus, we obtain $1202x$. We need one more procedure in order to reach $\mathbf{1201}x$. The first digit is fixed. The next digit, 2, remains the same because the configuration says that $(120) \rightarrow (1\mathbf{2}0)$. The next three digits are 202. The 0 in the middle of 202 remains the same since the configuration says that $(202) \rightarrow (2\mathbf{0}2)$. The next three digits are $02x$. Three configurations containing $02x$ are $(020) \rightarrow (0\mathbf{1}0)$, $(021) \rightarrow (0\mathbf{1}1)$ and $(022) \rightarrow (0\mathbf{1}2)$. No matter what the value of x will be, the 2 in the middle of $02x$ will change to 1. Thus, we obtain the sequence $\mathbf{1201}$.

Case D: $1010x$.

$$1010x \rightarrow 1212x \rightarrow 1202x \rightarrow \mathbf{1201}x. \qquad \text{(3TS)}$$

For **Case D**, one has initially $1010x$. Let's start with the first three digits. The first digit is fixed. The next digit, 0, turns to 2. This is because the configuration says that $(101) \rightarrow (1\mathbf{2}1)$. The next three digits are 010. The 1 in the middle of 010 remains as it is. This is because the configuration says that $(010) \rightarrow (0\mathbf{1}0)$. The next three digits are $10x$. Three configurations containing $10x$ are $(100) \rightarrow (1\mathbf{2}0)$, $(101) \rightarrow (1\mathbf{2}1)$ and $(102) \rightarrow (1\mathbf{2}2)$. No matter what the value of x will be, the 0 in the middle of $10x$ will change to 2. Thus, we obtain $1212x$. We start over again. The first digit is fixed. The next digit, 2, remains as it is. This is because the configuration says that $(121) \rightarrow (1\mathbf{2}1)$. The next three digits are 212. The 1 in the middle of 212 turns to 0 according to the configuration $(212) \rightarrow (2\mathbf{0}2)$. The next three digits are $12x$. Three configurations containing $12x$ are $(120) \rightarrow (1\mathbf{2}0)$, $(121) \rightarrow (1\mathbf{2}1)$ and $(122) \rightarrow (1\mathbf{2}2)$. No matter what the value of x will be, the 2 in the middle of $12x$ will remain as it is. Thus, we obtain $1202x$. We need one more procedure in order to reach $\mathbf{1201}x$. The first digit is fixed. The next digit, 2, remains the same because the configuration says that $(120) \rightarrow (1\mathbf{2}0)$. The next three digits are 202. The 0 in the middle of 202 remains the same since the configuration says that $(202) \rightarrow (2\mathbf{0}2)$. The next three digits are $02x$. Three configurations containing $02x$ are $(020) \rightarrow (0\mathbf{1}0)$, $(021) \rightarrow (0\mathbf{1}1)$ and $(022) \rightarrow (0\mathbf{1}2)$. No matter what the value of

x will be, the 2 in the middle of $02x$ will change to 1. Thus, we obtain the sequence **1201**.

Case E: $1011x$.

$$1011x \rightarrow 1212x \rightarrow 1202x \rightarrow \mathbf{1201}x. \qquad \text{(3TS)}$$

For **Case E**, one has initially $1011x$. Let's start with the first three digits. The first digit is fixed. The next digit, 0, turns to 2. This is because the configuration says that $(101) \rightarrow (1\mathbf{2}1)$. The next three digits are 011. The 1 in the middle of 011 remains as it is. This is because the configuration says that $(011) \rightarrow (0\mathbf{1}1)$. The next three digits are $11x$. Three configurations containing $11x$ are $(110) \rightarrow (1\mathbf{2}0)$, $(111) \rightarrow (1\mathbf{2}1)$ and $(112) \rightarrow (1\mathbf{2}2)$. No matter what the value of x will be, the 1 in the middle of $11x$ will change to 2. Thus, we obtain $1212x$. We start over again. The first digit is fixed. The next digit, 2, remains as it is. This is because the configuration says that $(121) \rightarrow (1\mathbf{2}1)$. The next three digits are 212. The 1 in the middle of 212 turns to 0 according to the configuration $(212) \rightarrow (2\mathbf{0}2)$. The next three digits are $12x$. Three configurations containing $12x$ are $(120) \rightarrow (1\mathbf{2}0)$, $(121) \rightarrow (1\mathbf{2}1)$ and $(122) \rightarrow (1\mathbf{2}2)$. No matter what the value of x will be, the 2 in the middle of $12x$ will remain as it is. Thus, we obtain $1202x$. We need one more procedure in order to reach $\mathbf{1201}x$. The first digit is fixed. The next digit, 2, remains the same because the configuration says that $(120) \rightarrow (1\mathbf{2}0)$. The next three digits are 202. The 0 in the middle of 202 remains the same since the configuration says that $(202) \rightarrow (2\mathbf{0}2)$. The next three digits are $02x$. Three configurations containing $02x$ are $(020) \rightarrow (0\mathbf{1}0)$, $(021) \rightarrow (0\mathbf{1}1)$ and $(022) \rightarrow (0\mathbf{1}2)$. No matter what the value of x will be, the 2 in the middle of $02x$ will change to 1. Thus, we obtain the sequence **1201**.

Case F: $1012x$.

$$1012x \rightarrow 1212x \rightarrow 1202x \rightarrow \mathbf{1201}x. \qquad \text{(3TS)}$$

For **Case F**, one has initially $1012x$. Let's start with the first three digits. The first digit is fixed. The next digit, 0, turns to 2. This is because the configuration says that $(101) \rightarrow (1\mathbf{2}1)$. The next three digits are 012. The 1 in the middle of 012 remains as it is. This is because the configuration says that $(012) \rightarrow (0\mathbf{1}2)$. The next three digits are $12x$. Three configurations containing $12x$ are $(120) \rightarrow (1\mathbf{2}0)$, $(121) \rightarrow (1\mathbf{2}1)$ and $(122) \rightarrow (1\mathbf{2}2)$. No matter what the value of x will be, the 2 in the middle of $12x$ will remain as it is. Thus, we obtain $1212x$. We start over again. The first digit is fixed. The next digit, 2, remains as it is. This is because the configuration says that $(121) \rightarrow (1\mathbf{2}1)$.

The next three digits are 212. The 1 in the middle of 212 turns to 0 according to the configuration $(212) \to (2\mathbf{0}2)$. The next three digits are $12x$. Three configurations containing $12x$ are $(120) \to (1\mathbf{2}0)$, $(121) \to (1\mathbf{2}1)$ and $(122) \to (1\mathbf{2}2)$. No matter what the value of x will be, the 2 in the middle of $12x$ will remain as it is. Thus, we obtain $1202x$. We need one more procedure in order to reach $\mathbf{1201}x$. The first digit is fixed. The next digit, 2, remains the same because the configuration says that $(120) \to (1\mathbf{2}0)$. The next three digits are 202. The 0 in the middle of 202 remains the same since the configuration says that $(202) \to (2\mathbf{0}2)$. The next three digits are $02x$. Three configurations containing $02x$ are $(020) \to (0\mathbf{1}0)$, $(021) \to (0\mathbf{1}1)$ and $(022) \to (0\mathbf{1}2)$. No matter what the value of x will be, the 2 in the middle of $02x$ will change to 1. Thus, we obtain the sequence $\mathbf{1201}$.

Case G: $1020x$.

$$1020x \to 1210x \to 1202x \to \mathbf{1201}x. \qquad \text{(3TS)}$$

For **Case G**, one has initially $1020x$. Let's start with the first three digits. The first digit is fixed. The next digit, 0, turns to 2. This is because the configuration says that $(102) \to (1\mathbf{2}2)$. The next three digits are 020. The 2 in the middle of 020 will change to 1. This is because the configuration says that $(020) \to (0\mathbf{1}0)$. The next three digits are $20x$. Three configurations containing $20x$ are $(200) \to (2\mathbf{0}0)$, $(201) \to (2\mathbf{0}1)$ and $(202) \to (2\mathbf{0}2)$. No matter what the value of x will be, the 0 in the middle of $20x$ will remain as it is. Thus, we obtain $1210x$. We start over again. The first digit is fixed. The next digit, 2, remains as it is. This is because the configuration says that $(121) \to (1\mathbf{2}1)$. The next three digits are 210. The 1 in the middle of 210 turns to 0 according to the configuration $(210) \to (2\mathbf{0}0)$. The next three digits are $10x$. Three configurations containing $10x$ are $(100) \to (1\mathbf{2}0)$, $(101) \to (1\mathbf{2}1)$ and $(102) \to (1\mathbf{2}2)$. No matter what the value of x will be, the 0 in the middle of $10x$ will change to 2. Thus, we obtain $1202x$. We need one more procedure in order to reach $\mathbf{1201}x$. The first digit is fixed. The next digit, 2, remains the same because the configuration says that $(120) \to (1\mathbf{2}0)$. The next three digits are 202. The 0 in the middle of 202 remains the same since the configuration says that $(202) \to (2\mathbf{0}2)$. The next three digits are $02x$. Three configurations containing $02x$ are $(020) \to (0\mathbf{1}0)$, $(021) \to (0\mathbf{1}1)$ and $(022) \to (0\mathbf{1}2)$. No matter what the value of x will be, the 2 in the middle of $02x$ will change to 1. Thus, we obtain the sequence $\mathbf{1201}$.

Case H: $1021x$.

$$1021x \to 1210x \to 1202x \to \mathbf{1201}x. \qquad \text{(3TS)}$$

For **Case H**, one has initially $1021x$. Let's start with the first three digits. The first digit is fixed. The next digit, 0, turns to 2. This is because the configuration says that $(102) \rightarrow (1\mathbf{2}2)$. The next three digits are 021. The 2 in the middle of 021 will change to 1. This is because the configuration says that $(021) \rightarrow (0\mathbf{1}1)$. The next three digits are $21x$. Three configurations containing $21x$ are $(210) \rightarrow (2\mathbf{0}0)$, $(211) \rightarrow (2\mathbf{0}1)$ and $(212) \rightarrow (2\mathbf{0}2)$. No matter what the value of x will be, the 1 in the middle of $21x$ will change to 0. Thus, we obtain $1210x$. We start over again. The first digit is fixed. The next digit, 2, remains as it is. This is because the configuration says that $(121) \rightarrow (1\mathbf{2}1)$. The next three digits are 210. The 1 in the middle of 210 turns to 0 according to the configuration $(210) \rightarrow (2\mathbf{0}0)$. The next three digits are $10x$. Three configurations containing $10x$ are $(100) \rightarrow (1\mathbf{2}0)$, $(101) \rightarrow (1\mathbf{2}1)$ and $(102) \rightarrow (1\mathbf{2}2)$. No matter what the value of x will be, the 0 in the middle of $10x$ will change to 2. Thus, we obtain $1202x$. We need one more procedure in order to reach $\mathbf{1201}x$. The first digit is fixed. The next digit, 2, remains the same because the configuration says that $(120) \rightarrow (1\mathbf{2}0)$. The next three digits are 202. The 0 in the middle of 202 remains the same since the configuration says that $(202) \rightarrow (2\mathbf{0}2)$. The next three digits are $02x$. Three configurations containing $02x$ are $(020) \rightarrow (0\mathbf{1}0)$, $(021) \rightarrow (0\mathbf{1}1)$ and $(022) \rightarrow (0\mathbf{1}2)$. No matter what the value of x will be, the 2 in the middle of $02x$ will change to 1. Thus, we obtain the stripe $\mathbf{1201}$.

Case I: $1022x$.

$$1022x \rightarrow 1210x \rightarrow 1202x \rightarrow \mathbf{1201}x. \qquad \text{(3TS)}$$

For **Case I**, one has initially $1022x$. Let's start with the first three digits. The first digit is fixed. The next digit, 0, turns to 2. This is because the configuration says that $(102) \rightarrow (1\mathbf{2}2)$. The next three digits are 022. The 2 in the middle of 022 will change to 1. This is because the configuration says that $(022) \rightarrow (0\mathbf{1}2)$. The next three digits are $22x$. Three configurations containing $22x$ are $(220) \rightarrow (2\mathbf{0}0)$, $(221) \rightarrow (2\mathbf{0}1)$ and $(222) \rightarrow (2\mathbf{0}2)$. No matter what the value of x will be, the 2 in the middle of $22x$ will change to 0. Thus, we obtain $1210x$. We start over again. The first digit is fixed. The next digit, 2, remains as it is. This is because the configuration says that $(121) \rightarrow (1\mathbf{2}1)$. The next three digits are 210. The 1 in the middle of 210 turns to 0 according to the configuration $(210) \rightarrow (2\mathbf{0}0)$. The next three digits are $10x$. Three configurations containing $10x$ are $(100) \rightarrow (1\mathbf{2}0)$, $(101) \rightarrow (1\mathbf{2}1)$ and $(102) \rightarrow (1\mathbf{2}2)$. No matter what the value of x will be, the 0 in the middle of $10x$ will change to 2. Thus, we obtain $1202x$. We need one more procedure in order to reach $\mathbf{1201}x$. The first digit is fixed. The next digit, 2, remains the same because the configuration says that $(120) \rightarrow (1\mathbf{2}0)$. The next

three digits are 202. The 0 in the middle of 202 remains the same since the configuration says that $(202) \to (2\mathbf{0}2)$. The next three digits are $02x$. Three configurations containing $02x$ are $(020) \to (0\mathbf{1}0)$, $(021) \to (0\mathbf{1}1)$ and $(022) \to (0\mathbf{1}2)$. No matter what the value of x will be, the 2 in the middle of $02x$ will change to 1. Thus, we obtain the sequence **1201**.

Case J: $1100x$.

$$1100x \to 1221x \to 1200x \to \mathbf{1201}x. \qquad \text{(3TS)}$$

For **Case J**, one has initially $1100x$. Let's start with the first three digits. The first digit is fixed. The next digit, 1, turns to 2. This is because the configuration says that $(110) \to (1\mathbf{2}0)$. The next three digits are 100. The 0 in the middle of 100 will change to 2. This is because the configuration says that $(100) \to (1\mathbf{2}0)$. The next three digits are $00x$. Three configurations containing $00x$ are $(000) \to (0\mathbf{1}0)$, $(001) \to (0\mathbf{1}1)$ and $(002) \to (0\mathbf{1}2)$. No matter what the value of x will be, the 0 in the middle of $00x$ will change to 1. Thus, we obtain $1221x$. We start over again. The first digit is fixed. The next digit, 2, remains as it is. This is because the configuration says that $(122) \to (1\mathbf{2}2)$. The next three digits are 221. The 2 in the middle of 221 turns to 0 according to the configuration $(221) \to (2\mathbf{0}1)$. The next three digits are $21x$. Three configurations containing $21x$ are $(210) \to (2\mathbf{0}0)$, $(211) to (2\mathbf{0}1)$ and $(212) \to (2\mathbf{0}2)$. No matter what the value of x will be, the 1 in the middle of $21x$ will change to 0. Thus, we obtain $1200x$. We need one more procedure in order to reach $\mathbf{1201}x$. The first digit is fixed. The next digit, 2, remains the same because the configuration says that $(120) \to (1\mathbf{2}0)$. The next three digits are 200. The 0 in the middle of 200 remains the same since the configuration says that $(200) \to (2\mathbf{0}0)$. The next three digits are $00x$. Three configurations containing $00x$ are $(000) \to (0\mathbf{1}0)$, $(001) \to (0\mathbf{1}1)$ and $(002) \to (0\mathbf{1}2)$. No matter what the value of x will be, the 0 in the middle of $00x$ will change to 1. Thus, we obtain the sequence **1201**.

Case K: $1101x$.

$$1101x \to 1221x \to 1200x \to \mathbf{1201}x. \qquad \text{(3TS)}$$

For **Case K**, one has initially $1101x$. Let's start with the first three digits. The first digit is fixed. The next digit, 1, turns to 2. This is because the configuration says that $(110) \to (1\mathbf{2}0)$. The next three digits are 101. The 0 in the middle of 101 will change to 2. This is because the configuration says that $(101) \to (1\mathbf{2}1)$. The next three digits are $01x$. Three configurations containing $01x$ are $(010) \to (0\mathbf{1}0)$, $(011) \to (0\mathbf{1}1)$ and

$(012) \rightarrow (01\mathbf{2})$. No matter what the value of x will be, the 1 in the middle of $01x$ will remain as it is. Thus, we obtain $1221x$. We start over again. The first digit is fixed. The next digit, 2, remains as it is. This is because the configuration says that $(122) \rightarrow (1\mathbf{2}2)$. The next three digits are 221. The 2 in the middle of 221 turns to 0 according to the configuration $(221) \rightarrow (2\mathbf{0}1)$. The next three digits are $21x$. Three configurations containing $21x$ are $(210) \rightarrow (2\mathbf{0}0)$, $(211)to(2\mathbf{0}1)$ and $(212) \rightarrow (2\mathbf{0}2)$. No matter what the value of x will be, the 1 in the middle of $21x$ will change to 0. Thus, we obtain $1200x$. We need one more procedure in order to reach $\mathbf{1201}x$. The first digit is fixed. The next digit, 2, remains the same because the configuration says that $(120) \rightarrow (1\mathbf{2}0)$. The next three digits are 200. The 0 in the middle of 200 remains the same since the configuration says that $(200) \rightarrow (2\mathbf{0}0)$. The next three digits are $00x$. Three configurations containing $00x$ are $(000) \rightarrow (0\mathbf{1}0)$, $(001) \rightarrow (0\mathbf{1}1)$ and $(002) \rightarrow (0\mathbf{1}2)$. No matter what the value of x will be, the 0 in the middle of $00x$ will change to 1. Thus, we obtain the sequence $\mathbf{1201}$.

Case L: $1102x$.

$$1102x \rightarrow 1221x \rightarrow 1200x \rightarrow \mathbf{1201}x. \qquad \text{(3TS)}$$

For **Case L**, one has initially $1102x$. Let's start with the first three digits. The first digit is fixed. The next digit, 1, turns to 2. This is because the configuration says that $(110) \rightarrow (1\mathbf{2}0)$. The next three digits are 102. The 0 in the middle of 102 will change to 2. This is because the configuration says that $(102) \rightarrow (1\mathbf{2}2)$. The next three digits are $02x$. Three configurations containing $02x$ are $(020) \rightarrow (0\mathbf{1}0)$, $(021) \rightarrow (0\mathbf{1}1)$ and $(022) \rightarrow (0\mathbf{1}2)$. No matter what the value of x will be, the 2 in the middle of $02x$ will change to 1. Thus, we obtain $1221x$. We start over again. The first digit is fixed. The next digit, 2, remains as it is. This is because the configuration says that $(122) \rightarrow (1\mathbf{2}2)$. The next three digits are 221. The 2 in the middle of 221 turns to 0 according to the configuration $(221) \rightarrow (2\mathbf{0}1)$. The next three digits are $21x$. Three configurations containing $21x$ are $(210) \rightarrow (2\mathbf{0}0)$, $(211)to(2\mathbf{0}1)$ and $(212) \rightarrow (2\mathbf{0}2)$. No matter what the value of x will be, the 1 in the middle of $21x$ will change to 0. Thus, we obtain $1200x$. We need one more procedure in order to reach $\mathbf{1201}x$. The first digit is fixed. The next digit, 2, remains the same because the configuration says that $(120) \rightarrow (1\mathbf{2}0)$. The next three digits are 200. The 0 in the middle of 200 remains the same since the configuration says that $(200) \rightarrow (2\mathbf{0}0)$. The next three digits are $00x$. Three configurations containing $00x$ are $(000) \rightarrow (0\mathbf{1}0)$, $(001) \rightarrow (0\mathbf{1}1)$ and $(002) \rightarrow (0\mathbf{1}2)$. No matter what the value of x will be, the 0 in the middle of $00x$ will change to 1. Thus, we obtain the sequence $\mathbf{1201}$.

Case M: $1110x$.

$$1110x \rightarrow 1222x \rightarrow 1200x \rightarrow \mathbf{1201x}. \qquad \text{(3TS)}$$

For **Case M**, one has initially 1110x. Let's start with the first three digits. The first digit is fixed. The next digit, 1, turns to 2. This is because the configuration says that $(111) \rightarrow (1\mathbf{2}1)$. The next three digits are 110. The 1 in the middle of 110 will change to 2. This is because the configuration says that $(110) \rightarrow (1\mathbf{2}0)$. The next three digits are $10x$. Three configurations containing $10x$ are $(100) \rightarrow (1\mathbf{2}0)$, $(101) \rightarrow (1\mathbf{2}1)$ and $(102) \rightarrow (1\mathbf{2}2)$. No matter what the value of x will be, the 0 in the middle of $10x$ will change to 2. Thus, we obtain $1222x$. We start over again. The first digit is fixed. The next digit, 2, remains as it is. This is because the configuration says that $(122) \rightarrow (1\mathbf{2}2)$. The next three digits are 222. The 2 in the middle of 222 turns to 0 according to the configuration $(222) \rightarrow (2\mathbf{0}2)$. The next three digits are $22x$. Three configurations containing $22x$ are $(220) \rightarrow (2\mathbf{0}0)$, $(221) \rightarrow (2\mathbf{0}1)$ and $(222) \rightarrow (2\mathbf{0}2)$. No matter what the value of x will be, the 2 in the middle of $22x$ will change to 0. Thus, we obtain $1200x$. We need one more procedure in order to reach $\mathbf{1201x}$. The first digit is fixed. The next digit, 2, remains the same because the configuration says that $(120) \rightarrow (1\mathbf{2}0)$. The next three digits are 200. The 0 in the middle of 200 remains the same since the configuration says that $(200) \rightarrow (2\mathbf{0}0)$. The next three digits are $00x$. Three configurations containing $00x$ are $(000) \rightarrow (0\mathbf{1}0)$, $(001) \rightarrow (0\mathbf{1}1)$ and $(002) \rightarrow (0\mathbf{1}2)$. No matter what the value of x will be, the 0 in the middle of $00x$ will change to 1. Thus, we obtain the sequence $\mathbf{1201}$.

Case N: $1111x$.

$$1111x \rightarrow 1222x \rightarrow 1200x \rightarrow \mathbf{1201x}. \qquad \text{(3TS)}$$

For **Case N**, one has initially $1111x$. Let's start with the first three digits. The first digit is fixed. The next digit, 1, turns to 2. This is because the configuration says that $(111) \rightarrow (1\mathbf{2}1)$. The next three digits are 111. The 1 in the middle of 111 will change to 2. This is because the configuration says that $(111) \rightarrow (1\mathbf{2}1)$. The next three digits are $11x$. Three configurations containing $11x$ are $(110) \rightarrow (1\mathbf{2}0)$, $(111) \rightarrow (1\mathbf{2}1)$ and $(112) \rightarrow (1\mathbf{2}2)$. No matter what the value of x will be, the 1 in the middle of $11x$ will change to 2. Thus, we obtain $1222x$. We start over again. The first digit is fixed. The next digit, 2, remains as it is. This is because the configuration says that $(122) \rightarrow (1\mathbf{2}2)$. The next three digits are 222. The 2 in the middle of 222 turns to 0 according to the configuration $(222) \rightarrow (2\mathbf{0}2)$. The next three digits are $22x$. Three configurations containing $22x$ are $(220) \rightarrow (2\mathbf{0}0)$, $(221) \rightarrow (2\mathbf{0}1)$ and $(222) \rightarrow (2\mathbf{0}2)$. No matter what the value of x will be, the 2 in the middle of $22x$ will change to 0. Thus, we obtain $1200x$.

We need one more procedure in order to reach $\mathbf{1201}x$. The first digit is fixed. The next digit, 2, remains the same because the configuration says that $(120) \rightarrow (1\mathbf{2}0)$. The next three digits are 200. The 0 in the middle of 200 remains the same since the configuration says that $(200) \rightarrow (2\mathbf{0}0)$. The next three digits are $00x$. Three configurations containing $00x$ are $(000) \rightarrow (0\mathbf{1}0)$, $(001) \rightarrow (0\mathbf{1}1)$ and $(002) \rightarrow (0\mathbf{1}2)$. No matter what the value of x will be, the 0 in the middle of $00x$ will change to 1. Thus, we obtain the sequence $\mathbf{1201}$.

Case O: $1112x$.

$$1111x \rightarrow 1222x \rightarrow 1200x \rightarrow \mathbf{1201x}. \qquad \text{(3TS)}$$

For **Case O**, one has initially $1112x$. Let's start with the first three digits. The first digit is fixed. The next digit, 1, turns to 2. This is because the configuration says that $(111) \rightarrow (1\mathbf{2}1)$. The next three digits are 112. The 1 in the middle of 112 will change to 2. This is because the configuration says that $(112) \rightarrow (1\mathbf{2}2)$. The next three digits are $12x$. Three configurations containing $12x$ are $(120) \rightarrow (1\mathbf{2}0)$, $(121) \rightarrow (1\mathbf{2}1)$ and $(122) \rightarrow (1\mathbf{2}2)$. No matter what the value of x will be, the 2 in the middle of $12x$ will remain as it is. Thus, we obtain $1222x$. We start over again. The first digit is fixed. The next digit, 2, remains as it is. This is because the configuration says that $(122) \rightarrow (1\mathbf{2}2)$. The next three digits are 222. The 2 in the middle of 222 turns to 0 according to the configuration $(222) \rightarrow (2\mathbf{0}2)$. The next three digits are $22x$. Three configurations containing $22x$ are $(220) \rightarrow (2\mathbf{0}0)$, $(221) \rightarrow (2\mathbf{0}1)$ and $(222) \rightarrow (2\mathbf{0}2)$. No matter what the value of x will be, the 2 in the middle of $22x$ will change to 0. Thus, we obtain $1200x$. We need one more procedure in order to reach $\mathbf{1201}x$. The first digit is fixed. The next digit, 2, remains the same because the configuration says that $(120) \rightarrow (1\mathbf{2}0)$. The next three digits are 200. The 0 in the middle of 200 remains the same since the configuration says that $(200) \rightarrow (2\mathbf{0}0)$. The next three digits are $00x$. Three configurations containing $00x$ are $(000) \rightarrow (0\mathbf{1}0)$, $(001) \rightarrow (0\mathbf{1}1)$ and $(002) \rightarrow (0\mathbf{1}2)$. No matter what the value of x will be, the 0 in the middle of $00x$ will change to 1. Thus, we obtain the sequence $\mathbf{1201}$.

Case P: $1120x$.

$$1120x \rightarrow 1200x \rightarrow 1200x \rightarrow \mathbf{1201x}. \qquad \text{(3TS)}$$

For **Case P**, one has initially $1120x$. Let's start with the first three digits. The first digit is fixed. The next digit, 1, turns to 2. This is because the configuration says that $(112) \rightarrow (1\mathbf{2}2)$. The next three digits are 120. The 2 in the middle of 120 will remain as

it is. This is because the configuration says that $(120) \to (1\mathbf{2}0)$. The next three digits are $20x$. Three configurations containing $20x$ are $(200) \to (2\mathbf{0}0)$, $(201) \to (2\mathbf{0}1)$ and $(202) \to (2\mathbf{0}2)$. No matter what the value of x will be, the 0 in the middle of $20x$ will remain as it is. Thus, we obtain $1220x$. We start over again. The first digit is fixed. The next digit, 2, remains as it is. This is because the configuration says that $(122) \to (1\mathbf{2}2)$. The next three digits are 220. The 2 in the middle of 220 turns to 0 according to the configuration $(220) \to (2\mathbf{0}0)$. The next three digits are $20x$. Three configurations containing $20x$ are $(200) \to (2\mathbf{0}0)$, $(201) \to (2\mathbf{0}1)$ and $(202) \to (2\mathbf{0}2)$. No matter what the value of x will be, the 0 in the middle of $20x$ will remain as it is. Thus, we obtain $1200x$. We need one more procedure in order to reach $\mathbf{1201}x$. The first digit is fixed. The next digit, 2, remains the same because the configuration says that $(120) \to (1\mathbf{2}0)$. The next three digits are 200. The 0 in the middle of 200 remains the same since the configuration says that $(200) \to (2\mathbf{0}0)$. The next three digits are $00x$. Three configurations containing $00x$ are $(000) \to (0\mathbf{1}0)$, $(001) \to (0\mathbf{1}1)$ and $(002) \to (0\mathbf{1}2)$. No matter what the value of x will be, the 0 in the middle of $00x$ will change to 1. Thus, we obtain the sequence $\mathbf{1201}$.

Case Q: $1121x$.

$$1121x \to 1200x \to 1200x \to \mathbf{1201x}. \qquad \text{(3TS)}$$

For **Case Q**, one has initially $1121x$. Let's start with the first three digits. The first digit is fixed. The next digit, 1, turns to 2. This is because the configuration says that $(112) \to (1\mathbf{2}2)$. The next three digits are 121. The 2 in the middle of 121 will remain as it is. This is because the configuration says that $(121) \to (1\mathbf{2}1)$. The next three digits are $21x$. Three configurations containing $21x$ are $(210) \to (2\mathbf{0}0)$, $(211) \to (2\mathbf{0}1)$ and $(212) \to (2\mathbf{0}2)$. No matter what the value of x will be, the 1 in the middle of $21x$ will change to 0. Thus, we obtain $1220x$. We start over again. The first digit is fixed. The next digit, 2, remains as it is. This is because the configuration says that $(122) \to (1\mathbf{2}2)$. The next three digits are 220. The 2 in the middle of 220 turns to 0 according to the configuration $(220) \to (2\mathbf{0}0)$. The next three digits are $20x$. Three configurations containing $20x$ are $(200) \to (2\mathbf{0}0)$, $(201) \to (2\mathbf{0}1)$ and $(202) \to (2\mathbf{0}2)$. No matter what the value of x will be, the 0 in the middle of $20x$ will remain as it is. Thus, we obtain $1200x$. We need one more procedure in order to reach $\mathbf{1201}x$. The first digit is fixed. The next digit, 2, remains the same because the configuration says that $(120) \to (1\mathbf{2}0)$. The next three digits are 200. The 0 in the middle of 200 remains the same since the configuration says that $(200) \to (2\mathbf{0}0)$. The next three digits are $00x$. Three configurations containing $00x$ are $(000) \to (0\mathbf{1}0)$, $(001) \to (0\mathbf{1}1)$ and $(002) \to (0\mathbf{1}2)$. No matter what the value of x will be, the 0 in the middle of $00x$ will change to 1. Thus, we obtain the sequence $\mathbf{1201}$.

Case R: $1122x$.

$$1122x \rightarrow 1200x \rightarrow 1200x \rightarrow \mathbf{1201x}. \qquad (3\text{TS})$$

For **Case R**, one has initially $1122x$. Let's start with the first three digits. The first digit is fixed. The next digit, 1, turns to 2. This is because the configuration says that $(112) \rightarrow (1\mathbf{2}2)$. The next three digits are 122. The 2 in the middle of 122 will remain as it is. This is because the configuration says that $(122) \rightarrow (1\mathbf{2}2)$. The next three digits are $22x$. Three configurations containing $22x$ are $(220) \rightarrow (2\mathbf{0}0)$, $(221) \rightarrow (2\mathbf{0}1)$ and $(222) \rightarrow (2\mathbf{0}2)$. No matter what the value of x will be, the 1 in the middle of $21x$ will change to 0. Thus, we obtain $1220x$. We start over again. The first digit is fixed. The next digit, 2, remains as it is. This is because the configuration says that $(122) \rightarrow (1\mathbf{2}2)$. The next three digits are 220. The 2 in the middle of 220 turns to 0 according to the configuration $(220) \rightarrow (2\mathbf{0}0)$. The next three digits are $20x$. Three configurations containing $20x$ are $(200) \rightarrow (2\mathbf{0}0)$, $(201) \rightarrow (2\mathbf{0}1)$ and $(202) \rightarrow (2\mathbf{0}2)$. No matter what the value of x will be, the 0 in the middle of $20x$ will remain as it is. Thus, we obtain $1200x$. We need one more procedure in order to reach $\mathbf{1201}x$. The first digit is fixed. The next digit, 2, remains the same because the configuration says that $(120) \rightarrow (1\mathbf{2}0)$. The next three digits are 200. The 0 in the middle of 200 remains the same since the configuration says that $(200) \rightarrow (2\mathbf{0}0)$. The next three digits are $00x$. Three configurations containing $00x$ are $(000) \rightarrow (0\mathbf{1}0)$, $(001) \rightarrow (0\mathbf{1}1)$ and $(002) \rightarrow (0\mathbf{1}2)$. No matter what the value of x will be, the 0 in the middle of $00x$ will change to 1. Thus, we obtain the sequence $\mathbf{1201}$.

Case S: $1200x$.

$$1200x \rightarrow \mathbf{1201x}. \qquad (1\text{TS})$$

For **Case S**, one has initially $1200x$. The first digit is fixed. The next digit, 2, remains the same because the configuration says that $(120) \rightarrow (1\mathbf{2}0)$. The next three digits are 200. The 0 in the middle of 200 remains the same since the configuration says that $(200) \rightarrow (2\mathbf{0}0)$. The next three digits are $00x$. Three configurations containing $00x$ are $(000) \rightarrow (0\mathbf{1}0)$, $(001) \rightarrow (0\mathbf{1}1)$ and $(002) \rightarrow (0\mathbf{1}2)$. No matter what the value of x will be, the 0 in the middle of $00x$ will change to 1. Thus, we obtain the sequence $\mathbf{1201}$.

Case S: $1201x$.

$$\mathbf{1201x}. \qquad (0\text{TS})$$

For **Case T**, the sequence **1201**x is already established.

Case U: $1202x$.

$$1202x \rightarrow \mathbf{1201x}. \qquad \text{(1TS)}$$

For **Case U**, one has initially $1202x$. The first digit is fixed. The next digit, 2, remains the same because the configuration says that $(120) \rightarrow (1\mathbf{2}0)$. The next three digits are 200. The 0 in the middle of 202 remains the same since the configuration says that $(202) \rightarrow (2\mathbf{0}2)$. The next three digits are $02x$. Three configurations containing $02x$ are $(020) \rightarrow (0\mathbf{1}0)$, $(021) \rightarrow (0\mathbf{1}1)$ and $(022) \rightarrow (0\mathbf{1}2)$. No matter what the value of x will be, the 2 in the middle of $02x$ will change to 1. Thus, we obtain the sequence **1201**.

Case V: $1210x$.

$$1210x \rightarrow 1202x \rightarrow \mathbf{1201x}. \qquad \text{(2TS)}$$

For **Case V**, one has initially $1210x$. The first digit is fixed. The next digit, 2, remains as it is. This is because the configuration says that $(121) \rightarrow (121)$. The next three digits are 210. The 1 in the middle of 210 turns to 0 according to the configuration $(210) \rightarrow (2\mathbf{0}0)$. The next three digits are $10x$. Three configurations containing $10x$ are $(100) \rightarrow (1\mathbf{2}0)$, $(101) \rightarrow (1\mathbf{2}1)$ and $(102) \rightarrow (1\mathbf{2}2)$. No matter what the value of x will be, the 0in the middle of $10x$ will change to 2. Thus, we obtain $1202x$. We need one more procedure in order to reach **1201**x. The first digit is fixed. The next digit, 2, remains the same because the configuration says that $(120) \rightarrow (1\mathbf{2}0)$. The next three digits are 200. The 0 in the middle of 202 remains the same since the configuration says that $(202) \rightarrow (2\mathbf{0}2)$. The next three digits are $02x$. Three configurations containing $02x$ are $(020) \rightarrow (0\mathbf{1}0)$, $(021) \rightarrow (0\mathbf{1}1)$ and $(022) \rightarrow (0\mathbf{1}2)$. No matter what the value of x will be, the 2 in the middle of $02x$ will change to 1. Thus, we obtain the sequence **1201**.

Case W: $1211x$.

$$1211x \rightarrow 1202x \rightarrow \mathbf{1201x}. \qquad \text{(2TS)}$$

For **Case W**, one has initially $1211x$. The first digit is fixed. The next digit, 2, remains as it is. This is because the configuration says that $(121) \rightarrow (121)$. The next three

digits are 210. The 1 in the middle of 211 turns to 0 according to the configuration $(211) \to (20\mathbf{1})$. The next three digits are $11x$. Three configurations containing $11x$ are $(110) \to (1\mathbf{2}0)$, $(111) \to (1\mathbf{2}1)$ and $(112) \to (1\mathbf{2}2)$. No matter what the value of x will be, the 1 in the middle of $10x$ will change to 2. Thus, we obtain $1202x$. We need one more procedure in order to reach $\mathbf{1201}x$. The first digit is fixed. The next digit, 2, remains the same because the configuration says that $(120) \to (1\mathbf{2}0)$. The next three digits are 200. The 0 in the middle of 202 remains the same since the configuration says that $(202) \to (2\mathbf{0}2)$. The next three digits are $02x$. Three configurations containing $02x$ are $(020) \to (0\mathbf{1}0)$, $(021) \to (0\mathbf{1}1)$ and $(022) \to (0\mathbf{1}2)$. No matter what the value of x will be, the 2 in the middle of $02x$ will change to 1. Thus, we obtain the sequence $\mathbf{1201}$.

Case X: $1212x$.

$$1211x \to 1202x \to \mathbf{1201x}. \qquad \text{(2TS)}$$

For **Case X**, one has initially $1212x$. The first digit is fixed. The next digit, 2, remains as it is. This is because the configuration says that $(121) \to (121)$. The next three digits are 210. The 1 in the middle of 212 turns to 0 according to the configuration $(212) \to (2\mathbf{0}2)$. The next three digits are $12x$. Three configurations containing $12x$ are $(120) \to (1\mathbf{2}0)$, $(121) \to (1\mathbf{2}1)$ and $(122) \to (1\mathbf{2}2)$. No matter what the value of x will be, the 2in the middle of $10x$ will remain as it is. Thus, we obtain $1202x$. We need one more procedure in order to reach $\mathbf{1201}x$. The first digit is fixed. The next digit, 2, remains the same because the configuration says that $(120) \to (1\mathbf{2}0)$. The next three digits are 200. The 0 in the middle of 202 remains the same since the configuration says that $(202) \to (2\mathbf{0}2)$. The next three digits are $02x$. Three configurations containing $02x$ are $(020) \to (0\mathbf{1}0)$, $(021) \to (0\mathbf{1}1)$ and $(022) \to (0\mathbf{1}2)$. No matter what the value of x will be, the 2 in the middle of $02x$ will change to 1. Thus, we obtain the sequence $\mathbf{1201}$.

Case Y: $1220x$.

$$1220x \to 1200x \to \mathbf{1201x}. \qquad \text{(2TS)}$$

For **Case Y**, one has initially $1220x$. The first digit is fixed. The next digit, 2, remains as it is. This is because the configuration says that $(122) \to (1\mathbf{2}2)$. The next three digits are 220. The 2 in the middle of 220 turns to 0 according to the configuration $(220) \to (2\mathbf{0}0)$. The next three digits are $20x$. Three configurations containing $20x$ are $(200) \to (2\mathbf{0}0)$, $(201) \to (2\mathbf{0}1)$ and $(202) \to (2\mathbf{0}2)$. No matter what the value of x will

be, the 0 in the middle of $20x$ will remain as it is. Thus, we obtain $1200x$. We need one more procedure in order to reach $\mathbf{1201}x$. The first digit is fixed. The next digit, 2, remains the same because the configuration says that $(120) \to (1\mathbf{2}0)$. The next three digits are 200. The 0 in the middle of 200 remains the same since the configuration says that $(200) \to (2\mathbf{0}0)$. The next three digits are $00x$. Three configurations containing $00x$ are $(000) \to (0\mathbf{1}0)$, $(001) \to (0\mathbf{1}1)$ and $(002) \to (0\mathbf{1}2)$. No matter what the value of x will be, the 0 in the middle of $00x$ will change to 1. Thus, we obtain the sequence $\mathbf{1201}$.

Case Z: $1221x$.

$$1221x \to 1200x \to \mathbf{1201x}. \qquad \text{(2TS)}$$

For **Case Z**, one has initially $1221x$. The first digit is fixed. The next digit, 2, remains as it is. This is because the configuration says that $(122) \to (1\mathbf{2}2)$. The next three digits are 221. The 2 in the middle of 221 turns to 0 because the configuration says that $(221) \to (2\mathbf{0}1)$. The next three digits are $21x$. Three configurations containing $21x$ are $(210) \to (2\mathbf{0}0)$, $(211) \to (2\mathbf{0}1)$ and $(212) \to (2\mathbf{0}2)$. No matter what the value of x will be, the 1 in the middle of $21x$ will change to 0. Thus, we obtain $1200x$. We need one more procedure in order to reach $\mathbf{1201}x$. The first digit is fixed. The next digit, 2, remains the same because the configuration says that $(120) \to (1\mathbf{2}0)$. The next three digits are 200. The 0 in the middle of 200 remains the same since the configuration says that $(200) \to (2\mathbf{0}0)$. The next three digits are $00x$. Three configurations containing $00x$ are $(000) \to (0\mathbf{1}0)$, $(001) \to (0\mathbf{1}1)$ and $(002) \to (0\mathbf{1}2)$. No matter what the value of x will be, the 0 in the middle of $00x$ will change to 1. Thus, we obtain the sequence $\mathbf{1201}$.

Case AA: $1222x$.

$$1222x \to 1200x \to \mathbf{1201x}. \qquad \text{(2TS)}$$

For **Case AA**, one has initially $1222x$. The first digit is fixed. The next digit, 2, remains as it is. This is because the configuration says that $(122) \to (1\mathbf{2}2)$. The next three digits are 222. The 2 in the middle of 222 turns to 0 because the configuration says that $(222) \to (2\mathbf{0}2)$. The next three digits are $22x$. Three configurations containing $22x$ are $(220) \to (2\mathbf{0}0)$, $(221) \to (2\mathbf{0}1)$ and $(222) \to (2\mathbf{0}2)$. No matter what the value of x will be, the 2 in the middle of $22x$ will change to 0. Thus, we obtain $1200x$. We need one more procedure in order to reach $\mathbf{1201}x$. The first digit is fixed. The next digit, 2, remains the same because the configuration says that $(120) \to (1\mathbf{2}0)$. The next

179

three digits are 200. The 0 in the middle of 200 remains the same since the configuration says that $(200) \rightarrow (2\mathbf{0}0)$. The next three digits are $00x$. Three configurations containing $00x$ are $(000) \rightarrow (0\mathbf{1}0)$, $(001) \rightarrow (0\mathbf{1}1)$ and $(002) \rightarrow (0\mathbf{1}2)$. No matter what the value of x will be, the 0 in the middle of $00x$ will change to 1. Thus, we obtain the sequence **1201**.

Thus, the slowest way of formation of periodic structure implies the formation of one stripe during 3 time-steps. Therefore in the medium containing k elements periodic structure (containing $k/3$ stripes) forms during k iterations. For other cases when starting from **0**xxx and **2**xxx, the procedures will be similar in order to reach **0120**x and **2012**x respectively.

Bibliography

[1] Bruce Alberts, Alexander Johnson, Julian Lewis, Martin Raff, Keith Roberts, and Peter Walter. *Molecular Biology of the Cell, fourth edition.* Garland Science, 2002.

[2] William L. Allen, Roland Baddeley, Nicholas E. Scott-Samuel, and Innes C. Cuthill. The evolution and function of pattern diversity in snakes. *Behavioral Ecology*, 2013.

[3] P.W. Anderson. More is different. *Science*, 177(4047):393–396, 1972.

[4] Alfonso Martinez Arias. *Drosophila melanogaster and the Development of Biology in the 20th Century*, volume 420 of *Methods in Molecular Biology*, book section 1, pages 1–25. Humana Press, 2008.

[5] R. F. Bachvarova. Establishment of anterior-posterior polarity in avian embryos. *Curr Opin Genet Dev*, 9(4):411–6, 1999.

[6] Philip Ball. *The Self-Made Tapestry: Pattern Formation in Nature.* Oxford University Press, 2001.

[7] Jonathan B. L. Bard. A unity underlying the different zebra striping patterns. *Journal of Zoology*, 183(4):527–539, 1977.

[8] N. Barkai and D. Ben-Zvi. 'big frog, small frog'- maintaining proportions in embryonic development. *Febs Journal*, 276(5):1196–1207, 2009.

[9] J. C. Beetschen and J. L. Fischer. Yves delage (1854-1920) as a forerunner of modern nuclear transfer experiments. *Int J Dev Biol*, 48(7):607–12, 2004.

[10] Danny Ben-Zvi and Naama Barkai. Scaling of morphogen gradients by an expansion-repression integral feedback control. *Proceedings of the National Academy of Sciences*, 107(15):6924–6929, 2010.

[11] Danny Ben-Zvi, Ben-Zion Shilo, Abraham Fainsod, and Naama Barkai. Scaling of the bmp activation gradient in xenopus embryos. *Nature*, 453(7199):1205–1211, 2008.

[12] Alistair Boettiger, Bard Ermentrout, and George Oster. The neural origins of shell structure and pattern in aquatic mollusks. *Proceedings of the National Academy of Sciences*, 106(16):6837–6842, 2009.

[13] Jerry L Bona, Thierry Colin, and David Lannes. Long wave approximations for water waves. *Archive for Rational Mechanics & Analysis*, 178(3):373–410, 2005.

[14] T.J. Bridges, F Dias, and D Menasce. Steady three-dimensional water-wave patterns on a finite-depth fluid. *Journal of Fluid Mechanics*, 436:145–175, 2001.

[15] Elena Castellani. On the meaning of symmetry breaking, 2002.

[16] M. Chuai and C. J. Weijer. Regulation of cell migration during chick gastrulation. *Curr Opin Genet Dev*, 19(4):343–9, 2009.

[17] C. M. Chuong and M. K. Richardson. Pattern formation today. *Int J Dev Biol*, 53(5-6):653–8, 2009.

[18] J. Cooke. Scale of body pattern adjusts to available cell number in amphibian embryos. *Nature*, 290(5809):775–8, 1981.

[19] Mathieu Coppey, Alexander M. Berezhkovskii, Yoosik Kim, Alistair N. Boettiger, and Stanislav Y. Shvartsman. Modeling the bicoid gradient: Diffusion and reversible nuclear trapping of a stable protein. *Developmental Biology*, 312(2):623–630, 2007.

[20] Stephen C. Cowin. How is a tissue built? *Journal of Biomechanical Engineering*, 122(6):553–569, 2000.

[21] Alex D. D. Craik. The origins of water wave theory. *Annual Review of Fluid Mechanics*, 36(1):1–28, 2004.

[22] S. J. Day and P. A. Lawrence. Measuring dimensions: the regulation of size and shape. *Development*, 127(14):2977–87, 2000.

[23] A. M. de Lachapelle and S. Bergmann. Precision and scaling in morphogen gradient read-out. *Mol Syst Biol*, 6:351, 2010.

[24] A.M. De Lachapelle and B. Bergmann. A new scaling measure quantifies the conservation of proportions of gene expression profiles. *Developing organic Shapes*, 2011.

[25] Edward M. De Robertis. Spemann's organizer and self-regulation in amphibian embryos. *Nat Rev Mol Cell Biol*, 7(4):296–302, 2006.

[26] A Dikansky. Fitzhugh-nagumo equations in a nonhomogeneous medium. *DIS-CRETE AND CONTINUOUS Website*, pages 216–224, 2005.

[27] W. Driever and C. Nusslein-Volhard. A gradient of bicoid protein in drosophila embryos. *Cell*, 54(1):83–93, 1988.

[28] A. Eldar, R. Dorfman, D. Weiss, H. Ashe, B. Z. Shilo, and N. Barkai. Robustness of the bmp morphogen gradient in drosophila embryonic patterning. *Nature*, 419(6904):304–8, 2002.

[29] Richard J. Field, Endre Koros, and Richard M. Noyes. Oscillations in chemical systems. ii. thorough analysis of temporal oscillation in the bromate-cerium-malonic acid system. *Journal of the American Chemical Society*, 94(25):8649–8664, 1972.

[30] R. Fitzhugh. Impulses and physiological states in theoretical models of nerve membrane. *Biophys J*, 1(6):445–66, 1961.

[31] RubnD Flores-saaib and AlbertJ Courey. Regulation of dorso/ventral patterning in the drosophila embryo by multiple dorsal-interacting proteins. *Cell Biochemistry and Biophysics*, 33(1):1–17, 2000.

[32] Gabor Forgacs and Stuart A. Newman. *Biological Physics of the Developing Embryo*. Cambridge University Press, 2005.

[33] V. Francois, M. Solloway, J. W. O'Neill, J. Emery, and E. Bier. Dorsal-ventral patterning of the drosophila embryo depends on a putative negative growth factor encoded by the short gastrulation gene. *Genes Dev*, 8(21):2602–16, 1994.

[34] Scott F Gilbert. *Developmental Biology*. 2010.

[35] Martin Golubitsky, William F. Langford, and Ian Stewart. Symmetry and bifurcation in biology. 2003.

[36] T. Gregor, W. Bialek, R. R. de Ruyter van Steveninck, D. W. Tank, and E. F. Wieschaus. Diffusion and scaling during early embryonic pattern formation. *Proc Natl Acad Sci U S A*, 102(51):18403–7, 2005.

[37] T. Gregor, A. P. McGregor, and E. F. Wieschaus. Shape and function of the bicoid morphogen gradient in dipteran species with different sized embryos. *Dev Biol*, 316(2):350–8, 2008.

[38] T. Gregor, D. W. Tank, E. F. Wieschaus, and W. Bialek. Probing the limits to positional information. *Cell*, 130(1):153–64, 2007.

[39] Thomas Gregor, Eric F. Wieschaus, Alistair P. McGregor, William Bialek, and David W. Tank. Stability and nuclear dynamics of the bicoid morphogen gradient. *Cell*, 130(1):141–152, 2007.

[40] O. Grimm, M. Coppey, and E. Wieschaus. Modelling the bicoid gradient. *Development*, 137(14):2253–64, 2010.

[41] DavidJ. Gross. The role of symmetry infundamentalphysics. *Proceedings of the National Academy of Sciences*, 93(25):14256–14259, 1996.

[42] Sarah Hake and Fred Wilt. *Principles of Developmental Biology*. W. W. Norton and Company, New York, NY, 2003.

[43] N. C. Harrison, D. R. del Corral, and B. Vasiev. Coordination of cell differentiation and migration in mathematical models of caudal embryonic axis extension. *PLoS ONE*, 6(7), 2011.

[44] M. Haskel-Ittah, D. Ben-Zvi, M. Branski-Arieli, E. D. Schejter, B. Z. Shilo, and N. Barkai. Self-organized shuttling: generating sharp dorsoventral polarity in the early drosophila embryo. *Cell*, 150(5):1016–28, 2012.

[45] R. M. Hazen. The emergence of patterning in lifes origin and evolution. *Int J Dev Biol*, 53(5-6):683–92, 2009.

[46] F. He, Y. Wen, J. Deng, X. Lin, L. J. Lu, R. Jiao, and J. Ma. Probing intrinsic properties of a robust morphogen gradient in drosophila. *Dev Cell*, 15(4):558–67, 2008.

[47] Willy Hereman. *Shallow Water Waves and Solitary Waves*, book section 96, pages 1520–1532. Springer New York, 2011.

[48] Patrick A. Hesp. Geomorphology of desert dunes, n. lancaster, publisher routledge, london (1995) (290 pp) 55.00 (hardback) isbn 0-415-06093-1 17.99 (paperback) isbn 0-415-06094-x. *Journal of Quaternary Science*, 12(1):78–78, 1997.

[49] Rebecca. Hoyle. *Pattern Formation. An introduction to methods*. Cambridge University Press, 2006.

[50] Herbert Jackle, Diethard Tautz, Reinhard Schuh, Eveline Seifert, and Ruth Lehmann. Cross-regulatory interactions among the gap genes of drosophila. *Nature*, 324(6098):668–670, 1986.

[51] J. Jaeger, S. Surkova, M. Blagov, H. Janssens, D. Kosman, K. N. Kozlov, Manu, E. Myasnikova, C. E. Vanario-Alonso, M. Samsonova, D. H. Sharp, and J. Reinitz. Dynamic control of positional information in the early drosophila embryo. *Nature*, 430(6997):368–71, 2004.

[52] Johannes Jaeger. Modelling the drosophila embryo. *Molecular BioSystems*, 5(12):1549–1568, 2009.

[53] Megan Kearl. The potency of the first two cleavage cells in echinoderm development. experimental production of partial and double formations" (1891-1892), by hans driesch. *Embryo Project Encyclopedia*, 2012.

[54] Michel Kerszberg and Lewis Wolpert. Specifying positional information in the embryo: Looking beyond morphogens. *Cell*, 130(2):205–209, 2007.

[55] O. Khaner. The potency of the first two cleavage cells in echinoderm development: the experiments of driesch revisited. *Roux's archives of developmental biology*, 202(4):193–197, 1993.

[56] A. D. Lander, F. Y. M. Wan, and Q Nie. Multiple paths to morphogen gradient robustness.

[57] A.D. Lander, F.Y.M. Wan, H.M. Elledge, C.M. Mizutani, E. Bier, and Q. Nie. Diverse paths to morphogen gradient robustness. 2005.

[58] T. J. Levario, M. Zhan, B. Lim, S. Y. Shvartsman, and H. Lu. Microfluidic trap array for massively parallel imaging of drosophila embryos. *Nat Protoc*, 8(4):721–36, 2013.

[59] R. Li and B. Bowerman. Symmetry breaking in biology. *Cold Spring Harb Perspect Biol*, 2(3):a003475, 2010.

[60] Pei-Hui Lin and Ruth Steward. *Drosophila Embryo: Dorsal-ventral Specification*. John Wiley & Sons, Ltd, 2001.

[61] Ian Livingstone, Giles F. S. Wiggs, and Corinne M. Weaver. Geomorphology of desert sand dunes: A review of recent progress. *Earth-Science Reviews*, 80(34):239–257, 2007.

[62] Jeremy A. Lynch and Siegfried Roth. The evolution of dorsalventral patterning mechanisms in insects. *Genes & Development*, 25(2):107–118, 2011.

[63] K Mainzer. *Symmetry and Complexity: The Spirit and Beauty of Nonlinear Science*, volume 51. World Scientific Publishing Company, Incorporated, 2005.

[64] P. McHale, W. J. Rappel, and H. Levine. Embryonic pattern scaling achieved by oppositely directed morphogen gradients. *Phys Biol*, 3(2):107–20, 2006.

[65] Hans Meinhardt. *The Algorithmic Beauty of Sea Shells*. Springer Publishing Company, Incorporated, 2009.

[66] Hans Meinhardt and Martin Klingler. A model for pattern formation on the shells of molluscs. *Journal of Theoretical Biology*, 126(1):63–89, 1987.

[67] J. D. Murray and M. R. Myerscough. Pigmentation pattern formation on snakes. *Journal of Theoretical Biology*, 149(3):339–360, 1991.

[68] James D Murray. How the leopard gets its spots. *Scientific American*, 258(3):80–87, 1988.

[69] James D Murray. *Mathematical Biology II: Spatial Models and Biomedical Applications*. 3rd edition, 2003.

[70] J Nagumo, S Arimoto, and S Yoshizawa. An active pulse transmission line simulating nerve axon. *Proceedings of the Institute of Radio Engineers*, (50):2061–2070, 1962.

[71] Hiraku Nishimori and Noriyuki Ouchi. Formation of ripple patterns and dunes by wind-blown sand. *Physical Review Letters*, 71(1):197–200, 1993.

[72] Flavio Nogueira. The symmetry-breaking paradigm. 2006.

[73] M Ohkusu and H Iwashita. Revisiting the unsteady wave pattern of a ship. *19th IWWWFB*, 2004.

[74] J. Parker. Morphogens, nutrients, and the basis of organ scaling. *Evol Dev*, 13(3):304–14, 2011.

[75] A. Pechenkin. B p belousov and his reaction. *J Biosci*, 34(3):365–71, 2009.

[76] N. Perrimon and A. P. Mahowald. Multiple functions of segment polarity genes in drosophila. *Dev Biol*, 119(2):587–600, 1987.

[77] Andrew J. Plater. Aeolian sand and sand dunes by k. pye and h. tsoar, unwin hyman limited, london, 1990. no. of pages: 396. price: 70.00 (hardback). *Geological Journal*, 26(3):274–275, 1991.

[78] William John Macquorn Rankine. On the exact form of waves near the surface of deep water. *Philosophical Transactions of the Royal Society of London*, 153:127–138, 1863.

[79] Gregory T Reeves, Nathanie Trisnadi, Thai V Truong, Marcos Nahmad, Sophie Katz, and Angelike Stathopoulos. Dorsal-ventral gene expression in the drosophila embryo reflects the dynamics and precision of the dorsal nuclear gradient. *Developmental Cell*, 22(3):544–557, 2012.

[80] J Sablic. Diffusion-based physical theories of morphogen propagation. 2012.

[81] I. Salazar-Ciudad, J. Jernvall, and S. A. Newman. Mechanisms of pattern formation in development and evolution. *Development*, 130(10):2027–37, 2003.

[82] Klaus Sander. *Wilhelm Roux on embryonic axes, sperm entry and the grey crescent*, book section 3, pages 7–9. Springer Berlin Heidelberg, 1997.

[83] Miguel A. F. Sanjun. Noise-induced phenomena in the environmental sciences, by luca ridolfi, paolo d'odorico and francesco laio. *Contemporary Physics*, 53(4):376–376, 2012.

[84] Stefania Scarsoglio, Francesco Laio, Paolo DOdorico, and Luca Ridolfi. Spatial pattern formation induced by gaussian white noise. *Mathematical Biosciences*, 229(2):174–184, 2011.

[85] G. Schwank and K. Basler. Regulation of organ growth by morphogen gradients. *Cold Spring Harb Perspect Biol*, 2(1):a001669, 2010.

[86] Robert P. Sharp. Wind ripples. *The Journal of Geology*, 71(5):617–636, 1963.

[87] S. Small and M. Levine. The initiation of pair-rule stripes in the drosophila blastoderm. *Curr Opin Genet Dev*, 1(2):255–60, 1991.

[88] Hans Spemann. *Embryonic development and induction*. New Haven, 1938.

[89] D. St Johnston and C. Nusslein-Volhard. The origin of pattern and polarity in the drosophila embryo. *Cell*, 68(2):201–19, 1992.

[90] C.D. Stern. Gastrulation in the chick. in: Gastrulation: from cells to embryo. *Cold Spring Harbor Press*, pages 219–232, 2004.

[91] C. J. Tomlin and J. D. Axelrod. Biology by numbers: mathematical modelling in developmental biology. *Nat Rev Genet*, 8(5):331–40, 2007.

[92] C. Tsai and J. P. Gergen. Gap gene properties of the pair-rule gene runt during drosophila segmentation. *Development*, 120(6):1671–83, 1994.

[93] Haim Tsoar. Bagnold, r.a. 1941: The physics of blown sand and desert dunes. london: Methuen. *Progress in Physical Geography*, 18(1):91–96, 1994.

[94] A. M. Turing. The chemical basis of morphogenesis. *Philosophical Transactions of the Royal Society of London. Series B, Biological Sciences*, 237(641):37–72, 1952.

[95] D. Umulis, M. B. O'Connor, and H. G. Othmer. Robustness of embryonic spatial patterning in drosophila melanogaster. *Curr Top Dev Biol*, 81:65–111, 2008.

[96] David M. Umulis. Analysis of dynamic morphogen scale invariance. *Journal of The Royal Society Interface*, 6(41):1179–1191, 2009.

[97] David M. Umulis and Hans G. Othmer. Mechanisms of scaling in pattern formation. *Development*, 140(24):4830–4843, 2013.

[98] J. E. Ungar and P. K. Haff. Steady state saltation in air. *Sedimentology*, 34(2):289–299, 1987.

[99] J. Van der Gucht and C. Sykes. Physical model of cellular symmetry breaking. *Cold Spring Harb Perspect Biol*, 1(1):a001909, 2009.

[100] Milton Van Dyke. *An album of fluid motion*. 1982.

[101] Bakhtier Vasiev, Ariel Balter, Mark Chaplain, James A. Glazier, and Cornelis J. Weijer. Modeling gastrulation in the chick embryo: Formation of the primitive streak. *PLoS ONE*, 5(5):1–14, 2010.

[102] Bakhtier N. Vasiev. Classification of patterns in excitable systems with lateral inhibition. *Physics Letters A*, 323(34):194–203, 2004.

[103] O. Vasieva, M. Rasolonjanahary, and B. Vasiev. Mathematical modelling in developmental biology. *Reproduction*, 145(6):R175–84, 2013.

[104] C. H. Waddington and Russell J. Cowe. Computer simulation of a mulluscan pigmentation pattern. *Journal of Theoretical Biology*, 25(2):219–225, 1969.

[105] Gabriel Wainer, Qi Liu, Olivier Dalle, and Bernard P. Zeigler. Applying cellular automata and devs methodologies to digital games: A survey. *Simul. Gaming*, 41(6):796–823, 2010.

[106] James Douglas Walker. An experimental study of wind ripples. *Master Thesis in Geology, MIT*, 1981.

[107] O. Wartlick, A. Kicheva, and M. Gonzalez-Gaitan. Morphogen gradient formation. *Cold Spring Harb Perspect Biol*, 1(3):a001255, 2009.

[108] A.S. Wilkins. The evolution of developmental pathways. *Journal of Heredity*, 93(6):460–461, 2001.

[109] Stephen Wolfram. *A new kind of science*. Wolfram Media Inc., 2002.

[110] L. Wolpert. Positional information and the spatial pattern of cellular differentiation. *Journal of Theoretical Biology*, 25(1):1–47, 1969.

[111] L. Wolpert. Positional information and pattern formation in development. *Dev Genet*, 15(6):485–90, 1994.

[112] L. Wolpert. Positional information and patterning revisited. *J Theor Biol*, 269(1):359–65, 2011.

[113] Lewis Wolpert, Rosa Beddington, Jeremy Brockes, Thomas Jessell, Peter Lawrence, and Elliot Meyerowitz. *Principles of Development*. Oxford University Press, Oxford, 1998.

[114] Lewis Wolpert, Elliot Meyerowitz, Peter Lawrence, Rosa Beddington, and Thomas Jessell. *Principles of development*. Oxford University Press, USA, 2 edition, 2001.

[115] Zhang Xiaojing, Chen Chung-Chu, R. W. Bernstein, S. Zappe, M. P. Scott, and O. Solgaard. Microoptical characterization and modeling of positioning forces on drosophila embryos self-assembled in two-dimensional arrays. *Microelectromechanical Systems, Journal of*, 14(5):1187–1197, 2005.

[116] Xin-She Yang and Y. Young. Cellular automata, pdes, and pattern formation. 2010.

[117] Hezi Yizhaq, Neil J. Balmforth, and Antonello Provenzale. Blown by wind: nonlinear dynamics of aeolian sand ripples. *Physica D: Nonlinear Phenomena*, 195(34):207–228, 2004.

[118] A. N. Zaikin and A. M. Zhabotinsky. Concentration wave propagation in two-dimensional liquid-phase self-oscillating system. *Nature*, 225(5232):535–537, 1970.